A Study of the Complications regarding the Derivation of Amplitude Equations via Weakly Nonlinear Expansions for Non-self-adjoint Partial Differential Equations

Catherine Drysdale

INSTITUT POLYTECHNIQUE DE PARIS

ÉCOLE POLYTECHNIQUE

IP PARIS

ONERA
THE FRENCH AEROSPACE LAB

Thèse de doctorat

A Study of the Complications regarding the Derivation of Amplitude Equations via Weakly Nonlinear Expansions for Non-self-adjoint Partial Differential Equations

Thèse de doctorat de l'Institut Polytechnique de Paris préparé à l'École Polytechnique et à l'Office National d'Études et de Recherches Aérospatiales

École doctorale n°626
École Doctorale de l'Institut Polytechnique de Paris (ED IP Paris)
Spécialité de doctorat: Mécanique des fluides et des solides

Thèse présentée et soutenue à Paris, le 13/12/2021, par

CATHERINE DRYSDALE

Composition du Jury :

Luc Pastur Professeur Associé, Institut Polytechnique of Paris (ENSTA)	Président
David Krejčiřík Professeur Associé, Czech Technical University in Prague (Faculty of Nuclear Sciences and Physical Engineering)	Rapporteur
Peter Schmid Professeur, KAUST (Physical Science and Engineering Division)	Rapporteur
Alessia E. Kogoj Professeure Associée, Universita degli Studi di Urbino Carlo Bo (Department of Pure and Applied Sciences)	Examinateur
David Needham Professeur Émérite, University of Birmingham (Department of Mathematics)	Examinateur
Grigoris A. Pavliotis Professeur, Imperial College London (Department of Mathematics)	Examinateur
Denis Sipp Directeur de recherche, ONERA (Departement Aérodynamique, Aéroélasticité, Acoustique)	Directeur de thèse

I would like to dedicate this PhD to my Uncle Brian.

Acknowledgements

I would like to thank my mother, father and Uncle Brian whose combined efforts lead me where I am today. My uncle Brian unfortunately passed away during my PhD, but his life ethos resonated through his immaculate collection of books on psychology, philosophy and sociology. Reading these, especially at the hopeless points of my PhD, reminded that the pursuit of truth in art and science is something that distinguishes the human spirit, and the nobility of this pursuit reinforces the human spirit instead of breaking it.

I would like to thank all of my my academic mentors. They all gave excellent advice and instruction at various points during my PhD, and I hope to have ongoing collaborations with all of them. I would like to thank Denis Sipp in particular for giving me a lot of freedom throughout my PhD to pursue what I wanted.

I would also like to thank Michael Woodley, Tom Crossland and Lucas Franceschini for assisting me with various numerical crises. I would also like to thank Kweku Abraham for responding to various mathematical questions, no matter how silly or badly written, and taking the time to work out what I was trying to ask. I would also like to thank my close friends in Paris for providing moral support of various kinds.

Last (and by no means least), I would like to thank Peter who made my time in Paris so much fun! I've experienced so much with you from cycling around the walls of Lucca to defining experiences of reading Russian short stories by Chekhov and Sologub aloud on the phone everyday when were separated owing to the pandemic. I hope that, wherever the future takes me, our dynamic remains as it is!

Contents

Chapter 1

Introduction

It is the purpose of an introduction to give an overview of thesis, review the literature as well as establish and legitimise the gap in the current research which the thesis fills. In order to do this, we have chosen a rather unusual structure for the introduction of the thesis as the author feels that it is best to have the issue of the thesis demonstrated as opposed to just described. Furthermore, some of the concepts in the literature review are best illustrated through numerical experiments on our test cases; after all that is why we chose the particular test-cases. It is for this reason that we give a brief introduction to the thesis where we avoid citing any literature (Section 1.1). Then we present our test cases (Section 1.2) and the derivations of first order approximations via WNLE. We then review the literature (Section 1.3) using our test cases to demonstrate various concepts with numerical experiments. Lastly, we give brief descriptions of the chapters of the thesis (Section 1.4).

1.1 Brief Introduction

To provide a mathematical description of open shear flows is an interesting and challenging task owing to the non-self-adjointness inherent in the linear operator and also the nonlinearity present in equations such as the Navier-Stokes equations and Ginzburg-Landau equation. It is also an important task when one considers the examples of mixing layers, jets, wakes and boundary layers found in industrial and geoscientific applications. The flows described by these equations can develop self-sustained oscillations in time, which have characteristic spatial distributions, saturation amplitudes and saturation frequencies. In the Fluid Mechanics community, these spatially-coherent structures are called “Global Modes”. For marginally unstable systems, which are systems where the largest eigenvalue is zero and the rest are negative, there have been several attempts at approximating these global modes by the spatial development of the leading eigenvector (the eigenvector that corresponds to the zeroth eigenvalue). The spatial development is categorised by an amplitude equation derived via methods such as normal form theory or weakly nonlinear expansions (WNLE). These methods are generally successful in the cases where the operator

is self-adjoint, but, for non-self-adjoint systems, only the early time characteristics are captured and the saturation characteristics are under-estimated.

In this thesis, we have taken a closer look at this problem by looking at specifically why first order approximations derived via weakly nonlinear expansions do not approximate the governing system well in non-self-adjoint cases. This is a historic problem that has been tacked in various ways. For instance, authors have tried to build higher order approximations including spatial structures different from the zeroth eigenvectors, but there is a problem regarding the non-uniqueness of higher order terms. Other authors have also tried to build higher order amplitude equations, i.e. more elaborate amplitude equations that describe the leading eigenvector. This approach can be seen as a way to circumvent the non-uniqueness. However, by still only approximating with the leading eigenvector, even though its temporal development is elaborated by a higher order amplitude equation, spatial structures different from the leading eigenvector are neglected.

For our purposes, we have chosen two particular test-cases in order to study the failure of first-order weakly non-linear expansions at approximating non-self-adjoint cases; the Real non-self-adjoint Ginzburg-Landau and Complex non-self-adjoint Ginzburg-Landau equations (labelled RnsaGL and CnsaGL respectively). They have similar properties to the Navier-Stokes equations in the sense that they are non-self-adjoint and nonlinear, but are different in the sense that the linear operators generate strongly-continuous semigroups (C_0-semigroups), which allow us to write the equations in integral form and in this way derive error bounds. Also, in the real case, we have a quasi-basis structure that allows us to expand our solutions into amplitude-eigenvector pairs, which cannot always be done meaningfully for non-self-adjoint systems (completeness of eigenvectors guarantees an expansion, but the amplitudes are not guaranteed to be finite). This is the first known application of the quasi-basis structure in Fluid Mechanics.

We begin by consolidating the literature and giving an overview of different mathematical descriptions of Fluid Mechanics. In the first chapter, we give an example of higher order amplitude equations regarding the RnsaGL; this should be seen as an extension to the introduction, as it is not necessarily new. Nevertheless, it demonstrates that for non-self-adjoint systems contributions from spatial structures different from the leading eigenvector are significant and therefore cannot be neglected. We also see that for higher order amplitude equations that the radius of convergence is very small thus limiting the utility of these higher order amplitude equations. We then derive higher order approximations with additional spatial structures. The problem of non-uniqueness persists, but we combat this using additional assumptions - these assumptions are different in comparison to the ones used by previous authors. We notice for the RnsaGL, where there is a quasi-basis structure, we can normalise the higher order spatial structures in two ways; we can either make them orthogonal to the zeroth direct eigenvector or the zeroth adjoint eigenvector. We then derive error bounds for the discrepancy between the direct and adjoint eigenvectors. A key part of the derivation of the error bounds is to transform the governing partial differential equations into integral form, which is possible owing to the fact the linear operators generate C_0-semigroups. However, these error

bounds remain theoretical tools that show a radius of convergence exists as opposed to telling us what that radius of convergence is. Lastly, we consider a stochastic homogenisation procedure, which is different from WNLE as it does not neglect all stable eigenmodes as a first step.

1.2 Test Cases and Derivation of First Order Approximations via WNLE

In Fluid Mechanics, we generally want to study equations of the form

$$\frac{\partial u}{\partial t} = \mathcal{L}u + \mathcal{N}(u) + \delta u \tag{1.1}$$

where $\mathcal{L}$ is a linear operator, $\mathcal{N}$ is the nonlinear operator and $0 < \delta < 1$ is the a constant perturbation from criticality. In this thesis, we have chosen Ginzburg-Landau-type equations for our test cases. Ginzburg-Landau equations have often been used as test cases in Fluid Mechanics (Cossu and Chomaz (1997) [28], Couairon and Chomaz (1999) [29]; Huerre and Monkevitz (1990) [54] and Chomaz (2005) [25] to name a few) as they exhibit similar features to the Navier-Stokes equations. A specificity of our Ginzburg-Landau-type equations is that increasing the advection velocity, U, makes both equations *more non-normal* - in the sense that the direct and adjoint spatial structures of eigenvectors move further apart - but the operator stays critical, meaning that the real part of the leading eigenvalue remains zero for increasing U but the real part of all other eigenvalues remains negative.

We have chosen both a real and a complex case as they display different phenomena. In the real case, there exists an unbounded transformation to transform the operator of the RnsaGL into a self-adjoint equation that allows us to use concepts from Non-Hermitian Quantum Mechanics. In the complex case, we can consider both the saturation frequency and the saturation amplitude. When we decompose the equation into the equation for the frequency and amplitude, i.e. let $u(x,t) = r(x,t)e^{i\phi(x,t)}$ where $r(x,t)$ is the amplitude and $\phi(x,t)$ is the frequency, only the linear operator for the amplitude demonstrates strong transient growth. Therefore, the saturation frequency is well captured as a first order expansion.

The real and complex test cases are respectively;

- Real non-self-adjoint Ginzburg-Landau equation

$$\frac{\partial u}{\partial t} = \mathcal{L}^{RGL}u - u^3 + \delta u \tag{RnsaGL}$$

where

$$\mathcal{L}^{RGL} = \frac{\partial^2}{\partial x^2} - U\frac{\partial}{\partial x} + \left(\frac{U^2}{4} + \sqrt{c_2} - c_2 x^2\right)$$

with boundary conditions $|u| \longrightarrow 0$ as $x \longrightarrow \pm\infty$.

- Complex non-self-adjoint Ginzburg-Landau equation

$$\frac{\partial u}{\partial t} = \mathcal{L}^{CGL}u - |u|^2 u + \delta u \tag{CnsaGL}$$

where

$$\mathcal{L}^{CGL} = (1-i)\frac{\partial^2}{\partial x^2} - (U+0.2i)\frac{\partial}{\partial x} + \left[C_1 + \frac{1}{8}(U^2 - 0.4U - 0.04)\right] - c_2 x^2$$

with $C_1 = \Re\{\sqrt{(1-i)c_2}\}$, with boundary conditions $|u| \longrightarrow 0$ as $x \longrightarrow \pm\infty$.

In the above equations, the real coefficient in front of the $\frac{\partial^2 u}{\partial x^2}$ is the diffusion constant, $c_2 > 0$ determines the non-parallelism of the flow (throughout this thesis and in all numerical experiments $c_2 = 0.005$) and U is the mean advection velocity. The two-dimensional form of this equation has been used in order to model cylinder flow Roussopoulous et al. (1996) [81].

WNLE is a procedure that combines the method of multiple scales and perturbation theory. It is often tailored to the application at hand. Therefore, there is no rigorous definition. However, loosely the three main steps are, for a problem of the form (1.1); firstly, introduce a diffusive scaling centered around a small parameter ϵ that allows the linear operator to remain dominant, secondly, introduce an expansion in terms of the small parameter, ϵ, in order to get a hierachy of equations, and, thirdly, use the Fredholm alternative repeatedly to obtain solvability conditions at each order to *elabourate* the terms of the expansion. We have chosen the word *elabourate* on purpose, because often it is not possible to determine the terms of the expansion fully owing to the Fredholm alternative.

Below, we give our two versions of the Fredholm alternative in order to reference them when we derive amplitude equations in our test cases. The versions of the Fredholm alternative used in this thesis are tailor-made in order to fit the decay boundary conditions and complexity of the equation in the case of the CnsaGL. The Fredholm Alternative as given in Evans [44] (see Theorem 4, Chapter 6.2) is given on a fixed interval L where the solution is in the space $H_0^1(L)$. In order to extend this to a real line for an elliptic PDE of non-constant coefficients, we considered the following space

$$\mathcal{H}^{\mathcal{L}^1} := \{u \in L^2(\mathbb{R}) : ||u||_{\mathcal{L}^1} < \infty\} \tag{1.2}$$

where

$$\mathcal{L}^1 = \frac{\partial}{\partial x} - x \qquad \text{and} \qquad ||\cdot||^2_{L^1} = \langle \mathcal{L}^1 \cdot, \mathcal{L}^1 \cdot \rangle. \tag{1.3}$$

$\mathcal{H}^{\mathcal{L}^1}$ is compactly embedded[1] into $L^2(\mathbb{R})$. We give both versions of the theorem, because, even though they are identical to look at, the complex version requires the Complex Lax-Milgram Theorem, so they are not identical in

[1] We have included key definitions such as "compact embedding" in the first section of the Appendix A before giving the proofs of in the real and complex case in the second and third sections respectively.

proof.

- Theorem (Tailored Fredholm Alternative for $\mathcal{L}^{RGL}$). Given $\mathcal{L}^{RGL}$ as in RnsaGL defined as above

  i Precisely one of the following statements holds:

  either

  (α) For each $f \in L^2(\mathbb{R})$[2], there exists a unique weak solution u of the equation[3]

  $$-\mathcal{L}^{RGL}u = f \qquad \text{in } L^2(\mathbb{R}) \tag{1.4}$$

  or else

  (β) There exists a weak solution, $u \neq 0$ of the homogeneous problem

  $$-\mathcal{L}^{RGL}u = 0 \qquad \text{in } L^2(\mathbb{R}) \tag{1.5}$$

  ii Furthermore, should assertion (β) hold, the dimension of the subspace $N \subset \mathcal{H}^{\mathcal{L}^1}$ of weak solutions of (1.5) is finite and equals the dimension of the subspace $N^\dagger \subset \mathcal{H}^{\mathcal{L}^1}$ of weak solutions of

  $$-(\mathcal{L}^{RGL})^\dagger v = 0 \qquad \text{in } L^2(\mathbb{R}) \tag{1.6}$$

  where $(\mathcal{L}^{RGL})^\dagger$ is the L^2-adjoint of $(\mathcal{L}^{RGL})$, i.e. $\langle (\mathcal{L}^{RGL})^\dagger u, v\rangle = \langle u, (\mathcal{L}^{RGL})v\rangle$ where $\langle\cdot,\cdot\rangle$ is the L^2-inner product.

  iii Finally, the boundary-value problem (1.4) has a weak solution if and only if

  $$\langle v, f\rangle = 0 \qquad \text{for all } v \in N^\dagger. \tag{1.7}$$

  Proof. This theorem with proof is given in Appendix A.2.

- Theorem (Tailored Fredholm Alternative for $\mathcal{L}^{CGL}$). Given $\mathcal{L}^{CGL}$ as in the CnsaGL defined as above

  i Precisely one of the following statements holds:

  either

  (α) For each $f \in L^2(\mathbb{R})$, there exists a unique weak solution u of the equation

  $$-\mathcal{L}^{CGL}u = f \qquad \text{in } L^2(\mathbb{R}) \tag{1.8}$$

[2]This is owing to the fact that $L^2(\mathbb{R}) \subset (\mathcal{H}^{\mathcal{L}^1})^*$ where the $*$ denotes the dual space.

[3]Note, we put the minus sign for the necessary ellipticity condition, the equation also takes on a minus sign when we consider the inhomogeneous problem in the weakly nonlinear expansions. We have added it to the other equations for the continuity of the presentation.

or else

(β) There exists a weak solution, $u \neq 0$ of the homogeneous problem

$$-\mathcal{L}^{CGL}u = 0 \qquad \text{in } L^2(\mathbb{R}) \tag{1.9}$$

ii Furthermore, should assertion (β) hold, the dimension of the subspace $N \subset \mathcal{H}^{\mathcal{L}^1}$ of weak solutions of (1.9) is finite and equals the dimension of the subspace $N^\dagger \subset \mathcal{H}^{\mathcal{L}^1}$ of weak solutions of

$$-(\mathcal{L}^{CGL})^\dagger v = 0 \qquad \text{in } L^2(\mathbb{R}) \tag{1.10}$$

where $(\mathcal{L}^{CGL})^\dagger$ is the L^2-adjoint of $\mathcal{L}^{CGL}$, i.e. $\langle(\mathcal{L}^{CGL})^\dagger u, v\rangle = \langle u, (\mathcal{L}^{CGL})v\rangle$ where $\langle\cdot,\cdot\rangle$ is the L^2-inner product.

iii Finally, the boundary-value problem (1.8) has a weak solution if and only if

$$\langle v, f\rangle = 0 \qquad \text{for all } v \in N^\dagger. \tag{1.11}$$

Proof. This theorem with proof is given in Appendix A.3.

We perform WNLE on the RnsaGL and the CnsaGL to illustrate this concretely in Example 1 and Example 2 respectively. In these examples, we have performed computations using a Hermite pseudo-spectral method for the discretisation of the operator in space and a finite-difference method in time. Details of the numerics can be found in the Appendix B. As we are always in situation (β) of the real or complex version of the Fredholm Alternative, i.e. $\mathcal{L}^{RGL}u = 0$ and $\mathcal{L}^{CGL} = 0$ have non-trivial solutions, we can never determine higher order terms uniquely.

- Example 1 (WNLE for the RnsaGL)

  In this case, we put the equation on the diffusive timescale $u = \epsilon^{\frac{1}{2}}v(x,\tau)$ where $\tau = \epsilon t$. Furthermore, we let $\delta = \epsilon\tilde{\delta}$ where $\tilde{\delta} = O(1)$. This gives the following equation

$$-\mathcal{L}^{RGL}v = \epsilon\left(\frac{\partial v}{\partial \tau} + \tilde{\delta}v - v^3\right). \tag{1.12}$$

  We expand $v = v_0 + \epsilon v_1 + ... + \epsilon^n v_n$ in order to get the following hierachy of equations

$$-\mathcal{L}^{RGL}v_0 = 0, \tag{1.13}$$

$$-\mathcal{L}^{RGL}v_1 = \left(\frac{\partial v_0}{\partial \tau} + \tilde{\delta}v_0 - v_0^3\right) \tag{1.14}$$

  From (1.13), we let $v_0 = C(\tau)e_0$, where e_0 solves the equation $\mathcal{L}^{RGL}e_0 = 0$ and $C(\tau)$ is the corresponding

amplitude of this spatial structure.

We apply the Fredholm alternative to (1.14). By this take the inner product with $(\hat{e}_0)^\dagger$, which solves the following equation

$$(\mathcal{L}^{RGL})^\dagger e_0^\dagger = 0 \tag{1.15}$$

where $(\mathcal{L}^{RGL})^\dagger$ is the L^2-adjoint of $\mathcal{L}^{RGL}$ given by

$$(\mathcal{L}^{RGL})^\dagger = a\frac{\partial^2}{\partial x^2} + U\frac{\partial}{\partial x} + \left(\frac{U^2}{4a} + \sqrt{ac_2} - c_2x^2\right), \tag{1.16}$$

in order to obtain the following amplitude equation

$$\frac{dC}{d\tau} = \tilde{\delta}C - \frac{\langle e_0^\dagger, e_0^3\rangle}{\langle e_0^\dagger, e_0\rangle}C^3. \tag{1.17}$$

The first order approximation, u_{app} to the solution of u, is given by

$$u_{app} = \epsilon^{\frac{1}{2}}C(\tau)e_0 = B(t)e_0 \tag{1.18}$$

where we have let $B(\tau) = \epsilon^{\frac{1}{2}}C(\tau)$. By doing this, we can write the amplitude equation (1.17) on the original timescale

$$\frac{dB}{dt} = \delta B - \underbrace{\frac{\langle e_0^\dagger, e_0^3\rangle}{\langle e_0^\dagger, e_0\rangle}}_{\lambda^1} B^3. \tag{1.19}$$

We call the constant in front of the cubic term λ^1 as is customary (this will be discussed further in the literature review). We obtain the saturation amplitude, B_{sat} by setting $\frac{dB}{dt}$ in (1.19) to zero. This gives

$$B_{sat} = \sqrt{\frac{\delta}{\lambda^1}}. \tag{1.20}$$

We illustrate the problem by comparing the difference $||u-u_{app}||_{L^2}$ for different values of U in Figure 1. We see that the approximation gets worse as U increases. However, for early time, in the linear regime we have that the global mode is well approximated by u_{app}. This suggests that the failure of approximation is a combination of non-normality and nonlinearity.

The next order approximation would be of the form $u_{app} = \epsilon^{\frac{1}{2}}(v_0 + \epsilon v_1)$. However, as we are in situation (β) of the Fredholm alternative demonstrated in (1.5), we cannot determine v_1 uniquely. We will discuss additional assumptions used to circumvent this problem in the literature review.

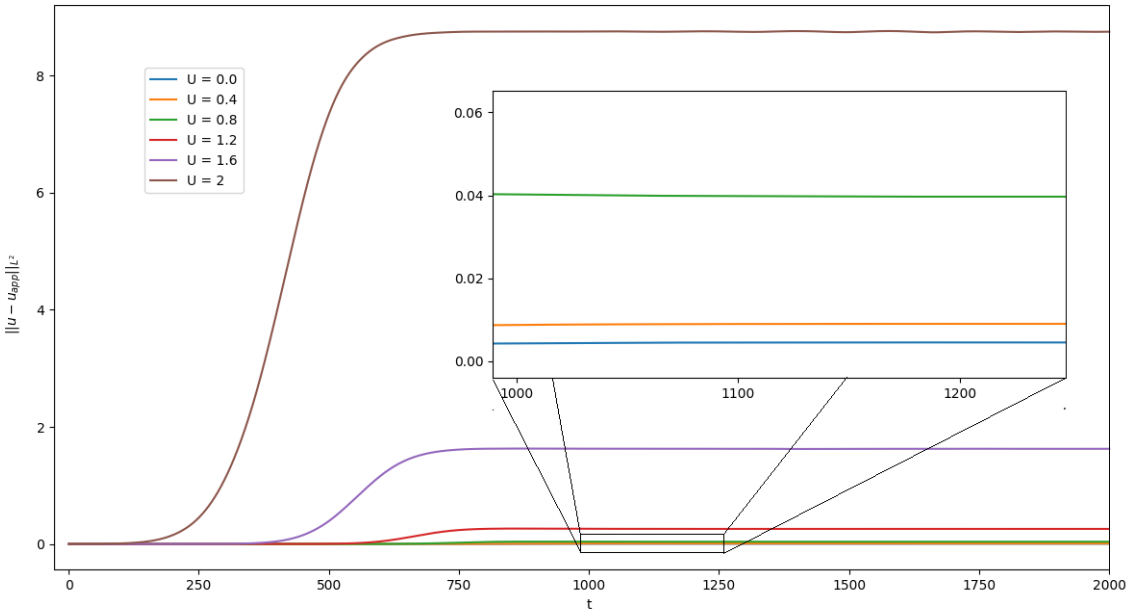

Figure 1. A plot of $||u - u_{app}||_{L^2}$ for various values of U shown in plot, with $\delta = 0.01$

- Example 2 (WNLE for the CnsaGL)

We let $u(x,t) = e^{i\omega_0 t}\epsilon^{\frac{1}{2}}v(x,\tau,t)$ in the CnsaGL equation. $\lambda_0 = i\omega_0$ with $\omega_0 \in \mathbb{R}$ is the largest eigenvalue corresponding to eigenvector e_0. The operator remains with this eigenvalue as the leading eigenvector as U increases. As the real part of λ_0 is zero, the operator is still critical.

$$\Big(i\omega_0 - \mathcal{L}^{CGL}\Big)v = \epsilon\Big(-\frac{\partial}{\partial\tau}v + \tilde{\delta}v - |v|^2 v\Big). \tag{1.21}$$

Introducing the expansion $v = v_0 + \epsilon v_1 + ... + \epsilon^n v_n$ in order to get the following hierarchy of equations

$$\Big(i\omega_0 - \mathcal{L}^{CGL}\Big)v_0 = 0, \tag{1.22}$$

$$\Big(i\omega_0 - \mathcal{L}^{CGL}\Big)v_1 = -\frac{\partial}{\partial\tau}v_0 + \tilde{\delta}v_0 - |v_0|^2 v_0 \tag{1.23}$$

As before, from the (1.22) we approximate $v_0 = C(\tau)e_0$ where e_0 solves the equation $\mathcal{L}^{RGL}\hat{e}_0 = 0$. The amplitude equation for $C(\tau)$ is obtained similarly to previous case by applying the Fredholm alternative

$$\frac{\partial C(\tau)}{\partial\tau} = \tilde{\delta}C(\tau) - \underbrace{\frac{\langle e_0, |e_0|^2 e_0\rangle}{\langle e_0^\dagger, e_0\rangle}}_{\lambda^1}|C(\tau)|^2 C(\tau) \tag{1.24}$$

where $e_0^\dagger$ solves the adjoint problem

$$(\mathcal{L}^{CGL})^\dagger e_0^\dagger = 0 \tag{1.25}$$

where $(\mathcal{L}^{CGL})^\dagger$ is the L^2-adjoint of $(\mathcal{L}^{CGL})$ given by

$$(\mathcal{L}^{CGL})^\dagger = (1+i)\frac{\partial^2}{\partial x^2} + (U-0.2i)\frac{\partial}{\partial x} + \left[C_1 + \frac{1}{8}(U^2 - 0.4U - 0.04)\right] - c_2 x^2 \tag{1.26}$$

We again label the coefficient of the cubic term λ^1.

We let $B = \epsilon^{\frac{1}{2}} e^{i\omega t} C(\tau)$. Then the amplitude equation in terms of B is then

$$\frac{dB}{dt} = (\delta + i\omega_0)B - |B|^2 B \tag{1.27}$$

and the approximation is given by u_{app}

$$u_{app} = Be_0. \tag{1.28}$$

We assume δ to be real and consider the real and imaginary parts of B in polar coordinates, i.e. $B = re^{i\phi}$. Furthermore, we write $\lambda^1 = \lambda^r + i\lambda^i$ We obtain the following two equations

$$\frac{dr}{dt} = \delta r - \lambda_r r^3. \qquad \text{and} \qquad \frac{\partial \phi}{\partial t} = \omega_0 - \lambda_i r^2. \tag{1.29}$$

From the equations in (1.29) we see that the saturation amplitude r_A and saturation frequency ϕ_A are given by $r_A = \sqrt{\frac{\delta}{\lambda_r}}$ and $\phi_A = \omega_0 - \lambda_i \frac{\delta}{\lambda_r}$.

In order compare the solutions to the approximation. Firstly, we consider the solution difference in amplitude. We decompose our solution as $u = Re^{i\Phi}$, and we consider $||R-r||_{L^2}$ for different values of U. In Figure 2a, we plot this. We see the same phenomena as last time where the amplitude is underestimated by the first order approximation as the non-normality increases. Secondly, we look at the saturation frequency by considering the time signal of the solution at a particular point x. We choose $x = -\frac{4\alpha_2}{\alpha_1^2}$, as this is the maximum point of the spatial structure $\hat{e}_0$, so it is equally where we expect the signal to be the strongest. We obtain the saturation frequency by performing the Fast Fourier transform on the signal between $t = 1500$ and $t = 1750$ where we assume the flow has saturated from looking at the graph. In Table 1, we give values from performing the Fourier transform on the time signal of the solution and $e^{i\phi_A t}$. The values correspond to the frequency of the single peak of the energy spectrum, which is computed via the numpy FFT package, We see that the approximations capture the frequency well in all cases.

We comment as we did in the previous test case, at the next order of the expansion, the approximation would be of the form $u_{app} = \epsilon^{\frac{1}{2}} e^{i\omega_0 t}(v_0 + \epsilon v_1)$. However, as we are in situation (β) of the Fredholm alternative demonstrated in (1.9), we cannot determine v_1 uniquely.

The phenomena of the saturation frequency's being well approximated and the saturation amplitude's not

being approximated well can be seen in other cases; notably, in the case of cylinder flow, where Sipp and Lebedev (2007) [92] use WNLE to determine saturation characteristics for cylinder flow whereas Carini et al. (2015) [21] use the method of Coullet and Spiegel (1983) [30] that is based on normal form theory. In the literature review, we perform numerical experiments on the CnsaGL to theorise why this is the case. We save these for the literature review, as it requires a notion of transient growth that is built up in the literature review. We expect these results extend to the linearised Navier-Stokes operator but this needs to be confirmed by numerical experiments.

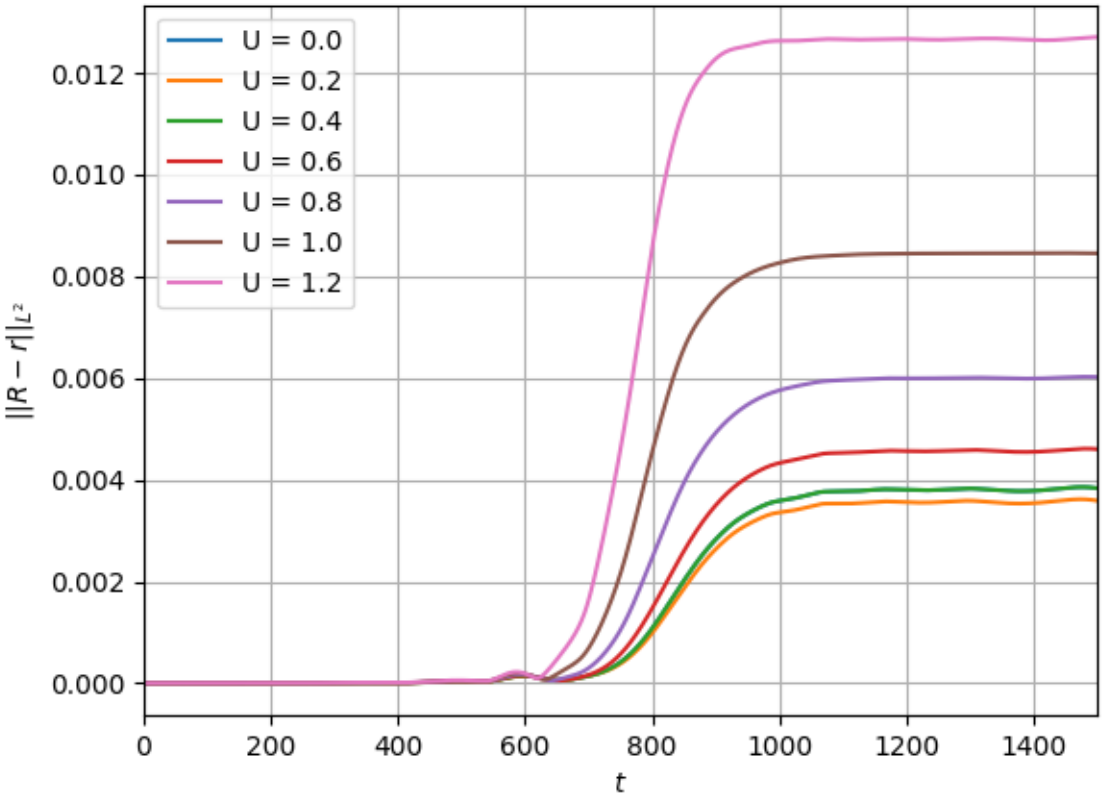

Figure 2. A plot of various $||R - r||_{L^2}$ for various values of U shown in plot, with $\delta = 0.01$.

Frequency (Hz)	U						
	0.0	0.2	0.4	0.6	0.8	1.0	1.2
$e^{i\phi_A t}$	0.006	0.0004	0	-0.006	-0.0014	-0.0022	-0.0032
u	0.006	0.0004	0	-0.006	-0.0014	-0.0022	-0.0032

Table 1. A table of the frequencies in Hz corresponding to the single peak (as there is only one frequency) of the energy spectrum of u and $e^{i\phi_A t}$. The values of u are shown in plot with $\delta = 0.01$

1.3 Literature Review

In order to provide a mathematical description of Fluid Mechanics, different approaches have been taken. In our exploration of the issues with WNLE, we have notably connected different aspects of different linear descriptions together. Therefore, to understand the relevance of this thesis, not only as a presentation of new results, but, also as a pedagogical resource, it is important to understand what these linear approaches entail. The method WNLE is one of many "nonlinear" approaches, and, as the thesis is focused on trying to improve this method, we have not considered any of the other nonlinear methods. Examples of nonlinear approaches include the use of Lyapunov functions to establish the stability of nonlinear systems; this removes the problem of the loss of information as a result of linearisation. However, for us, the loss of information is exactly the issue we study.

We have therefore divided the literature review intro two sections to facilitate this; "The Mathematics of Linear Approaches" and "Examples of Amplitude Equations in Fluid Mechanics and Elsewhere". The first section brings together the mathematics of linear approaches as the title would suggest, whereas the second section evaluates the approaches that other authors have taken to deal with the loss of information demonstrated in the previous section. The latter section also considers the following amplitude equation given by equation

$$\frac{dB}{dt} = \delta B - \lambda^1 |B|^2 B \tag{1.30}$$

which is historical, (1.30) was firstly derived by Landau in the 1940s but with the form of the constant λ^1 not explicitly derived. In the 1960s, in the midst of new computational power, attempts were made to fit these coefficients for various fluid flows, but the fitting only worked in the linear regime for very small δ. In this thesis, we build notions as to why this is the case.

1.3.1 The Mathematics of Linear Approaches

The Linear Approaches to Fluid Mechanics problems loosely fit into three categories, the Local Framework, the Global Framework and the Non-modal Framework. Each of these categories align themselves with a different mathematical object namely Green's functions, Resolvent Operators and Eigenvalues. How these objects are connected together is how the different descriptions are connected together. The reader may find it helpful to consider Figure 1, where we have drawn a diagram that gives the framework and the corresponding mathematical objects the various approaches and connects them together. In the following points, we elabourate on each of these approaches, citing important works and definitions. Afterwards, we discuss how these objects are mathematically connected together.

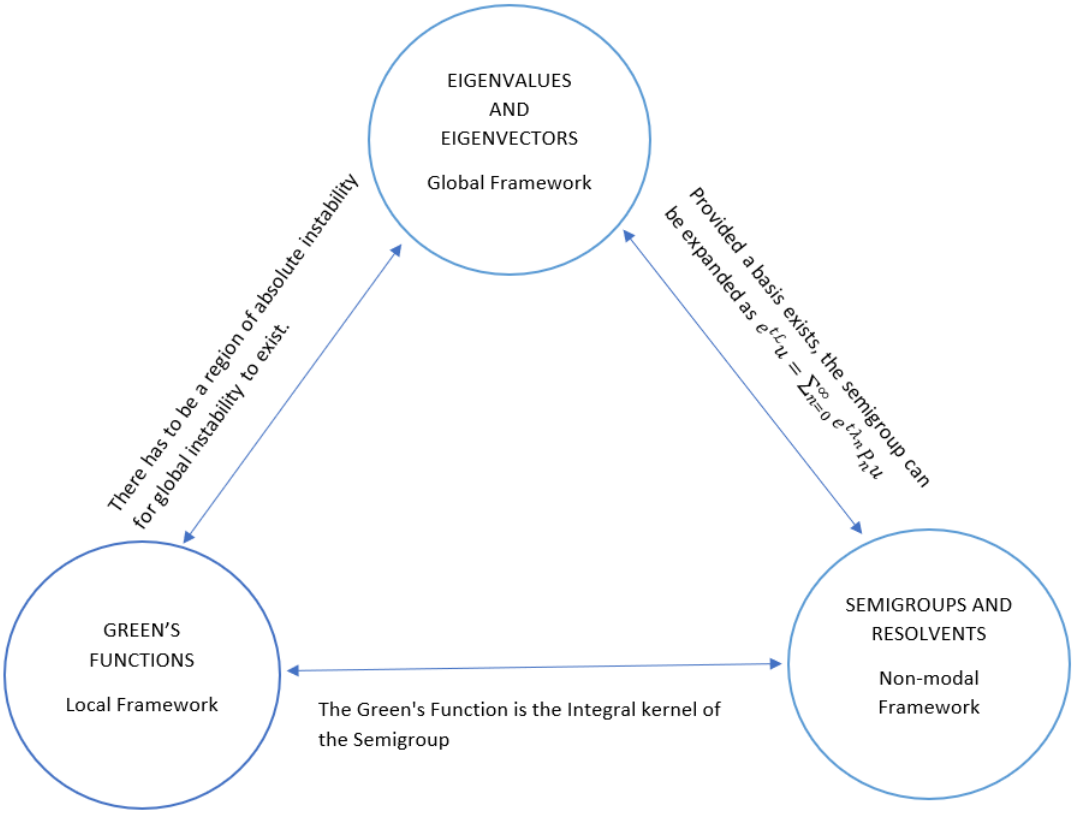

Figure 1. A pictorial representation of how different mathematical approaches to Fluid Mechanics, namely the global approach, the local approach and the non-modal approach connect together.

- The Local Framework The local framework considers whether or not flows are absolutely or convectively unstable. We present the definitions of absolute and convective stability from the review article by Huerre and Monkevitz (1990) [54]. These definitions, as remarked by Huerre and Monkevitz, originated in Plasma physics before finding more general application (see Landau and Lifshitz (1954, 1959) [62, 63]). For these definitions, we need the following reference equation

$$\left(\frac{\partial}{\partial t} - \mathcal{L}\right) u = 0, \tag{1.31}$$

with initial condition $u(t = 0) = u_0$. $\mathcal{L}$ is a linear operator, t is time and u is the unknown. The equation corresponding to the Green's function $G(x, t)$ on to the operator on the left-hand-side of (1.31) is given by

$$\left(\frac{\partial}{\partial t} - \mathcal{L}\right) G(x, t) = \delta(t)\delta(x) \tag{1.32}$$

where δ is the Dirac delta function.

The basic flow described by u is said to be

  - *linearly stable* if $\lim_{t\to\infty} G(x, t) \longrightarrow 0$ along rays $\frac{x}{t} = constant$,
  - *linearly unstable* if $\lim_{t\to\infty} G(x, t) \longrightarrow \infty$ along at least one ray $\frac{x}{t} = constant$.

From the linearly unstable flows, there are two types of impulse response. The basic flow is said to be

- *absolutely unstable* if $\lim_{t\to\infty} G(x,t) \longrightarrow \infty$ along the ray $\frac{x}{t} = 0$,
- *convectively unstable* if $\lim_{t\to\infty} G(x,t) \longrightarrow 0$ along the ray $\frac{x}{t} = 0$.

These are local phenomena as they are based on the behaviour along the ray $\frac{x}{t}$. They can be contrasted with the definition of global stability; the flow described by u is said to be

- *globally unstable* if $\lim_{t\to\infty} G(x,t) \longrightarrow \infty$ for some x.

For illustration, we give the following diagrams from the book in Figure 2 by Schmid and Henningson (2002) [83] that depict absolute and convective instability.

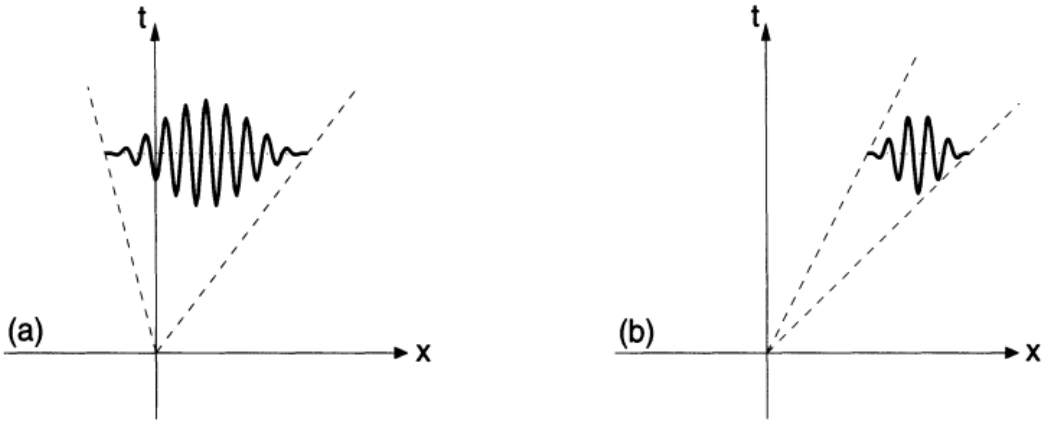

Figure 2. From Schmid and Henningson (2002), two diagrams illustrating absolute (left) and convective instability (right). The impulse was applied at the origin of the $(x-t)$ diagram.

These definitions allow us to describe a flow through the impulse response of the governing linear operator. Furthermore, there are tools available that enable us see whether a flow described by the dispersion relation (1.31) is absolutely or convectively unstable. We invite the reader to consult the book by Schmid and Henningson (2002) [83], which gives a detailed explanation of the Briggs Method. Briggs (1964) [20] developed the method of categorising instabilities via complex analysis originally for plasma physics. In order to apply the Briggs criterion, the problem (1.31) must be considered in $(k-\omega)$-space, which is achievable via Laplace and Fourier transforms.

In the local framework, we have the restriction that the impulse occurred at precise point x. When one considers parallel flows, this is not a problem as the linear operator $\mathcal{L}$ does not change with respect to x. For non-parallel flows, we can circumvent this problem by calculating the Green's function at each position s. Now,

for a spatially-varying operator, i.e. an operator with a well potential, we solve the following equation;

$$\left(\frac{\partial}{\partial t} - \mathcal{L}\right) G(x, s, t) = \delta(x - s)\delta(t). \tag{1.33}$$

By using this approach, In Chomaz (1991) [26], demonstrated the necessary condition that, in order for global instability to occur, there has to be a finite region of absolute instability. This condition was established using WKB theory, see Schmid and Henningson (2002) [83] for more details.

- The Global Approach Let the solution of (1.31) be decomposed as $u = e^{\lambda t}\hat{u}$. We then obtain the following eigenvalue equation for $\hat{u}$.

$$\lambda \hat{u} = \mathcal{L}\hat{u} \tag{1.34}$$

This equation has multiple solutions that we will label $\hat{u} = \hat{u}_n$ for corresponding $\lambda = \lambda_n$. If any of the λ_n are such that $\Re\{\lambda_n\} > 0$, the solution then the solution u grows in time. This definition coincides with the definition of a globally unstable flow that we defined in the last section. We will demonstrate this after giving a summary of each approach.

This kind of linear stability analysis has a rather old basis that can be traced back to Poincaré's work "On the Curves defined by Differential Equations" (in French "Mémoire sur les courbes définies par une équation différentielle") (1882) [77]. In this work, he developed the field known as "the qualitative study of differential equations". That being said, efficient numerical calculation of the spectrum of two-dimensional and three-dimensional systems continues to be a dynamic area of research. The author invites the reader to consider the review article by Theofilus (2011) [96]. Furthermore, for the Navier-Stokes equations, there is the problem of establishing the appropriate form form of $\mathcal{L}$ such that a change of parameter leads to the flow becoming globally unstable. This issue is discussed in the beginning of the article by Sipp and Lebedev [92] in the context of whether $\mathcal{L}$ should be taken as the linearisation of the Navier-Stokes operator around the base flow or mean flow.

- The Non-modal Approach The non-modal framework is characterised by considering the norm of the matrix exponential $||e^{t\mathcal{L}}||$. This quantity can be interpreted as the maximum response over all initial conditions, but also coincides with the definition of the semigroup of a linear operator $\mathcal{L}$. We will discuss this more when we build the connections between these approaches. For a Fourier transformed system one can consider the maximum frequency response that is given by the norm of the operator $(i\omega - \mathcal{L})^{-1}$. Studying this quantity for various values of ω is at the heart of the field called "Resolvent Analysis". The purpose of this non-modal framework is to identify the transient growth of a system. The eigenvalues of a system provide the asymptotic nature but may not capture the bump before decaying. The reader is invited to consider the article by Schmid [82] for a passionate review of this subject explicitly arguing against the eigenvalue-based approach that we

described in the last section.

We demonstrate the phenomenon of transient growth via the RnsaGL before relating this to the idea of pseudospectra. In Figure 3, we plot the norm of the semigroup $||e^{t(\mathcal{L}^{RGL}+\delta)}||_{L^2}$ for the critical case ($\delta = 0$) and sub-critical case ($\delta = -0.01$) for two values of U; we choose $U = 0$ (the self-adjoint case) in Figure 3a and $U = 1$ in the non-self-adjoint case (Figure 3b) respectively. We compute this matrix exponential using the "expm" function in the NumPy package in Python. Note that in both of these cases, $||e^{t\mathcal{L}}||_{L^2}$ is not divergent, so they are globally stable.

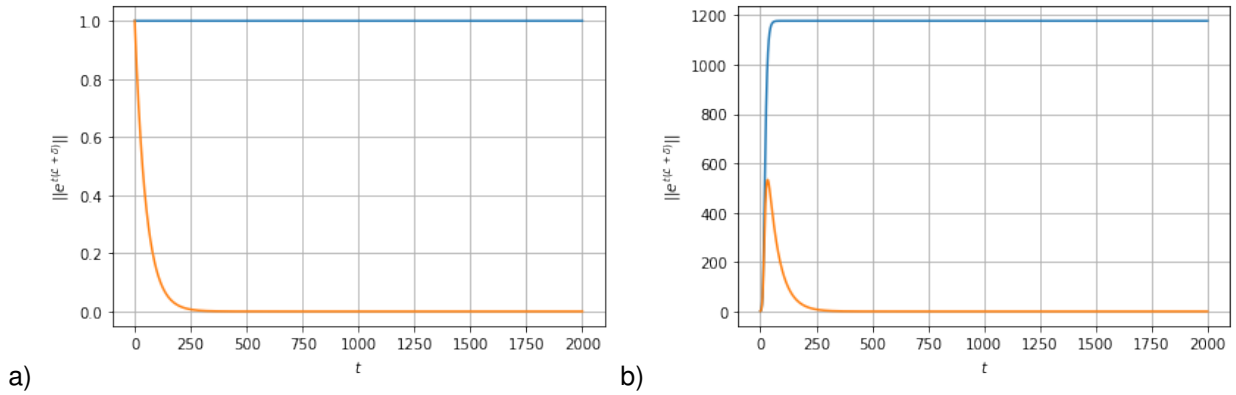

a) b)

Figure 3. The L^2 norm of $||e^{t(\mathcal{L}^{RGL}+\delta)}||$ for a) $U = 0$ (left) and b) $U = 1$ right respectively. In both figures, the orange lines represent the case where $\delta = -0.01$ and the blue lines represent the case $\delta = 0$.

We notice that the "bump" only occurs in the non-self-adjoint case and also that the semigroup bound is much larger. The physical interpretation of this is that the impulse excites the non-orthogonal modes, which forms a wave packet or "bump" that eventually decay. For the full equation with the nonlinearity, this bump interacts with the zeroth eigenvector via the non-linearity. In the self-adjoint case, there is no wave packet to interact with the global mode hence the solution is predominantly the spatial development of the leading eigenvector. The Figures 1 and 2 in the previous section (Section 1.3) showcase this property.

One can estimate the size of the bump shown in Figure 3a using pseudospectra; the definition of the pseudospectra is given as follows

– Definition (ϵ-pseudospectra). Let $\mathcal{L}$ be a closed operator and let $\epsilon > 0$ be arbitrary. The ϵ- pseudospectra is the set of $z \in \mathbb{C}$ defined by

$$||(z - \mathcal{L})^{-1}|| \geq \epsilon^{-1}. \tag{1.35}$$

Sometimes, the "ϵ" is dropped in the nomenclature and we refer to this as simply "pseudospectra".

The pseudospectra is connected to the norm of the semigroup $e^{t\mathcal{L}}$ using the theorems in Chapter 4 in the book "Spectra and Pseudospectra" by Trefethen and Embree (2005). A consequence of these theorems can

be seen in Schmid (2007) [82], where the so-called “Kreiss Constant” is used to give a lower bound on the norm of the semigroup

Computing the norm of the semigroup is non-self-adjoint cases more time-intensive, especially for multi-dimensional systems in Fluid Mechanics. For self-adjoint operators, the L^2-norm is given by $||e^{t\mathcal{L}}||_{L^2} = e^{\lambda_0 t}$ where λ_0 is the biggest eigenvalue (E. B. Davies [33]). Hence, in the critical case we get $||e^{t(\mathcal{L}+\delta)}||_{L^2} = 1$ and the sub-critical case, we get $||e^{t(\mathcal{L}+\delta)}||_{L^2} = e^{-0.01t}$. In Cossu and Chomaz (1997) [28], similar plots are made for their linear operator [28], which is similar to the CnsaGL but without the quality of remaining at criticality for any advection velocity. Their plots however were done with respect to the supremum norm and they relied on Hunt’s form of the Green’s function to calculate the semigroup norm. The author believes the choice of norm may have been a result of the computational power available.

Non-modal theory, particularly regarding pseudospectra, has been developed further in the field of Non-Hermitian Quantum Mechanics. The link between this work and Fluid Mechanics can be seen from the point of view that the $\mathcal{L}^{RGL}$ and $\mathcal{L}^{CGL}$ can be recast in the following way

$$\mathcal{L} := \bigg(-i\frac{d}{dx} + a \bigg)^2 + bx^2 \tag{1.36}$$

where a and b are constants. This is can be recognised as a Schödinger operator. In particular with a and b to be purely real, the quantum-mechanics interpretation of (self-adjoint) $\mathcal{L}$ would be that of an electron interacting with the magnetic field of vector potential a and a harmonic-oscillator electric field of frequency b. In the paper Krejčiřík et al. (2015) [61], theorems were derived that allowed us to extract basis properties from the pseudospectra of operators with a compact resolvent. It is meaningful to define what a Quasi-Hermitian operator as well as give the theorems that relate the pseudospectra to the basis properties, as we can consider the early Fluid Mechanics paper by Reddy et al. (1993) [79] where the pseudospectra for the Orr-Sommerfeld operator was computed.

We firstly define a Quasi-Hermitian operator and a Riesz basis:

– Definition (Quasi-Hermitian Operator). Let $\mathcal{H}$ be a Hilbert Space and $\mathcal{L}$, if there exists a positive operator G such that for an operator $\mathcal{L}$

$$\mathcal{L}^\dagger G = G\mathcal{L}, \tag{1.37}$$

where G is a positive operator called a metric operator where $\mathcal{L}^\dagger$ denotes the adjoint in the Hilbert space $\mathcal{H}$. The operator is said to be Quasi-Hermitian.

– Definition (Riesz or Unconditional Basis, as given in [61]). Let $\mathcal{H}$ be a Hilbert Space. Let $\{e_n\}_{k=0}^{\infty}$ be a collection of functions, normalised to 1 in $\mathcal{H}$. $\{e_n\}_{k=0}^{\infty}$ is a Riesz or unconditional basis if it forms a basis

and for all functions $\phi \in X$ the inequality

$$C^{-1}||\phi||^2 \leq \sum_{k=1}^{\infty} |\langle e_n, \phi \rangle|^2 \leq C||\phi||^2. \tag{1.38}$$

The Riesz basis ensures that all projections onto the collection of vectors are bounded, which is very powerful for practical applications. Other notions of bases, such as the Abel-Lidskii basis are looser, often requiring only completeness and are not as useful in practical applications. The following theorem connects the Riesz basis to the existence of the metric operator;

– Theorem (Riesz Basis if and only if Bounded Metric Operator with Bounded Inverse). Let $\mathcal{L}$ be an operator with a compact resolvent in a Hilbert space $\mathcal{H}$. Then the eigenvectors of $\mathcal{L}$ form a Riesz basis if and only if $\mathcal{L}$ is Quasi-Hermitian and possesses a bounded and boundedly-invertible metric operator.
Proof. See Proposition 4 in Krejčiřík et al. (2015) [61]. □

We can use this theorem in conjunction with the following definition of "trivial pseudospectra" and the following theorem that connects the quasi-hermiticity of the operator with implications about the pseudospectra.

– Definition (Trivial Pseudospectra). We say that the pseudo-spectrum of $\mathcal{L}$ is trivial if there exists a fixed constant C such that, for all $\epsilon > 0$,

$$\sigma_\epsilon(\mathcal{L}) \subseteq \{z \in \mathbb{C} | \text{ dist}(z, \sigma(\mathcal{L})) < C\epsilon\}. \tag{1.39}$$

– Theorem (Quasi-Hermitian Implications for Pseudospectra). Let H be quasi-Hermitian with a positive, bounded and boundedly-invertible metric. Then the pseudospectrum of H is trivial.
Proof. See Proposition 3 in Krejčiřík et al. (2015) [61]. □

In Reddy et al. (1993) [79] the pseudospectra was used to estimate the size of the transient growth using methods described earlier in this section. Furthermore, it was reinforced that the a sufficient condition for no transient growth is that the numerical range of the linear operator is restricted to the left half plane - this was established as the extension of the Hille-Yosida Theorem. In Figure 4, we give the pseudospectra plots [74] for the Orr-Sommerfeld operator, $\mathcal{L}_{OS}$ as well as the Davies Oscillator $\mathcal{L}_D$ (these operators are shown in shot) that were given in the talk by Novák (2015) [74]. The former demonstrates an operator with trivial pseudospectra and the latter demonstrates an operator with non-trivial pseudospectra. In Reddy et al. (1993) [79], the projection coefficients, $\langle e_n, \phi \rangle$ in (1.39), were calculated and found to be large.

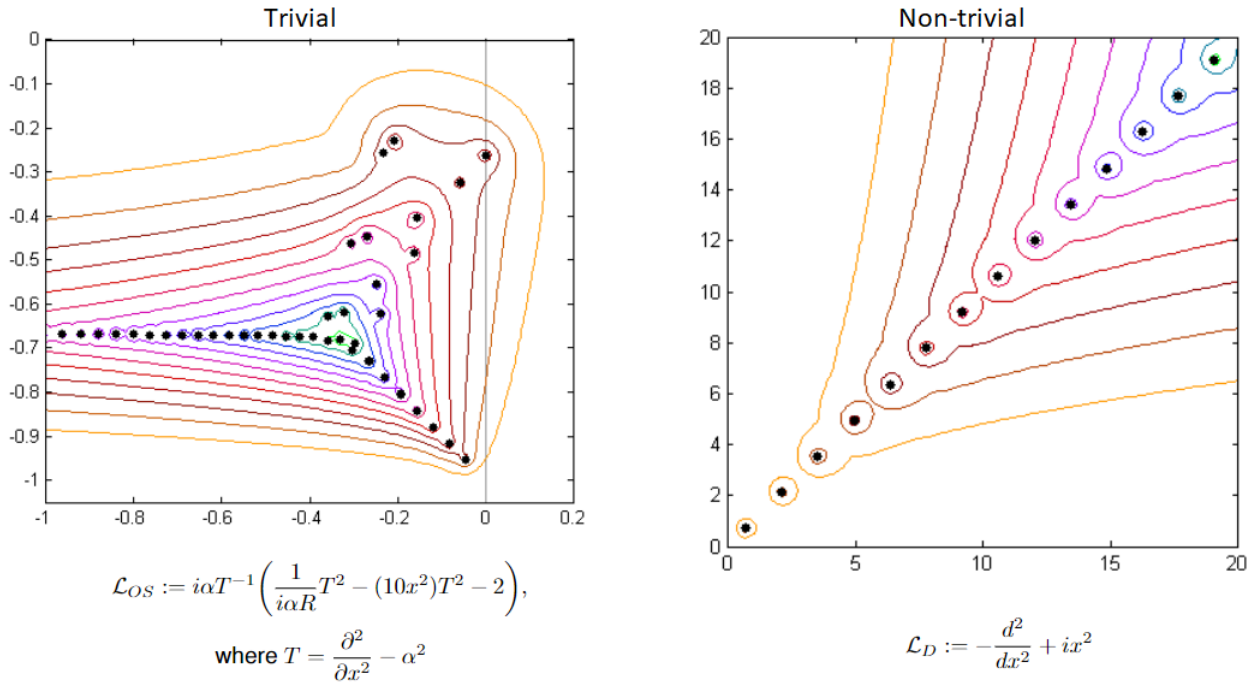

Figure 4. Plots of the pseudospectra given in the talk by Novák [74]. The scale of the contour lines are on a logarithmic scale (orange to green) from -8 to -2 in increments of 0.5.

This demonstrates how we can use the above theorems, namely solely in the reverse implication. From the computations regarding the Davies operator, one visualise what seems to be non-trivial pseudospectra. Often, the non-triviality of pseudospectra can be proven rigorously using semi-classical analysis and defining the pseudomodes when the structure of the eigenmodes cannot be easily deduced - the reader is invited to see Davies (2004) et al. [35], Dencker at al. (2003) [37] and Krejčiřík et al. (2015) [61]. Many examples concerning non-trivial pseudospectra are centred around the imaginary cubic oscillator, which has a complete set of eigenvectors which do not form a Riesz basis; this can be established via the non-existence of trivial pseudospectra. In contrast, we cannot determine the existence of a Riesz basis from the existence of trivial pseudospectra, hence we cannot assume the eigenvectors of the Orr-Sommerfeld operator form a Riesz basis. One can circumvent this problem by considering the metric operator directly, but establishing the form of the metric operator is a highly non-trivial task. The interested reader is invited to consider Ergun (2013) [42] that provides examples about how to establish the metric operator in particular cases. The reader is also invited to consider the works of Shubov (1996, 2016, 2017, 2020) [87, 88, 89, 90], who looks at the basis properties for mechanical systems including flutter, damped waves and energy harvesting.

We now relate these approaches together by considering the mathematical objects. We take special care to emphasize where the non-normality creates difficulty. We will first describe these relationships with words before

describing them mathematically. The Global Framework is related to the Local Framework by considering the eigenvector expansion of the green's function. This connection only requires that the eigenvectors are complete. As previously discussed, some notions of basis only require completeness, and these bases sometimes are not appropriate for expanding the functions in. The connection between the Global Framework and the Non-modal Framework can be observed particularly with self-adjoint operators when considering the L^2-norm of the semigroup is $||e^{t\mathcal{L}}||_{L^2} = e^{\lambda_0 t}$ where λ_0 is the biggest eigenvalue (E. B. Davies [33]). Thus in the self-adjoint case, the leading eigenvector captures everything from the initial growth, to the transient growth as well as the asymptotic behaviour. These three things are strongly differentiated in the non-self-adjoint case. The Non-modal Framework and the Local Framework are connected by considering the relationship between Green's function and semigroup.

Now, let us recreate these relationships mathematically. We firstly consider the eigenvalue equation

$$\mathcal{L}e_n(x) = \lambda_n e_n(x) \tag{1.40}$$

where $\{e_n\}_{n=0}^{\infty}$ are the eigenvectors of $\mathcal{L}$ form a complete set and $\{\lambda_n\}_{n=0}^{\infty}$ are the constant corresponding constant eigenvalues. Now consider the eigenvalue equation for L^2-adjoint of $\mathcal{L}$,

$$\mathcal{L}^{\dagger}e_n^{\dagger}(x) = \lambda_n^{\dagger}e_n^{\dagger}(x) \tag{1.41}$$

where $\{e_n^{\dagger}\}_{n=0}^{\infty}$ are the adjoint eigenvectors of $\mathcal{L}^{\dagger}$, which also form a complete set, and $\{\lambda_n^{\dagger}\}_{n=0}^{\infty}$ are the corresponding constant eigenvalues. We have that $(\lambda_n)^* = \lambda^{\dagger}$ where $*$ denotes the complex conjugate. We assume that $\{e_n\}_{n=0}^{\infty}$ and $\{e_n^{\dagger}\}_{n=0}$ are bi-orthonormal to each other such that $\langle e_m^{\dagger}, e_n\rangle = \delta_{nm}$. Therefore, considering the expansion of u into (1.31) into amplitude-eigenvectors pairs $\sum_{n=0}^{\infty} a_n e_n$. We then get the following equation

$$\sum_{n=0}^{\infty} e_n \frac{da_n}{dt} = \sum_{n=0}^{\infty} \lambda_n a_n e_n. \tag{1.42}$$

We take the inner product of (1.42) with each $e_n^{\dagger}$ in order to get the infinite-dimensional dynamical system,

$$\frac{da_n}{dt} = \lambda_n a_n, \tag{1.43}$$

which should be solved with appropriate initial conditions, i.e $a_n(t=0) = \langle \hat{e}_n^{\dagger}, u_0\rangle$, thus $u_0 = \sum_{n=0}^{\infty} a_n(t=0)e_n$. Thus, the solution of (1.31) can be written as

$$u = \sum_{n=0}^{\infty} e^{\lambda_n t} \underbrace{a_n(t=0)e_n(x)}_{u_0} = \int_{s_1}^{s_2} G(s,x,t) \underbrace{a_n(t=0)e_n(s)}_{u_0} ds \tag{1.44}$$

where the Green's function is given by $G(x,s,t) = \sum_{n=0}^{\infty} e^{\lambda_n t} e_n^{\dagger}(s)e_n(x)$ (s_1 and s_2 are the endpoints of the boundary

(in the case of the RnsaGl and CnsaGL will be $s_1 = -\infty$ and $s_2 = \infty$). In this way, we have related the Global Framework and the Local Framework together.

In order to relate the Global Framework to the non-modal approach one recognises that, provided the eigenvectors form a complete set,

$$e^{t\mathcal{L}} = \sum_{n=0}^{\infty} e^{\lambda_n t} P_n \tag{1.45}$$

where P_n is the projection operator onto each eigenvector of $\mathcal{L}$ and λ_n are the eigenvalues of $\mathcal{L}$. In this case, it is clear as to why an eigenvalue with positive real part equates to global instability. However, the additional difficulty comes from the fact that completeness is not enough to ensure that the projection operators are bounded. One needs a stronger notion of a basis that ensures the projection operators are bounded. The non-modal approach relies on different representations of the semigroup $e^{t\mathcal{L}}$ when the projection operators are unbounded; these include the same formula one uses for matrix exponentials when the linear operator is a bounded operator

$$e^{ta} u_0 = e^{tA} u_0 = e^{t\mathcal{L}} u_0 = \sum_{n=0}^{\infty} \frac{t^n}{n!} \mathcal{L}^n. \tag{1.46}$$

and also the Cauchy integral formula which works in the case of unbounded operator

$$e^{t\mathcal{L}} = \frac{1}{2\pi i} \int_{+\partial U} e^{\lambda t} R(\lambda, \mathcal{L}) d\lambda \tag{1.47}$$

where $R(\lambda, \mathcal{L}) = (\lambda - \mathcal{L})^{-1}$ is the resolvent operator for $\lambda \notin \sigma(\mathcal{L})$ where $\sigma(\mathcal{L})$ is the spectrum of $\mathcal{L}$ containing the eigenvalues λ_n. For a full discussion of formulas through which the evolution operator $e^{t\mathcal{L}}$ can be expressed, the author suggests Section II.3.3 of the book "One parameter evolution semigroups for Linear Evolution Equations" by Engel and Nagel (2000) [41]. In this way, the global approach and the non-modal approach are connected together.

Lastly, we related the non-modal approach and the local approach together. This is done by recognising that the Green's function $G(x, s, t)$ is the integral kernel of the semigroup $e^{t\mathcal{L}}$, i.e.

$$e^{t\mathcal{L}} u = \int_{s_1}^{s_2} G(x, s, t) u(s) ds. \tag{1.48}$$

One can also see this from (1.44). As an example of the intersection between the different frameworks , we can consider Cossu and Chomaz (1997) [28]. In Cossu and Chomaz (1997) [28], the global instability of a Ginzburg-Landau operator (this was the same as the CnsaGL up to constants) was inferred from local properties by considering the Green's function, $G(x, s, t)$ on each point of the domain. In this way, they essentially reconstituted the Green's function on the right-hand-side of (1.48) and then considered the following norm

$$||e^{\mathcal{L}t}||_{\infty} = \sup_{-\infty \leq x \leq \infty} \int_{\infty}^{\infty} |G(x, s, t)| ds. \tag{1.49}$$

They did not refer to the operator on the left-hand-side of (1.49) as a semigroup but instead an evolution operator. Global instability was then corresponds to the divergence of $||e^{\mathcal{L}t}||_\infty$. However, this technique of establishing global instability via Green's functions is not universal and the existence of the Green's function for a non-self-adjoint operator was specific to the case chosen in Cossu and Chomaz (1997) [28]. In Cossu and Chomaz (1997) [28], the form of the Green's function was deduced by Hunt and Crighton (1991) [55] using perturbation theory. Having an analytical form for the Green's function is somewhat unusual for operators in Fluid Mechanics, but this is precisely why it was an elucidating test case.

In the author's opinion, it is better to redefine global instability as when the quantity $e^{t\mathcal{L}}$ diverges. This is more harmonious and does not force the definition of a Green's function when there does not exist a Green's function as the integral kernel of $e^{t\mathcal{L}}$. The difficulty is as $e^{t\mathcal{L}}$ is an operator it has to be measured in terms of norm, so it is possible that the quantity $||e^{t\mathcal{L}}||$ may be divergent in norms like the supremum norm or energy norm, but may be convergent in more *exotic* norms.

Interestingly, we obtain the Green's function derived by Hunt (1991) [55] by considering the eigenvalue expansion as he does using perturbation theory. This exemplifies that often the definition of a basis can be adapted to fit for a purpose, i.e. completeness for defining a Green's function, but something stronger such as a Riesz basis for expanding an arbitrary function in the eigenvectors. We demonstrate this in the following derivation. For references on the construction of Green's function of eigenvector expansions, the reader is invited to consider Dolph (1961) [39], Greenlee (1982) [50] and Friedman and Mishoe (1956) [46].

- Derivation of Green's Function for CnsaGL.

  Recall the linear operator from the CnsaGL;

$$\mathcal{L}^{CGL} = (1-i)\frac{\partial^2}{\partial x^2} - (U+0.2i)\frac{\partial}{\partial x} + \left[C_1 + \frac{1}{8}(U^2 - 0.4U - 0.04)\right] - c_2 x^2 \tag{1.50}$$

  where $C_1 = \Re\{(1-i)c_2\}$.

  The eigenfunctions and eigenvalues of $\mathcal{L}^{CGL}$ are given by

$$e_n = \exp\{-\frac{1}{4}(\alpha_1 x)^2 + \alpha_2 x\} He_n(\alpha_1 x) \quad \text{and} \quad \lambda_n = -(1+2n)\sqrt{(1-i)c_2} - i\frac{\left[U^2 + 0.4U - 0.04\right]}{8} + C_1 \tag{1.51}$$

  where $He_n(\alpha_1 x)$ are Probabilists' Hermite polynomials where $\alpha_1 = (\frac{4c_2}{1-i})^{\frac{1}{4}}$ and $\alpha_2 = \frac{U+0.2i}{2(1-i)}$.

  We denote the L^2-adjoint linear operator of $\mathcal{L}^{CGL}$ by $(\mathcal{L}^{CGL})^\dagger$. $(\mathcal{L}^{CGL})^\dagger$ and its eigenvectors $\{e_n^\dagger\}_{n=0}^\infty$ are given by

$$(\mathcal{L}^{CGL})^\dagger = (1+i)\frac{\partial^2}{\partial x^2} + (U-0.2i)\frac{\partial}{\partial x} + \left[C_1 + \frac{1}{8}(U^2 - 0.4U - 0.04)\right] \quad \text{and} \quad e_n^\dagger = \exp\{-\frac{1}{4}(\beta_1 x^2) - \beta_2 x\} He_n(\beta_1 x) \tag{1.52}$$

where $\beta_1 = \alpha_1^*$ and $\beta_2 = \alpha_2^*$ The eigenvalues of $\mathcal{L}^\dagger$ are the complex conjugates of λ_n, i.e. $\lambda_n^\dagger = (\lambda_n)^*$. We normalise the direct and adjoint eigenvectors such that $\langle \hat{e}_m^\dagger, \hat{e}_n \rangle = \tilde{\delta}_n$, where $\langle \cdot, \cdot \rangle$ is the L^2-inner product on the real line, i.e. for $\langle f, g \rangle = \int_{-\infty}^{\infty} \bar{f} g dx$ where the bar, $^-$, denotes complex conjugation[4], via the normalisation constant $\hat{e}_n = \frac{1}{Z_n} e_n$ and $\hat{e}^\dagger = \frac{1}{Z_n} e_n^\dagger$ where $Z_n = (\frac{n!\sqrt{2\pi}}{\alpha_1})^{\frac{1}{2}}$.

For the time-dependent operator $(\frac{\partial}{\partial t} - \mathcal{L}^{CGL})$, generating a set eigenvectors with a corresponding set of adjoint eigenvectors, the formula for the Green's function is given by [105]

$$G(x, s, t) = \sum_{n=0}^{\infty} e^{-\lambda_n t} (\bar{\hat{e}}_n^\dagger(s))(\hat{e}_n(x)). \tag{1.53}$$

$$G(x, s, t) = \sum_{n=0}^{\infty} e^{-\lambda_n t} \frac{\alpha_1}{n!\sqrt{2\pi}} He_n(\alpha_1 s) He_n(\alpha_1 x). \tag{1.54}$$

We rearrange this in the following way

$$G(x, s, t) = C \exp\{-\frac{\alpha_1^2}{4}(s^2 + x^2) + \alpha_2(x - s)\} \sum_{n=0}^{\infty} \frac{(e^{t\sqrt{4(1-i)c_2}})^n}{n!} He_n(\alpha_1 s) He_n(\alpha_1 x), \tag{1.55}$$

where the constant $C = \frac{\alpha_1}{\sqrt{2\pi}} \exp\{-\sqrt{(1-i)c_2} - \frac{i}{8}(U^2 + 0.4U - 0.04) + C_1\}$. Let $\rho(t) = e^{t\sqrt{4(1-i)c_2}}$. The application of Mehler's formula (1866) [66] gives the following

$$G(x, s, t) = \frac{C}{\sqrt{1 - \rho(t)^2}} \exp\left\{ \frac{1}{1 - \rho(t)^2} \left[-\frac{(\alpha_1)^2}{4}(s^2 + x^2)(1 + \rho^2(t)) + (\alpha_1)^2 \rho(t) xs + \alpha_2(x - s)(1 - \rho^2) \right] \right\}, \tag{1.56}$$

which is the same as the solution derived by Hunt (1991) [55] and used by Cossu and Chomaz (1997) [28].

Previously, we said that we would perform numerical experiments on the CnsaGL in order to showcase the phenomena of the saturation frequency's being well captured and the saturation amplitude's not being well captured. We have built up a notion of transient growth throughout this literature review, but now we hope to showcase it with this example. As previously stated, the pseudospectra and the semigroup are closely related. We will start by presenting plots of the pseudospectra for the operators $\mathcal{L}^{RGL}$ and $\mathcal{L}^{CGL}$ before going more in-depth on the complex case.

- Pseudospectra of $\mathcal{L}^{RGL}$ and $\mathcal{L}^{CGL}$. We plot the following pseudospectra for $\mathcal{L}^{RGL}$ and $\mathcal{L}^{CGL}$ in Figure 5 and Figure 6 respectively. Details of the numerics can be found in Appendix B. In all figures, the analytically-derived eigenvalues are in orange and the numerically derived eigenvalues are in blue. The grey areas indicate the positive real axis. We also note in all of our plots (apart from the self-adjoint case for the $\mathcal{L}^{RGL}$ when $U = 0$), we have spectral pollution, which is the difference between the analytical eigenvectors and the numerically

[4] We use two notations for complex conjugation, namely the bar $^-$ for functions and the $*$ for constants. Regarding spaces $*$ denotes the dual space.

computed eigenvectors. This is clear in Figure 5 and would be clear in Figure 6 if we showed a larger domain. A discussion of spectral pollution, which is a particular problem for non-self-adjoint operators, can be found in Aboud et al. (2020) [1]. Also, spectral pollution can also be a problem for certain classes of self-adjoint operators, the interested reader is directed toward the paper by Davies et al. (2004) [35].

In Figure 5, left, we see pseudospectra of $\mathcal{L}^{RGL}$ with $U = 0$, i.e. the self-adjoint case. We know for the RnsaGL when $U = 0$, we have a basis as the operator is self-adjoint, hence the pseudospectra is trivial. We would have to zoom in order to see the tubular neighbourhoods indicating trivial pseudospectra. We notice that in the cases of $U = 1$ and $U = 2$, the pseudospectra extends to the right-hand-side hence in these cases we see transient growth. For the case $U = 0$, we can see the smallest contour corresponding to 10^0 extending hence we cannot interpret transient growth from this.

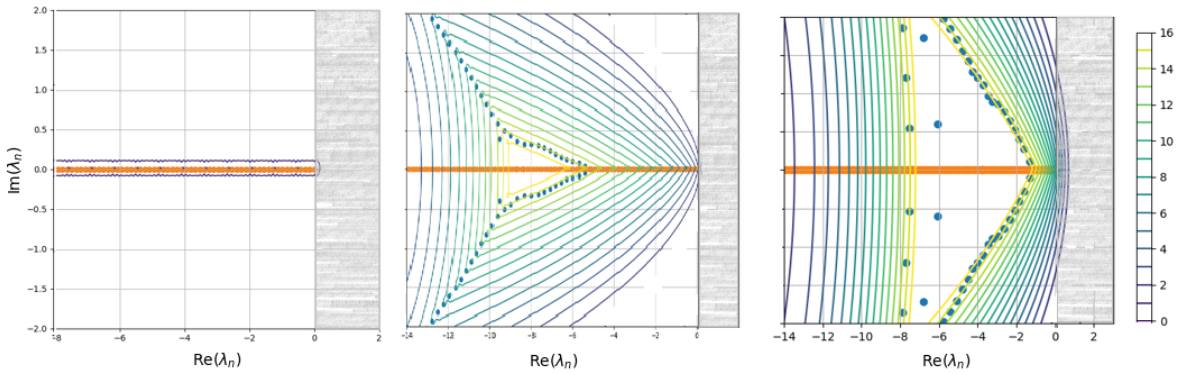

Figure 5. A plot the pseudospectra for the RnsaGL with $\delta = 0$ for $U = 0$ (left), $U = 1$ (center) and $U = 2$ (right). The contour plots are presented on a logarithmic scale with 10^0 being the smallest contour and 10^{16} being the largest contour. The analytical eigenvalues are in orange and the numerically derived eigenvalues are in blue. The grey areas indicate the positive real axis.

In Figure 6, left, we see pseudospectra of $\mathcal{L}^{CGL}$ with $U = 0$, i.e. the self-adjoint case. We know for the RnsaGL when $U = 0$, the operator is still not self-adjoint, but we see what we would call minimal transient growth. It is not clear that we have the tubular neighbourhoods as we had in the real case. For $U = 1$ and $U = 2$, the pseudospectra extends to the right-hand-side hence in these cases we see transient growth.

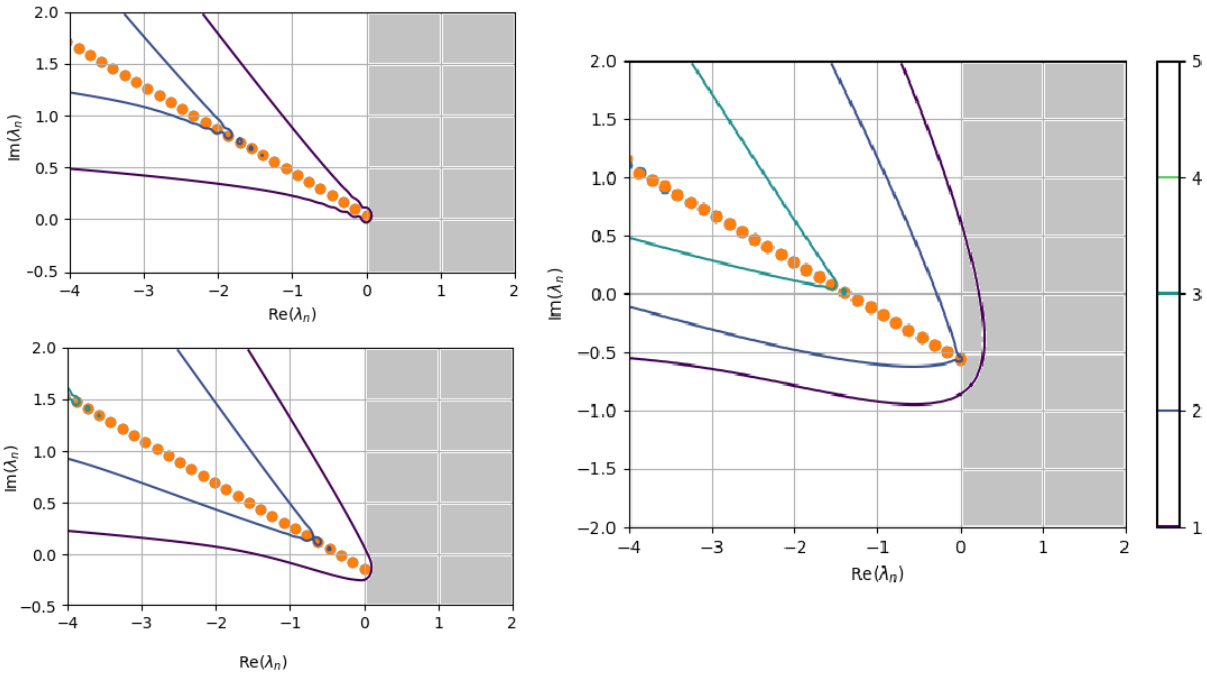

Figure 6. A plot the pseudospectra for the CnsaGL with $\delta = 0$ for $U = 0$ (top left), $U = 1$ (bottom left) and $U = 2$ (right). The contour plots are presented on a logarithmic scale with 10^1 being the smallest contour and 10^5 being the largest contour. The analytical eigenvalues are in orange and the numerically derived eigenvalues are in blue. The grey areas indicate positive real axis.

- Transient Growth of Amplitude but not Frequency for the CnsaGL We let $u = Re^{i\Phi}$ in the CnsaGL, separating the equation into the real and imaginary parts gives the following two equations

$$\frac{\partial R}{\partial t} = \mathcal{L}_R R - \mathcal{N}_R(R, \Phi) + \delta R \tag{1.57}$$

and

$$\frac{\partial \Phi}{\partial t} = \mathcal{L}_\Phi \Phi - \mathcal{N}_\Phi(R, \Phi) \tag{1.58}$$

where

$$\mathcal{L}_R = \frac{\partial^2}{\partial x^2} - U\frac{\partial}{\partial x} + \left[C_1 + \frac{1}{8}(U^2 - 0.4U - 0.04)\right] - c_2 x^2 \quad \text{and} \quad \mathcal{L}_\Phi = \frac{\partial^2}{\partial x^2} - U\frac{\partial}{\partial x}, \tag{1.59}$$

$$\mathcal{N}_R = 2\left(\frac{\partial R}{\partial x}\right)\left(\frac{\partial \Phi}{\partial x}\right) - R\left(\frac{\partial \Phi}{\partial x}\right)^2 + R\left(\frac{\partial^2 \Phi}{\partial x^2}\right) - R\left(\frac{\partial R}{\partial x}\right) - 0.2R\left(\frac{\partial \theta}{\partial x}\right) - R^3$$

and

$$\mathcal{N}_\Phi = -\frac{1}{R}\left(\frac{\partial^2 R(x,t)}{\partial x}\right) + \frac{2}{R}\left(\frac{\partial R}{\partial x}\right)\left(\frac{\partial \Phi}{\partial x}\right) + \left(\frac{\partial \Phi}{\partial x}\right)^2 + 0.2\frac{1}{R}\left(\frac{\partial R}{\partial x}\right).$$

We plot the matrix exponentials of $\mathcal{L}_R + \delta$ and $\mathcal{L}_\Phi + \delta$ in Figure 7 where $\delta = -0.01$. Again, we use a slightly

sub-critical operator to demonstrate transient growth. In Figure 4b, we still see transient growth which can be attributed to the superposition of non-orthogonal modes but it is only small. We notice also that with appropriate boundary conditions $\mathcal{L}_\Phi$ is sub-critical unlike $\mathcal{L}_R$.

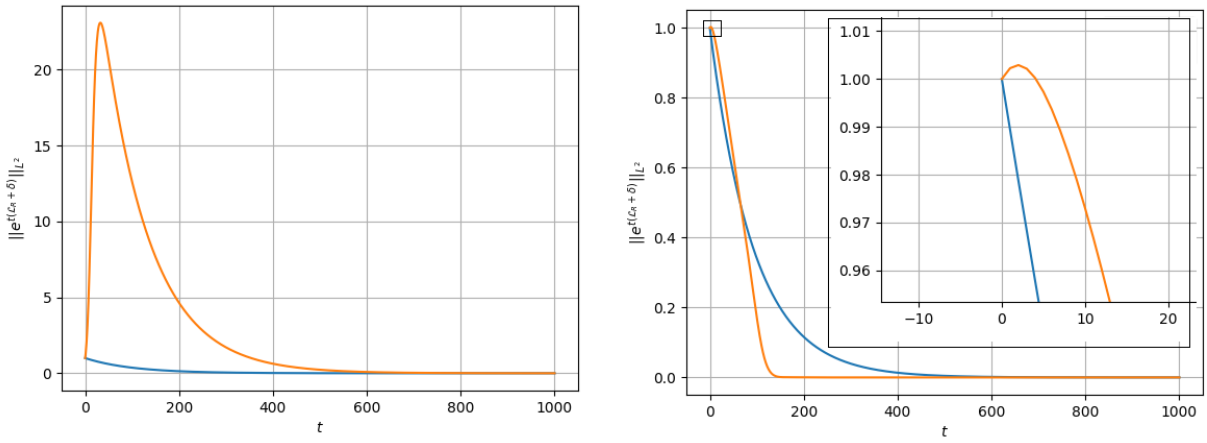

Figure 7. (Left) The L^2 norm of $||e^{t(\mathcal{L}_R+\delta)}||$ for a) $U=0$ (blue) and $U=1$ (orange). (Right) The L^2 norm of $||e^{t(\mathcal{L}_\Phi+\delta)}||$ for $U=0$ (blue) and $U=1$ (orange). The magnified figure is a zoomed view of what is in the box at in the top left-hand corner of the figure.

1.3.2 Examples of Amplitude Equations in Fluid Mechanics and Elsewhere

In this section, we look specifically at amplitude equations as approximations to partial differential equations. We begin with amplitude equations in Fluid Mechanics which takes us from Landau's research in the 1940s to applications of WNLE analysis in the last two decades. We then look at the approaches taken in other fields such as stochastic mathematics. We also consider the evaluation of amplitude equations via error bounds, in particular cases involving the Kuramoto-Sivashinsky equation and Swift-Hohenburg equation.

Landau (1945) [63] first described the amplitude of a single fluid instability using what we call the family Stuart-Landau equation. The starting point is a flow v, being decomposed as $v = v_0 + v_1$ where v_0 is a steady solution to the Navier-Stokes and v_1, is a small unsteady perturbation. By what is now classical argument, he showed that a small unsteady perturbation, v_1, could be written as

$$v_1 = A(t)f(x,y,z)$$

where $f(x,y,z)$ is a coherent structure. We have called $f(x,y,z)$ deliberately a coherent structure because the vocabulary of global modes was used later by Drazin [40] in 1974. $A(t)$ satisfies

$$\frac{dA}{dt} = \delta A(t) - \lambda^1 |A(t)|^2 A(t) \tag{1.60}$$

where δ is the distance to critical Reynolds number and λ^1 is known as the λ^1 constant or the "Landau" constant. Landau did not work out the value of the constant constant, but it was firstly derived by Stuart (1960) [93] for Poiseuille Flow. Numerical values of the λ^1-constant derived by Stuart were calculated by Reynolds and Potter (1967) [80] and Pekeris and Shkoller (1967) [76] who found that the amplitude equation was only valid for very small δ and for early times only[5]. In essence, this is similar to what we saw in the examples for the RnsaGL and CnsaGL in the last section (In Section 1.2, Figures 1 and 2 show that there is no difference in norm at early times between the solution of the RnsaGL and the CnsaGL and their respective first order approximations.). The amplitude equations approximated the solution well at early times.

It is for this reason that higher order approximations of the solution were sought. However, for higher order terms there were issues of non-uniqueness when determining the higher order spatial coefficients; again this corresponds how we had difficulty establishing v_1 in (1.14) and (1.23) in the RnsaGL and CnsaGL owing to being in situation β of the real and complex Fredholm alternative. Therefore, additional assumptions were needed to specify these coefficients. Herbert (1983) [52] circumvented the problem by introducing normalisation condition which ensured that the $A(t)$ took a particular value at a particular reference point. This idea was used by subsequent authors including Crouch (1993) [31] and Fujimura (1989) [47]. However, the higher order terms would differ depending on where the reference point was taken. In Watson (1960) [102], a way of obtaining higher order amplitude equations was introduced. This method was called the amplitude expansion method. The idea was with these new higher order amplitude equations, one could describe the coherent structure $f(x, y, z)$ more *elaborately* by having more terms of the form $|A|^{2m}A$ on the right-hand-side of (1.3.2) and therefore capture more of the flow. Fujimura (1989) [47] showed that higher order amplitude equations derived via WNLE coincide with amplitude equations made such as the amplitude expansion method (we demonstrate higher order amplitude equations made via WNLE in the next chapter). Fujimura (1991) [48] also showed that approximations obtained via WNLE coincide with those obtained through an application of centre manifold theory provided the disturbance amplitude is correctly defined in each setting. Additionally, Coullet and Spiegel (1983) used normal form theory to make higher order amplitude equations [30].

Three of these methods, namely the amplitude expansion method, WNLE and the method of Coullet and Spiegel, are conveniently connected together in later works by the same test case for cylinder flow. Sipp and Lebedev (2007) [92] successfully approximated the saturation frequency of the first bifurcation of a cylinder flow via WNLE with a first order expansion, but the saturation amplitude was underestimated. We should compare this to the transient growth analysis performed in the last section on the CnsaGL where we considered the linear operator concerning the frequency and the amplitude separately. We found that although non-self-adjoint, the transient growth was minimal unlike the operator for the amplitude. Carini et al. (2015) [21] used the method of Coullet and Spiegel (1983) [30], a method based on normal form theory, in order to derive a higher order amplitude expansion describing the flow past

[5] In this thesis, we do not consider a large range of parameters for δ, but we will show that error bounds that we derive increase with δ and U.

a circular cylinder as well as codimension-two bifurcation arising in the flow past two side-by-side circular cylinders. Concerning cylinder flow, the authors Sipp and Lebedev (2007) [92] and Carini et al. (2015) [21]) obtained the same first order amplitude equation, which, when contrasted with numerical experiments of Giannetti and Luchini (2007) [49], approximated well the dynamics at early times and not at saturation. Carini et al. (2015) explored the convergence of the terms in the higher order amplitude equation and it was found to be vanishingly small. The interpretation in this case was that the amplitude expansion was an asymptotic series as opposed to a convergent one, and hence an appropriate truncation of the series provides a good physical approximation. A non-coincidence at this point is the correspondence between the theoretical work of Sipp and Lebedev (2007) [92] and Carini et al. [21] (2015) and the numerical experiments of Giannetti and Luchini [49] is the same as the validity as the Stuart-Landau equation for Poiseuille flow, i.e. a slightly critical value of δ and only at early times. Again, we reason that the spatial development of the leading eigenvector approximates the early times well because the other modes have not been strongly mixed by the nonlinearity yet.

An important article is Chomaz (2005) [25], in which a Ginzburg-Landau equation exhibiting the same features as the CnsaGL (his version did not have the same constants to maintain the equation at criticality for any value of U). He established that "when the non-normality is strong, the bifurcation is abrupt and the weakly nonlinear analysis becomes invalid". He also noticed that if one forces the equation by adding a term such as $\epsilon f(x,t)$ to the right-hand-side of the CnsaGL, the forcing response was inversely proportional to the quantity $\langle e_0^\dagger, e_0 \rangle$. For the complex Ginzburg-Landau operator used in his equation, but also any operator where the non-normality manifests in the direct and adjoint eigenvectors moving further apart, this quantity becomes smaller as the parameter governing non-normality increases. He determined some physical consequences; the region where the direct and adjoint modes overlap, sometimes called the wave-maker region, is crucial for determining the global mode frequency. Therefore, the size of the spatial structures themselves[6] does not affect the resulting saturation amplitude.

As a response to the failure of weakly nonlinear analysis, in the same article (Chomaz (2005) [25]), the author considered the importance of "nonlinear global modes" and the adaptation of concepts like absolute and convective instability to the nonlinear setting. We give these definitions so that the reader can see that they are similar to the previous definitions, but the Green's function structure has been replaced by the fully-nonlinear response. These definitions were first introduced in Chomaz (1992) [24] and have since become part of the standard lexicon used by various authors considering nonlinear global modes, some of which we will discuss afterwards. Let a system at $t = 0$ be in the state s, we call this system the "basic state", we define the following;

- The basic state of system is *nonlinearly convective*, if for all initial perturbations of finite extent and finite amplitude, the system relaxes to the basic state everywhere in the laboratory frame.

- The basic state of a system is *nonlinear absolute* if for some initial condition of finite extent and amplitude, the

[6] In the case where the direct and adjoint eigenvectors are normalised with respect to themselves, i.e. for e_n, $\langle \hat{e}_n, \hat{e}_n \rangle = \tilde{\delta}_{nm}$ where δ_{nm} is the Kronecker δ. Thus, $\hat{e}_n = \frac{\hat{e}_n}{||e_n||}$.

system does not relax to the basic state everywhere in the laboratory frame.

- The basic state of a system is *nonlinearly stable* if, for all initial perturbations of finite extent and amplitude, the system relaxes to the basic state in any moving frame. It is nonlinearly unstable if it is not nonlinearly stable.

Systems under consideration are often explored by reducing the problem to the front or leading edge. The selection problem for the front velocities that has been long explored via amplitude equations. The terminology of pulled fronts and pushed fronts is used to describe the fronts when the selected frequency is associated with the linear upstream region or nonlinear downstream region. In Chomaz (2005) [25], he cites different research on pushed and pulled fronts in Ginzburg-Landau systems, but does not remark that the pulled front arises from a self-adjoint system system (Dee and Lander (1983) [36]) whereas pushed fronts occur in various configurations of complex Schrödinger equations (van Saarloos and Hohenberg (1992) [99]), which are non-self-adjoint. Furthermore, he concludes the review article with the following statement; "the reason why the majority of open flows seem to follow linear front velocity selection is still mysterious and it should ultimately be interpreted and modeled before concluding that the present theory is complete". By present theory, he means the analysis of nonlinear global modes (or fronts) with the nonlinear generalisations of the definitions present. This statement summarises the other perspective to take, i.e. why can so much be extrapolated via linear analysis from some equations and not others which have the same nonlinear operators?

It is useful here to clarify here as to why the response the failure of WNLE in Chomaz (2005) [25] in a non-self-adjoint setting is a fully nonlinear framework. Especially, as it has been the tendency over the years to make strong distinctions between the effects of non-normality and nonlinearity in Fluid Mechanics (The reader is invited to consider Waleffe (1995) [101] and Balasubramanian et al. (2008) [12]). At first glance, the saturation frequency and saturation amplitude may seem to be more a feature of the full nonlinear operator as opposed to non-normal linear operator because saturation occurs once all the modes have been mixed by the nonlinearity. However, there have been many examples where the leading eigenvector and amplitude have approximated a system with a nonlinear operator; the difference was that these systems had a normal linear operator (Collet and Eckmann (1990) [27], Kirrman et al. (1992) [58] for the Swift-Hohenberg equation, and Schneider (1994) [85], where the Ginzburg-Landau equation is derived as an approximation to the Kuramoto-Sivashinksy equation), thus reinforcing the conclusions in Chomaz (2005) [25]. The reason why Chomaz's response to non-normality was a fully nonlinear framework is therefore not due to the nonlinearity itself but rather that in a nonlinear framework that nothing is "thrown away".

In this thesis, we decided to explore the discrepancy by deriving error bounds between the solution and the approximation. The validity of reduced order models for systems of PDEs has been explored in the examples with normal linear operators was in the previous paragraph. However, in these cases, the linear operator generated a strongly-continuous semigroup, and the error bounds were derived using the integral form of the PDE. We have chosen the RnsaGL and the CnsaGL because the linear operators in both of these cases generate strongly contin-

uous semigroups so we can follow the same methodology of to a large extent. In this thesis, we do follow the proof by Kirrman et al. in [58]. The proof is achieved via bootstrap argument[7]. In the literature, there are many results deriving error bounds in this way, but, in this thesis, we continually emphasize that these are theoretical tools and not practical ones. For instance, one cannot ascertain the minimum order that an expansion needs to go be within a certain threshold or necessarily what values for ϵ the expansion $v = v_0 + \epsilon v_1 + ...+$ converges.

Similar error bounds were derived by Blömker et al. (2005) (2007) (2011) [14, 15, 16] for SPDEs where the stochastic PDE was derived via infinite-dimensional homogenisation. By similar we mean that, let u be the function and u_A be its corresponding approximation. In the deterministic case, the error bound is of the form $||u - u_A|| \leq b\epsilon$, where b is a constant. In the stochastic case, the error bound is of the form $\mathbb{P}(\sup_{t\in[0,T]} ||u(t) - u_A|| \geq c\epsilon) \leq d\epsilon$, where c and d are constants. In all of these papers assumptions are made to ensure a mild solution. In Blömker et al, i.e. the linear operator generates a C_0-semigroup and the nonlinearity is dissipative. In Blömker (2005), the Rayleigh-Bernard problem [14] was considered. In this problem, the linear operator is non-self-adjoint and a corresponding first order approximation was derived. However, there are a no numerical experiments that explore the validity of this approximation for different values of the perturbing parameter (analogous to the role of δ in our equations). An intriguing point about stochastic homogenisation is that it does not discard all stable modes as a first step but instead uses an invariant measure in order to average over all of them. In the last chapter of the thesis, we do numerical experiments with noise on the RnsaGL where the quasi-basis structure exists to see if the first order approximation derived via the infinite-dimensional stochastic homogenisation approximates the solution of the governing equations well. We choose a strength of noise in particular that should not have any effect on the first order amplitude equation (Mohammed et al. (2014) [71]), with the notion that this may yield a different result from the Stuart-Landau equation in the deterministic system.

Furthermore, studying the convergence of $v = v_0+\epsilon v_1+...+$ directly is useful but one cannot ascertain whether or not the approximation converges towards the solution. In Vishik and Lyusternik (1960) [100], linear non-self-adjoint elliptic operators were considered with elliptic perturbations. As the authors were studying the elliptic problem, they did not have the non-uniqueness at higher terms which occurs in the parabolic problem. Additionally, the authors proved convergence of their approximating expansion using results from Koshelev (1958) [59]. Although many of Koshelev's important works were translated into English, the paper that was cited had not been translated and the author of this thesis struggled to retrace the argument. He proved the convergence of the sequence

[7]We give a small bootstrap argument, this can be found in Johnathan Ben-Artzi's lecture notes on diffusive equations (https://jbenartzi.github.io/2015.Dispersive/index.html) and is extremely illustrative. Although bootstrap arguments are standard, the logic is often unclear to the reader precisely the logic if they have never seen one before;
Example (Bootstrap Argument)
Theorem. Let $f : [0, T) \longrightarrow [0, \infty)$ be continuous, where $0 < T \leq \infty$, and fix a constant $C > 0$. Suppose the following conditions hold:

1. $f(0) \leq C$.
2. $f(t) \leq 4C$ for some $t > 0$, then in fact $f(t) \leq 2C$.

Then, $f(t) \leq 4C$ (and hence $f(t) \leq 2C$) for all $t \in [0, T)$.
Proof. Let $A := \{t \in [0, T)|f(s) \leq 4C$ for all $0 \leq s \leq t\}$. Note that A is non-empty, since $0 \in A$, and that A is closed, since f is continuous. Now, if $t \in A$, then the second assumption implies $f(t) \leq 2C$, so that $t + \delta \in A$ for small enough $\delta > 0$. Thus A is a non-empty, closed and open subset of the connected set $[0, T)$ and hence, $A = [0, T)$.

$v = v_0 + \epsilon v_1 + ...$ for the case where the problem was “off the eigenvalue” and therefore in situation (α) of the Fredholm alternative. It is not clear how to adapt this proof the nonlinear case, but also in the case where we are in (β) of the Fredholm Alternative. One possibility for considering the nonlinear case where we are in situation (α) of the Fredholm alternative is to use the Adomian polynomials, but this is outside the scope of this thesis. The reader is invited to consider Adomian (1994) for an overview [2] and Cherruault (1989) [22] for a criteria on the convergence of the polynomials..

Lastly, we mention two areas of research for completeness, namely “non-modal nonlinear stability analysis” and “weak convergence methods for nonlinear partial differential equations”. These topics do not fall under the purview of this thesis, as we reiterate that the objective of the thesis is to understand where WNLE go awry, but nevertheless they are important for contextualising the research in a broader sense.

Non-modal nonlinear stability analysis is the extension of non-modal analysis to nonlinear systems. It is important to note that this is not a response to WNLE. The problem is stated as thus; given a nonlinear system (unlike what we saw in the Linear Framework), what is the most dangerous initial condition in terms of energy. The most dangerous initial condition can often result in new findings about solutions that have not previously been anticipated as it is necessary to consider the whole parameter-space as opposed to just an expansion around a fixed point. In our example, we restrict ourselves to a small perturbation δ. When δ goes from negative to positive the leading eigenvector crosses the imaginary axis resulting in a pitchfork bifurcation in the case of the RnsaGL and limit cycle in the case of the CnsaGL. In more complicated systems, there could be different behaviours accessible by different dangerous initial conditions. In comparison to finding the most dangerous initial condition in the case of (1.31), the problem in the nonlinear case is a fully nonlinear optimisation problem. The interested reader can discover the article by Kerswell (2018) [57].

Weak convergence methods of nonlinear partial differential equations deals with the following problem. Given an equation with nonlinear operator $\mathcal{A}$

$$\mathcal{A}u = f \tag{1.61}$$

where u is the unknown and f is a forcing function and a series of approximating problems

$$\mathcal{A}_k u_k = f_k. \tag{1.62}$$

such that $\mathcal{A}_k \longrightarrow \mathcal{A}$ and $f_k \longrightarrow f$. How can we guarantee that $u_k \longrightarrow u$? Techniques for solving dealing with this problem can be found in the book by Evans (1990) [43]. The approach of taking an additional timescale ϵt (or spatial scale ϵx), and comparing whether the homogenised valid is still relevant as $\epsilon \longrightarrow 0$ forms the basis of ”Two-Scale Convergence”, which has been extensively studied by G. Allaire (1992) [3], Furthermore, a non-self-adjoint example was studied by Allaire (2007) [4] on a periodic domain. In this work, the use of the two scales in space was justified as $\epsilon \longrightarrow 0$. Another technique used to justify the convergence of a homogenised equation to the governing equation

is the so-called energy method of Tartar, which is also applicable to non-self-adjoint operators. The author of this recommends the book by Tartar (2009) [95] that goes over the subtleties of different types of convergence as well as contextualising them historically.

1.4 Structure of Thesis

The reader can find below a summary of all of the core chapters after which follows a conclusion and appendices. In each chapter, we have put an emphasis on derivations, so as to make this thesis useful for those in the Fluid Mechanics community who want to recreate the derivations.

- In Chapter 2, "An Argument Against Higher Order Amplitude Equations", we compute higher order amplitude equations using WNLE on the RnsaGL. We perform numerical experiments that demonstrate as U increases a smaller percentage of U is along the zeroth eigenvector. Thus reiterating that non-normality is a problem in space instead of a problem in time.

- In Chapter 3, "Equations and their Properties", we derive some properties of the RnsaGl and CnsaGL. We show that the linear operators in the RnsaGL and CnsaGL generate strongly continuous one parameter (C_0-semigroups). As also the nonlinearity in each case is dissipative, we can write the equations in integral form and use this to prove the existence of local solutions.

- In Chapter 4, "Properties of the Eigenvectors of the $\mathcal{L}^{RGL}$ and $\mathcal{L}^{CGL}$", we prove that neither the eigenvectors of the $\mathcal{L}^{RGL}$ or $\mathcal{L}^{CGL}$ for bases. We see in the case of $\mathcal{L}^{RGL}$ that owing to the existence of a unbounded metric operator, the eigenvectors of the linear operator form a quasi-basis. This means that we can express functions that exist in a certain Hilbert-Space (embedded into the L^2-Space) using the eigenvectors of $\mathcal{L}^{RGL}$.

- In Chapter 5, "Amplitude Equations - Derivations and Analysis", we derive higher order approximations for the RnsaGL and the CnsaGL. We then perform numerical experiments that showcase their validity. In particular, the fact that the linear operator of the RnsaGL forms a quasi-basis allows us two possible normalisation choices of higher order terms.

- In Chapter 6, "Error Bound Analysis", we derive the amplitude equations via a bootstrapping argument. We also use the results of Chapter 3, by writing the equation for the discrepancy in integral form. We then perform numerical experiments in order to show that these error bounds grossly over estimate the difference between the solution and the approximation.

- In Chapter 7, "Stochastic Amplitude Equations", we consider a SPDE with noise strength such that the noise should not effect the first order approximation. This has been justified via a theorem for self-adjoint SPDEs. We add noise of the same strength to the RnsaGL and derive a first order approximation of the resulting

system. Afterwards, we perform numerical experiments to see how noise affects the non-self-adjoint system in comparison to the self-adjoint system. Furthermore, we adapt some stochastic notions to the quasi-basis structure.

Chapter 2

An Argument Against Higher Order Amplitude Equations

In this chapter, we derive and analyse higher order amplitude equations for the RnsaGL using the method of multiple scales, described in Fujimura (1989) [47], who showed that this method is equivalent to the amplitude expansion method. This chapter should really be considered an extension of the introduction as it demonstrates to the reader specifically why we neglect higher order expansions. As we only consider the RnsaGL, we have dropped on $\mathcal{L}^{RGL}$, so as to just have $\mathcal{L}$.

2.1 Derivation

We introduce two new timescales $\tau_0 = \epsilon t$ and $\tau_1 = \epsilon^2 t$ in the RnsaGL and also introduce the diffusive scaling $u = \epsilon^{\frac{1}{2}} w(\tau_1, \tau_2)$. This yields the following PDE

$$\epsilon \frac{\partial w}{\partial \tau_1} + \epsilon^2 \frac{\partial}{\partial \tau_2} = \mathcal{L}w - \epsilon w^3 + \epsilon \tilde{\delta} w. \tag{2.1}$$

We expand $w = w_0 + \epsilon w_1 + \epsilon^2 w_2 + \epsilon^3 w_3 + ...$ in order to get the following hierachy of equations;

- $O(1)$

$$-\mathcal{L}w_0 = 0 \tag{2.2}$$

gives $w_0 = C_0(\tau_0, \tau_1)\hat{e}_0$ where C_0 is the amplitude and $\hat{e}_0$ is the eigenvector corresponding to $\lambda_0 = 0$.

- $O(\epsilon)$

$$-\mathcal{L}w_1 = -\frac{\partial w_0}{\partial \tau_0} - w_0^3 + \tilde{\delta} v_0 \tag{2.3}$$

We input w_0 and then we apply the Fredholm alternative in order to obtain

$$\frac{\partial C_0}{\partial \tau_0} = \tilde{\delta} C_0 - \lambda^1 C_0^3 \tag{2.4}$$

where $\lambda^1 = \langle \hat{e}_0^\dagger, \hat{e}_0^3 \rangle$. $\hat{e}_0^\dagger$ is the solution to the adjoint eigenproblem that we previously defined in Section 1.2. Note that we have normalised the direct and adjoint eigenvectors such that $\langle \hat{e}_n^\dagger, \hat{e}_n \rangle = \delta_{nm}$ where δ_{nm} is the Kronecker delta.

Putting (2.4) back into the equation (2.3), we establish that w_1 has the structure $w_1 = C_1 \hat{e}_0 + C_0^3 \hat{w}_1$, where $\langle \hat{e}_0, \hat{w}_1 \rangle = 0$. We can find $\hat{w}_1$ by inverting the singular operator on the right-hand-side of 2.3 with the condition $\langle \hat{e}_0, \hat{w}_1 \rangle = 0$.

- $O(\epsilon^2)$

$$-\mathcal{L} w_2 = -\frac{\partial w_1}{\partial \tau_0} - \frac{\partial w_0}{\partial \tau_1} - 3 w_0^2 w_1 + \tilde{\delta} w_1 \tag{2.5}$$

We apply the Fredholm alternative in order to get the following equation

$$\frac{\partial C_1}{\partial \tau_0} + \frac{\partial C_0}{\partial \tau_1} = -2 C_0^3 \tilde{\delta} \langle \hat{e}_0^\dagger, \hat{w}_1 \rangle + 3 C_0^5 [\lambda^1 \langle \hat{e}_0^\dagger, \hat{w}_1 \rangle - \langle \hat{e}_0^\dagger, \hat{w}_1 e_0^2 \rangle] - 3 C_0^2 C_1 \lambda^1 + \tilde{\delta} C_1 \tag{2.6}$$

We use (2.6) to remove the derivative terms from (2.5) from the above equation in order to get an expression for v_2. In this way, we obtain

$$-\mathcal{L} w_2 = 2 C_0^3 \tilde{\delta} [\langle \hat{e}_0^\dagger, \hat{w}_1 \rangle \hat{e}_0 - \hat{w}_1] + 3 C_0^5 [\lambda^1 \hat{w}_1 - \lambda^1 \langle \hat{e}_0^\dagger, \hat{w}_1 \rangle \hat{e}_0 + \langle \hat{e}_0^\dagger, \hat{w}_1 e_0^2 \rangle \hat{e}_0 - \hat{e}_0^2 \hat{w}_1] + 3 C_0^2 C_1 [\lambda^1 \hat{e}_0 - \hat{e}_0^3]. \tag{2.7}$$

Therefore, $w_2 = C_2 \hat{e}_0 + \hat{w}_2(C_0, C_1, x)$ where $\hat{w}_2 = 2 C_0^3 \tilde{\delta} \hat{w}_2^a + 3 C_0^5 \hat{w}_2^b + 3 C_0^2 C_1 \hat{w}_2^c$ and the spatial terms $\hat{w}_2^a$, $\hat{w}_2^b$ and $\hat{w}_2^c$ are obtained from (2.7) using the conditions $\langle \hat{e}_0, \hat{w}_2^a \rangle = 0$, $\langle \hat{e}_0, \hat{w}_2^b \rangle = 0$ and $\langle \hat{e}_0, \hat{w}_c^2 \rangle = 0$. We can see that $\hat{w}_2^c = \hat{w}_1$.

- $O(\epsilon^3)$

$$-\mathcal{L} w_3 = -\frac{\partial w_2}{\partial \tau_0} - \frac{\partial w_1}{\partial \tau_1} - \frac{\partial w_0}{\partial \tau_2} - 3 w_0^2 w_2 - 3 w_1^2 w_0 + \tilde{\delta} w_2 \tag{2.8}$$

Applying the Fredholm alternative gives the following equation

$$\frac{\partial C_2}{\partial \tau_0}+\frac{\partial C_1}{\partial \tau_1}+\frac{\partial C_0}{\partial \tau_2}= \\ C_1C_0^4\Big[6\lambda^1\langle\hat{e}_0^\dagger,\hat{w}_1\rangle+9\lambda^1\langle\hat{e}_0^\dagger,\hat{w}_1\rangle-15\langle\hat{e}_0^\dagger,\hat{e}_0^2\hat{w}_1\rangle\Big]-4C_0^3\tilde{\delta}^2\langle\hat{e}_0^\dagger,\hat{w}_2^a\rangle-6\tilde{\delta}C_1C_0^2\langle\hat{e}_0^\dagger,\hat{w}_1\rangle \\ -3C_0^2C_2\lambda^1-3C_1^2C_0\lambda^1+\tilde{\delta}C_2+\tilde{\delta}C_0^5\Big[6\lambda^1\langle\hat{e}_0^\dagger,\hat{w}_2^a\rangle-12\langle\hat{e}_0^\dagger,\hat{w}_2^b\rangle+6\langle\hat{e}_0^\dagger,\hat{w}_1\rangle^2-6\langle\hat{e}_0^\dagger,\hat{e}_0^2\hat{w}_2^a\rangle\Big] \\ +C_0^7\Big[15\lambda^1\langle\hat{e}_0^\dagger,\hat{w}_2^b\rangle-9\lambda^1\langle\hat{e}_0^\dagger,\hat{w}_1\rangle^2+9\langle\hat{e}_0^\dagger,\hat{w}_1(\hat{e}_0)^2\rangle\langle\hat{e}_0^\dagger,\hat{w}_1\rangle-9\langle\hat{e}_0^\dagger,\hat{e}_0^2\hat{w}_2^b\rangle-3\langle\hat{e}_0^\dagger,\hat{e}_0\hat{w}_1^2\rangle\Big]. \quad (2.9)$$

In order to obtain a second order amplitude equation, it is not necessary to work out C_1, C_2 explicitly hence we do not have to deal with the non-uniqueness. We define $C=\epsilon^{\frac{1}{2}}(C_0+\epsilon C_1+\epsilon^2C_2...)$, and therefore

$$\frac{dC}{dt}=\epsilon^{\frac{3}{2}}\frac{\partial C_0}{\partial \tau_0}+\epsilon^{\frac{5}{2}}\left(\frac{\partial C_1}{\partial \tau_0}+\frac{\partial C_0}{\partial \tau_1}\right)+\epsilon^{\frac{7}{2}}\left(\frac{\partial C_2}{\partial \tau_0}+\frac{\partial C_1}{\partial \tau_1}+\frac{\partial C_0}{\partial \tau_2}\right)+.... \quad (2.10)$$

We input the right-hand-side terms in brackets using (2.4), (2.6) and (2.9) and rewrite them in terms of C,

$$\frac{dC}{dt}=\delta C-\mu_1C^3+\mu_2C^5-\mu_3C^7 \quad (2.11)$$

where

$$\mu_1=\lambda^1+\delta\mu_1^1+\delta^2\mu_1^2 \quad (2.12)$$

with

$$\mu_1^1=2\langle\hat{e}_0^\dagger,\hat{w}_1\rangle \qquad \text{and} \qquad \mu_1^2=4\langle\hat{e}_0^\dagger,\hat{w}_2^a\rangle, \quad (2.13)$$

$$\mu_2=\mu_2^1+\delta\mu_2^2 \quad (2.14)$$

with

$$\mu_2^1=3\lambda^1\langle\hat{e}_0^\dagger,\hat{w}_1\rangle-3\langle\hat{e}_0^\dagger,\hat{w}_1\hat{e}_0^2\rangle \qquad \text{and} \qquad \mu_2^2=6\lambda^1\langle\hat{e}_0^\dagger,\hat{w}_2^a\rangle-12\langle\hat{e}_0^\dagger,\hat{w}_2^b\rangle+6\langle\hat{e}_0^\dagger,\hat{w}_1\rangle^2-6\langle\hat{e}_0^\dagger,\hat{e}_0^2\hat{w}_2^a\rangle, \quad (2.15)$$

and lastly

$$\mu_3=9\langle\hat{e}_0^\dagger,\hat{e}_0^2\hat{w}_2^b\rangle+3\langle\hat{e}_0^\dagger,\hat{e}_0\hat{w}_1^2\rangle+9\lambda^1\langle\hat{e}_0^\dagger,\hat{w}_1\rangle^2-15\lambda^1\langle\hat{e}_0^\dagger,\hat{w}_2^b\rangle-9\langle\hat{e}_0^\dagger,\hat{w}_1\hat{e}_0^2\rangle\langle\hat{e_0}^\dagger,\hat{w}_1\rangle. \quad (2.16)$$

Therefore, truncating (2.10), we obtain a first-order, second-order and third-order amplitude equation; respectively given by

$$\frac{dC^{1st}}{dt}=\delta C^{1st}-\lambda^1(C^{1st})^3, \quad (2.17)$$

$$\frac{dC^{2nd}}{dt} = \delta C^{2nd} - [\lambda^1 + \delta\mu_1^1](C^{2nd})^3 + [\mu_2^1](C^{2nd})^5 \tag{2.18}$$

and

$$\frac{dC^{3rd}}{dt} = \delta C^{3rd} - \mu_1(C^{3rd})^3 + \mu_2(C^{3rd})^5 - \mu_3(C^{3rd})^7. \tag{2.19}$$

where we have denoted the solutions to the first order amplitude equations, second order amplitude equations and third order amplitude equations by C^{1st}, C^{2nd} and C^{3rd} respectively. Just to clarify the notation, all of these amplitude equations describe the evolution of the leading eigenvector e_0, but the spatial development of e_0 happens across the timescales τ_1 and τ_2. However, we label them after the order of ϵ at which they are determined.

From these, we construct the following three approximations, $u_A^1 = C^{1st}\hat{e}_0$, $u_A^2 = C^{2nd}\hat{e}_0$ and $u_A^3 = C^{3rd}\hat{e}_0$ that we analyse in the following section.

2.2 Analysis of Approximation Abilities

2.2.1 Radius of Convergence

We plot the approximation u_A^1, u_A^2 and u_A^3 as well as the PDE in Figure 1 at a point near the origin $x = 0.22$ for $U = 0$ (left) and $U = 1$ (right) respectively. This is the closest point to the 0 in its discretisation. At this point, the eigenvector $\hat{e}_0(U = 0) \approx \hat{e}_0(U = 1)$. We firstly notice even in the normal case, C^{1st} is the better approximation but this is just one spatial point, so is not really indicative of how well the approximation performs. However, we showcase these plots not necessarily to evaluate the approximations, but discuss their radius of convergence. We notice from the plot on the right in Figure 1, u_A^1 diverges hence there is an underlying problem.

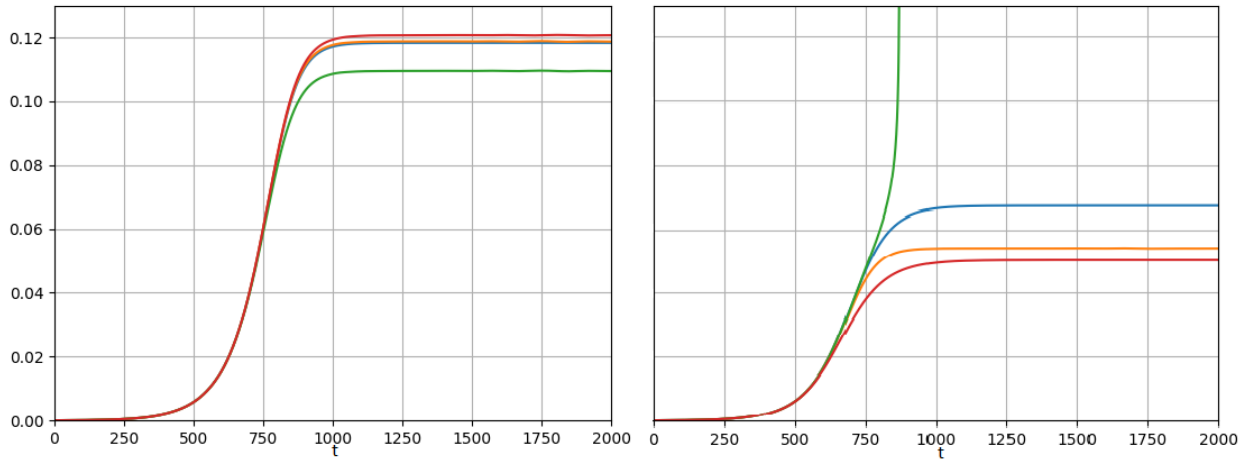

Figure 1. A plot of C^{1st} (orange), C^{2nd} (green), C^{3rd} (red) and u (blue) at $x = 0.22$, with $\delta = 0.01$ against t for different values of U, $U = 0$ (left) and $U = 1$ (right).

In order to explore the underlying problem, we consider the radius of convergence as in [47] and [21], we apply the uniform convergence criterion on the terms we have, i.e. finding a δ that satisfies the following inequalities from (2.12) and (2.14)

$$\delta\frac{|\mu_1^1|}{|\lambda^1|}<1, \qquad \delta\frac{|\mu_1^2|}{|\mu_1^1|}<1, \qquad \text{and} \qquad \delta\frac{|\mu_2^2|}{|\mu_2^1|}<1. \tag{2.20}$$

We remark that tells us to what extent our finite approximations are valid, but it does not tell us whether an infinite series expansion would be valid or not, as it may converge ultimately despite having some large coefficients in early terms. This gives us the possibility of re-summing the terms in order to create an expansion with a larger radius of convergence. The reader is invited to consider Bender and Orszag (2013) [13] for techniques concerning Borel Resummation and Padé approximations. The table below (Table 2) gives values the smallest value of δ satisfying all three inequalities in (2.20).

U	Radius of Convergence
0	0.0746
1	0.0069
2	0.0001

Table 2. The radius of convergence defined by the smallest δ that satisfies the inequalities in (2.20).

Whilst, this is not indicative of the radius of convergence for the entire expansion, it is indicative of the upper bound for the radius of convergence for the truncated expansions. Using Table 2, we safely assume why we did not have convergence in the case of $U=1$ as our value δ was too large. Therefore, the approach of higher order amplitude equations is limited if we want to model larger perturbations and larger values of δ.

2.2.2 Ability to Capture Spatial Structures Orthogonal to the Zeroth Eigenvector

When studying non-self-adjoint systems, it is reasonable question to ask is how much of the solution is along the $\hat{e}_0$? We create the following quantity u_p, which is the fraction of the overall solution that is along the unit vector $\frac{\hat{e}_0}{||\hat{e}_0||}$;

$$u_p=\frac{\langle\frac{\hat{e}_0}{||\hat{e}_0||_{L^2}},u\rangle}{||u||_{L^2}}. \tag{2.21}$$

Note that we do not take the inner product with the adjoint eigenvector, because this would be falsely assuming that a basis property exists. In Figure 3, we plot the time evolution of u_p for different values of U.

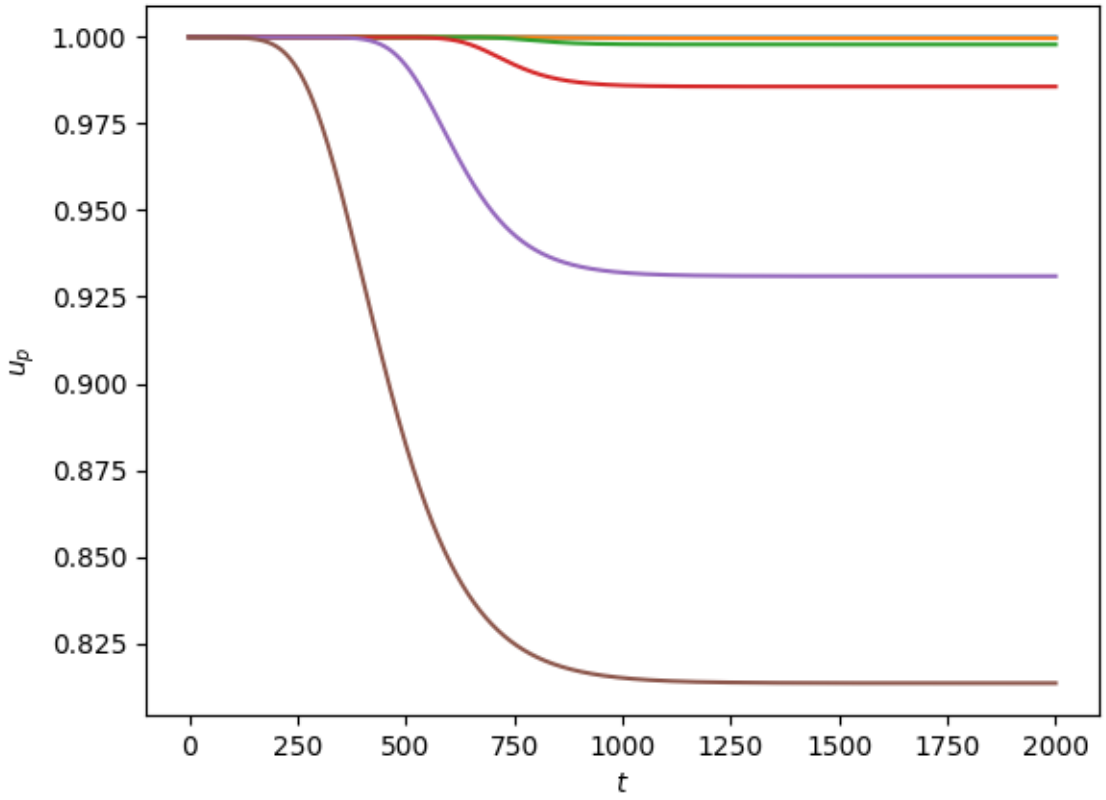

Figure 1. A plot of u_f against t for different values of U, namely $U = 0$ (blue), $U = 0.4$ (orange), $U = 0.8$ (green), $U = 1.2$ (red), $U = 1.6$ (purple) and $U = 2$ (brown).

We see that as the non-normality increases u_p becomes smaller at saturation. This shows that to obtain good approximations of the flow at saturation, it is important to take into consideration other spatial structures as opposed to just the leading eigenvectors. Therefore a higher order approximation, no matter how elabourate, will not capture the overall solution. We also see that at early times, regardless of the non-normality, the solution is totally projected along $\hat{e}_0$. The physical interpretation of this is that it takes time for the modes to be mixed by the nonlinearity.

2.3 Summary of Chapter

In this chapter, we derived higher order amplitude for the RnsaGL equations and performed numerical experiments. The first numerical experiments show the radius of convergence for a amplitude equation seemingly decreases as the order increases, when comparing terms using the uniform convergence criterion. Therefore, the utility of the amplitude equations for even describing the trajectory of the zeroth eigenvector is limited. This could potentially be improved by re-summation. The second set of numerical experiments show the non-normality causes the overall solution to contain significant spatial structures other than the zeroth eigenvector. Therefore, higher order amplitude

equations, which solely describe the temporal development of the zeroth eigenvector, are unsuitable for modelling a non-self-adjoint system.

Chapter 3

Equations and their Properties

soul In the introduction, we gave the RnsaGL and the CnsaGL. We then cited examples where error bounds had been derived to capture the difference between solutions and their approximations. These error bounds were derived largely owing to the fact the solution could be written in integral form. Two components necessary to write the solution to a PDE in integral form are, firstly the linear operator generates a strongly-continuous semigroup and that nonlinearity is sufficiently well-behaved. In this chapter, we prove that we can write the RnsaGL and the CnsaGL in integral form. We use the semigroup properties in order to prove also that the local solutions exist.

In the first section (Section 3.1), we give the definitions of the linear operators in the point of view of their domains. As the linear operators have unbounded coefficients, we have to essentially use tailor made spaces as was done in the case of Metafune et al. (2006) [67]. In second section (Section 3.2), we briefly give the motivation behind strongly continuous one-parameter semigroups (C_0-semigroups) before proving that $\mathcal{L}^{RGL}$ and $\mathcal{L}^{CGL}$ as defined in Section 3.1 generate C_0-semigroups. We prove that $\mathcal{L}^{RGL}$ and $\mathcal{L}^{CGL}$ generate C_0-semigroups using different strategies. In the former case, we rely heavily on the work of Metafune et al. (2005) [67], whereas in the latter case we rely on standard theorems from the study of non-Hermitian operators [23]. Lastly, we prove in this case, existence and uniqueness theorems for the the RnsaGL and the CnsaGL using the modern theory of semilinear parabolic equations (Miklavčič (1998) [69], Henry (2006) [51], Yagi (2009) [104]). This relies us The uniqueness of solutions is juxtaposed with the method of weakly nonlinear expansions in the next chapter.

3.1 Definitions of Linear Operators

In this thesis, we consider unbounded operators. The definition of an unbounded operator is given as follows by Cheverry and Raymond (2009) [23];

- Definition (Unbounded operator from Cheverry and Raymond (2019) [23]) Let E and F be Banach spaces. An

unbounded operator $T : E \longrightarrow F$ is a pair $(D(T), T)$ where

- $D(T)$ is a linear subspace of E;
- T is a linear map from $D(T)$ to F.

It can be helpful to refer to $D(T)$ as the "chosen domain" in contrast to the maximal domain given by, $D^m(T)$,

$$D^m(T) = \{u \in F : ||Tu||_F < \infty\}. \tag{3.1}$$

It is often difficult to establish precisely what the maximal domain $D^m(T)$ is or characterise it in terms of a few characteristics such as the existence of a certain number of weak derivatives. The domain $D(T)$ is often chosen with respect to these characteristics and this is what we have done in the case of the RnsaGL and CnsaGL. Let us recall the $\mathcal{L}^{RGL}$ and $\mathcal{L}^{CGL}$ in the context of their equations that we presented in the introduction. These are given as follows;

- Real non-self-adjoint Ginzburg-Landau equation

$$\frac{\partial u}{\partial t} = \mathcal{L}^{RGL}u - u^3 + \delta u \tag{RnsaGL}$$

where

$$\mathcal{L}^{RGL} = \frac{\partial^2}{\partial x^2} - U\frac{\partial}{\partial x} + \left(\frac{U^2}{4} + \sqrt{c_2} - c_2x^2\right)$$

with boundary conditions $|u| \longrightarrow 0$ as $x \longrightarrow \pm\infty$.

- Complex non-self-adjoint Ginzburg-Landau equation

$$\frac{\partial u}{\partial t} = \mathcal{L}^{CGL}u - |u|^2u + \delta u \tag{CnsaGL}$$

where

$$\mathcal{L}^{CGL} = (1-i)\frac{\partial^2}{\partial x^2} - (U + 0.2i)\frac{\partial}{\partial x} + \left[C_1 + \frac{1}{8}(U^2 - 0.4U - 0.04)\right] - c_2x^2$$

with $C_1 = \Re\{\sqrt{(1-i)c_2}\}$, with boundary conditions $|u| \longrightarrow 0$ as $x \longrightarrow \pm\infty$.

We consider the operators as unbounded operators in $L^2(\mathbb{R}, \mathbb{R})$ and $L^2(\mathbb{R}, \mathbb{C})$ in the case of the $\mathcal{L}^{RGL}$ and complex case $\mathcal{L}^{CGL}$. We determine their domains by firstly considering the boundary conditions $u \longrightarrow 0$ as $|x| \longrightarrow \pm\infty$ before dealing with the unbounded terms c_2x^2 in the linear operator. We encode the boundary conditions by considering domain of the operator to be a subsection of the space $H^2(\mathbb{R})$. To see why this satisfies our boundary conditions, let us first consider the space $H_0^1(\mathbb{R})$, we mean the closure of the space $C_c^\infty(\mathbb{R})$ in the H^1-norm. This

means that for functions $f \in H_0^1(\mathbb{R})$

$$\lim_{x \longrightarrow \infty} f = 0 \qquad \text{and} \qquad \lim_{x \longrightarrow -\infty} f = 0. \tag{3.2}$$

There is a subtlety that occurs on the real-line as opposed to finite intervals that means we do not need to specify that the functions vanish at infinity; as the space $C_c^1(\mathbb{R})$ is dense in $W^{1,p}(\mathbb{R}^N)$, $W_0^{1,p}(\mathbb{R}^N) = W^{1,p}(\mathbb{R}^N)$ (as demonstrated in Brezis (2011) [19], Chapter 9, 287). In this way, the function space $H^2(\mathbb{R})$ also encodes the boundary conditions, $u \longrightarrow 0$ as $|x| \longrightarrow \infty$. This viewpoint can be reinforced by considering that differentiability implies uniform continuity (by Morrey's inequality, see Evans (2010) [44] Theorem 4, Section 5.6.2) which implies on the real line the functions vanish at infinity[1].

We now consider the operators, $\hat{\mathcal{L}}_n^{RGL}$ and $\hat{\mathcal{L}}_n^{CGL}$

$$\hat{\mathcal{L}}_n^{RGL} = \frac{\partial^2}{\partial x^2} - U\frac{\partial}{\partial x} - (1 + c_2 x^2), \tag{3.3}$$

and

$$\hat{\mathcal{L}}_n^{CGL} = (1 - i)\frac{\partial^2}{\partial x^2} - (U + 0.2i)\frac{\partial}{\partial x} - (1 + c_2 x^2). \tag{3.4}$$

These operators are similar to the operators $\mathcal{L}^{RGL}$ and $\mathcal{L}^{CGL}$, but instead we have removed the constant term and moreover subtracted the identity operator. This is to put ensure that these operators are of the form of the operators used in the theorems by Metafune et al. (2005) [67]. Later on we will prove that these operators are sectorial that will allow us to prove our existence and uniqueness theorems. However, currently, we write them in this way in order to motivate the form of the following potential $V = (1 + c_2 x^2)$, and introduce the following space

$$H_V^2(\mathbb{R}) = \{u \in H^2(\mathbb{R}) : Vu \in L^2(\mathbb{R})\}. \tag{3.5}$$

We consider this space for the RnsaGL and the CnsaGL, but we remind the reader that in the real case the inner product on $L^2(\mathbb{R}, \mathbb{R})$ is without conjugation on the first argument as we only want to consider real-valued functions. We can clarify this with the following notation

$$H_{Vr}^2(\mathbb{R}) = \{u \in H^2(\mathbb{R}, \mathbb{R}) : Vu \in L^2(\mathbb{R}, \mathbb{R})\} \tag{3.6}$$

and

$$H_{Vc}^2(\mathbb{R}) = \{u \in H^2(\mathbb{R}, \mathbb{C}) : Vu \in L^2(\mathbb{R}, \mathbb{C})\}. \tag{3.7}$$

[1] These notions could possibly be formalised further by extending the real number line $\bar{\mathbb{R}} = \mathbb{R} \cup \{-\infty, \infty\}$, so we have that $f(\infty) = f(-\infty) = 0$.

The spaces H^2_{Vr} and H^2_{Vc}, equipped with the respective norms

$$||u||_{H_{Vr}} = ||u||_{H^2(\mathbb{R},\mathbb{R})} + ||Vu||_{L^2(\mathbb{R},\mathbb{R})} \tag{3.8}$$

and

$$||u||_{H_{Vc}} = ||u||_{H^2(\mathbb{R},\mathbb{C})} + ||Vu||_{L^2(\mathbb{R},\mathbb{C})}, \tag{3.9}$$

are Banach spaces. We use this spaces as the following operator domains,

$$D(\mathcal{L}^{RGL}) := H^2_{Vr} \qquad \text{and} \qquad D(\mathcal{L}^{CGL}) := H^2_{Vc} \tag{3.10}$$

respectively. However, the distinction to such an extent between the real and complex case is not necessary.

We note that for all $u \in D(\mathcal{L}^{RGL})$

$$\begin{aligned}
||\mathcal{L}^{RGL}u||^2_{L^2} = ||\frac{\partial^2 u}{\partial x^2}||^2_{L^2} + U^2||\frac{\partial u}{\partial x}||^2_{L^2} + c_1^2||u||^2_{L^2} + ||(1+c_2x^2)u||^2_{L^2} \\
+ 2c_1\langle u, \frac{\partial^2 u}{\partial x^2}\rangle - 2c_1U\langle u, \frac{\partial u}{\partial x}\rangle - 2c_1\langle u, (1+c_2x^2)u\rangle \\
- 2U\langle \frac{\partial^2 u}{\partial x^2}, \frac{\partial u}{\partial x}\rangle - 2\langle \frac{\partial^2 u}{\partial x^2}, (1+c_2x^2)u\rangle + 2U\langle \frac{\partial u}{\partial x}, (1+c_2x^2)u\rangle \\
\leq ||\frac{\partial^2 u}{\partial x^2}||^2_{L^2} + U^2||\frac{\partial u}{\partial x}||^2_{L^2} + c_1^2||u||^2_{L^2} + ||(1+c_2x^2)u||^2_{L^2} \\
+ 2c_1||u||^2_{L^2}||\frac{\partial^2 u}{\partial x^2}||_{L^2} + 2c_1U||u||_{L^2}||\frac{\partial u}{\partial x}||_{L^2} + 2c_1||u||_{L^2}||(1+c_2x^2)u||_{L^2} \\
+ 2U||\frac{\partial^2 u}{\partial u^2}||_{L^2}||\frac{\partial u}{\partial u}||_{L^2} + 2||\frac{\partial^2 u}{\partial u^2}||_{L^2}||(1+c_2x^2)u||_{L^2} + 2U||\frac{\partial u}{\partial x}||_{L^2}||(1+c_2x^2)u||_{L^2} < \infty
\end{aligned} \tag{3.11}$$

where on the right-hand-side we have used the Cauchy-Schwartz inequality as well as the abbreviation $c_1 = \frac{U^2}{4} + \sqrt{c_2} + 1$. A similar inequality holds for the $\mathcal{L}^{CGL}$ but with modified cross terms to suit the complexity. In this way, we have that $D(\mathcal{L}^{RGL}) \subseteq D^m(\mathcal{L}^{RGL})$. It can be shown in the same manner that $D(\mathcal{L}^{CGL}) \subseteq D^m(\mathcal{L}^{CGL})$.

Thus we are in a position to formally define the operators as pairs as in the definition of an unbounded operator. We have that $\mathcal{L}^{RGL} : D(\mathcal{L}^{RGL}) \longrightarrow L^2(\mathbb{R},\mathbb{R})$ and $\mathcal{L}^{CGL} : D(\mathcal{L}^{CGL}) \longrightarrow L^2(\mathbb{R},\mathbb{C})$. From now on, we will denote $\mathcal{L}^{RGL} : D(\mathcal{L}^{RGL}) \longrightarrow L^2(\mathbb{R},\mathbb{R})$ and $\mathcal{L}^{CGL} : D(\mathcal{L}^{CGL}) \longrightarrow L^2(\mathbb{R},\mathbb{C})$ by the pairs $(D(\mathcal{L}^{RGL}), \mathcal{L}^{RGL})$ and $(D(\mathcal{L}^{CGL}), \mathcal{L}^{CGL})$ respectively.

3.2 Semigroup Properties of the Linear Operators

In the introduction, we motivated the following form of the semigroup for a linear operator $\mathcal{L}$

$$e^{t\mathcal{L}} = \sum_{n=0}^{\infty} e^{\lambda_n t} P_n \tag{3.12}$$

where P_n is the projection operator onto each eigenvector of $\mathcal{L}$ and λ_n are the eigenvalues of $\mathcal{L}$, but said that this viewpoint is only valid providing the eigenvectors form a complete set. Nevertheless, this motivates regarding the semigroup in this way as a generalisation of the exponential function; i.e. in the same way that $u = e^{ta}u_0$ solves the following equation

$$\frac{du}{dt} = au, \qquad u(t=0) = u_0, \tag{3.13}$$

where a is a constant, the definition of a C_0-semigroup gives meaning to the expression $u = e^{t\mathcal{L}}u_0$ for the following abstract Cauchy problem

$$\frac{\partial u}{\partial t} = \mathcal{L}u, \qquad u(t=0) = u_0, \tag{3.14}$$

where $\mathcal{L}$ is a linear operator.

The definition of the C_0-semigroup and its generator (definitions can be found in Miklavčič (1998) [69] but are standard) are given by

- Definition (C_0-semigroup). A family of bounded linear operators $\{T(t)\}_{t\geq 0}$ on a Banach space X is called a strongly-continuous semigroup (or C_0 semigroup) if

  1. $T(0) = I$ where I is the identity operator on X
  2. $\forall t, s \geq 0$: $T(t+s) = T(t)T(s)$
  3. $\forall x_0 \in X : ||T(t)x_0 - x_0|| \longrightarrow 0$ as $t \downarrow 0$

  Furthermore, a contraction is a C_0-semigroup such that $||T(t)|| \leq 1$ for all $t \geq 0$.

- Definition (Infinitesimal Generator of a C_0-semigroup). Let $\{Q(t)\}_{t\geq 0}$ be a C_0 semigroup on a Banach space X. Define $D(\mathcal{L})$ to be the set of all $xinX$ for which there exists $y \in X$ such that

$$\lim_{t \longrightarrow 0+} ||\frac{1}{t}(x - T(t)x) - y|| = 0; \tag{3.15}$$

  for such x and y define $Ax = y$. The linear operator, $-A$, is called the generator (or the infinitesimal generator) of the semigroup.

The theorem that we use to prove that the $\mathcal{L}^{RGL}$ proves that the semigroup generated by $\mathcal{L}^{RGL}$ is not only a C_0-semigroup, but also an analytic semigroup. It is for this reason that we give the definition of an analytic semigroup

as follows as well as the theorem connecting analytic semigroups to sectorial operators. Sectorial operators are highly useful when determining the existence of solutions as they are easily bounded in norm. The definitions that we use in this case can be found in Henry (2006) [51], but are again standard and align perfectly with those given in other standard texts about semigroups[2].

- Definition (Sectorial Operator as given in Henry (2006) [51], (Definition 1.3.1)). We call a linear operator $-\mathcal{L}$ a sectorial operator if it is closed, densely-defined operator such that, for some ϕ in $(0, \frac{\pi}{2})$ and some $M \geq 1$ and real a,

  (a) the sector

  $$S_{a,\phi} = \{\phi \leq |arg(\lambda - a)| \leq \pi, \lambda \neq a\} \tag{3.16}$$

  is contained in the resolvent set $\rho(-\mathcal{L})$, and

  (b)

  $$||(\lambda - \mathcal{L})^{-1}|| \leq \frac{M}{|\lambda - a|} \qquad \text{for all} \qquad \lambda \in S_{a,\phi}. \tag{3.17}$$

- Definition (Analytic Semigroup as given in Henry (2006) [51] (Definition 1.3.3)). An analytic semigroup on a Banach space X is a family of continuous linear operators on X, $\{T(t)\}_{t\geq 0}$, satisfying

  1. $T(0) = I$ where I is the identity operator on X
  2. $\forall t, s \geq 0$: $T(t + s) = T(t)T(s)$
  3. $\forall x_0 \in X : ||T(t)x_0 - x_0|| \longrightarrow 0$ as $t \downarrow 0$.
  4. $t \longrightarrow T(t)x$ is real analytic on $0 < t < \infty$ for each $x \in X$.

- Theorem (Analytic Semigroups and Sectorial Operators as given in Henry (2006) [51] (Theorem 1.3.4)). $-\mathcal{L}$ is a sectorial operator if and only if[3] an analytic semigroup $\{e^{-t\mathcal{L}}\}_{t\geq 0}$, where

  $$e^{-\mathcal{L}t} = \frac{1}{2\pi i}\int_{\gamma}(\lambda + \mathcal{L})^{-1}e^{\lambda t}d\lambda \tag{3.18}$$

  where Γ is a contour in $\rho(-\mathcal{L})$ with $\arg\lambda \longrightarrow \pm\theta$ as $|\lambda| \longrightarrow \infty$ for some θ in $(\frac{\pi}{2}, \pi)$.

  Proof. See Theorem 1.3.4 in Henry (2006) [51] and the references therein. □

We use the following theorem to prove that $\hat{\mathcal{L}}_n^{RGL}$ generates an analytic semigroup and therefore $-\mathcal{L}_n^{RGL}$ is a sectorial operator by the theorem "Analytic Semigroups and Sectorial Operators".

[2]Often on the topic of semigroups, the author's preference can effect what is given as a definition and what is given as a theorem. For example, what are presented as theorems in Kato (2013) [56] are presented as theorems in Pazy [75] (2012).

[3]In Henry (2006) [51], the author proves the forward implication and then cites the proves of the backward implication in Friedman (1969)[45] and Hoppenstadt (1969) [53].

- Theorem (Generation of Analytic Semigroup from Metafune et al. (2005) [67]). Consider the operator, T of the following form

$$Tu = \frac{\partial^2 u}{\partial x^2} + U\frac{\partial u}{\partial x} - Vu \tag{3.19}$$

where $V \in C^1(\mathbb{R})$ and U is a constant. Assume the following

(a) $|\frac{\partial V}{\partial x}| < \gamma V^{\frac{3}{2}}$

(b) There exists a κ such that $U \leq \kappa V^{\frac{1}{2}}$ and $(\frac{\gamma}{2})\kappa + (\frac{\gamma}{2})^2 \leq 1$

then $(T, H_V^2(\mathbb{R}))$ is closed and $(T, H_V^2(\mathbb{R}))$ generates an analytic C_0-semigroup $T_2(\cdot)$ in $L^2(\mathbb{R})$, such that $T_2(z) \leq 1$ for $|arg(z)| \leq \phi_p$ and some $\phi_p > 0$.

Proof. See Theorem 3.2 for the closedness and Theorem 3.4 for the generation of the analytic semigroup in Metafune et al. (2005) [67][4]. □

- Corollary ($(D(\mathcal{L}^{RGL}), \hat{\mathcal{L}}_n^{RGL})$ is a Sectorial Operator). $(D(\mathcal{L}^{RGL}), \hat{\mathcal{L}}_n^{RGL})$ is a sectorial operator.

Proof. We firstly use the theorem "Generation of Analytic Semigroup" from Metafune et al. (2005) [67] on the operator $(D(\mathcal{L}^{RGL}), \hat{\mathcal{L}}_n^{RGL})$; we have (3.19) $V = (1 + c_2x^2)$ and $U = U$. We can take $\gamma = 1$ and $\kappa = U$[5]. Therefore, we have that $\hat{\mathcal{L}}_n^{RGL}$ generates an analytic semigroup. By the Theorem "Analytic Semigroups and Sectorial Operators" it follows that $\hat{L}_n^{RGL}$ is a sectorial operator. □.

Lastly, by the following theorem, it follows that $\mathcal{L}^{RGL}$ generates a C_0-semigroup that we prove as a corollary;

- Theorem (Perturbations by Bounded Linear Operators as given in Pazy (2012) [75]). Let X be a Banach space and let $\mathcal{L}$ be the infinitesimal generator of a C_0-semigroup $T(t)$ on X satisfying $||T(t)|| \leq Me^{\omega t}$. If B is a bounded linear operator on X, then $\mathcal{L} + B$ is the infinitesimal generator of C_0-semigroup $S(t)$ on X, satisfying $||S(t)|| \leq Me^{(\omega + M||B||)t}$ Proof. See Chapter 3, Section 3.1, Theorem 1.1 of Pazy (2012) [75]. □

- Corollary ($(D(\mathcal{L}^{RGL}), \mathcal{L}^{RGL})$ generates a C_0-semigroup). $(D(\mathcal{L}^{RGL}), \mathcal{L}^{RGL})$ generates a C_0-semigroup.

Proof. We can consider $\mathcal{L}^{RGL} - \hat{\mathcal{L}}_n^{RGL}$ as a bounded perturbation. Therefore, that $((D(\mathcal{L}^{RGL}, \mathcal{L}^{RGL})$ generates a C_0-semigroup follows from "Perturbations by Bounded Linear Operators as given in Pazy (2012).

As the theorems by Metafune et al. (2005) [67] have the condition that the coefficient of $\frac{\partial^2}{\partial x^2}$ is real-valued we cannot use the same approach to prove that $\hat{\mathcal{L}}_n^{CGL}$ is a sectorial operator. We instead use another approach that uses theorems from non-hermitian quantum mechanics that can be found in Cheverry and Raymond (2019) [23] in Appendix C.

[4] We have set $M = 1, p = 2$ in our presentation of this theorem as the theorem given in Metafune et al. (2005) [67] is more general.

[5] In this case, condition (b) gives the condition $U \leq \frac{3}{2}$ but this can be compensated by adjusting the potential V, i.e. we took $V = (1 + c_2x^2)$ but we can take also $V = (a + c_2x^2)$ where a is a constant chosen to create a more flexible condition.

3.3 Integral form of the RnsaGL and CnsaGL and the Existence and Uniqueness of Solutions

In the introduction to this section, we said that the two components necessary to write an equation in integral form was that the operator generated a C_0-semigroup and that the nonlinearity was sufficiently well-behaved. There are different ways to characterise how well behaved a nonlinearity is in terms of dissipativity and Lipschitz continuity. For our intent and purpose, we consider nonlinearities in the space[6] $\mathcal{N}(u) \in C([0,T),X)$.

We are in a position to prove the following theorem that allows us to write a PDE under certain assumptions satisfied by the CnsaGL and RnsaGL in integral from. This theorem is an amalgamation of several theorems from Miklavčič (1998) [69] that we have put together. In Miklavčič (1998) [69], this combination of theorems was used as the first step in Theorem 6.4.3, which gives conditions under which a semilinear parabolic equation has a solution when the operator is sectorial (and therefore must generate a C_0-semigroup).

- Theorem (Integral form with C_0-semigroup and well-behaved nonlinearity). Assume $u_0 \in X$ and u, $\mathcal{N}(u) \in C([0,T),X)$ and $\mathcal{L}$ generates a C_0 semigroup on X. Then we can write the equation

$$\frac{\partial u}{\partial t} = \mathcal{L}u + \mathcal{N}(u) + \delta u \qquad u(t=0) = u_0 \tag{3.21}$$

as

$$u = e^{t\mathcal{L}}u_0 + \int_0^t e^{t\mathcal{L}}(N(u(s)) + \delta u(s))ds. \tag{3.22}$$

Proof. Choose $t \in (0,T)$, and let $v(s) = e^{(t-s)\mathcal{L}}u(s)$ for $0 < s \leq t$. Let $s, s+h \in (0,t], \neq 0$. We want to find the derivative of $v(s)$ and then apply the fundamental theorem of calculus. To this end, we consider

$$\begin{aligned}
\frac{v(s+h)-v(s)}{h} &= \frac{1}{h}\left[e^{(t-s-h)\mathcal{L}}u(s+h) - e^{(t-s)\mathcal{L}}u(s)\right] \\
&= \frac{1}{h}\left[e^{(t-s-h)\mathcal{L}}u(s+h) - e^{(t-s)\mathcal{L}}u(s)\right] \\
&\quad + \frac{1}{h}\left[e^{(t-s-h)\mathcal{L}}u(s) - e^{(t-s-h)\mathcal{L}}u(s)\right] + \frac{1}{h}\left[e^{(t-s-h)\mathcal{L}}u'(s) - e^{(t-s)\mathcal{L}}u'(s)\right] \\
&= e^{(t-s-h)\mathcal{L}}u'(s) - \frac{1}{h}\left[e^{(t-s-h)\mathcal{L}} - e^{(t-s)\mathcal{L}}\right]u(s)
\end{aligned} \tag{3.23}$$

The first equality is simply by writing $v(s) = e^{(t-s)\mathcal{L}}u(s)$, the second equality is from adding and subtracting the

[6] We clarify this notation as hybrid spaces $C((0,T],X)$ are not used uniformly in the literature on semilinear parabolic equations [44]. We define $C((0,T],X)$ as the following

- Definition ($C([0,T],X)$, as defined in [44]). Let X denote a Banach space with norm $||\cdot||$, then the space $C([0,T];X)$ comprises of all continuous functions $u : [0,T] \longrightarrow X$ with the norm

$$||u||_{C([0,T];X)} := \max_{0\leq t\leq T} \sup ||u(t)|| < \infty. \tag{3.20}$$

same terms in order to get the third inequality. Now, as $\mathcal{L}$ generates a C_0-semigroup, for continuous function $f(s)$ we have the following limit

$$\frac{1}{h}\left[e^{(-h)\mathcal{L}} - 1\right] e^{(t-s)\mathcal{L}} f(s) = \mathcal{L}f(s) \tag{3.24}$$

(this follows from (2) in the definition of a C_0 semigroup). Therefore, may write in the limit $h \longrightarrow 0$

$$\frac{dv(s)}{ds} = e^{(t-s)\mathcal{L}}\left[u'(s) + \mathcal{L}u(s)\right] = e^{(t-s)\mathcal{L}}(\mathcal{N}(u(s) + \delta u(s)) \tag{3.25}$$

Therefore, recognising that as $s \longrightarrow 0$, we have $v(0) = e^{t\mathcal{L}}u_0$ (this follows from (3) in the definition of C_0-semigroup), and that $v(t) = u(t)$. We can apply the fundamental theorem of calculus to obtain

$$u(t) = e^{t\mathcal{L}}u_0 + \int_0^t e^{(t-s)\mathcal{L}}(\mathcal{N}(u(s) + \delta u(s))ds \tag{3.26}$$

and hence prove the theorem. □

Now, for us to write RnsaGL and CnsaGL in integral from we have to choose the space X in the theorem "Integral form with C_0-semigroup and well-behaved nonlinearity". We discuss to motivate the choice of this space. Firstly, a solution u of equation (3.21) must satisfy the following equation

$$u = \Phi(u) \tag{3.27}$$

where $\Phi(u)$ is the mapping given by the integral form of the equation

$$\Phi(u) = e^{t\mathcal{L}}u_0 + \int_0^t e^{(t-s)\mathcal{L}}(\mathcal{N}(u(s) + \delta u(s))ds. \tag{3.28}$$

In other words, we are looking to show that equation (3.27) has a fixed point. We can do this by considering Banach's fixed point theorem;

- Theorem (Banach's Fixed-Point Theorem). Let $(Y, ||\cdot||)$ be a non-empty complete metric space with contraction mapping $C : Y \longrightarrow Y$. Then C admits a unique fixed-point x^* in X.

In order to use Banach's fixed point theorem, we need to establish, for a complete metric space X (this space coincides with the space in the theorem "Integral form with C_0-semigroup and well-behaved nonlinearity") that is also the same space as in the theorem show that $\Phi(u) : X \longrightarrow X$ and then show Φ is a contraction. We have shown that $\hat{\mathcal{L}}_n^{RGL}$ and $\hat{\mathcal{L}}_n^{CGL}$ are sectorial operators in order to use the rich theory of semilinear parabolic equations that uses the fractional powers of operators. The idea is to define the space X as a space that between the domain defined in 3.1 and the range of the operator ($L^2(\mathbb{R})$) that provides the conditions of Banach's fixed point theorem. Often an approach is to define the nonlinearity in an interpolation space, i.e. $H_1(\mathbb{R})$, but in such spaces we often

have issues with differential operator not commuting with the linear operator (and thereby the semigroup). Therefore, it is difficult to make arguments about the relative size of semigroup in the interpolation space. Studying the sectorial operators circumvents this problem as the fractional powers of the sectorial operators, $\mathcal{L}^\alpha$ are well defined, i.e.

- Definition (Fractional powers of Operators, as defined in [51]). Suppose $-\mathcal{L}$ is a sectorial operator and $\Re(\sigma(\mathcal{L})) < 0$; then for any $\alpha > 0$

$$(-\mathcal{L})^{-\alpha} = \frac{1}{\Gamma(\alpha)} \int_0^\infty t^{\alpha-1} e^{\mathcal{L}t} dt. \tag{3.29}$$

  We define $(-\mathcal{L})^\alpha =$ inverse of $A^{-\alpha}$ $(\alpha > 0)$, $D(-\mathcal{L}^\alpha) = R(A^{-\alpha})$; $A^0 = I$.

We use these fractional powers of operators in to define the space where we prove the conditions of Banach's fixed point theorem. Let X^α be defined as the following space

$$X^\alpha = \{u \in X : ||u||_\alpha \leq \infty\}. \tag{3.30}$$

where $||u||_\alpha = ||(-\mathcal{L})^\alpha u||$. Then the space

$$\mathcal{X}(T) = C([0,T], X^\alpha) \tag{3.31}$$

equipped with the norm $||\cdot||_{\mathcal{X}(T)} = \sup_{0\leq t\leq T} ||u||_\alpha$ is a complete metric space.

We now present the next two theorems that are useful when proving the existence of solutions. The first theorem enables us to determine what restrictions there need to be on α in order to satisfy the conditions of Banach's theorem and the second theorem allows us to estimate the norm of the semigroup multiplied by the linear operator;

- Theorem (Useful Embeddings). Suppose $\Omega \subset R^n$ is an open set having the C^m extension property, $1 \leq p < \infty$, and A is a sectorial operator in $X = L_p(\Omega)$ with $D(A) = X^1 \subset W^{m,p}(\Omega)$ for some $m \geq 1$. Then for $0 \leq \alpha \leq 1$.

$$X^\alpha \subset W^{k,q}(\Omega) \qquad \text{when} \qquad k - \frac{n}{q} < m\alpha - \frac{n}{p}, \quad q \geq p, \tag{3.32}$$

$$X^\alpha \subset C^\nu(\Omega) \qquad \text{when} \qquad 0 \leq \nu < m\alpha - \frac{n}{p} \tag{3.33}$$

  Proof. See Theorem 1.6.1 in Henry (2006) [51]. □

- Theorem (Bounds on Semigroup in X^α). Suppose $(-\mathcal{L})^\alpha$ is sectorial and $\Re(-\mathcal{L})^\alpha > \delta_1 > 0$. For $\alpha \geq 0$, there exists a $C_\alpha < \infty$ such that

$$||(-\mathcal{L})^\alpha e^{\mathcal{L}t}||_{L^2} \leq C_\alpha t^{-\alpha} e^{-\delta_1 t} \tag{3.34}$$

  for $t > 0$.

Proof. See Theorem 1.4.3 in Henry (2006) [51]. □

We are now in a position to prove the existence of local solutions to the RnsaGL and the CnsaGL. We prove only the existence of local solutions RnsaGL; the CnsaGL follows in the same way as in Appendix C we prove that $\hat{\mathcal{L}}_n^{CGL}$ is a sectorial operator.

- Theorem (Existence and Uniqueness of Solution to the RnsaGL). Let us define the two spaces X^α and $\mathcal{X}(S)$ as in (3.30) and (3.31) with $X = L^2(\mathbb{R})$, $\mathcal{L} = -\hat{\mathcal{L}}_n^{RGL}$ and $\alpha \in (\frac{1}{2}, 1)$. There exists a unique[7] solution to the $u \in \mathcal{X}$ to the RnsaGL for initial data $u_0 \in X^\alpha$.

  Proof. Let us begin by recasting the RnsaGL in the following way;

$$\frac{\partial u}{\partial t} = \hat{\mathcal{L}}_n^{RGL} u + \hat{\mathcal{N}}(u) \tag{3.35}$$

  where $\hat{\mathcal{N}}(u) = (\mathcal{L}^{RGL} - \hat{\mathcal{L}}_n^{RGL})u + \delta u - u^3$.

  From the theorem "Integral form with C_0-Semigroup and well-behaved nonlinearity". We can write (3.35) in the following way;

$$u = e_0^{t\hat{\mathcal{L}}_n^{RGL}} u_0 + \int_0^t e^{t\hat{\mathcal{L}}_n^{RGL}} \hat{\mathcal{N}}(u) dx. \tag{3.36}$$

  It remains to show that the map, $\hat{\Phi}(u)$ on the right-hand-side of (3.36)

$$\hat{\Phi}(u) = e_0^{t\hat{\mathcal{L}}_n^{RGL}} u_0 + \int_0^t e^{t\hat{\mathcal{L}}_n^{RGL}} \hat{\mathcal{N}}(u) dx \tag{3.37}$$

  maps $\mathcal{X}(S)$ to $\mathcal{X}(S)$ and is a contraction. We split the proof up into two steps:

  1. Firstly, we show that $\hat{\Phi}(u) : \mathcal{X}(S) \longrightarrow \mathcal{X}(S)$. Consider the following inequality

$$||u^3||_{L^2} \leq ||u^3||_{H^1} \leq C_2 ||u||_{H^1}^3 \leq C_3 ||u||_\alpha^3 \tag{3.38}$$

     where C_1, C_2 and C_3 are positive constants. The first and third inequality follow from (3.32) and the second inequality comes from the product formula.

     Therefore, we have that

$$||\hat{\Phi} u||_\alpha \leq ||e^{t\hat{\mathcal{L}}_n^{RGL}} u_0||_\alpha + C \int_0^t ||(-\hat{\mathcal{L}}_n^{RGL})^\alpha e^{(t-s)\hat{\mathcal{L}}_n^{RGL}}|| \bigg(||u||_\alpha + ||u||_\alpha^3 \bigg) ds \tag{3.39}$$

     where the constant C_α comes from (3.34) and the constant C absorbs the constants $(\mathcal{L}^{RGL} - \hat{\mathcal{L}}^{RGL}) + \delta$ and C_3.

[7] In our case, the uniqueness follows from Banach's Fixed-Point Theorem, but there are cases where the initial data is rougher. The reader is invited to consider Step 4 in the proof of Theorem 4.1 of Yagi (2009) [104] for a more intricate proof of uniqueness and also the discussion above example 6.4.1 in Miklavčič (1998).

We split the integral on the right-hand-side into two parts

$$||\hat{\Phi}u||_\alpha \leq ||e^{t\hat{\mathcal{L}}_n^{RGL}}u_0||_\alpha + \underbrace{C\int_0^s ||(-\hat{\mathcal{L}}_n^{RGL})^\alpha e^{(s-\tau)\hat{\mathcal{L}}_n^{RGL}}||\bigg(||u||_\alpha + ||u||_\alpha^3\bigg)d\tau}_{I_1}$$
$$+ C\underbrace{\int_s^t ||(-\hat{\mathcal{L}}_n^{RGL})^\alpha e^{(t-\tau)\hat{\mathcal{L}}_n^{RGL}}||\bigg(||u||_\alpha + ||u||_\alpha^3\bigg)d\tau}_{I_2} \quad (3.40)$$

We consider I_2 first. Let

$$M = \sup_{0\leq s\leq T}\bigg(||u||_\alpha + ||u||_\alpha^3\bigg) \quad (3.41)$$

then

$$\int_s^t ||(-\hat{\mathcal{L}}_n^{RGL})^\alpha e^{(t-\tau)\hat{\mathcal{L}}_n^{RGL}}||\bigg(||u||_\alpha + ||u||_\alpha^3\bigg)d\tau \leq MC_\alpha\int_s^t (t-\tau)^{-\alpha}e^{-\delta_1(t-\tau)}d\tau$$
$$\leq MC_\alpha\int_s^t (t-\tau)^{-\alpha}d\tau \leq MC_\alpha\frac{(t-s)^{1-\alpha}}{(1-\alpha)}, \quad (3.42)$$

therefore I_2 is bounded.

For I_1, we consider the following quantity

$$A_\alpha = \sup_{0\leq\tau\leq T} t^\alpha||(-\hat{\mathcal{L}}_n^{RGL})^\alpha e^{\hat{\mathcal{L}}_n^{RGL}t}||, \quad (3.43)$$

then it follows that

$$I_1 = \int_0^s ||(-\hat{\mathcal{L}}_n^{RGL})^\alpha e^{(t-\tau)\hat{\mathcal{L}}_n^{RGL}}||\bigg(||u||_\alpha + ||u||_\alpha^3\bigg)d\tau \leq MA_\alpha\int_0^s (s-\tau)^{-\alpha}d\tau \leq MA_\alpha\frac{(s)^{1-\alpha}}{(1-\alpha)}. \quad (3.44)$$

Moreover, we have that $I_1 \longrightarrow 0$ as $s \longrightarrow 0$.

Lastly,

$$||(-\hat{\mathcal{L}}_n^{RGL})^\alpha e^{t\hat{\mathcal{L}}_n^{RGL}}u_0|| \leq ||e^{t\hat{\mathcal{L}}_n^{RGL}}||\,||(-\hat{\mathcal{L}}_n^{RGL})^\alpha u_0|| \leq ||u_0||_\alpha. \quad (3.45)$$

From (3.42), (3.44) and (3.45), we have $\hat{\Phi}(u) : \mathcal{X}(S) \longrightarrow \mathcal{X}(S)$.

2. Now, we prove $\hat{\Phi}(u) : \mathcal{X}(s) \longrightarrow \mathcal{X}(s)$. We consider two functions $u, v \in \mathcal{X}(S)$. We begin by stating the inequality

$$u^3 - v^3 = (u-v)(u^2+v^2+uv). \quad (3.46)$$

Therefore, we have

$$||u^3 - v^3|| \leq ||u^3 - v^3||_{H^1} \leq ||u - v||_{H_0^1} \left[||u||_{H^1}^2 + ||v||_{H^1}^2 + ||u||_{H_0^1} ||v||_{H^1} \right] \leq C_N ||u - v||_\alpha. \tag{3.47}$$

By result (3.32), we have that the quantities $||u||_{H^1}$ and $||v||_{H^1}$ are bounded, hence we can contain them in the constant C_N.

Suppose u and v have the same initial data, then

$$\begin{aligned} ||\hat{\Phi}(u) - \hat{\Phi}(v)||_\alpha &\leq C \int_0^t ||(-\mathcal{L})^\alpha e^{(t-s)\hat{\mathcal{L}}^{RGL}}|| \; ||u - v|| ds \\ &\leq C \sup_{0 \leq s \leq t} \{||u - v||\} A_\alpha \int_0^t \frac{1}{(t-s)^\alpha} ds \leq C \frac{t^{(1-\alpha)}}{(1-\alpha)}. \end{aligned} \tag{3.48}$$

Therefore, providing S such that $(0, t] \in S$ is sufficiently small, we have that $\hat{\Phi}(u)$ is a contraction.

As we have shown that the two conditions of Banach's theorem are satisfied for $\hat{\Phi}(u)$ in the complete metric space $\mathcal{X}(S)$, there exists a unique fixed point of (3.27). It follows that there exists a unique solution to the RnsaGL with initial data in X^α. □

3.4 Summary of Chapter

In this chapter, we firstly defined fully the $\mathcal{L}^{RGL}$ and $\mathcal{L}^{CGL}$ with the appropriate domains. These domains coincided with the ones established by Metafune et al. (2005) [67] to prove regularity for elliptic problems with unbounded coefficients. We proved that $\mathcal{L}^{RGL}$ generated a C_0-semigroup using the theorems of Metafune et al. (2005) [67] (there is an analogous proof for $\mathcal{L}^{CGL}$ in Appendix C). As the nonlinearity is dissipative in the cases of the RnsaGL and the CnsaGL, these equations can be written in integral form using the fact that the linear operators generate C_0-semigroups. We used the integral form to prove existence and uniqueness for the RnsaGL when the initial condition had appropriate regularity. The regularity condition can be relaxed somewhat and has been in the references Yagi [104] (2009), Miklavčič (1998) [69] and Henry (2006) [51].

Chapter 4

Properties of the Eigenvectors of the $\mathcal{L}^{RGL}$ and $\mathcal{L}^{CGL}$

In this chapter, we explore to what degree the eigenvectors of the $\mathcal{L}^{RGL}$ and $\mathcal{L}^{CGL}$ form a basis. In the first section, we discuss different notions of a basis and prove that the eigenvectors of the $\mathcal{L}^{RGL}$ and $\mathcal{L}^{CGL}$ do not from bases that allow us to meaningfully expand arbitrary L^2-functions in eigenvector-amplitude pairs (except in the case of $U = 0$ for the $\mathcal{L}^{RGL}$). In the following section, we recognise that $\mathcal{L}^{RGL}$ is a Quasi-Hermitian Operator with an unbounded metric operator. We give the relevant definitions which define a Lattice of Hilbert Spaces (LHS). In the third section, we define a quasi-basis that allows us to expand functions that are in a subset of L^2, namely an extremal space of the LHS, into eigenvector-amplitude pairs. This has ramifications in terms of the normalisation choices with respect to higher order terms using WNLE. Furthermore, the quasi-basis structure allows us to perform the infinite-dimensional homogenisation of Blömker et al. (2005, 2007, 2011) [14, 15, 16].

4.1 (Lack of) Basis Properties for $\mathcal{L}^{RGL}$ and $\mathcal{L}^{CGL}$

A significant reason why we chose the RnsaGL and the CnsaGL as our test-cases was largely owing to knowing what the form of the eigenvectors without computation. Furthermore, these eigenvectors have compact resolvents that allows us to use the theorems from Krejčiřik et al. (2015) [61]. We prove the fact that these operators have compact resolvents in Appendix D.

Let us denote the direct and adjoint eigenvectors for the $\mathcal{L}^{RGL}$ are denoted by $\{e_n\}$ and $\{e_n^\dagger\}$ respectively. Let us also denote the $\mathcal{L}^{CGL}$, we denote the direct and adjoint eigenvectors by $\{e_n^c\}$ and $\{(e_n^c)^\dagger\}$ respectively. This is the only time that the $\mathcal{L}^{RGL}$ and $\mathcal{L}^{CGL}$ will be considered in the same section. We describe the normalisation constant in the real case by Z and the complex case by Z^c. The forms of $\{e_n\}$, $\{e_n^\dagger\}$, $\{e_n^c\}$ and $\{e_n^\dagger\}$ are given as follows

•

$$\hat{e}_n = \frac{1}{Z_n}\exp\{-\frac{1}{4}(\alpha_1 x)^2 + \frac{U}{2a}x\}He_n(\alpha_1 x) \tag{4.1}$$

•

$$\hat{e}_n^{\dagger} = \frac{1}{Z_n}\exp\{-\frac{1}{4}(\alpha_1 x)^2 - \frac{U}{2a}x\}He_n(\alpha_1 x) \tag{4.2}$$

•

$$\hat{e}_n^{c} = \frac{1}{Z_n^c}\exp\{-\frac{1}{4}(\alpha_1^c x)^2 + \alpha_2^c x\}He_n(\alpha_1^c x) \tag{4.3}$$

•

$$(\hat{e}_n^{c})^{\dagger} = \frac{1}{Z_n^c}\exp\{-\frac{1}{4}(\beta_1^c x)^2 - \beta_2^c x\}He_n(\beta_1^c x) \tag{4.4}$$

where we have real constant $\alpha_1 = (4c_2)^{\frac{1}{4}}$ and complex constants $\alpha_1^c = (\frac{4c_2}{1-i})^{\frac{1}{4}}$, $\alpha_2^c = \frac{U+0.2i}{2(1-i)}$, $\beta_1^c = (\alpha_1^c)^*$, $\beta_2^c = (\alpha_2^c)^*$. The normalisation constants Z_n and Z_n^c are given by $Z_n = (\frac{n!\sqrt{2\pi}}{\alpha_1})^{\frac{1}{2}}$ and $Z_n^c = (\frac{n!\sqrt{2\pi}}{\alpha_1^c})^{\frac{1}{2}}$

Let us consider the following definitions of a basis before we prove that neither the eigenvectors of $\mathcal{L}^{RGL}$ or $\mathcal{L}^{CGL}$ form a basis. Below we give both the definitions of a conditional basis and an unconditional basis. These are just two examples that exist in the literature. There are other definitions of a basis in the literature, some relying on just completeness, but these are not appropriate for expanding functions in eigenvector-amplitude pairs.

- Definition (Schauder or Conditional Basis, as given in Krejčiřik (2015) [61]) Let X be a Banach space, $\{e_n\}_{k=0}^{\infty}$ is a Schauder basis or conditional basis if every $e_n \in X$ has a unique expansion in the vectors $\{e_n\}_{k=0}^{\infty}$.

- Definition (Riesz or Unconditional Basis, as given in Krejčiřik (2015) [61]) Let X be a Banach space, $\{e_n\}_{k=0}^{\infty}$, normalised to 1 in X, is a Riesz or unconditional basis if it forms a basis and for all functions $\phi \in X$ the inequality

$$C^{-1}||\phi||^2 \leq \sum_{k=1}^{\infty}|\langle e_n, \phi\rangle^2 \leq C||\phi||^2 \tag{4.5}$$

holds with a positive constant C independent of ϕ.

We give the following two theorems (they are also presented in Section 2); the first is a theorem from Davies (2007) [34] that provides context for the second theorem given in Krejčiřik (2015) [61] of which we use the reverse-implication to prove that the eigenvectors of the $\mathcal{L}^{RGL}$ and $\mathcal{L}^{CGL}$ do not form a basis.

- Theorem (Biorthogonality of Basis vectors from Davies (2007) [34]). Let X be a Banach space and f be a function in X. If $\{\psi_n\}_{n=1}^{\infty}$ is a basis in a Banach space X, then there exists a $\phi_n \in X^*$ such that the Fourier coefficients α_n are given by $\alpha_n := \langle f, \phi_n\rangle$. The pair of sequences $\{\psi_n\}_{n=1}^{\infty}$, $\{\phi_n\}_{n=1}^{\infty}$ is biorthogonal in the sense that $\langle f_n, \phi_m\rangle = \tilde{\delta}_{n,m}$ for all m, n,

  Proof. See Lemma 3.3.1 from Davies (2007) [34].

- Theorem (Condition of the Uniform Boundedness of Projections). Let X be a Banach space. Let $\mathcal{L}$ be an operator with a compact resolvent and let us denote that has a basis of eigenvectors by ϕ_n. Let us denote the associated one-dimensional projections as

$$P_k := \psi_k \langle \phi_k, \cdot \rangle. \tag{4.6}$$

If $\{\phi_k\rangle_{k=0}^{\infty}$ is a basis, then both P_k and $\sum_{k=0}^{N}$ are uniformly bounded in X.

Proof. See Krejčiřik et al. (2015) [61].

In the next two theorems, we prove that the the projections onto the eigenvectors are unbounded in both cases thus proving that the eigenvectors of $\mathcal{L}^{RGL}$ and $\mathcal{L}^{CGL}$ do not form bases. All the references of the expansion polynomials formula that we use can be found in Mityagin et al. (2013) [70].

- Theorem (Divergence of Projections for eigenvectors of $\mathcal{L}^{RGL}$). Let $\hat{e}_n$ and $\hat{e}_n^{\dagger}$ be defined as in (4.1) and (4.2) respectively with $U \neq 0$. These form a biorthogonal set. We define the projections

$$P_n = \langle \hat{e}_n^{\dagger}, \cdot \rangle e_n. \tag{4.7}$$

We have that

$$||P_n|| = \frac{e^{2(nC)^{\frac{1}{2}}}}{2\sqrt{\pi}(C)^{\frac{1}{4}} n^{\frac{1}{2}}}(1 + O(n^{-\frac{1}{2}})) \tag{4.8}$$

and hence diverge as $n \longrightarrow \infty$.

Proof.

We have that

$$||P_n|| = ||\hat{e}_n^{\dagger}||_{L^2} ||\hat{e}_n||_{L^2} \tag{4.9}$$

Looking at the individual terms gives

$$||\hat{e}_n||_{L^2} = \frac{1}{Z_n^2} \sqrt{\int_{-\infty}^{\infty} \exp\Big\{ -\frac{1}{2}\alpha_1^2 x^2 + \frac{U}{a} x \Big\} He_n(\alpha_1 x) He_n(\alpha_1 x) dx}. \tag{4.10}$$

Note, we have that we have the formula for physicist polynomials

$$\int_{-\infty}^{\infty} e^{-(x-y)^2} H_m(x) H_n(x) dx = 2^n \pi^{\frac{1}{2}} m! y^{n-m} L_n^{n-m}(-2y^2), \tag{4.11}$$

where $L_n^{n-m}(x)$ are the Laguerre polynomials. Therefore, firstly by noticing that $He_n(\alpha_1 x) = 2^{-\frac{n}{2}} H_n(\frac{\alpha_1}{\sqrt{2}} x)$.

Then, we perform the change of variables $y = \frac{\alpha_1}{\sqrt{2}}x$ in order to obtain

$$\int_{-\infty}^{\infty} \exp\Big\{ -\frac{1}{2}\alpha_1^2 x^2 + \frac{U}{a}x \Big\} He_n(\alpha_1 x) He_n(\alpha_1 x) dx$$
$$= 2^{-n}\frac{\sqrt{2}}{\alpha_1} e^{\frac{1}{2\alpha_1^2}\frac{U^2}{a^2}} \int_{-\infty}^{\infty} \exp\Big\{ -\Big(y - \frac{1}{\alpha_1\sqrt{2}}\frac{U}{a}\Big)^2 \Big\} H_n(y) H_n(y) dy$$
$$= \frac{\sqrt{2}}{\alpha_1} e^{\frac{1}{2\alpha_1^2}\frac{U^2}{a^2}} \pi^{\frac{1}{2}} n! L_n^0\Big(-2\Big(\frac{1}{\alpha_1\sqrt{2}}\frac{U}{a}\Big)^2\Big) \quad (4.12)$$

We now use the following asymptotic formula for the Laguerre Polynomials,

$$\forall x \in \mathbb{C}\setminus\mathbb{R}_+, \qquad L_k^0(x) = \frac{e^{\frac{x}{2}} e^{2(-kx)^{\frac{1}{2}}}}{2\sqrt{\pi}(-x)^{\frac{1}{4}} k^{\frac{1}{2}}}(1 + O(k^{-\frac{1}{2}})) \quad (4.13)$$

Therefore, let $C = 2(\frac{1}{\alpha_1\sqrt{2}}\frac{U}{a})^2 > 0$ We have

$$||e_n||_{L^2}^2 = \frac{e^{2(nC)^{\frac{1}{2}}}}{2\sqrt{\pi}(C)^{\frac{1}{4}} n^{\frac{1}{2}}}(1 + O(n^{-\frac{1}{2}})) \quad (4.14)$$

which diverges as $n \longrightarrow \infty$

We notice that by replacing U by $-U$, we obtain the same formula for $||e_n^\dagger||_{L^2}$;

$$||e_n^\dagger||_{L^2}^2 = \frac{e^{2(nC)^{\frac{1}{2}}}}{2\sqrt{\pi}(C)^{\frac{1}{4}} n^{\frac{1}{2}}}(1 + O(n^{-\frac{1}{2}})) \quad (4.15)$$

.

Therefore, we have that

$$||P_n|| = \frac{e^{2(nC)^{\frac{1}{2}}}}{2\sqrt{\pi}(C)^{\frac{1}{4}} n^{\frac{1}{2}}}(1 + O(n^{-\frac{1}{2}})) \quad (4.16)$$

which diverges as $n \longrightarrow \infty$. □

Theorem (Divergence of Projections for eigenvectors of $\mathcal{L}^{CGL}$). Let $\hat{e}_n^c$ and $(\hat{e}_n^c)^\dagger$ be defined as in (4.1) and (4.2) respectively, which form a biorthogonal set. We define the projections

$$P_n = \langle (\hat{e}_n^c)^\dagger, \cdot \rangle e_n^c. \quad (4.17)$$

As $n \longrightarrow \infty$

$$||P_n|| \geq |\frac{e^{2(nC)^{\frac{1}{2}}}}{2\sqrt{\pi}(C)^{\frac{1}{4}} n^{\frac{1}{2}}}| \quad (4.18)$$

thus $||P_n||_{L^2}$ diverges as $n \longrightarrow \infty$.

Proof. We have that

$$||P_n|| = ||(\hat{e}_n^c)^\dagger||_{L^2}||(\hat{e}_n^c)||_{L^2} \tag{4.19}$$

Looking at the individual terms gives

$$||\hat{e}_n^c||_{L^2} = \sqrt{\frac{1}{|Z_n^c|^2}\int_{-\infty}^{\infty} |\exp\Big\{-\frac{1}{4}(\alpha_1^c x)^2 + \alpha_2^c x\Big\} He_n(\alpha_1^c x)|^2 dx}. \tag{4.20}$$

By acknowledging that

$$|\int_{-\infty}^{\infty} \hat{e}_n^2 dx| \leq \int_{\infty}^{\infty} |\hat{e}_n|^2 dx, \tag{4.21}$$

we can proceed in the same way as last time, and prove that $||P_n||$ is bounded below by something divergent. Note, we have that we have the formula for physicist polynomials

$$\int_{-\infty}^{\infty} e^{-(x-y)^2} H_m(x) H_n(x) dx = 2^n \pi^{\frac{1}{2}} m! y^{n-m} L_n^{n-m}(-2y^2), \tag{4.22}$$

where $L_{n^{n-m}(x)}$ are the Laguerre polynomials with complex argument. Therefore, firstly by noticing that $He_n(\alpha_1^c x) = 2^{-\frac{n}{2}} H_n(\frac{\alpha_1^c}{\sqrt{2}}x)$. Then, we perform the change of variables $y = \frac{\alpha_1^c}{\sqrt{2}}x$ and complete the square

$$-y^2 + 2\frac{\alpha_2^c\sqrt{2}}{\alpha_1^c} = -(y^2 - 2\frac{\alpha_2^c\sqrt{2}}{\alpha_1^c}) = -\Big[(y - \frac{\alpha_2^c\sqrt{2}}{\alpha_1^c})^2 - \frac{2(\alpha_2^c)^2}{(\alpha_1^c)^2}\Big]. \tag{4.23}$$

We consider the following integral

$$\begin{aligned}\int_{-\infty}^{\infty} \exp\Big\{-\frac{1}{2}(\alpha_1^c)^2 x^2 + 2(\alpha_2^c)x\Big\} He_n(\alpha_1^c x) He_n(\alpha_1^c x) dx \\ = 2^{-n}\frac{\sqrt{2}}{\alpha_1^c} e^{2\frac{(\alpha_2^c)^2}{(\alpha_1^c)^2}} \int_{-\infty}^{\infty} \exp\Big\{-\Big(y - \frac{(\alpha_2^c)\sqrt{2}}{\alpha_1^c}\Big)^2\Big\} H_n(y) H_n(y) dy \\ = 2^{-n}\frac{\sqrt{2}}{\alpha_1^c} e^{2\frac{(\alpha_2^c)^2}{(\alpha_1^c)^2}} \pi^{\frac{1}{2}} n! L_n^0\Big(-2\Big(\frac{(\alpha_2^c)\sqrt{2}}{(\alpha_1^c)}\Big)^2\Big)\end{aligned} \tag{4.24}$$

We now use the following asymptotic formula for the Laguerre Polynomials,

$$\forall x \in \mathbb{C} \setminus \mathbb{R}_+, \qquad L_k^0(x) = \frac{e^{\frac{x}{2}} e^{2(-kx)^{\frac{1}{2}}}}{2\sqrt{\pi}(-x)^{\frac{1}{4}} k^{\frac{1}{2}}}(1 + O(k^{-\frac{1}{2}})) \tag{4.25}$$

Therefore, let $C = 2(\frac{\alpha_2\sqrt{2}}{\alpha_1})^2 > 0$ We have as $n \longrightarrow \infty$

$$|\int_{-\infty}^{\infty} (\hat{e}_n^c)^2 dx| \approx |\frac{e^{2(nC)^{\frac{1}{2}}}}{2\sqrt{\pi}(C)^{\frac{1}{4}} n^{\frac{1}{2}}}| \tag{4.26}$$

In the case of $(\hat{e}_n^c)^\dagger$ we find that the same argument but we replace α_2 by $-\alpha_2$ on the grounds that $|\exp\{-\frac{1}{4}(\alpha_1^c x)^2 - \alpha_2^c x\}He_n(\alpha_1^c x)|^2 = |\exp\{-\frac{1}{4}(\beta_1^c x)^2 - \beta_2^c x\}He_n(\beta_1^c x)|^2$. We see that this gives us the same formula as $n \longrightarrow \infty$

$$|\int_{-\infty}^{\infty}((\hat{e}_n^c)^\dagger)^2 dx| \approx |\frac{e^{2(nC)^{\frac{1}{2}}}}{2\sqrt{\pi}(C)^{\frac{1}{4}}n^{\frac{1}{2}}}| \tag{4.27}$$

Therefore, from (4.20) and (4.21) we have that

$$||P_n||^2 = ||(\hat{e}_n^c)^\dagger||^2||\hat{e}_n^c||^2 \tag{4.28}$$

Therefore we have that as $n \longrightarrow \infty$

$$||P_n||^2 \geq |\frac{e^{2(nC)^{\frac{1}{2}}}}{2\sqrt{\pi}(C)^{\frac{1}{4}}n^{\frac{1}{2}}}|^2. \tag{4.29}$$

Therefore, we have that

$$\left(||P_n|| - |\frac{e^{2(nC)^{\frac{1}{2}}}}{2\sqrt{\pi}(C)^{\frac{1}{4}}n^{\frac{1}{2}}}|\right)\left(||P_n|| + |\frac{e^{2(nC)^{\frac{1}{2}}}}{2\sqrt{\pi}(C)^{\frac{1}{4}}n^{\frac{1}{2}}}|\right) \geq 0 \tag{4.30}$$

which leads to

$$||P_n|| \geq |\frac{e^{2(nC)^{\frac{1}{2}}}}{2\sqrt{\pi}(C)^{\frac{1}{4}}n^{\frac{1}{2}}}| \tag{4.31}$$

The right-hand-side diverges as $n \longrightarrow \infty$, hence $||P_n||_{L^2}$ diverges. □

4.2 Quasi-Hermiticity of $\mathcal{L}^{RGL}$

In the following, we are going to define and motivate the lattice of Hilbert-spaces based around a generic metric operator, G, before defining G for $\mathcal{L}^{RGL}$. Our construction is the same as that found in Antoine et al. (2015) [7]. For a didactic reference on the construction of partial inner product spaces, the reader is invited to consider the book by Antoine and Trapani (2012) [5].

We firstly define a Quasi-Hermitian Operator and the corresponding metric operator;

- Definition (Quasi-Hermitian Operator in the sense of Dieudonné (1960) [38]). A closed operator $\mathcal{L}$, with dense domain $D(\mathcal{L})$ is called quasi-Hermitian if there exists a self-adjoint, positive operator G, known as the metric operator, with dense domain $D(G)$ such that $D(\mathcal{L}) \subseteq D(G)$[1] and

$$\langle \mathcal{L}u, Gv\rangle = \langle Gu, \mathcal{L}v\rangle, \qquad u, v \in D(\mathcal{L}). \tag{4.32}$$

[1]The condition that $D(\mathcal{L}) \subset D(\mathcal{G})$ is imposed to make sure there are interesting things in $D(\mathcal{G})$ to consider as opposed to just $\{0\}$.

Now, let us considering the operator $G^{\frac{1}{2}}$ in a Hilbert Space $\mathcal{H}$, the domain of this operator is given by

$$D(G^{\frac{1}{2}}) = \{u \in \mathcal{H} : ||G^{\frac{1}{2}}u||_{\mathcal{H}} \leq \infty\}. \tag{4.33}$$

We equip this space with various norms that can be induced by an inner product. For instance, equipping the space $D(G^{\frac{1}{2}})$ with the norm $||\cdot||_G = ||G^{\frac{1}{2}} \cdot || = \sqrt{\langle G^{\frac{1}{2}}\cdot, G^{\frac{1}{2}}\cdot\rangle}$, yields a Hilbert Space that we denote $\mathcal{H}(G)$. Equipping the space with the norm $||\cdot||_{1+G} = ||(1+G)^{\frac{1}{2}} \cdot || = \sqrt{\langle (1+G)^{\frac{1}{2}}\cdot, (1+G)^{\frac{1}{2}}\cdot\rangle}$, yields a Hilbert Space that we denote $\mathcal{H}(1+G)$. It follows that $\mathcal{H}(1+G) = \mathcal{H} \cap \mathcal{H}(G)$. Likewise, we consider the domain of the metric operator $(G^{\frac{1}{2}})^{-1}$, $D((G^{\frac{1}{2}})^{-1})$ defined as

$$D((G^{\frac{1}{2}})^{-1}) = \{u \in \mathcal{H} : ||(G^{\frac{1}{2}})^{-1}u||_{\mathcal{H}} \leq \infty\} \tag{4.34}$$

and define the spaces $||\cdot||_{G^{-1}}$ and $||\cdot||_{1+G^{-1}}$. It follows that $\mathcal{H}(G) = D(G^{\frac{1}{2}})$ and $\mathcal{H}(G^{-1}) = D((G^{\frac{1}{2}})^{-1})$.

Furthermore, the conjugate dual space, that we denote by a superscript X is given by $\mathcal{H}(G+1)^X$ is the space $\mathcal{H}(\frac{1}{1+G})$. Therefore, one gets the following triplet

$$\mathcal{H}(1+G) \subset \mathcal{H} \subset \mathcal{H}(\frac{1}{1+\mathcal{G}}). \tag{4.35}$$

Likewise, these relations hold for the inverse, G^{-1}. In this way, we can define the extreme spaces $\mathcal{H}(G) \cap \mathcal{H}(G^{-1}) = \mathcal{H}(1+G) \cap \mathcal{H}(1+G^{-1})$ and $\mathcal{H}(G) + \mathcal{H}(G^{-1}) = \mathcal{H}(\frac{1}{1+G}) + \mathcal{H}(\frac{1}{1+G^{-1}})$. We equip the spaces $\mathcal{H}(G) \cap \mathcal{H}(G^{-1})$ and $\mathcal{H}(G) + \mathcal{H}(G^{-1})$ with the inductive norm and projective norm respectively. These are given by

$$||f||_{\mathcal{H}(G)\cap\mathcal{H}(G^{-1})} = ||f||_G + ||f||_{G^{-1}} \tag{4.36}$$

and

$$||f||_{\mathcal{H}(G)+\mathcal{H}(G^{-1})} = \inf_{f=g+h}\{||g||_G + ||h||_{G^{-1}} : g \in \mathcal{H}(G), h \in \mathcal{H}(G^{-1})\}. \tag{4.37}$$

These spaces together generate a Lattice of Hilbert Spaces (LHS) that is shown in Figure 1. This picture is the same as the one in [5], but we have doctored the arrows to fit our notation. The arrows denote continuous and dense embeddings.

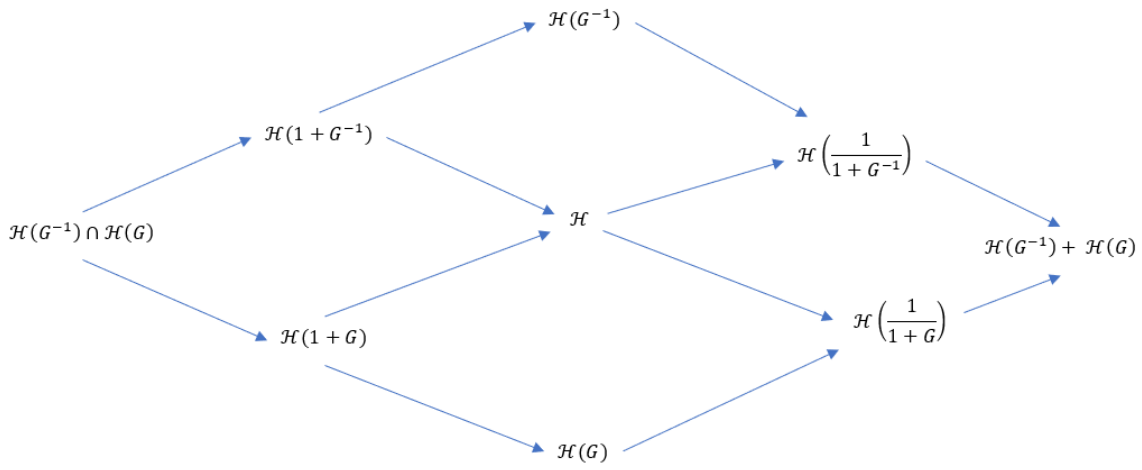

Figure 1. The lattice of Hilbert space as demonstrated in [5, 6] but adapted to the notation used. All of the arrows represent continuous embeddings with dense range.

It follows that $\mathcal{L}^{RGL}$ is a Quasi-Hermitian operator with respect to the metric operator $G = e^{-\frac{U}{a}x}$. We can consolidate this in the following theorem so we can refer to it later;

- Theorem (Quasi-Hermiticity of $\mathcal{L}^{RGL}$). $\mathcal{L}^{RGL}$ is Quasi Hermitian with respect to the metric operator $G = e^{-\frac{U}{a}x}$.

  Proof. The proof follows from the definition of a "Quasi-Hermitian Operator" given at the start of this section. □

We note that the eigenvectors of $\mathcal{L}^{RGL}$ and $(\mathcal{L}^{RGL})^{\dagger}$ form orthonormal bases in the spaces $\mathcal{H}(e^{-\frac{U}{a}x})$ and $\mathcal{H}(e^{\frac{U}{a}x})$ respectively. However, as the metric operator is unbounded, the spaces $\mathcal{H}(e^{-\frac{U}{a}x})$ and $\mathcal{H}$ and $\mathcal{H}(e^{\frac{U}{a}x})$ are not comparable as the norms induced by the inner product are not equivalent. Moreover, when one considers $\mathcal{L}^{RGL}$ in the space $\mathcal{H}(e^{\frac{U}{a}x})$, one is considering a non-Hermitian realisation of the quantum oscillator Mostafazedeh (2010, 2013) [72, 73].

4.3 Quasi-Basis Structure for the $\mathcal{L}^{RGL}$

The reason why we are interested in this construction is because the direct eigenvectors of $\mathcal{L}^{RGL}$, $\{e_n\}_{n=0}^{\infty}$, and the adjoint eigenvectors. $\{e_n^{\dagger}\}_{n=0}^{\infty}$, can be used to describe functions from the space $\mathcal{H}(e^{\frac{U}{a}x}) \cap \mathcal{H}(e^{-\frac{U}{a}x})$. In the following, we will describe this construction generally with a metric operator G before making precise to our case. The reader is invited to consider the following papers by Bagarello et al. (2010, 2010, 2013) [8, 9, 10] in which the mathematical aspects are developed more so than they are in this thesis. Quasi-bases in particular were motivated by the need to describe coherent states for non-Hermitian systems with an underlying structure. The definition of quasi-basis is given as follows

- Definition (Quasi-Basis, as defined in [10]). Given a suitable dense subspace X_1 of a Hilbert space $\mathcal{H}$. Let $E_{\mathcal{L}} = \{e_n\}_{n=0}^{\infty}$ and $E_{\mathcal{L}^{\dagger}} = \{e_n^{\dagger}\}_{n=0}^{\infty}$ be two orthogonal sets such that all $e_n \in X_1$ and all $e_n^{\dagger} \in X_1$. $E_{\mathcal{L}}$ and $E_{\mathcal{L}^{\dagger}}$

are X_1 quasi-bases if, for all $f, g \in X_1$,

$$\langle f, g\rangle = \sum_{n=0}\langle f, e_n\rangle\langle e_n^\dagger, g\rangle = \sum_{n=0}\langle f, e_n^\dagger\rangle\langle e_n, g\rangle. \tag{4.38}$$

We note that, although our choices of $\{e_n\}$ and $\{e_n^\dagger\}$ are derived from the direct and adjoint eigenvectors of $\mathcal{L}^{RGL}$. The idea of a quasi-basis a much more general concept that need not be motivated by an operator $\mathcal{L}$ and can just exist based on a metric operator. This can be shown in the following theorem where there is no operator $\mathcal{L}$;

- Theorem (The Existence of Quasi-Bases under certain conditions). Let $\hat{E} = \{\hat{e}_n\}_{n=0}^{\infty}$ be an orthonormal basis in a Hilbert Space $\mathcal{H}$. Consider the two sets $E = \{e_n\}_{n=0}^{\infty}{}^{\infty}$ and $E^\dagger = \{e_n^\dagger\}_{n=0}^{\infty}$, such that for the metric operator $G^{\frac{1}{2}}$ where $G^{\frac{1}{2}}e_n = \hat{e}_n$ and $(G^{\frac{1}{2}})^{-1}e_n^\dagger = \hat{e}_n$. Let the domain, $D(G^{\frac{1}{2}})$ of $G^{\frac{1}{2}}$ and $D((G^{\frac{1}{2}})^{-1})$ be defined as in (4.33) and (4.34). Given the following assumptions:

  - E_n and $\hat{E}_n$ are bi-orthogonal.
  - If $f \in \mathcal{H}(G)$ is orthogonal to all the e_n then $f = 0$.
  - If $f \in \mathcal{H}(G^{-1})$ is orthogonal to all the $e_n^\dagger$ then $f = 0$.

    The E_n and $\hat{E}_n$ are quasi-basis for the space $H(G^{-1}) \cap H(G)$.

  Proof. See Bagarello (2013) [10].

Furthermore, we can make it explicit as to why quasi-bases are useful for our application in the following theorem.

- Theorem (Expressing elements of $H(G) \cap H(G^{-1})$ in terms of non-orthogonal basis vectors). Let $\hat{E} = \{\hat{e}_n\}_{n=0}^{\infty}$ be an orthonormal basis in a Hilbert Space $\mathcal{H}$. Consider the two sets $E = \{e_n\}_{n=0}^{\infty}{}^{\infty}$ and $E^\dagger = \{e_n^\dagger\}_{n=0}^{\infty}$, such that for the metric operator G where $G^{\frac{1}{2}}e_n = \hat{e}_n$. Furthermore, $(G^{\frac{1}{2}})^{-1}e_n^\dagger = \hat{e}_n$ and $G^{-1}e_n^\dagger = e_n$. Then each element of $u \in \mathcal{H}(G) \cap \mathcal{H}(G^{-1})$ (with the spaces $\mathcal{H}(G)$ and $\mathcal{H}(G^{-1})$ defined by (4.34) and (4.33) respectively) can be expressed as $u = \sum_{n=0}^{\infty}\langle e_n, u\rangle e_n^\dagger = \sum_{n=0}^{\infty}\langle e_n^\dagger, u\rangle e_n$.
  Proof. Let $f \in \mathcal{H}(G) \cap \mathcal{H}(G^{-1})$. As $\hat{e}_n$ is an orthonormal basis, we can write $f = \sum_{n=0}^{\infty}\langle \hat{e}_n, f\rangle \hat{e}_n$. We apply $G^{\frac{1}{2}}$, which gives $G^{\frac{1}{2}}f = \sum_{n=0}^{\infty}\langle \hat{e}_n, G^{\frac{1}{2}}f\rangle \hat{e}_n = \sum_{n=0}^{\infty}\langle \hat{e}_n^\dagger, f\rangle \hat{e}_n$. Then it follows that

$$||f - \sum_{n=0}^{\infty}\langle e_n, f\rangle e_n^\dagger|| = ||(G^{\frac{1}{2}})^{-1}\bigg(G^{\frac{1}{2}}f - \sum_{n=0}^{\infty}\langle \hat{e}_n^\dagger, f\rangle \hat{e}_n\bigg)|| \leq ||(G^{\frac{1}{2}})^{-1}||\,||\bigg(G^{\frac{1}{2}}f - \sum_{n=0}^{\infty}\langle \hat{e}_n^\dagger, f\rangle \hat{e}_n\bigg)|| \tag{4.39}$$

  Note, we have that for all $f \in \mathcal{H}(G) \cap \mathcal{H}(G^{-1})$, $G^{\frac{1}{2}}$ is a unitary operator from $\mathcal{H}(G)$ on $\mathcal{H}$, and likewise $(G^{\frac{1}{2}})^{-1}$ is a unitary operator from $\mathcal{H}(G^{-1})$ on $\mathcal{H}$. Therefore, we want to show that $\mathcal{G}^{\frac{1}{2}}f \in \mathcal{H}(G^{-1})$, provided that $f \in \mathcal{H}(G) \cap \mathcal{H}(G^{-1})$. In this way, we can use that $(G^{\frac{1}{2}})^{-1} : \mathcal{H}(G^{-1}) \longrightarrow \mathcal{H}$ and thus $||(G^{\frac{1}{2}})^{-1}|| = 1$ in (4.39).

Given that $(G^{\frac{1}{2}})^{-1} : \mathcal{H}(G^{-1}) \longrightarrow \mathcal{H}$ is bounded, we have that

$$||G^{\frac{1}{2}} f||_{\mathcal{H}(G^{-1})} = ||(G^{\frac{1}{2}})^{-1} G^{\frac{1}{2}} f||_{\mathcal{H}} = ||f||_{\mathcal{H}}, \tag{4.40}$$

which is bounded as $f \in \mathcal{H}(G) \cap \mathcal{H}(G^{-1})$.

Therefore, it follows from (4.39)

$$||f - \sum_{n=0}^{\infty} \langle e_n, f \rangle e_n^{\dagger}|| \leq ||\Bigg(G^{\frac{1}{2}} f - \sum_{n=0}^{\infty} \langle \hat{e}_n^{\dagger}, f \rangle \hat{e}_n \Bigg)|| \longrightarrow 0 \tag{4.41}$$

as higher and higher terms are taken in $\sum_{n=0}^{\infty} \langle \hat{e}_n^{\dagger}, f \rangle \hat{e}_n$.

Thus we have shown that f can be written in the following way $f = \sum_{n=0}^{\infty} \langle e_n, f \rangle \hat{e}_n^{\dagger}$. Showing f can be written as $f = \sum_{n=0}^{\infty} \langle \hat{e}_n^{\dagger}, f \rangle e_n$ follows the same pattern. □

Lastly, we can see that this is true for the direct and adjoint eigenvectors of the $\mathcal{L}^{RGL}$;

- Theorem (Quasi-Basis Structure for RnsaGL). RnsaGL has a quasi-basis structure in the above set-up with underlying Hilbert Space $\mathcal{H} = L^2$ and $G = e^{-\frac{U}{2a}}$.

  Proof. We use the proof entitled "The existence of Quasi-Bases under certain conditions" that was just given. We can see for the eigenvectors $\{e_n\}_{n=0}^{\infty}$ and $\{e_n^{\dagger}\}_{n=0}^{\infty}$ are biorthogonal from their explicit form. Moreover, they both form complete sets hence the second and third conditions of the theorem are met. □

4.4 Summary of Chapter

In this chapter, we considered the eigenvectors of the RnsaGL and the CnsaGL. We proved that neither of these eigenvectors formed a useful basis because the projections on the sets of eigenvectors were unbounded. We could prove this only as we had the forms of the eigenvectors. We saw that $\mathcal{L}^{RGL}$ was a Quasi-Hermitian operator with respect to the metric operator $G = e^{-\frac{U}{a}x}$. We constructed a lattice of Hilbert spaces from an arbitrary metric operator G, before discussing the ramifications of this underlying lattice operator for our unbounded metric operator. We have that owing to the underlying quasi-basis structure we can use the direct and adjoint eigenvectors for $\mathcal{L}^{RGL}$ in order expand the functions in the space $\mathcal{H}(e^{-\frac{U}{a}x}) \cap \mathcal{H}(e^{\frac{U}{a}x})$ in terms of eigenvector-amplitude pairs where the amplitudes are guaranteed to be finite.

Chapter 5

Amplitude Equations - Derivations and Analysis

In this chapter, we derive amplitude equations for the RnsaGL and the CnsaGL and then perform numerical experiments to evaluate them. As we deal with each case separately, we have abbreviated $\mathcal{L}^{RGL}$ and $\mathcal{L}^{CGL}$ to $\mathcal{L}$ as it is obvious which space we are considering. Regarding the real case, we have a quasi-basis structure that allows us to have two normalisation choices for higher order terms. We verify these and compare them numerically. We also perform WNLE in the space $\mathcal{H}(G)$ and thus show that the first order approximation provides a good approximation of the solution in this space where the operator $\mathcal{L}^{RGL}$ is self-adjoint.

5.1 Real Case

5.1.1 Derivation

We begin by putting the RnsaGL equation on a dissipative timescale $u = \epsilon^{\frac{1}{2}} v(x, \tau)$ where $\tau = \epsilon t$;

$$\epsilon \frac{\partial v}{\partial \tau} = \mathcal{L}v - \epsilon v^3 + \epsilon \tilde{\delta} v. \tag{5.1}$$

We introduce the expansion

$$v = \underbrace{C\hat{e}_0}_{v_0'} + \epsilon \underbrace{[v_1(C,x) + \gamma_1(C)\hat{e}_0]}_{v_1'} + \epsilon^2 \underbrace{[v_2(C,x) + \gamma_2(C)\hat{e}_0]}_{v_2'} + \epsilon^3 \underbrace{[v_3(C,x) + \gamma_3(C)\hat{e}_0]}_{v_3'} + o(\epsilon^3)... \tag{5.2}$$

to we obtain the following hierachy of equations

$$-\mathcal{L}v_0' = 0, \qquad -\mathcal{L}v_1' = N^1(v_0'), \qquad -\mathcal{L}v_2' = N^2(v_0', v_1'), \qquad \dots, \qquad -\mathcal{L}v_n' = N^n(v_0', v_1', ..., v_n') \tag{5.3}$$

where

$$N^{n+1}(v_0', ..., v_n') = -\frac{\partial v_n'}{\partial \tau} + \tilde{\delta} v_n' - \left(\sum_{i=0}^{n} \sum_{k=0}^{n-i} \epsilon^{\frac{1}{2}+(n+1)} v_i' v_k' v_{n-i-k}' \right) \tag{5.4}$$

for all $n \geq 1$.

We put the expansion (5.1) into the equation (5.2) and compare terms at like order;

- O(1)

$$C\mathcal{L}\hat{e}_0 = 0 \tag{5.5}$$

- $O(\epsilon)$

$$-\mathcal{L}v_1 = N^1(v_0') = -\frac{\partial C}{\partial \tau}\hat{e}_0 + \tilde{\delta} C \hat{e}_0 - C^3(\hat{e}_0)^3 \tag{5.6}$$

We apply the Fredholm alternative to (5.6) in order to get the amplitude equation

$$\frac{\partial C}{\partial \tau} = \tilde{\delta} C - \lambda^1 C^3, \tag{5.7}$$

where $\lambda^1 = \langle \hat{e}_0^\dagger, (e_0)^3 \rangle$. We substitute (5.7) back into (5.6) in order to obtain

$$-\mathcal{L}v_1 = C^3[\lambda^1 \hat{e}_0 - (\hat{e}_0)^3]. \tag{5.8}$$

We let $v_1(C, x) = C^3 \hat{v}_1$ and we invert the singular operator $\mathcal{L}$ with the normalisation condition $\langle \hat{e}_0, \hat{v}_1 \rangle = 0$ to obtain $\hat{v}_1$, i.e. we consider the augmented system

$$\begin{pmatrix} \mathcal{L} & e_0 \\ \langle \hat{e}_0, \cdot \rangle & 0 \end{pmatrix} \begin{pmatrix} \hat{v}_1 \\ c \end{pmatrix} = \begin{pmatrix} -(e_0^\dagger)^3 \\ 0 \end{pmatrix} \tag{5.9}$$

where we treat c as an unknown. Upon inverting the matrix, we obtain $c = -\lambda^1$. This provides a nice numerical check that the inversion was performed properly.

- $O(\epsilon^2)$

$$-\mathcal{L}v_2 = N^1(v_0', v_1') = -\frac{\partial [C^3 \hat{v}_1 + \gamma_1(C)\hat{e}_0]}{\partial \tau} + \tilde{\delta}[C^3 \hat{v}_1 + \gamma_1(C)\hat{e}_0] - 3C^2(\hat{e}_0)^2[C^3 \hat{v}_1 + \gamma_1(C)\hat{e}_0] \tag{5.10}$$

Applying the Fredholm alternative to this equation gives

$$0 = \frac{\partial \gamma_1(C)}{\partial C} - \frac{(\tilde{\delta} - 3C^2\lambda^1)}{(\tilde{\delta}C - \lambda^1 C^3)}\gamma_1(C) + \frac{2\tilde{\delta}C^3\lambda^2 - 3C^5(\lambda^1\lambda^2 - \lambda^3)}{(\tilde{\delta}C - \lambda^1 C^3)} \tag{5.11}$$

where $\lambda^2 = \langle e_0^\dagger, \hat{v}_1 \rangle$ and $\lambda^3 = \langle \hat{e}_0^\dagger, \hat{v}_1(\hat{e}_0)^2 \rangle$.

We integrate the above equation (5.11) using the integrating factor in order to obtain the following representation for γ_1 where D is a constant to be determined;

$$\gamma_1(C) = \frac{1}{2(\lambda^1)^2}\left[(\lambda^1\lambda^2 - 3\lambda^3)\tilde{\delta}C + 3(\lambda^1\lambda^2 - \lambda^3)(\tilde{\delta}C - \lambda^1 C^3)\log(\tilde{\delta} - \lambda^1 C^2)\right] + D(\tilde{\delta}C - \lambda^1 C^3). \tag{5.12}$$

We introduce an assumption to establish D. The assumption is that all of the linear behaviour is dealt with at first order, and therefore there must be no contributions at higher order terms to the linear behaviour of the approximation. This is an assumption based on the empirical results that we saw in the introduction, where the first order approximation captured the behaviour well at early times. We consider the linearisation of $\gamma_1(C) = \gamma_1^{lin}(C)$

$$\gamma_1^{\text{lin}}(C) = \frac{1}{2(\lambda^1)^2}\left[(\lambda^1\lambda^2 - 3\lambda^3)\tilde{\delta}C + 3(\lambda^1\lambda^2 - \lambda^3)(\tilde{\delta}C)\log(\tilde{\delta})\right] + D(\tilde{\delta}C) \tag{5.13}$$

and set this equal to zero in order to obtain

$$D = -\frac{1}{2(\lambda^1)^2}\left[(\lambda^1\lambda^2 - 3\lambda^3) + 3(\lambda^1\lambda^2 - \lambda^3)\log(\tilde{\delta})\right]. \tag{5.14}$$

This gives the full version of $\gamma_1(C)$ as

$$\gamma_1(C) = \frac{1}{2(\lambda^1)^2}\left[(\lambda^1\lambda^2 - 3\lambda^3)(\lambda^1 C^3) + 3(\lambda^1\lambda^2 - \lambda^3)(\tilde{\delta}C - \lambda^1 C^3)\log\left(\frac{\tilde{\delta} - \lambda^1 C^2}{\tilde{\delta}}\right)\right]. \tag{5.15}$$

Inserting $\gamma_1(C)$ into (5.10) gives the following representation of v_2;

$$-\mathcal{L}v_2 = 2\tilde{\delta}C^3[\lambda^2\hat{e}_0 - \hat{v}_1] + 3C^5\left[[\lambda^1\hat{v}_1 - \lambda^1\lambda^2\hat{e}_0] + [\lambda^3\hat{e}_0 - \hat{v}_1(\hat{e}_0)^2]\right] + 3C^2\gamma_1(C)[\lambda^1\hat{e}_0 - (\hat{e}_0)^3]. \tag{5.16}$$

We let $v_2 = 2\tilde{\delta}C^3\hat{v}_2^a + 3C^5\hat{v}_2^b + 3C^2\gamma_1(C)\hat{v}_1$ and obtain $\hat{v}_a^2$ and $\hat{v}_b^2$ by solving the following augmented systems;

$$\begin{pmatrix} \mathcal{L} & e_0 \\ \langle \hat{e}_0, \cdot \rangle & 0 \end{pmatrix} \begin{pmatrix} \hat{v}_a^2 \\ c_a \end{pmatrix} = \begin{pmatrix} -\hat{v}_1 \\ 0 \end{pmatrix} \tag{5.17}$$

and

$$\begin{pmatrix} \mathcal{L} & e_0 \\ \langle \hat{e}_0, \cdot \rangle & 0 \end{pmatrix} \begin{pmatrix} \hat{v}_b^2 \\ c_b \end{pmatrix} = \begin{pmatrix} [\lambda^1 \hat{v}_1 - \lambda^1 \lambda^2 \hat{e}_0] - \hat{v}_1 (\hat{e}_0)^2 \\ 0 \end{pmatrix}, \tag{5.18}$$

where we obtain $c_a = -\lambda^2$ and $c_b = -\lambda^3$, which is consistent with (5.16).

- O(ϵ^3)

$$-\mathcal{L}v_3(C,x) = -\frac{\partial[v_2(C,x)+\gamma_2(C)\hat{e}_0]}{\partial\tau} + \tilde{\delta}[v_2(C,x)+\gamma_2(C)\hat{e}_0] - 3[v_1(C,x)+\gamma_1(C)\hat{e}_0]^2 C(\hat{e}_0) - 3[v_2(C,x)+\gamma_2(C)\hat{e}_0]C^2(\hat{e}_0)^2 \tag{5.19}$$

We will use this order to show that often we do not need to solve an ODE if we want to obtain the saturation value of γ_2. Furthermore, for just working out the saturation amplitude, we remove the problem of non-uniqueness at higher order terms, i.e. we do not need to determine another constant like D at the previous order[1].

We firstly apply the Fredholm alternative to (5.19) and set all of the time derivatives equal to zero; this gives

$$\gamma_2(C_{sat}) = \frac{1}{2\tilde{\delta}} \langle \hat{e}_0^\dagger, \tilde{\delta} v_2(C_{sat},x) - 3[v_1(C_{sat},x)+\gamma_1(C_{sat})\hat{e}_0]^2 C_{sat}(\hat{e}_0) - 3[v_2(C_{sat},x)C_{sat}^2(\hat{e}_0)^2 \rangle. \tag{5.23}$$

Now, we change back to the original timescale $u = \epsilon^{\frac{1}{2}} u(x, \epsilon t)$. We let $B(t) = \epsilon^{\frac{1}{2}} C(\tau)$. The governing amplitude on this timescale is given by

$$\frac{dB}{dt} = \delta B - \lambda^1 B^3. \tag{5.24}$$

We label the following approximations for the solutions of the RnsaGL as zeroth order, u^{0th}, first order, u^{1st} and second order approximation u_{sat}^{2nd} (calculated at the saturated value) respectively;

$$u^{0th} = B\hat{e}_0, \tag{5.25}$$

[1] We note that if we set $\frac{\partial u}{\partial t} = 0$ to zero in the governing equation we obtain an elliptic equation that was dealt with in Vishik and Lyusternik (1960) [100]. We notice that there is no non-uniqueness in this case. We compute the first few terms on the stationary case below;

$$\mathcal{L}v_0 = 0 \tag{5.20}$$
$$\mathcal{L}v_1 = \tilde{\delta}u_0 - u_0^3 \tag{5.21}$$
$$\mathcal{L}v_2 = \tilde{\delta}(v_1 + \gamma_1\hat{e}_0) + 3u_0^2(v_1+\gamma_1\hat{e}_0) \tag{5.22}$$

From applying first term, we obtain $u = C_1\hat{e}_0$ where C_1 is a constant. Applying the Fredholm alternative at second order we obtain $C_1 = \sqrt{\frac{\tilde{\delta}}{\lambda^1}}$. At second order, we can let $v_1 = (\frac{\tilde{\delta}}{\lambda^1})^{\frac{3}{2}}\hat{v}_1$ and obtain $\hat{v}_1$ via the augmented system (5.32). Lastly, in this case we would have $\gamma_1 = \frac{\delta}{2(\lambda^1)^2}\frac{\tilde{\delta}}{\lambda^1}[\lambda^1\lambda^2 - 3\lambda^3]$, which coincides with the definition of (5.12) at saturation.

$$u^{1st} = (B + \gamma_1'(B))\hat{e}_0 + B^3\hat{v}_1 \tag{5.26}$$

and

$$u_{\text{sat}}^{2nd} \approx (B_{\text{sat}} + \gamma_1'(B_{\text{sat}}) + \gamma_2'(B_{\text{sat}}))\hat{e}_0 + B_{\text{sat}}^3\hat{v}_1 + v_2'(B_{\text{sat}}, x) \tag{5.27}$$

where $\gamma_1'(B)$, $v_2'(B)$ and $\gamma_2'(B_{\text{sat}})$ are given by;

$$\gamma_1'(B) = \frac{1}{2(\lambda^1)^2}\left[(\lambda^1\lambda^2 - 3\lambda^3)(\lambda^1 B^3) + (\delta B - \lambda^1 B^3)\log\left(\frac{\delta - \lambda^1 B^2}{\delta}\right)\right], \tag{5.28}$$

$$v_2'(B, x) = \delta B^3 \hat{v}_2^a(x) + 3B^5\hat{v}_2^b(x) + 3B^2\gamma_1(C)\hat{v}_1(x) \tag{5.29}$$

and

$$\gamma_2'(B_{sat}) = \frac{1}{2\delta}\langle \hat{e}_0^\dagger, \delta v_2(B_{sat}, x) - 3[v_1(B_{sat}, x) + \gamma_1(B_{sat})\hat{e}_0]^2 B_{sat}(\hat{e}_0) - 3v_2(B_{sat}, x)B_{sat}^2(\hat{e}_0)^2\rangle \tag{5.30}$$

where the addition of the primes is to distinguish the different timescales τ and t.

5.1.2 Two normalisation choices

Note that owing to the underlying quasi-basis structure and the fact that our solution exists in the space $\mathcal{H}(G) \cap \mathcal{H}(G^{-1})$, we have two normalisation choices for our higher order terms. Previously, we chose to normalise v_1, $\hat{v}_2^a$ and $\hat{v}_2^b$ such that $\langle \hat{e}_0, \hat{v}_1\rangle = 0$, $\langle \hat{e}_0^\dagger, \hat{v}_2^a\rangle = 0$ and $\langle \hat{e}_0^\dagger, \hat{v}_2^b\rangle = 0$. As we are able to write $u = \sum_{n=0}^{\infty}\langle \hat{e}_0^\dagger, u\rangle \hat{e}_n$ owing to the quasi-basis structure, we can use the normalisation conditions $\langle \hat{e}_0^\dagger, \tilde{v}_1\rangle = 0$, $\langle \hat{e}_0^\dagger, \tilde{v}_2^a\rangle = 0$ and $\langle \hat{e}_0^\dagger, \tilde{v}_2^b\rangle = 0$, where we have differentiated these normalisation conditions to the previous normalisation conditions by using tildes $\tilde{}$.

Let us consider the $O(\epsilon)$ equation as an example,

$$-\mathcal{L}v_1 = C^3[\lambda^1\hat{e}_0 - (\hat{e}_0)^3]. \tag{5.31}$$

We can let $v_1 = C^3\tilde{v}_1$ and invert the equation (5.31) with the condition $\langle \hat{e}_0^\dagger, \tilde{v}_1\rangle = 0$, i.e. the augmented system (5.32) becomes

$$\begin{pmatrix} \mathcal{L} & e_0 \\ \langle \hat{e}_0^\dagger, \cdot\rangle & 0 \end{pmatrix}\begin{pmatrix} \tilde{v}_1 \\ c \end{pmatrix} = \begin{pmatrix} -(e_0^\dagger)^3 \\ 0 \end{pmatrix} \tag{5.32}$$

where the inner product in the lower right-hand-corner now contains a $\hat{e}_0$ instead of a $\hat{e}_0^\dagger$.

Note that applying the normalisation against the adjoint eigenvector $\hat{e}_0^\dagger$ results in different forms of $\tilde{v}_2'$, i.e.

$$\tilde{\gamma}_1'(B) = -\frac{3\lambda^3}{2(\lambda^1)^2}\left((\delta B - \lambda^1 B^3)\log\left(\frac{\delta - \lambda^1 B^2}{\delta}\right) + \lambda^1 B^3\right), \tag{5.33}$$

$$\tilde{\gamma}_2'(B_{sat}) = -\frac{3}{2\delta}\left[B_{sat}^7\langle\hat{e}_0^\dagger, (\tilde{v}_1)^2\hat{e}_0\rangle + B_{sat}(\gamma_1(B_{sat}))^2\lambda^1 + 2B_{sat}^4\gamma_1(B_{sat})\lambda^3 + \langle\hat{e}_0^\dagger, \tilde{v}_2(B_{sat}, x)B_{sat}^2(\hat{e}_0)^2\rangle\right] \tag{5.34}$$

and

$$\tilde{v}_2'(B_{sat}, x) = \delta B_{sat}^3\tilde{v}_2^a(x) + 3B_{sat}^5\tilde{v}_2^b(x) + 3B_{sat}^2\gamma_1(B_{sat})\tilde{v}_1(x), \tag{5.35}$$

where $\tilde{v}_2^a(x)$, $\tilde{v}_2^b(x)$, $\tilde{v}_1(x)$ are obtained from inverting the analogous equation[2] to (5.16) with the conditions $\langle\hat{e}_0^\dagger, \tilde{v}_2^a(x)\rangle = 0$ and $\langle\hat{e}_0^\dagger, \tilde{v}_2^b(x)\rangle = 0$.

We also denote the different approximations with tildes;

$$\tilde{u}^{0th} = B\hat{e}_0, \tag{5.38}$$

$$\tilde{u}^{1st} = (B + \gamma_1'(B))\hat{e}_0 + B^3\tilde{v}_1, \tag{5.39}$$

and

$$\tilde{u}_{\text{sat}}^{2nd} \approx (B_{\text{sat}} + \gamma_1'(B_{\text{sat}}) + \gamma_2'(B_{\text{sat}}))\hat{e}_0 + B_{\text{sat}}^3\tilde{v}_1 + \tilde{v}_2'(B_{\text{sat}}, x) \tag{5.40}$$

where B is given by (5.24).

5.1.3 Numerical Experiments

In the previous two sections, we worked out the following approximations u^{0th}, u^{1st} and u^{2nd}, where higher terms were normalised to be orthogonal to the direct eigenvector and $\tilde{u}^{0th}$, $\tilde{u}^{2nd}$ and $\tilde{u}^{3rd}$ where higher order terms were normalised with respect to the adjoint eigenvector; these equations can be found in (5.25), (5.26) and (5.27), and (5.38), (5.39) and (5.40) respectively.

We firstly concentrate on the spatial structures $\hat{v}_1$, $\hat{v}_2^a$ and $\hat{v}_2^b$ with the direct normalisation and $\tilde{v}_1$, $\tilde{v}_2^a$ and $\tilde{v}_2^b$ with

[2]The analogous equation to (5.16) is given by

$$\mathcal{L}v_2 = \tilde{\delta}C^3\hat{v}_1 + 3C^5\left[\lambda^3\hat{e}_0 - (\hat{e}_0)^2\hat{v}_1\right] + 3C^2\gamma_1(C)\left[\lambda^1\hat{e}_0 - (\hat{e}_0)^3\right] \tag{5.36}$$

We can see that it is the same as (5.16) but with $\lambda_2 = 0$, and also the coefficient of $\tilde{\delta}C^3\hat{v}_1$ is 1 instead of 2. We obtain $\tilde{v}_2^a$ by augmented matrix on the left hand side of

$$\begin{pmatrix} \mathcal{L} & e_0 \\ \langle\hat{e}_0, \cdot\rangle & 0 \end{pmatrix}\begin{pmatrix} \tilde{v}_a^2 \\ c \end{pmatrix} = \begin{pmatrix} \hat{v}_1 + \hat{e}_0 \\ 0 \end{pmatrix} \tag{5.37}$$

where we get $c = 1$; thus the mathematical trick of making this well-posed numerically is to $\hat{e}_0$ to both sides.

the adjoint normalisation. There are two fundamental points of interest that we deliver with relevant figures;

- As the non-normality increases, we see that the spatial structures normalised with respect to the direct eigenvector, $\hat{v}_1$ (Figure 1a), $\hat{v}_2^a$ (Figure 1b) and $\hat{v}_2^b$ (Figure 1c), as well as the spatial structures normalised with respect to the adjoint eigenvectors, $\tilde{v}_1$ (Figure 1d), $\tilde{v}_2^a$ (Figure 1e) and $\tilde{v}_2^b$ (Figure 1f), become more distinct and grow in size. This demonstrates that as the linear operator becomes more non-normal, higher order spatial structures become more important as they exist.

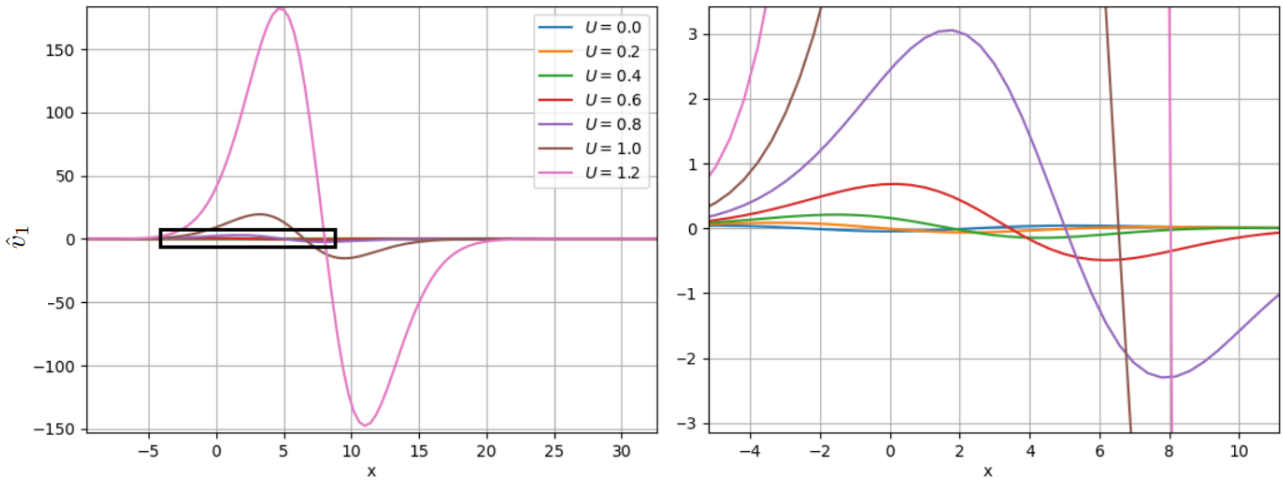

Figure 1a. (Left) A plot of $\hat{v}_1$ against x for various values of U shown in plot. The black box represents the zoomed in area shown in the figure on the right. (Right) A zoomed in region of $\hat{v}_1$ against x.

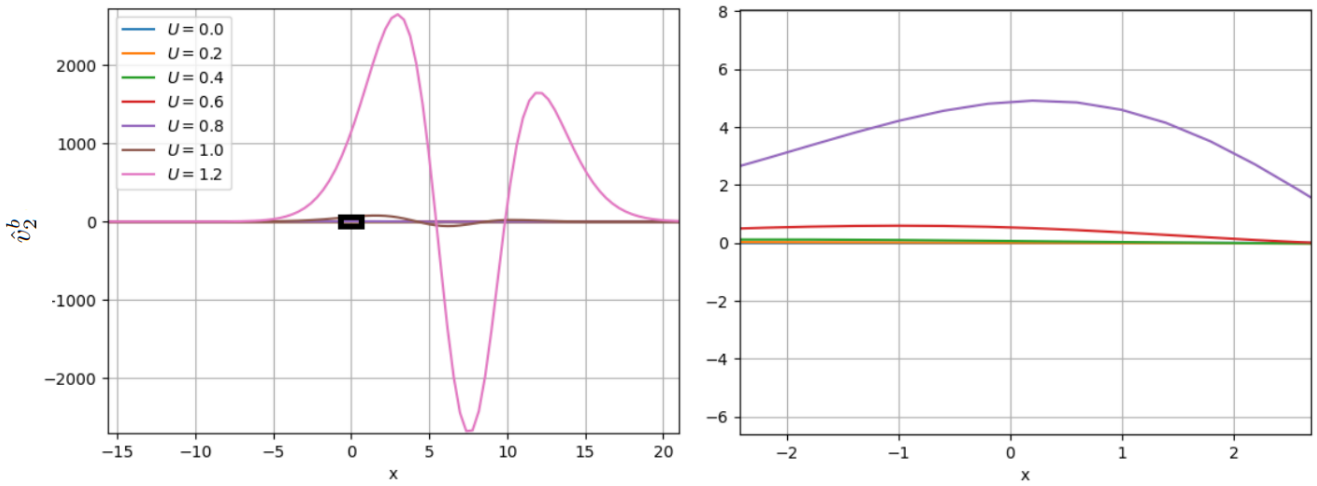

Figure 1b. (Left) A plot of $\hat{v}_2^a$ against x for various values of U shown in plot. The black box represents the zoomed in area shown in the figure on the right. (Right) A zoomed in region of $\hat{v}_2^a$ against x.

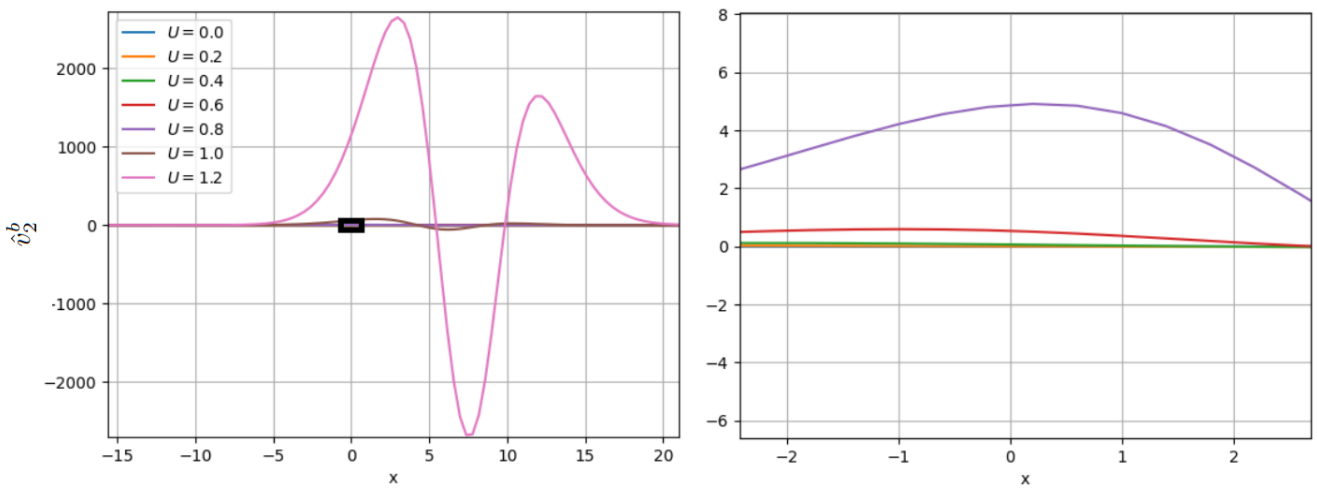

Figure 1c. (Left) A plot of $\hat{v}_2^b$ against x for various values of U shown in plot. The black box represents the zoomed in area shown in the figure on the right. (Right) A zoomed in region of $\hat{v}_2^b$ against x.

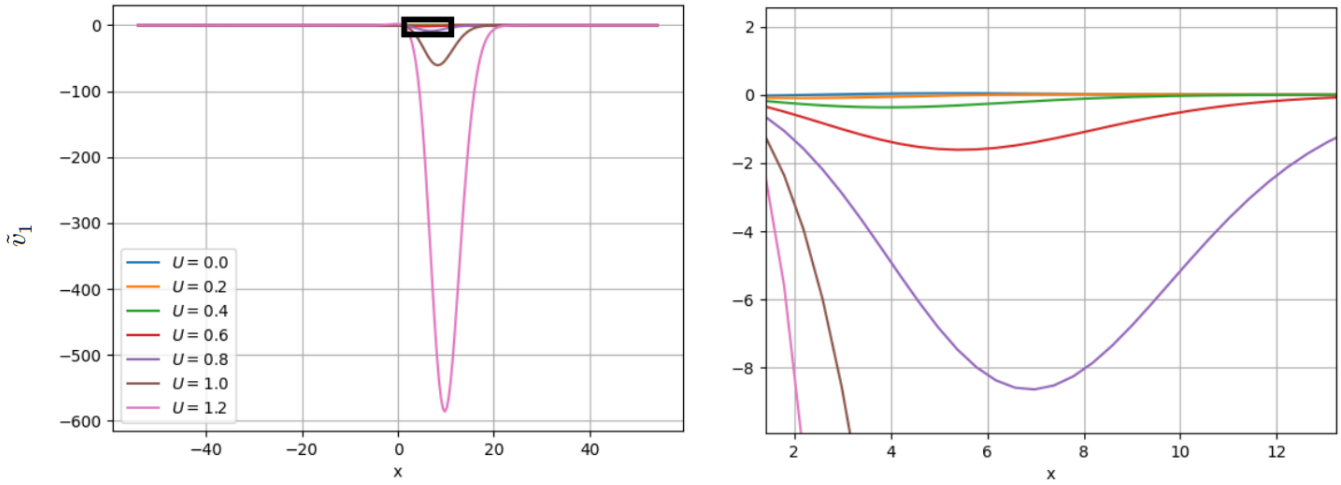

Figure 1d. (Left) A plot of $\tilde{v}_1$ against x for various values of U shown in plot. The black box represents the zoomed in area shown in the figure on the right. (Right) A zoomed in region of $\tilde{v}_1^b$ against x.

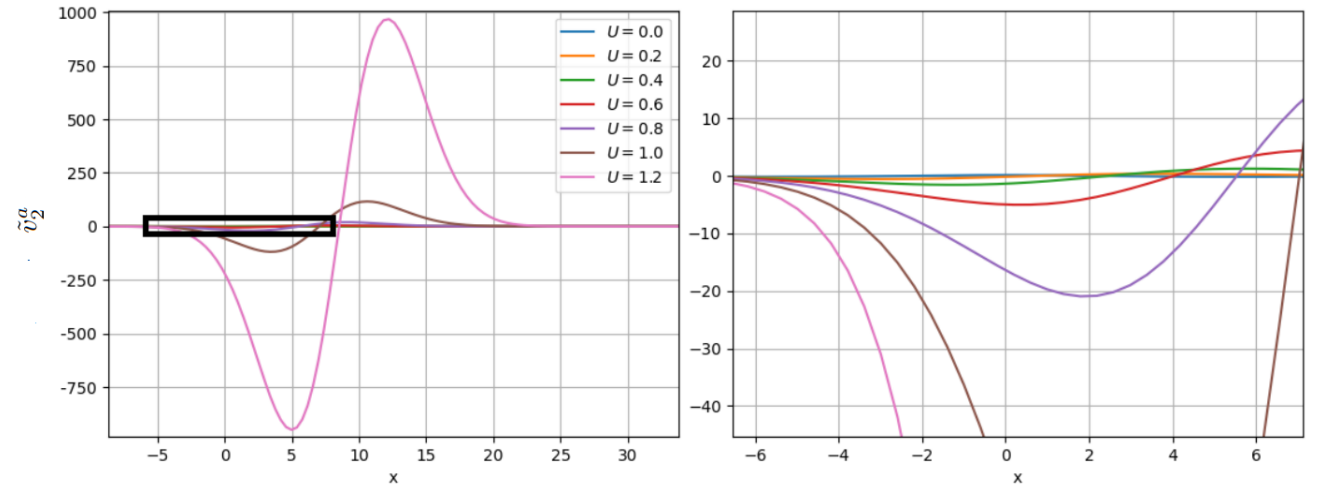

Figure 1e. (Left) A plot of $\tilde{v}_2^a$ against x for various values of U shown in plot. The black box represents the zoomed in area shown in the figure on the right. (Right) A zoomed in region of $\tilde{v}_2^a$ against x.

in area shown in the figure on the right. (Right) A zoomed in region of $\tilde{v}_2^a$ against x.

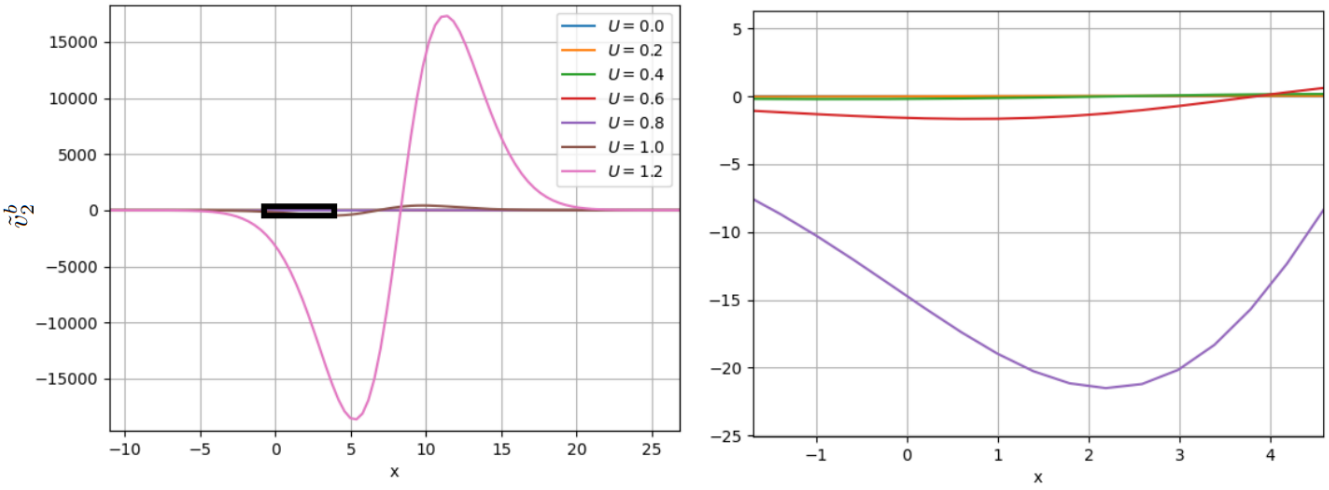

Figure 1f. (Left) A plot of $\tilde{v}_2^b$ against x for various values of U shown in plot. The black box represents the zoomed in area shown in the figure on the right. (Right) A zoomed in region of $\tilde{v}_2^b$ against x.

- We recall that $v_n' = v_n(C, x) + \gamma_n(C)\hat{e}_0$. Let $\tilde{v}_n' = \tilde{v}_n' + \tilde{\gamma}_n(C)\hat{e}_0$. We see that there is no difference in the structures of v_n' and $\tilde{v}_n'$ no matter what the non-normality. We plot these spatial structures for time points $t = 0$, $t = 1000$ and $t = 2000$ for three different values of U, namely $U = 0$, $U = 0.6$ and $U = 1.2$ in Figure 2a, Figure 2b and Figure 2c, respectively, and in each plot the figures overlap. We notice how the spatial structures are exceedingly small for $t = 0$ and $t = 1000$. This is because the energy from the zeroth eigenvector has not been transferred to the other modes by the nonlinearity yet. In Figure 3, we also plot v_2' and $\tilde{v}_2'$ at saturation for $U = 0$, $U = 0.6$ and $U = 1.2$, and again they overlap completely.

  Whilst it is perhaps not a surprising result that our two normalisation choices overlap, it reinforces the notion that there exists a quasi-basis structure underneath. Furthermore, in our subsequent analysis. we only consider one choice of normalisation as the results in terms of proximity to the real solution in norm are the same for both.

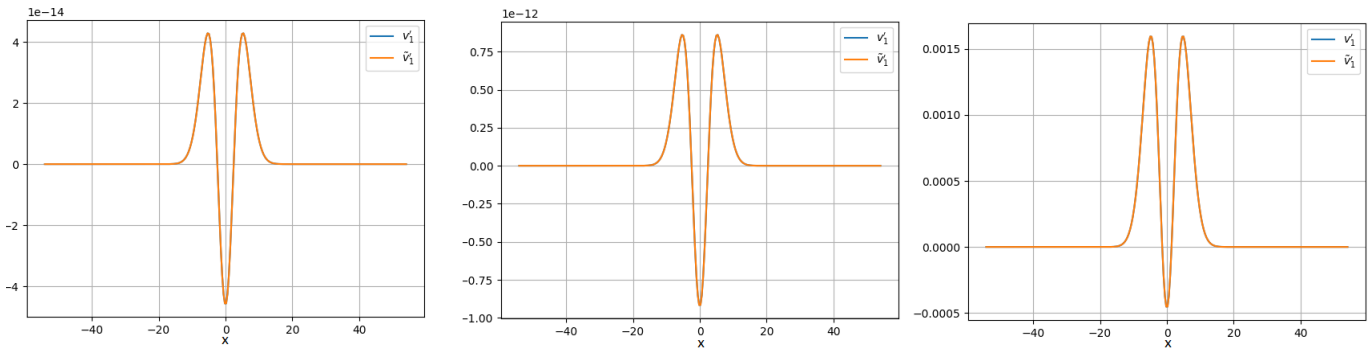

Figure 2a. The spatial structures of $\tilde{v}_1'$ and $\hat{v}_1$ for $U = 0$ at $t = 0$ (left), $t = 1000$ (center) and $t = 2000$ (right).

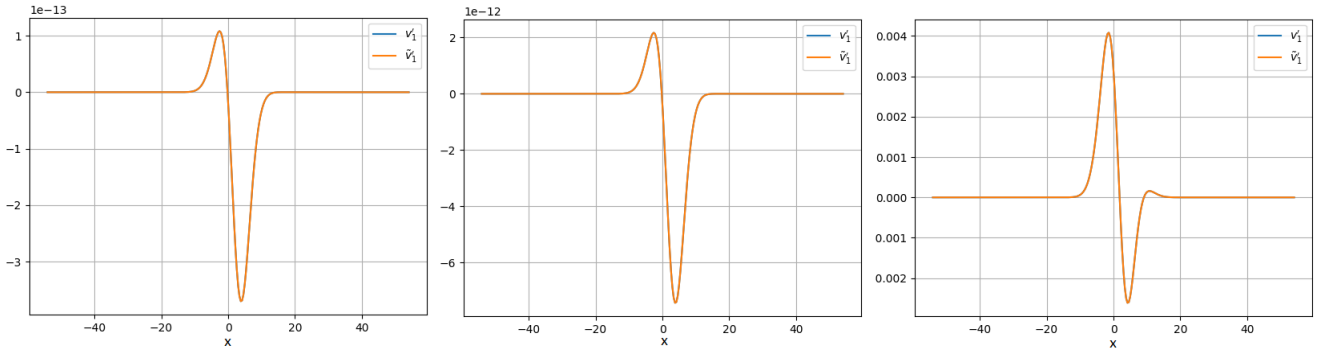

Figure 2b. The spatial structures of $\tilde{v}_1'$ and $\hat{v}_1$ for $U = 0.6$ at $t = 0$ (left), $t = 1000$ (centre) and $t = 2000$ (right).

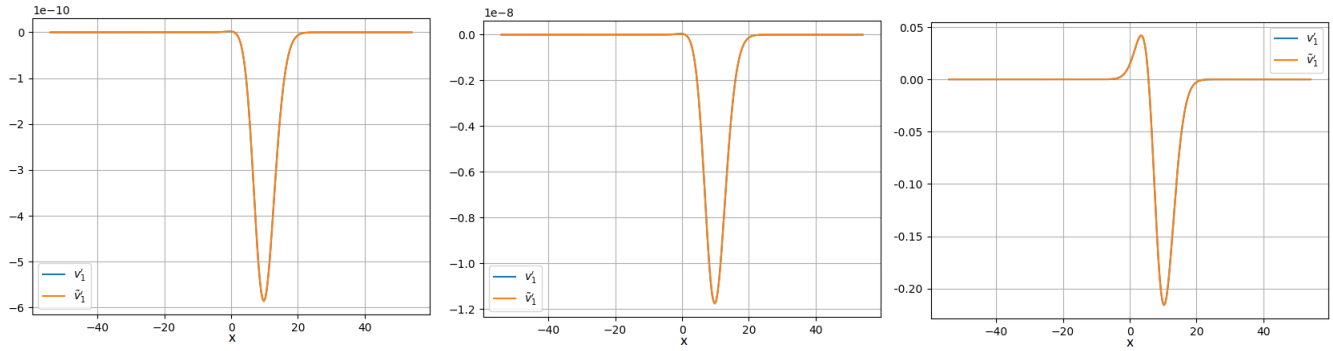

Figure 2c. The spatial structures of $\tilde{v}_1'$ and $\hat{v}_1$ for $U = 1.2$ at $t = 0$ (left), $t = 1000$ (centre) and $t = 2000$ (right).

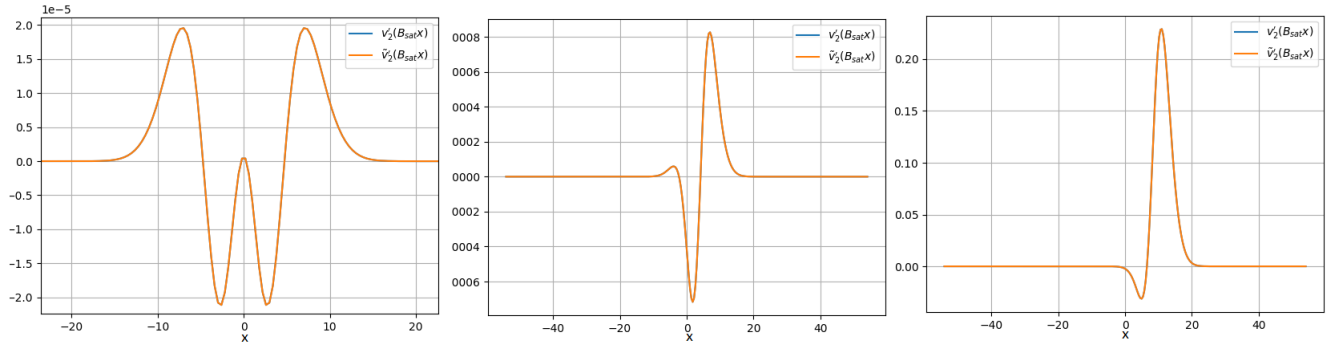

Figure 3. A plot of $v_2'(B_{sat}, x)$ and $\tilde{v}_2'(B_{sat}, x)$ for $U = 0$ (left), $U = 1$ (center) and $U = 2$ (right).

In this thesis, we are concerned with successfully approximating the saturation characteristics. After a certain time, the solution starts converging to particular spatial structure asymptotically hence true saturation time is $t = \infty$, but we are "asymptotically close" earlier in time. We choose T_{sat} as it is the last point in our time domain, $T = 2000$.

We firstly begin by comparing u with the approximations u^{nth} at $T_{sat} = 2000$ in L^2 by considering the difference given by $||u(T_{sat}) - u^{nth}(T_{sat})||_{L^2}$ in Figure 4. The crosses refer to the highest order approximation we derived $||u(T_{sat}) - u^{2nd}(T_{sat})||_{L^2}$ (u^{2nd} is given by (5.27)), and the stars refer to $||u(T_{sat}) - u^{1st}(T_{sat})||_{L^2}$ (u^{1st} is given by (5.26)). The circles refer to $||u(T_{sat}) - u^{0th}(T_{sat})||_{L^2}$ (u^{0th} is given by (5.25)), which is the result that we were trying to improve. In these plots $\delta = 0.01$. All plots are on a logarithmic scale and on the x axis, we have the value

of the advection velocity. The squares refer to $||u||_{L^2}$ and are there as a reference. From Figure 4, we can see that the higher order terms give us the best approximations in all cases apart from $U = 1.2$, which we will discuss imminently with regard to Figure 5. It should be noticed that also in all cases apart from $U = 1.2$ and $U = 1$, the discrepancy reduced by at least one order of magnitude by going higher in order, i.e. the discrepancy for $U = 0$ given by $||u - u^{nth}||_{L^2}$ is of order 10^{-4} for $n = 0$, 10^{-7} for $n = 1$ but nearly 10^{-12} for $n = 2$. For the case of $U = 1$, there is still significant improvement, but not as much, and the improvement is not so important considering the size of u itself. Furthermore, in general, there is a concertina of the different approximations as we go higher in order.

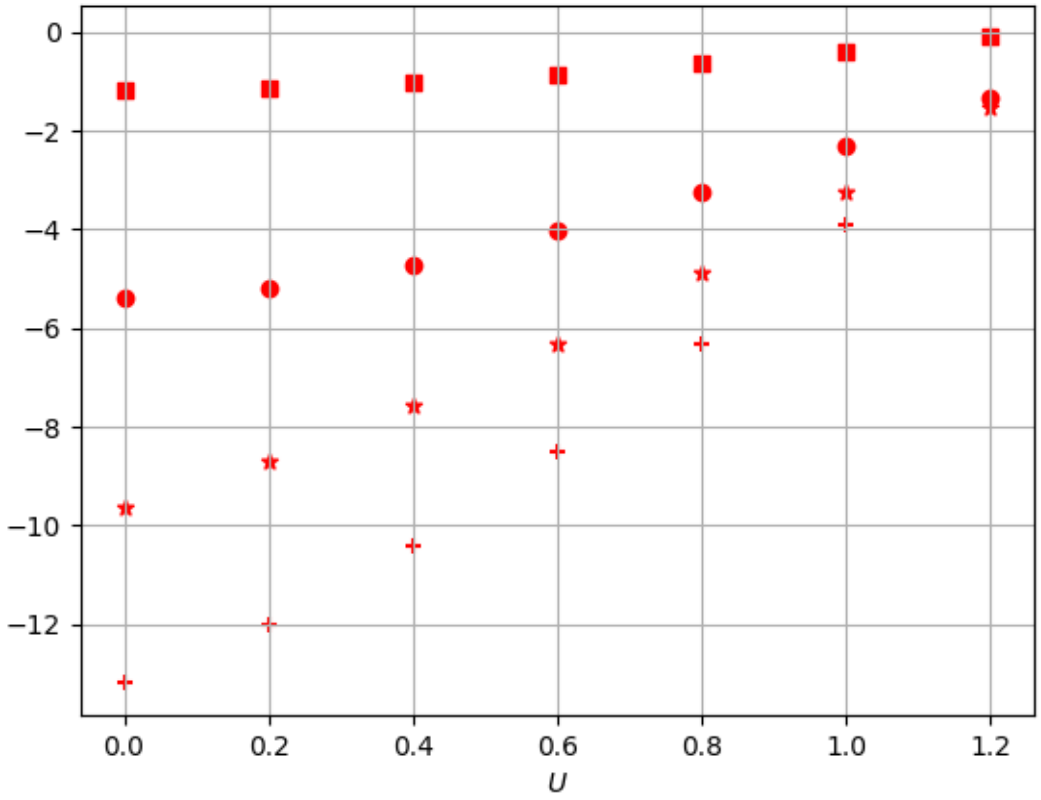

Figure 4. A scatter plot of the following quantities at $T_{sat} = 2000$ against U on a logarithmic scale; Red points: $||u||_{L^2}$ (square), $||u - u^{0th}||_{L^2}$ (filled circle), $||u - u^{1st}||_{L^2}$ (star), $||u - u^{2nd}||_{L^2}$ (cross).

In Figure 5, we plot the spatial profiles for u^{0th}, u^{1st}, and u^{2nd} with u at T_{sat} for $U = 0.6$ and $U = 1.2$. We see for $U = 0.6$. u^{1st} and u^{2nd} improve upon u and capture the solution. However, for $U = 1.2$, the order u^{1st} is a better approximation of the solution than u^{2nd}. However, from the plot the solution u lies "in between" the first and second approximation. This leaves open the possibility that the approximations will successively overestimate and then underestimate before converging to the solution.

We now compare the values of $\sup_{0\leq t\leq T_{sat}} ||u - u^{0th}||_{L^2}$ and $\sup_{0\leq t\leq T_{sat}} ||u - u^{1st}||_{L^2}$ in Figure 6. The key is the same as in Figure 4, and also given in the figure label. This quantity gives us a notion of how the solutions work

over time. We plot this against $\sup_{0\leq t\leq T_{sat}} ||u||_{L^2}$. This plot implies that the assumption regarding the preservation of linear behaviour does not cause anything to go awry. For further evidence of this, we plot the difference between $||u - u^{1st}||_{L^2}$ over time for a range of U values in Figure 7. We see for early times, the graph is flat suggesting that the linear regime has not been contaminated. We see that there is a slight bump for higher order non-normal terms, which suggests that the approximation does not capture well the transition between the linear regime and the nonlinear regime. This feature becomes more exaggerated with non-normality.

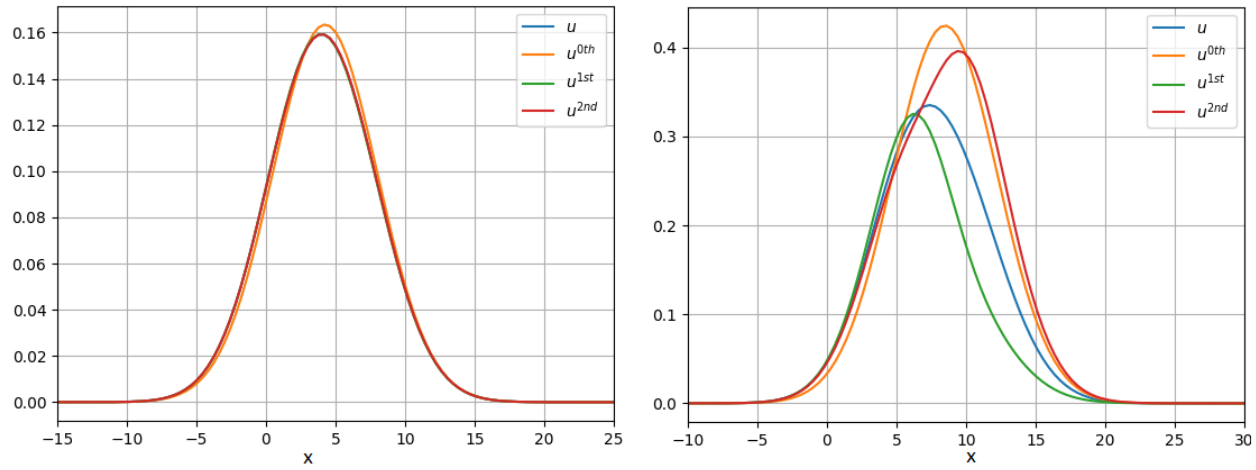

Figure 5. (Left) The spatial structures of u_0, u^{1st}, u^{2nd} and u at T_{sat} for $U = 0.6$ with $\delta = 0.01$. (Right) The spatial structures of u_0, u^{1st}, u^{2nd} and u at T_{sat} for $U = 1.2$ with $\delta = 0.01$.

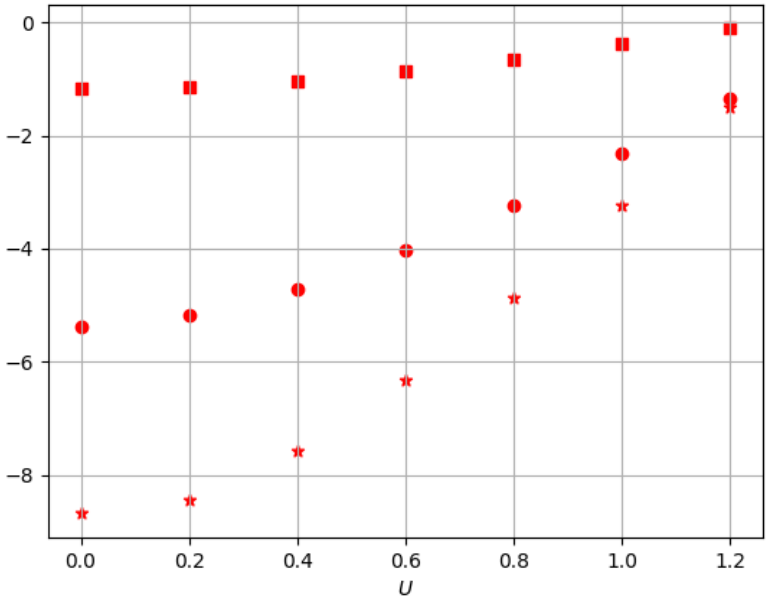

Figure 6. A scatter plot of $\sup_{0\leq t\leq T_{sat}} ||u||_{L^2}$ (square), $\sup_{0\leq t\leq T_{sat}} ||u - u^{0th}||_{L^2}$ (filled circle) and $\sup_{0\leq t\leq T_{sat}} ||u - u^{1st}||_{L^2}$ (star) against U for $\delta = 0.01$

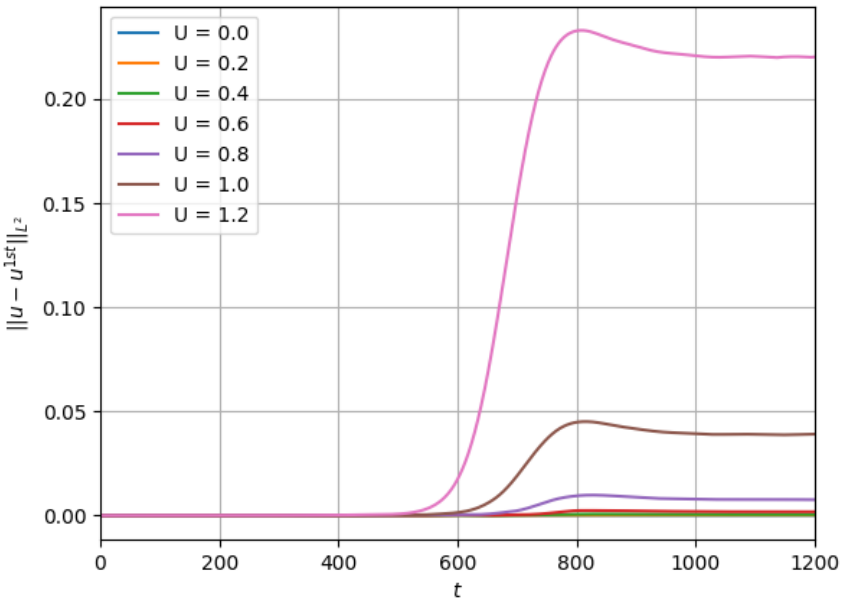

Figure 7. A plot of $||u - u^{1st}||_{L^2}$ for different values of U shown in plot.

In the next set of plots, we increase δ. This has some interesting effects on our approximations. For increased δ and increased U, the higher order approximations are no longer reliable. In Figure 8a, we plot the differences in norm given by $||u(T_{sat}) - u^{nth}(T_{sat})||_{L^2}$, but this time for $\delta = 0.05$. The key is the same as in Figures 4 and 6 and also given in label. In Figure 8b, we plot the the supremum of the difference in norm given by $\sup_{0 \leq t \leq T_{sat}} ||u - u^{0th}||_{L^2}$ and $\sup_{0 \leq t \leq T_{sat}} ||u - u^{1st}||_{L^2}$. As before, all plots are on a logarithmic scale.

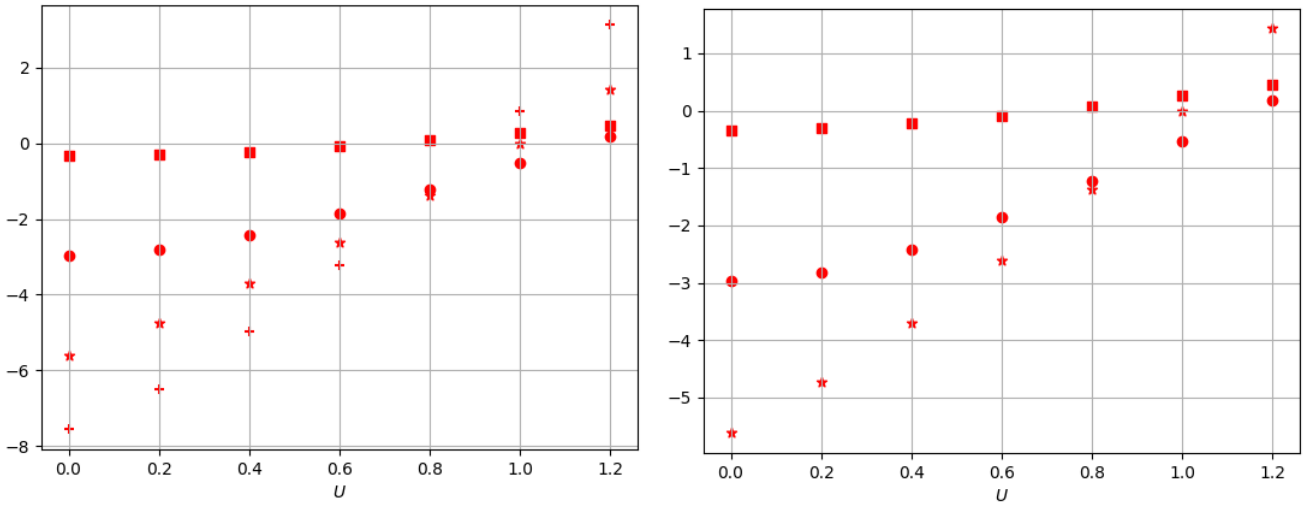

Figure 8. (a) A scatter plot of the following quantities at $T_{sat} = 2000$ against U on a logarithmic scale; $||u||_{L^2}$ (square), $||u - u^{0th}||_{L^2}$ (filled circle), $||u - u^{1st}||_{L^2}$ (star), $||u - u^{2nd}||_{L^2}$ (cross), with $\delta = 0.05$. (b) A scatter plot of $\sup_{0 \leq t \leq T_{sat}} ||u||_{L^2}$ (square), $\sup_{0 \leq t \leq T_{sat}} ||u - u^{0th}||_{L^2}$ (filled circle) and $\sup_{0 \leq t \leq T_{sat}} ||u - u^{1st}||_{L^2}$ (star) againt U with $\delta = 0.05$

In Figure 9, we look more closely at $U = 0.6$ and $U = 1.2$ as we did previously in Figure 5. For $U = 0.6$, the structure u^{2nd} is still the closest, but for $U = 1.2$, u^{2nd} is the worst approximation. In order to explore this further, the convergence of the expansion given by (5.2) must be explored[3].

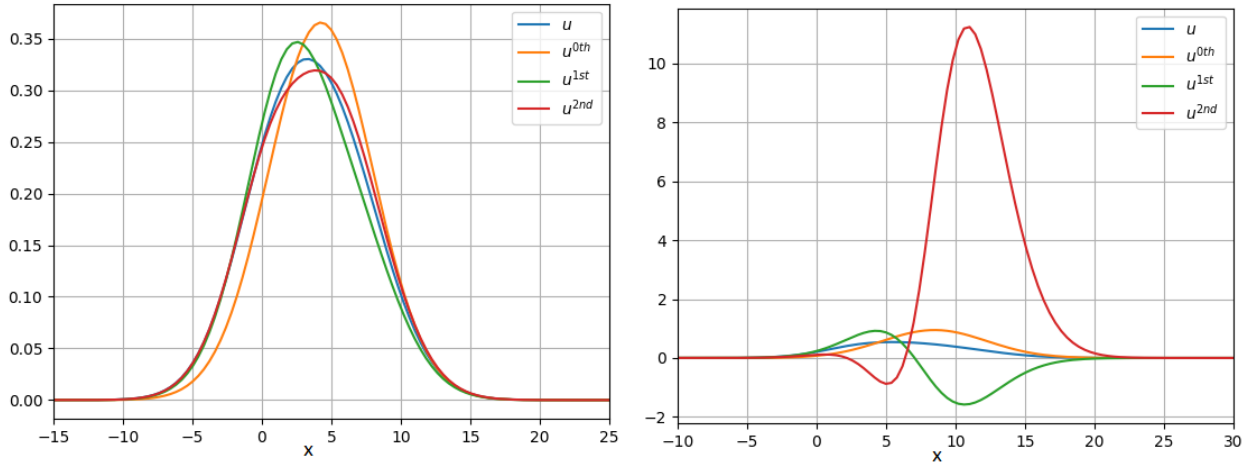

Figure 9. (Left) The spatial structures of u_0, u^{1st}, u^{2nd} and u at T_{sat} for $U = 0.6$ with $\delta = 0.01$. (Right) The spatial structures of u_0, u^{1st}, u^{2nd} and u at T_{sat} for $U = 1.2$ with $\delta = 0.01$.

Lastly, we present a numerical experiment that shows how the solution behaves in the space $\mathcal{H}(G)$. In the following, we plot $||u||_{\mathcal{H}(G)}$, $||u^{0th}||_{\mathcal{H}(G)}$, $||u||_{L^2}$ and $||u^{0th}||$ for $U = 1$. We see in Figure 10 that the approximation and the solution are much closer in the space $\mathcal{H}(G)$. However, one should be aware that this is a non-Hermitian representation of a self-adjoint system. Thus, these norms are not comparable.

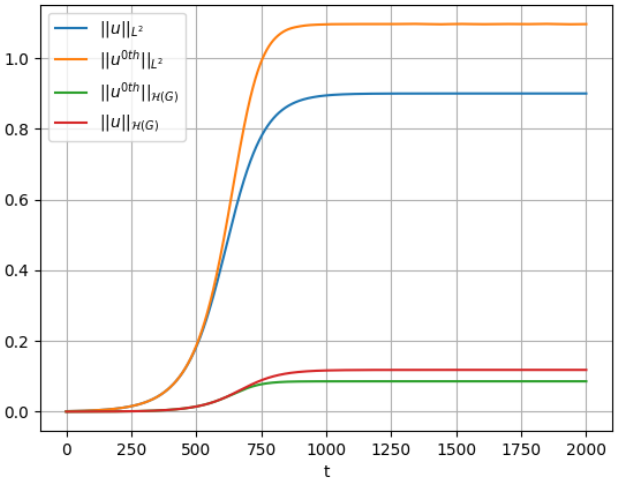

Figure 10. A plot of $||u||_{\mathcal{H}(G)}$, $||u^{0th}||_{\mathcal{H}(G)}$, $||u||_{L^2}$ and $||u^{0th}||$ against time for $U = 1$

[3]We do not explore the convergence in this thesis, but an example of the convergence of a series concerning a linear equation can be found in the article by Vishik and Lyusternik (1960) [100] for an linear elliptic PDE, as mentioned in the literature review. It is not clear to the author how to extend the methodology of Vishik and Lyusternik (1960) [100] to a nonlinear parabolic PDE.

5.2 Complex Case

5.2.1 Derivation

As before, we put the solution on a diffusive timescale $u = e^{i\omega_0 t}\epsilon^{\frac{1}{2}}v(x,\tau)$ but we include an $e^{i\omega_0 t}$ coefficient as the zeroth eigenvector is $i\omega_0$;

$$(i\omega_0 - \mathcal{L}) = -\epsilon\left(\frac{\partial v}{\partial \tau} + \tilde{\delta}v - v^3\right). \tag{5.41}$$

We then expand the solution as

$$v = e^{i(\theta_0+\epsilon\theta_1+\epsilon^2\theta_2+...)\tau}\Big[r\hat{e}_0 + \epsilon(v_1(r,x)+\gamma_1(r)\hat{e}_0) + \epsilon^2(v_2(r,x)+\gamma_2(r)\hat{e}_0) + ...\Big]. \tag{5.42}$$

We compare terms at like orders

- $O(1)$

$$(i\omega_0 - \mathcal{L})\hat{e}_0 = 0 \tag{5.43}$$

- $O(\epsilon)$

$$(i\omega_0 - \mathcal{L})v_1(r,x) = -\left(\frac{\partial r}{\partial \tau} + ir\frac{\partial \theta_0}{\partial \tau}\right)\hat{e}_0 + \tilde{\delta}r\hat{e}_0 - r^3|\hat{e}_0|^2\hat{e}_0 \tag{5.44}$$

  Applying the Fredholm alternative gives

$$\frac{\partial r}{\partial \tau} + ir\frac{\partial \theta_0}{\partial \tau} = \tilde{\delta}r - \langle \hat{e}_0^\dagger, |\hat{e}_0|^2\hat{e}_0\rangle r^3. \tag{5.45}$$

  We let $\lambda^1 = \langle \hat{e}_0^\dagger, |\hat{e}_0|^2\hat{e}_0\rangle$, and consider also the real and imaginary parts $\lambda^1 = \lambda_r^1 + i\lambda_i^1$. This gives us the real and imaginary equations

$$\frac{\partial r}{\partial \tau} = \tilde{\delta}r - \lambda_r^1 r^3 \tag{5.46}$$

  and

$$\frac{\partial \theta_0}{\partial \tau} = -\lambda_i^1 r^2 \tag{5.47}$$

  respectively.

  We put this back into the equation, letting $v_1(x) = r^3\hat{v}_1$ and we get

$$(i\omega_0 - \mathcal{L})\hat{v}_1 = \lambda^1\hat{e}_0 - |\hat{e}_0|^2\hat{e}_0. \tag{5.48}$$

  We invert this matrix to find $\hat{v}_1$ using the condition $\langle \hat{e}_0, \hat{v}_1\rangle = 0$.

- O(ϵ^2)

$$(i\omega_0 - \mathcal{L})v_2(r,x) = -i\left(\frac{\partial\theta_1}{\partial\tau}r\hat{e}_0 + \frac{\partial\theta_0}{\partial\tau}(v_1(r,x)+\gamma_1(r)\hat{e}_0)\right) - \left[\frac{\partial v_1(r,x)}{\partial\tau}\hat{v}_1 + \frac{\partial\gamma_1(r)}{\partial r}\frac{\partial r}{\partial\tau}\hat{e}_0\right]$$
$$- \left(2r^2|\hat{e}_0|^2(v_1(r,x)+\gamma_1(r)\hat{e}_0) + r^2(\hat{e}_0)^2(\bar{v}_1(r,x)+\gamma_1(r)\bar{\hat{e}}_0)\right) + \tilde{\delta}(v_1(r,x)+\gamma_1(r)\hat{e}_0) \quad (5.49)$$

Taking the Fredholm alternative and splitting real and imaginary parts gives us the following two equations

$$\frac{\partial\gamma_1(r)}{\partial r} - \frac{(\tilde{\delta} - 3r^2\lambda_r^1)}{(\tilde{\delta}r - \lambda_r^1 r^3)}\gamma_1(r) = -\frac{2r^3\lambda_r^2\tilde{\delta} - \hat{C}_1 r^5}{(\tilde{\delta}r - \lambda_r^1 r^3)} \quad (5.50)$$

and

$$\frac{\partial\theta_1}{\partial\tau} = \Big(- 2\lambda_i^2\tilde{\delta}r^2 + \tilde{C}_1 r^4 - 2r(\lambda_i^1)\gamma_1(r)\Big) \quad (5.51)$$

where $\hat{C}_1 = (3\lambda_r^2\lambda_r^1 - \lambda_r^3 - \lambda_i^1\lambda_i^2)$ and $\tilde{C}_1 = [3\lambda_i^2\lambda_r^1 + \lambda_r^2\lambda_i^1 - (\lambda_i^3)]$.

Solving this equation by the same procedure as we did in the last section gives us the following form for $\gamma_1(r)$,

$$\gamma_1(r) = \frac{1}{2(\lambda_r^1)^2}\left[(\hat{C}_1 - 2\lambda_r^1\lambda_r^2)\lambda_r^1 r^3 + \hat{C}_1(\tilde{\delta}r - \lambda_r^1 r^3)\log\left(\frac{\tilde{\delta} - \lambda_r^1 r^2}{\tilde{\delta}}\right)\right], \quad (5.52)$$

which we can substitute into (5.51).

Now, have to find an expression for v_2, substituting $\gamma_1(r)$ in (5.49) gives us the following equation

$$(i\omega_0 - \mathcal{L})v_2(r,x) = 2\tilde{\delta}r^3[\lambda^2\hat{e}_0 - \hat{v}_1]$$
$$+ r^5\left[\lambda^3\hat{e}_0 - \left(2|\hat{e}_0|^2\hat{v}_1 + (\hat{e}_0)^2\bar{\hat{v}}_1\right) + \left(3\lambda_r^1 + i\lambda_i^1\right)(\hat{v}_1 - \lambda^2\hat{e}_0)\right] + 3\gamma_1(r)r^2[\lambda^1\hat{e}_0 - |\hat{e}_0|^2\hat{e}_0]. \quad (5.53)$$

From this equation, we can choose an appropriate form of v_2. We $v_2(r,x) = 2\tilde{\delta}r^3 v_2^a + r^5 v_2^b + 3\gamma_1(r)r^2\hat{v}_1$. Then the augmented systems that we consider are

$$\begin{pmatrix}(i\omega_0 - \mathcal{L}) & \hat{e}_0\\ \langle\hat{e}_0,\cdot\rangle & 0\end{pmatrix}\begin{pmatrix}\hat{v}_2^a\\ -\lambda^2\end{pmatrix} = \begin{pmatrix}\hat{v}_1\\ 0\end{pmatrix} \quad (5.54)$$

and

$$\begin{pmatrix}(i\omega_0 - \mathcal{L}) & \hat{e}_0\\ \langle\hat{e}_0,\cdot\rangle & 0\end{pmatrix}\begin{pmatrix}\hat{v}_2^b\\ -\lambda^3\end{pmatrix} = \begin{pmatrix}-\left(2|\hat{e}_0|^2\hat{v}_1 + (\hat{e}_0)^2\bar{\hat{v}}_1\right) + \left(3\lambda_r^1 + i\lambda_i^1\right)(\hat{v}_1 - \lambda^2\hat{e}_0)\\ 0\end{pmatrix}. \quad (5.55)$$

Inverting these matrices on the left of (5.55) and (5.54) gives us the full form of $\hat{v}_2$.

- O(ϵ^3)

$$(i\omega_0 - \mathcal{L})v_3 = -i(v_2 + \gamma_2(r)\hat{e}_0)\left[\frac{\partial\theta_0}{\partial\tau}\right] - i(v_1 + \gamma_1(r)\hat{e}_0)\left[\frac{\partial\theta_1}{\partial\tau}\right] - ir\hat{e}_0\left[\frac{\partial\theta_2}{\partial\tau}\right] - \frac{\partial r}{\partial t}\left[\frac{\partial v_2}{\partial r} + \frac{\partial\gamma_2(r)}{\partial r}\hat{e}_0\right]$$
$$- \left[[2r^2|\hat{e}_0|^2 v_2 + \bar{v}_2(e_0)^2] + 2|v_1 + \gamma_1(r)\hat{e}_0|^2 r\hat{e}_0 + (v_1 + \gamma_1(r)\hat{e}_0)^2 r\bar{\hat{e}}_0] - 3\gamma_2(r(T_{sat}))|\hat{e}_0|^2 e_0\right]$$
$$+ \tilde{\delta}(v_2 + \gamma_2(r)\hat{e}_0) \quad (5.56)$$

By taking the Fredholm alternative and setting $\frac{dr}{d\tau} = 0$, we obtain the following equations for $\gamma_2(r(T_{sat}))$ and $\left[\frac{\partial\theta_2}{\partial\tau}\right]_{r(T_{sat})}$,

$$\gamma_2(r(T_{sat})) = \frac{1}{2\tilde{\delta}}\Re\Big\{\langle\hat{e}_0^\dagger, -i(v_2(r(T_{sat}, x))\left[\frac{\partial\theta_0}{\partial\tau}\right]_{r(T_{sat})} - i(v_1(r(T_{sat}), x) + \gamma_1(r)\hat{e}_0)\left[\frac{\partial\theta_1}{\partial\tau}\right]_{r(T_{sat})}$$
$$- \Big[[2r^2|\hat{e}_0|^2 v_2(r(T_{sat}), x), +\bar{v}_2(r(T_{sat}), x)(e_0)^2]$$
$$+ 2|v_1(r(T_{sat}), x) + \gamma_1(r)\hat{e}_0|^2 r\hat{e}_0 + (v_1(r(T_{sat}), x) + \gamma_1(r(T_{sat}))\hat{e}_0)^2 r(T_{sat})\bar{\hat{e}}_0\Big] + \tilde{\delta}v_2(r(T_{sat}), x)\rangle\Big\} \quad (5.57)$$

and

$$\left[\frac{\partial\theta_2}{\partial\tau}\right]_{r(T_{sat})} = \frac{1}{r(T_{sat})}\Im\Big\{\langle\hat{e}_0^\dagger, -i(v_2(r(T_{sat}), x) + \gamma_2(r(T_{sat}))\hat{e}_0)\left[\frac{\partial\theta_0}{\partial\tau}\right]_{T_{sat}}$$
$$- i(v_1(r(T_{sat}), x) + \gamma_1(r(T_{sat}))\hat{e}_0)\left[\frac{\partial\theta_1}{\partial\tau}\right]_{T_{sat}}$$
$$- \Big[[2r^2(T_{sat})|\hat{e}_0|^2 v_2(r(T_{sat}), x) + \bar{v}_2(r(T_{sat}), x)(e_0)^2]$$
$$+ 2|v_1(r(T_{sat}), x) + \gamma_1(r(T_{sat}))\hat{e}_0|^2 r(T_{sat})\hat{e}_0 + (v_1(r(T_{sat}), x) + \gamma_1(r(T_{sat}))\bar{\hat{e}}_0)^2 r(T_{sat})\bar{\hat{e}}_0\Big]$$
$$- 3\gamma_2(r(T_{sat}))|\hat{e}_0|^2 e_0 + \tilde{\delta}(v_2 + \gamma_2(r)\hat{e}_0)\rangle\Big\} \quad (5.58)$$

We now present the following approximations where we have let $r' = \epsilon^{\frac{1}{2}} r$,

$$u^{0th}(r'(t), t) = e^{i[\omega_0 + \theta_0(r')]t} r'\hat{e}_0, \quad (5.59)$$

$$u^{1st}(r'(t), t) = e^{i[\omega_0 + \theta_0(r') + \theta_1(r')]t}\Big[r'\hat{e}_0 + (v_1(r', x) + \gamma_1(r')\hat{e}_0)\Big], \quad (5.60)$$

and

$$u^{2nd}(r'(T_{sat}),T_{sat}) = e^{i[\omega_0+\theta_0(r'(T_{sat}))+\theta_1(r'(T_{sat}))+_2(r'(T_{sat}))]t}\Bigg[r'(T_{sat})\hat{e}_0 + [\hat{v}_1(r'(T_{sat}),x)+\gamma_1(r'(T_{sat}))\hat{e}_0]+[\hat{v}_2(r'(T_{sat}),x)+\gamma_1(r'(T_{sat})]\Bigg], \quad (5.61)$$

where r' solves

$$\frac{dr'}{dt} = \delta r' - \lambda_r^1 (r')^3. \quad (5.62)$$

We have also that

$$\hat{v}_1(r') = (r')^3 \hat{v}_1, \quad (5.63)$$

$$\hat{v}_2(r') = 2\delta(r')^3 v_2^a + (r')^5 v_2^b + 3\gamma_1(r')(r')^2\hat{v}_1, \quad (5.64)$$

$$\gamma_1(r') = \frac{1}{2(\lambda_r^1)^2}\left[(\hat{C}_1 - 2\lambda_r^1\lambda_r^2)\lambda_r^1(r')^3 + \hat{C}_1(\delta(r') - \lambda_r^1(r')^3\log\left(\frac{\delta-\lambda_r^1(r')^2}{\delta}\right)\right], \quad (5.65)$$

and

$$\gamma_2(r'(T_{sat})) = \frac{1}{2\delta}\Re\Bigg\{\langle\hat{e}_0^\dagger, -i(v_2(r'(T_{sat},x))\left[\frac{\partial\theta_0}{\partial t}\right]_{r'(T_{sat})} - i(v_1(r'(T_{sat}),x)+\gamma_1(r')\hat{e}_0)\left[\frac{\partial\theta_1}{\partial t}\right]_{r'(T_{sat})} - \Bigg[[2r^2|\hat{e}_0|^2 v_2(r'(T_{sat}),x), +\bar{v}_2(r'(T_{sat}),x)(e_0)^2] + 2|v_1(r'(T_{sat}),x)+\gamma_1(r')\hat{e}_0|^2 r'\hat{e}_0 + (v_1(r'(T_{sat}),x)+\gamma_1(r'(T_{sat}))\hat{e}_0)^2 r'(T_{sat})\bar{\hat{e}}_0\Bigg] + \tilde{\delta}v_2(r'(T_{sat}),x)\rangle\Bigg\}, \quad (5.66)$$

where

$$\frac{\partial\theta_0}{\partial t} = -\lambda_i^1(r')^2 \quad (5.67)$$

and

$$\frac{\partial\theta_1}{\partial t} = \Bigg(-2\lambda_i^2\delta(r')^2 + \tilde{C}_1(r')^4 - 2r'(\lambda_i^1)\gamma_1(r')\Bigg). \quad (5.68)$$

Furthermore,

$$\left[\frac{\partial\theta_2}{\partial t}\right]_{r'(T_{sat})} = \frac{1}{r'(T_{sat})}\Im\Big\{\langle\hat{e}_0^\dagger, -i(v_2(r'(T_{sat}),x)+\gamma_2(r'(T_{sat}))\hat{e}_0)\left[\frac{\partial\theta_0}{\partial t}\right]_{T_{sat}}$$
$$- i(v_1(r'(T_{sat}),x)+\gamma_1(r'(T_{sat}))\hat{e}_0)\left[\frac{\partial\theta_1}{\partial t}\right]_{T_{sat}}$$
$$- \Big[[2(r')^2(T_{sat})|\hat{e}_0|^2 v_2(r'(T_{sat}),x)+\bar{v}_2(r'(T_{sat}),x)(e_0)^2]$$
$$+ 2|v_1(r'(T_{sat}),x)+\gamma_1(r'(T_{sat}))\hat{e}_0|^2 r'(T_{sat})\hat{e}_0 + (v_1(r'(T_{sat}),x)+\gamma_1(r'(T_{sat}))\bar{\hat{e}}_0)^2 r'(T_{sat})\bar{\hat{e}}_0\Big]$$
$$- 3\gamma_2(r'(T_{sat}))|\hat{e}_0|^2 e_0 + \delta(v_2(r'(T_{sat}),x)+\gamma_2(r')\hat{e}_0)\rangle\Big\}. \quad (5.69)$$

We have that as $t \longrightarrow \infty$, (the "value" of T_{sat}),

$$\theta_0 \sim -\lambda_i^1(r'(T_{sat}))^2, \quad (5.70)$$

$$\theta_1 \sim \Big(- 2\lambda_i^2\delta(r')^2 + \tilde{C}_1(r')^4 - 2r'(\lambda_i^1)\gamma_1(r')\Big) \quad (5.71)$$

and

$$\theta_2 \sim \frac{1}{r'(T_{sat})}\Im\Big\{\langle\hat{e}_0^\dagger, -i(v_2(r'(T_{sat}),x)+\gamma_2(r'(T_{sat}))\hat{e}_0)\left[\frac{\partial\theta_0}{\partial t}\right]_{T_{sat}}$$
$$- i(v_1(r'(T_{sat}),x)+\gamma_1(r'(T_{sat}))\hat{e}_0)\left[\frac{\partial\theta_1}{\partial t}\right]_{T_{sat}}$$
$$- \Big[[2(r')^2(T_{sat})|\hat{e}_0|^2 v_2(r'(T_{sat}),x)+\bar{v}_2(r'(T_{sat}),x)(e_0)^2]$$
$$+ 2|v_1(r'(T_{sat}),x)+\gamma_1(r'(T_{sat}))\hat{e}_0|^2 r'(T_{sat})\hat{e}_0 + (v_1(r'(T_{sat}),x)+\gamma_1(r'(T_{sat}))\bar{\hat{e}}_0)^2 r'(T_{sat})\bar{\hat{e}}_0\Big]$$
$$- 3\gamma_2(r'(T_{sat}))|\hat{e}_0|^2 e_0 + \delta(v_2(r'(T_{sat}),x)+\gamma_2(r')\hat{e}_0)\rangle\Big\} \quad (5.72)$$

5.2.2 Numerical Experiments

In the previous section, we obtained the following approximations u^{0th}, u^{1st} and u^{2nd}. In this section, we test these approximations against the solution.

We firstly begin by comparing saturation frequency. As addressed in the introduction, if we decompose the solution as $u = Re^{i\Phi}$. We compute the fast Fourier transforms of $e^{i\theta^{nth}}$ at where the saturation frequencies θ^{nth} given by $\theta_0^{th} = \omega_0 + \theta_0$, $\theta^{1st} = \omega_0 + \theta_0 + \theta_1$ and $\theta^{2nd} = \omega + \theta_0 + \theta_1 + \theta_2$, as well as the Fast Fourier transform of the solution at solution at a point in the domain where the signal was of significant strength. We computed the signal between $t = 1750$ and $t = 2000$ as the flow is saturated during these times. In Table 1, we plot these frequencies.

Frequency(Hz)	U						
	0.0	0.2	0.4	0.6	0.8	1.0	1.2
$e^{i\theta^{0th}t}$	0.006	0.0004	0	-0.006	-0.0014	-0.0022	-0.0032
$e^{i\theta^{1st}t}$	0.006	0.0004	0	-0.006	-0.0014	-0.0022	-0.0032
$e^{i\theta^{2nd}}$	0.006	0.0004	0	-0.006	-0.0014	-0.0022	-0.0032
u	0.006	0.0004	0	-0.006	-0.0014	-0.0022	-0.0032
$e^{i\omega_0 t}$	0.006	0.0004	0	-0.006	-0.0014	-0.0022	-0.0032

Figure 1. A table of the frequencies in Hz computed via the FFT in python. The values of u are shown in plot with $\delta = 0.01$

We see that the frequency is well approximated no matter the order of the expansion. We relate this to the plots shown in the introduction where the linear operator governing the frequency demonstrates less transient growth when the norm of the semigroup is calculated.

In Figure 2, we consider the difference in amplitude, let $r^{nth} = |u^{nth}|$. We then compare $||R - r^{nth}||_{L^2}$ where n refers to the order of the approximation. In this way, we remove any difference in energy that may be attributed to the graphs being out of phase. We begin by comparing this quantity at $T_{sat} = 2000$, as in the last section. The crosses refer to the highest order approximation we derived $||R(T_{sat}) - r^{2nd}(T_{sat})||_{L^2}$ ($r^{2nd} = |u^{2nd}|$ where u^{2nd} is given by (5.61)), and the stars refer to $||r(T_{sat}) - R^{1st}(T_{sat})||_{L^2}$ ($r^{1st} = |u^{1st}|$ where u^{1st} is given by (5.60)). The circles refer to $||r(T_{sat}) - r^{0th}(T_{sat})||_{L^2}$ ($r^{0th} = |u^{0th}|$ where u^{0th} (5.59)), which is the result that we were trying to improve. As before, we have given the $||r||_{L^2}$ as a reference. We notice that there is generally an improvement between the approximation r^{0th} and the approximations r^{1st} and r^{2nd}, but sometimes the approximation r^{1st} is better that r^{2nd} on the logarithmic scale, but in these cases the differences are really minute. In Figure 3, we investigate this further by plotting $\log(|r(T_{sat}) - r^{1st}(T_{sat}|)$ (blue) and $\log(|r(T_{sat}) - r^{2nd}(T_{sat})|)$ (orange) against x for $U = 1$ (left) and $U = 1.2$. We see that we cannot tell the difference between plots in this case as they overlap. In Figure 4, we plot $\sup_{0 \leq T_{sat}} ||R - r^{nth}||_{L^2}$ for a variety of U-values where $n = 0$ and $n = 1$. This is a measure of how the approximation performs over time. We see that u^{1st} performs better that u^{0th} for all values of U considered.

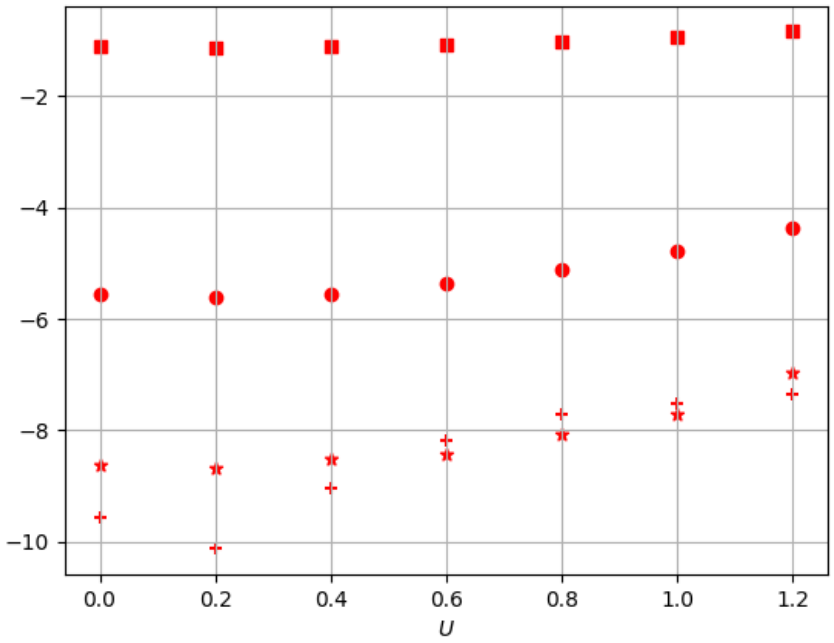

Figure 2. A scatter plot of the following quantities at $T_{sat} = 2000$ against U on a logarithmic scale; Red points: $||R||_{L^2}$ (square), $||R - r^{0th}||_{L^2}$ (filled circle), $||R - r^{1st}||_{L^2}$ (star), $||R - r^{2nd}||_{L^2}$ (cross). In both cases, $\delta = 0.01$.

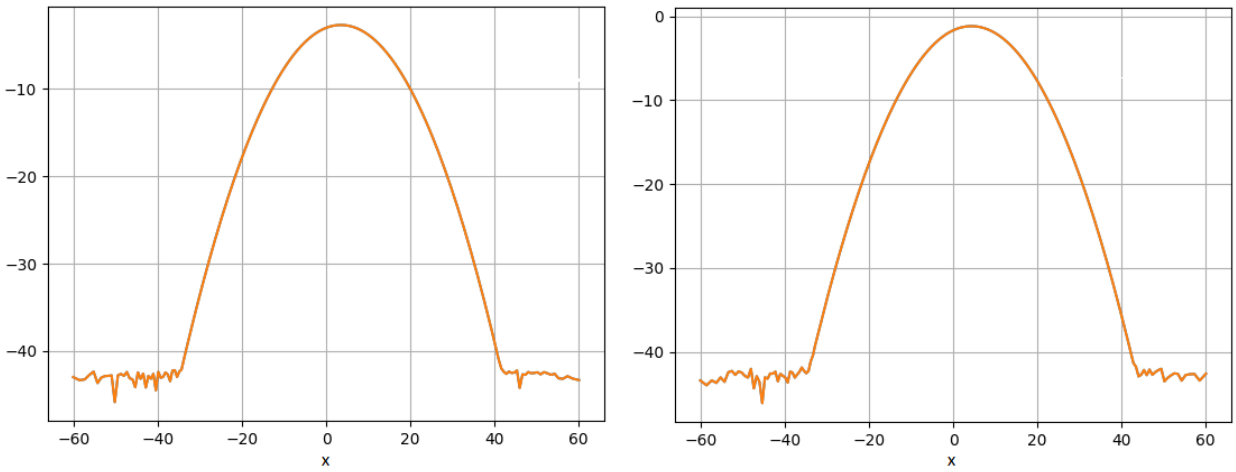

Figure 3. A plot of $\log(|r(T_{sat}) - r^{1st}(T_{sat}|)$ (blue) and $\log(|r(T_{sat}) - r^{2nd}(T_{sat})|)$ (orange) against x for $U = 1$ (left) and $U = 1.2$. In both cases $\delta = 0.01$.

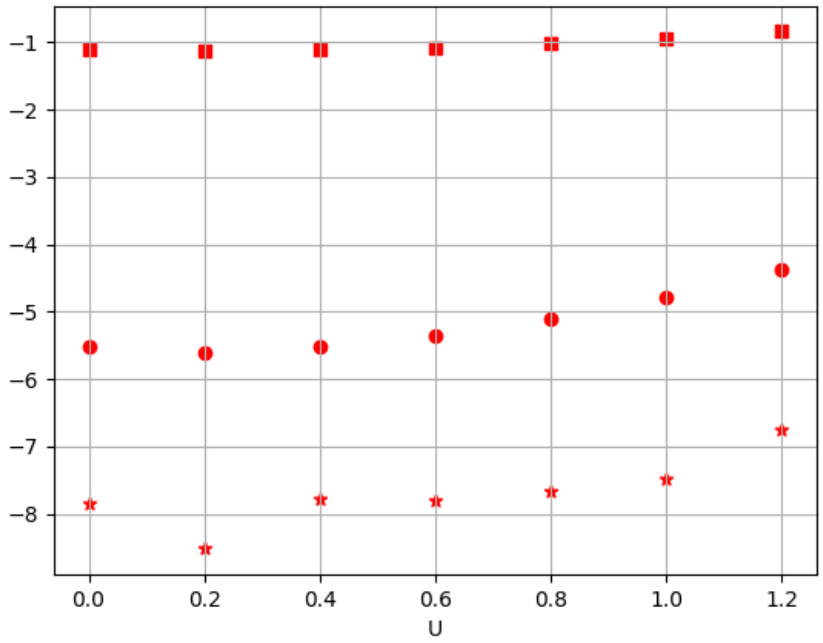

Figure 4. A scatter plot of $\sup_{0\leq t\leq T_{sat}} ||u||_{L^2}$ (square), $\sup_{0\leq t\leq T_{sat}} ||u-u^{0th}||_{L^2}$ (filled circle) and $\sup_{0\leq t\leq T_{sat}} ||u-u^{1st}||_{L^2}$ (star) for various values of U with $\delta = 0.01$.

5.3 Summary of Chapter

In this chapter, we have showcased the derivation of higher order approximations for the RnsaGL and CnsaGL using a method that has not been used before. We also showed a consequence of the quasi-basis structure that exists for the RnsaGL, that we were able to normalise the higher order terms in the expansion in two ways, namely for the terms to be orthogonal to the zeroth direct eigenvector or the zeroth adjoint eigenvector. We then explored these approximations via numerical experiments. In the case of the RnsaGL, we found that the higher order approximations generally provide an improvement to the first order WNLE expansions derived in the introduction. The only suspect cases were the extreme values of U and δ that we considered; but, without considering the convergence of the series expansion given by (5.2), we cannot know the nature of these suspect cases. i.e. is it the case that the expansion will oscillate to the solution or whether or not we are outside of the radius of convergence. In the complex case, we saw the phenomena outlined in the introduction as in that the frequency is well-approximated no matter the non-normality. Lastly, it should be noted we do not have the two choices of normalisation in the case of CnsaGL. The reader is invited to try the expansion for themselves and one can see the results are not particularly useful. We suspect that this is basis property does not exist as the complexity is significant in the case of Krejcirik

and Siegl (2019) [60]. [4]. An interpretation of the fact we get nonsensical results with by normalising $\hat{v}_1$, $\hat{v}_2$ etc. to be orthogonal to $\hat{e}_0^\dagger$ is that this normalisation causes spatial contributions along $\hat{e}_0^\dagger$ to be missed. These will not be compensated by the terms $\gamma_1(C)\hat{e}_0$, $\gamma_2(C)\hat{e}_0$, etc. as they are in the case of the RnsaGL.

[4] A result that would ensure that a quasi-basis structure does not exist in the case of the CnsaGL would be to prove the non-existence of the metric operator. Results that the non-existence of the metric operator for the imaginary cubic oscillator can be found in the paper by Krejcirik and Siegl (2012) [91]. In the conclusion, we discuss this more in the context of a future project.

Chapter 6

Error Bound Analysis

In this chapter, there are two sections. In the first section, we derive error bounds for the RnsaGL via a bootstrapping argument. We restrict our studies to the RnsaGL (hence we drop the superscripts) in this case but the same methodology can be applied to the CnsaGL. The process of deriving error bounds for amplitude equation is fairly standard and based on a bootstrap argument. An interested reader can see the example of Kirrmann et al. (1992) [58] for an example that follows ours extremely closely. However, there are other notable examples in Schneider (1994a) [84], Schneider (1994b) [85] and Mielke et al. (1995) [68]. In the second section, we consider the practicality of these error bounds. The need for this is based in the fact that error bounds between approximations and solutions generally tell us that there exists a radius of convergence for the small parameter ϵ where an approximation is within a fixed distance to the solution of the governing equation in norm, but not what the radius of convergence is[1]. We explore the question that, given a solution and an means of calculating an approximation, can we tell how high we need to go in the order of the approximation or what is the range of ϵ we can take using the error bounds?

6.1 Error Bound Derivation

In this section, we prove that there exists a radius of convergence for the parameter ϵ for which. When the value of ϵ is with this radius, the difference between the solution and the approximation in norm is below a particular threshold. For our purposes, we use the L^2-norm, which shows that the are close in terms of energy[2].

[1] For clarity, we distinguish two notions of the radius of convergence here. The first notion is the radius of convergence can be given by the ϵ chosen such that the series given by (5.2) converges. We explored this using the uniform convergence criterion for higher order amplitude equations in chapter two. The error bounds that we derive give a fixed distance between the approximation and the solution dependent on a small parameter. For certain values of the small parameter, the difference between the solution and approximation is below a certain threshold. Thus it is up to us what discrepancies are tolerable. We refer to values that the small parameter can take also as the radius of convergence and that is what we will be considering in this chapter. Both of these criteria give conditions for the size of the small parameter, in our case ϵ, but the latter often comes from practical application.

[2] We remark that equally we could have used the L^1 norm which quantifies the difference between the solutions along the entire domain. Semigroups bounds behave differently in different norms as demonstrated in Davies (2005) [33].

We start by defining the following quantities

$$u'_n = \epsilon^{\frac{1}{2}+n} v'_n \tag{6.1}$$

where the v'_n are defined in (5.2). We then define the sum

$$U_N = \sum_{n=0}^{N} u'_n = \sum_{n=0}^{N} \epsilon^{\frac{1}{2}+n} v'_n. \tag{6.2}$$

We now derive the error bounds in the following theorem,

- Theorem (Traditional Error Bounds). Let u be a solution of the RnsaGL and U_N be the expansion defined in (6.2). Let the initial data be such that $||u(0,x) - u_N(0,x)||_\alpha \leq d\epsilon^N$. Then, for each $T > 0$ and $d > 0$, there exists an $\epsilon \in (0, \epsilon_0)$ and a $C > 0$ such that the estimate

$$||u(t) - U_N(t)||_{L^2} \leq C\epsilon^N, \qquad \forall \quad (t,x) \in [0,T] \times \mathbb{R} \tag{6.3}$$

is satisfied.

Proof. The goal of this proof is to establish the size of the relative error $u(t,x) - u_N(t,x)$ in norm. If we substitute just $u_N(t,x)$ we are left with a residual term, so it is simpler to take the next order expansion and then use a further argument to infer the size of $u(t,x) - u_N(t,x)$. We let

$$u = U_{N+1} + \epsilon^N R, \tag{6.4}$$

where R stands for the residual. We put this into the RnsaGL in order to get the following equation

$$\frac{dR}{dt} = \mathcal{L}R + \delta R + N(U_{N+1}(\epsilon, t), R(t)) \tag{6.5}$$

where

$$\begin{aligned} N(U_{N+1}(\epsilon,t), R(t)) &= \frac{1}{\epsilon^N}\left[-\frac{dU_{N+1}}{dt} + \delta U_{N+1} - (U_{N+1} + \epsilon^N R)^3 \right] && (6.6) \\ &= \frac{1}{\epsilon^N}\left[\left(-\frac{\partial u'_{N+1}}{\partial t} + \delta u'_{N+1} + \sum_{n=0}^{N} \left(\sum_{i=0}^{n} \sum_{k=0}^{n-i} u'_i u'_k u'_{n-i-k} \right) \right) - u^3 \right], && (6.7) \end{aligned}$$

where the square brackets contain terms of ϵ^{N+1} or higher. Importantly, in (6.5), we have no terms of order $\epsilon^{\frac{1}{2}}$.

We split the operator $\mathcal{L}$ into $\hat{\mathcal{L}}_n + (\mathcal{L} - \hat{\mathcal{L}}_n)$ where $\hat{\mathcal{L}}_n$ was the sectorial operator defined in Section 3.1 of the

thesis. We label $C_1 = (\mathcal{L} - \hat{\mathcal{L}}_n) + \delta$. Then from the results of Section 3.3, we can write our equation in integral form as

$$R(x,t) = e^{t\hat{\mathcal{L}}_n} R(x,0) + \int_0^t e^{(t-s)\hat{\mathcal{L}}_n} \Big[C_1 R + N(U_{N+1}(\epsilon,t), R(t)) \Big] ds. \tag{6.8}$$

We consider the L^2 norm of the above equation in order to obtain

$$||R(x,t)|| \leq ||e^{t\hat{\mathcal{L}}_n} R(x,0)|| + || \int_0^t e^{(t-s)\hat{\mathcal{L}}_n} \Big[C_1 R + N(U_{N+1}(\epsilon,t), R(t)) \Big] ds|| \tag{6.9}$$

Then, for every $D_1 > 0$, we have that $\sup_{0\leq s\leq t}\{||N(U_{N+1}(\epsilon,t), R(t))||_{L^2}\} \leq M(\epsilon)$ for all $||R||_{L^2} \leq D_1$. As $\hat{\mathcal{L}}_n$ is a contraction, we have the following inequality

$$||R(x,t)||_{L^2} \leq \Big[(d + M(\epsilon)t) + C_1 \int_0^t ||R(x,t)||_{L^2} ds \Big]. \tag{6.10}$$

We use Gronwall's inequality to write the equation as

$$||R(x,t)||_{L^2} \leq (d + M(\epsilon)t) e^{C_1 t}. \tag{6.11}$$

The bootstrapping occurs as follows; let ϵ be chosen such that $M(\epsilon) < M$. Let $D_2 = (d + Mt)e^{C_1 t}$. Then it follows that $||R(x,t)||_{L^2} \leq D_2$. However, the bound (6.11) is more strict, and so it follows that $||R(x,t)||_{L^2} \leq D_2$.

Using the triangle inequality with $u - U_N = u - U_{N+1} + u'_{N+1}$, we have that therefore the difference between the approximation U_N and u is

$$||u(t) - U_N(t)||_{L^2} \leq \epsilon^N (d + Mt) e^{C_1 t} + ||u'_{N+1}(x,t)||_{L^2}, \tag{6.12}$$

where we can write

$$||u(t) - U_N(t)||_{L^2} \leq C\epsilon^N \tag{6.13}$$

with absorbing constant $C = (d + MT)e^{C_1 T} + ||u'_{N+1}(x,t)||_{L^2}$ for specific fixed T. □

6.2 Error Bound Functionality

In the last section, we established that there exists a radius of convergence. In this section, we focus on the utility of error bounds, i.e. "can we use the error bounds derived in the last section to ascertain what values of ϵ or what order we need to go to, so that the approximation works well?".

We begin by considering the following error bound that was derived in the last section;

$$||u(t) - U_{N+1}(t)||_{L^2} \leq \epsilon^N (\sup_{0\leq s\leq t} \{||N(U_{N+1}(\epsilon,t), R(t))||_{L^2}\}t) e^{C_1 t} \tag{6.14}$$

where we have just replaced all of the quantities in (6.11) by there explicit forms and set $d = 0$ as the governing equation and the approximation are initialised in the same way. As $C_1 = \frac{U^2}{4} + \sqrt{c_2} + \delta + 1$, we see from the right-hand-side of (6.15) that the error bound is governed by the U and δ, T_{sat} (we do not vary c_2). Also, we recall $\delta = \tilde{\delta}\epsilon$.

We begin by defining the right-hand-side of (6.14) as $\mathcal{F}(t)$.

$$\mathcal{F}(N,\epsilon,t) = \epsilon^N (\sup_{0\leq s\leq t} \{||N(U_{N+1}(\epsilon,t), R(t))||_{L^2}\}t) e^{C_1 t}. \tag{6.15}$$

In the following numerical computations, we vary U and δ to see how $\mathcal{F}(N.\epsilon,t)$ We also consider different values of t. We fix N to obtain

$$||N(U_1(\epsilon,t), R(t))||_{L^2} = -\frac{\partial u_1'}{\partial t} + \delta u_1' + u_0^3 - u^3 \tag{6.16}$$

for $N = 0$ and

$$||N(U_2(\epsilon,t), R(t))||_{L^2} = ||\bigg(- \frac{\partial u_2'}{\partial t} + \delta u_2' + u_0^3 + 3u_0^2 u_1 - u^3 \bigg)||_{L^2} \tag{6.17}$$

for[3] $N = 1$.

[3]For the purposes of this section, we computed $u_2'(x,t) = v_2(x,t) + \gamma_2(B)\hat{e}_0$. $v_2(B)$ was given in the previous chapter, but $\gamma_2(B)$ was only calculated at saturation. Applying our normalisation procedure gives

$$\begin{aligned}
\gamma_2(B) = -\frac{\delta}{2(\lambda^1)^2}\Big[&18\langle \hat{e}_0^\dagger, (\hat{e}_0)^2 v_2^b\rangle + 6(C^A)^2\lambda^1 + \lambda^1[6\langle \hat{e}_0^\dagger, (\hat{e}_0)^2 v_2^a\rangle - 18\langle \hat{e}_0^\dagger, v_2^b\rangle - 2\langle \hat{e}_0^\dagger, v_2^a\rangle\lambda^1] - 18C^A\lambda^1\lambda^2 + 30C^A\lambda^3 \\
&+ 6C^A C^B(\lambda^1)^2 + 3C^B\lambda^1[2C^B(\lambda^1)^2 - 3\lambda^1\lambda^2 + 5\lambda^3] + 6\langle \hat{e}_0^\dagger, \hat{v}_1\hat{v}_1\hat{e}_0\rangle\Big]B^3 \\
&\frac{3}{2(\lambda^1)}\Big[\Big(3\langle \hat{e}_0^\dagger, \hat{e}_0\hat{e}_0 v_2^b\rangle + (C^A)^2\lambda^1 - 5\langle \hat{e}_0^\dagger, v_2^b\rangle\lambda^1 + C^A(2C^B(\lambda^1)^2 - 5(\lambda^1)(\lambda^2) + 5\lambda^3) \\
&+ C^B\lambda^1(2C^B(\lambda^1)^2 - 3(\lambda^1)(\lambda^2) + 5\lambda^3) + \langle \hat{e}_0^\dagger, \hat{v}_1\hat{v}_1\hat{e}_0\rangle\Big)\Big]B^5 \\
&- \frac{3\delta}{2(\lambda^1)^3}\Big[6\langle \hat{e}_0^\dagger, (\hat{e}_0)^2 v_2^b\rangle + 2(C^A)^2\lambda^1 + 2C^A(C^B(\lambda^1)^2 - 3\lambda^1\lambda^2 + 5\lambda^3) + 2\langle \hat{e}_0^\dagger, \hat{v}_1\hat{v}_1\hat{e}_0\rangle \\
&+ \lambda^1[2\langle \hat{e}_0^\dagger, (\hat{e}_0)^2 v_2^a\rangle - 6\langle \hat{e}_0^\dagger, v_2^b\rangle - 2\langle \hat{e}_0^\dagger, v_2^a\rangle\lambda^1 + 2(C^B)^2(\lambda^1)^2 - 3C^B\lambda^1\lambda^2 + 5C^B\lambda^3]\Big](\tilde{\delta}B - \lambda^1 B^3)\log\Big(\frac{\delta - \lambda^1 B^2}{\delta}\Big) \\
&+ \frac{3}{2(\lambda^1)}\Big[C^B(2C^A\lambda^1 + 2C^B(\lambda^1)^2 - 5\lambda^1\lambda^2 + 5\lambda^3)\Big](\delta B - \lambda^1 B^3)B^2\log\Big(\frac{\delta - \lambda^1 B^2}{\delta}\Big) \\
&- \frac{3\delta}{4(\lambda^1)^2}C^B\Big(-2C^A\lambda^1 + (3\lambda^1\lambda^2 - 5\lambda^3)\Big)(\delta B - \lambda^1 B^3)\Big[\log\Big(\frac{\delta - \lambda^1 B^2}{\delta}\Big)\Big]^2 \\
&+ \frac{3}{2}(C^B)^2(\delta - \lambda^1 C^2)(\delta B - \lambda^1 B^3)\Big[\log\Big(\frac{\delta - \lambda^1 B^2}{\delta}\Big)\Big]^2.
\end{aligned} \tag{6.18}$$

where we have computed the terms using Wolfram Mathematica.

In this section, we focus on the difference between $\log(||u - U_{N+1}||)$ and $\log(||\mathcal{F}(N, \epsilon, t)||)$. We focus on different features, namely how the norms change with δ and U. In our first range of figures (Figure 1), we have fixed $\delta = 0.01$. We plot $\log(||u - U_{N+1}||)$ (U_0 with red stars and U_1 with blue stars) and $\log(||\mathcal{F}(N, \epsilon = 0.01, t)||)$ for $N = 0$ and $N = 1$ (red crosses and blue crosses respectively) increasing U for $t = 100$, $t = 1000$ and $t = 2000$ in Figures 1a, 1b and 1c respectively. We notice the error bound increases owing to the exponential dependence on T. We notice also that for $t = 100$ and $t = 1000$, that one approximation is not necessarily better as we are still in the linear regime. For $t = 2000$, the $N = 1$ approximation is slightly better. One could say this is reflected in the more conservative error bound.

In our second range of figures (Figure 2), we have fixed $\delta = 0.05$. We plot $\log(||u - U_{N+1}||)$ (U_0 with red stars and U_1 with blue stars) and $\log(||\mathcal{F}(N, \epsilon = 0.01, t)||)$ for $N = 0$ and $N = 1$ (red crosses and blue crosses respectively) increasing U for $t = 100$, $t = 1000$ and $t = 2000$ in Figures 2a, 2b and 2c respectively. In this case, we notice that error bounds always present the first approximation as being better even when this is sometimes dubious. We find that the approximation given by $N = 0$ is slightly better larger U. We attribute this to our approximations poorly approximating the transitions from the linear regime to the saturated regime. One of the limitations of these error bounds is that the error bound relating to $U = 1$ is uniformly better even though this may not be the case.

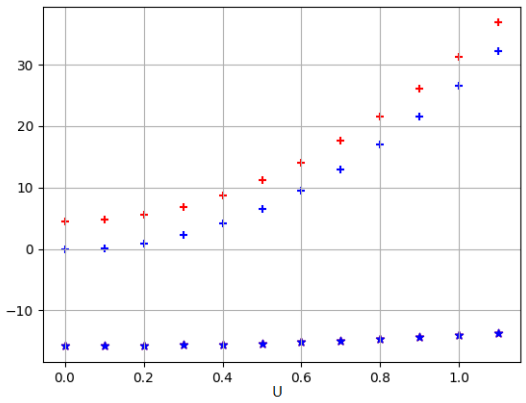

a)

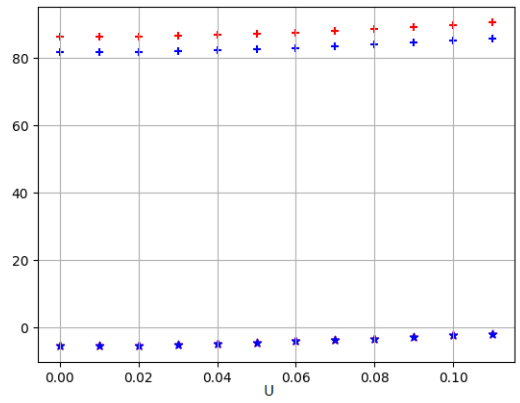

b)

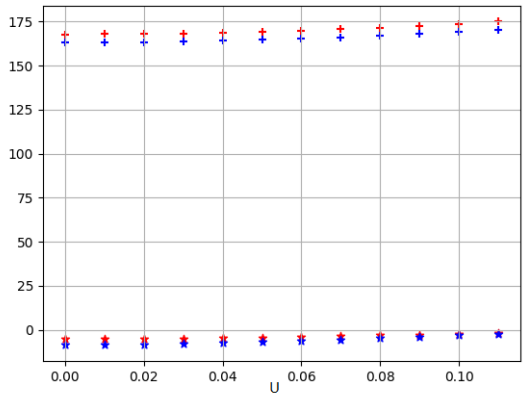

c)

Figure 1. Plots of $\log(||u - U_0||)$ (red stars) and $\log(||u - U_1||)$ (blue stars) for $\delta = 0.01$ with $\log(||\mathcal{F}(0, \epsilon = 0.01, t)||$

(red crosses) and $\log(||\mathcal{F}(1, \epsilon = 0.01, t)||$ for the following times $t = 100$ (a), $t = 1000$ (b) and $t = 2000$ (c).

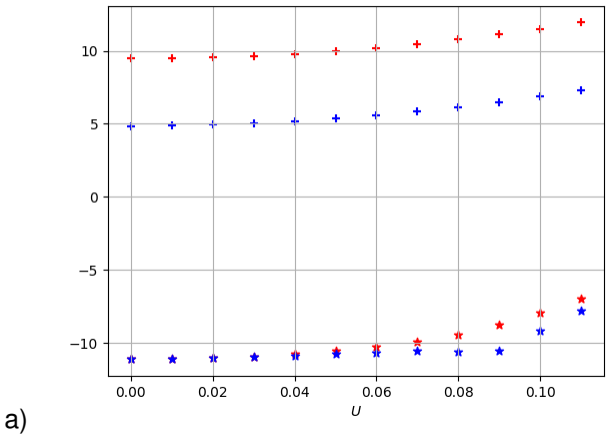

a)

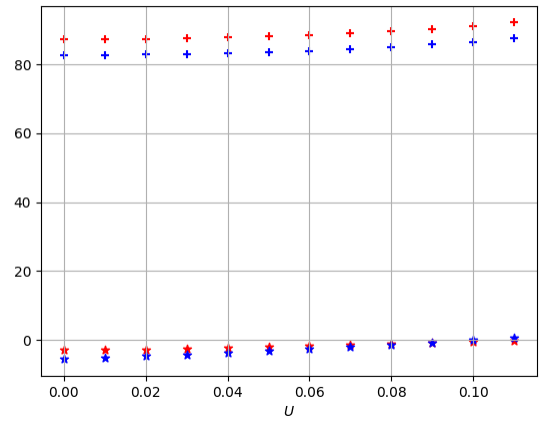

b)

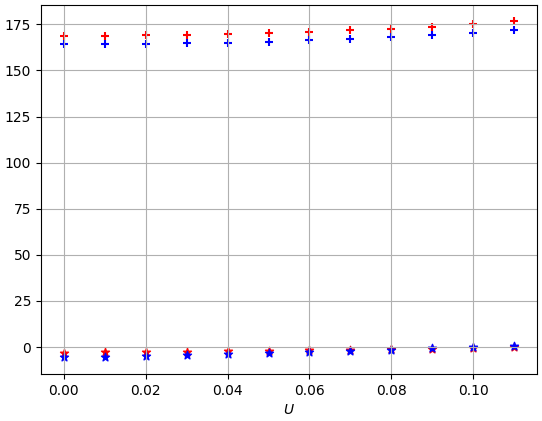

c)

Figure 2. Plots of $\log(||u - U_0||)$ (red stars) and $\log(||u - U_1||)$ (blue stars) for $\delta = 0.05$ with $\log(||\mathcal{F}(0, \epsilon = 0.01, t)||$ (red crosses) and $\log(||\mathcal{F}(1, \epsilon = 0.01, t)||$ for the following times $t = 100$ (a), $t = 1000$ (b) and $t = 2000$ (c).

After a certain time the solution does not grow anymore but instead converges asymptotically to a particular value. Therefore, if we pick a time point, T_c when the solution is on this "asymptotic approach", we can input this value T_c into the formula for the error bound (6.14), and this error values will apply from for the entire time domain, as $\mathcal{F}(N, \epsilon, t)$ is an increasing function. This is especially useful when we increase δ which reduces the saturation time. In Figure 3, we plot the $||u||_{L^2}$ for a range of δ. From this value, it is shown that we could pick earlier times for T_c for increasing δ and thus make the error bounds tighter.

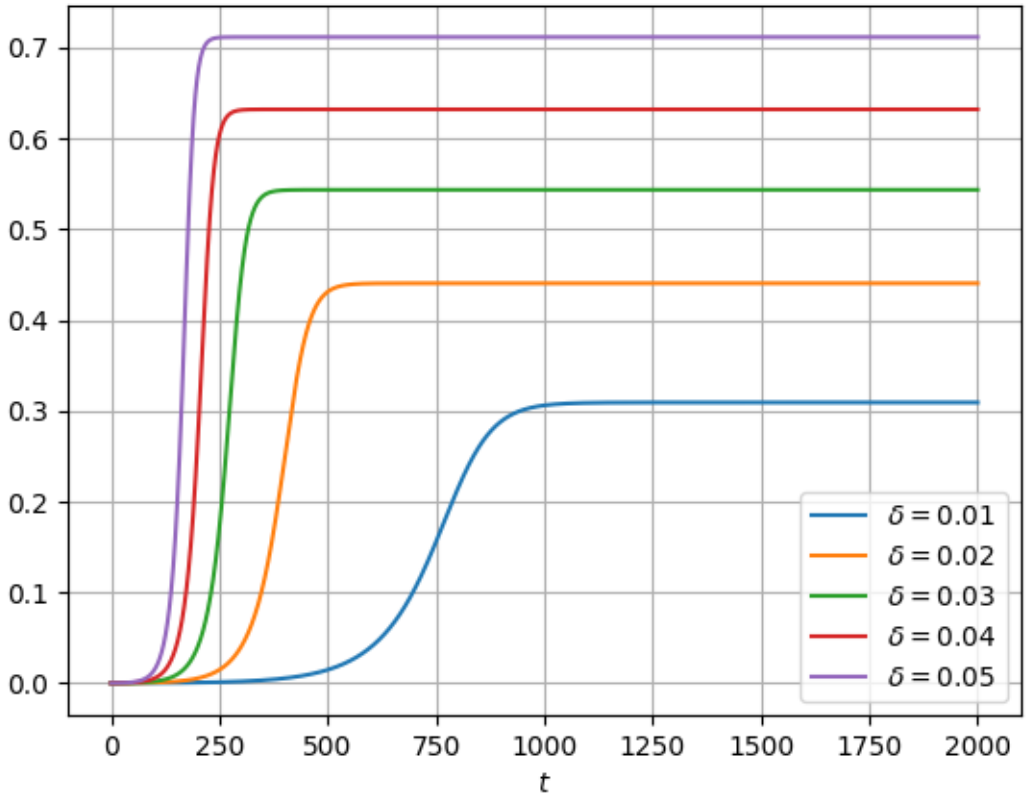

Figure 3. A plot of $||u||_{L^2}$ against t for a range of δ shown in plot.

6.3 Summary of Chapter

In the first section of this chapter, we derived error bounds for the RnsaGL (error bounds for the CnsaGL can be derived similarly). We did this via a bootstrapping argument that was facilitated by being able to write our operator in integral form. The bootstrapping argument showed us that a radius of convergence existed, but did not elucidate the what the radius of convergence was. These error bounds were importantly dependent on U and δ. In the second part of the chapter, we explored the error bound for various parameters. We saw that the error bound overestimates the discrepancy between the approximation and the solution to an enormous extent, thus demonstrating that these theoretical error bounds are not useful for providing guidance regard to what order to take the approximation up to or how big ϵ should be. The error bounds can be improved by picking the earliest time point when the solution is on the "asymptotic approach". This would provide tighter more nuanced error bounds, particularly as the solution saturates earlier for higher delta.

Chapter 7

Stochastic Amplitude Equations

In the papers of Blömker et al. (2005, 2007, 2011) [14, 15, 16] and Mohammed et al. (2011) [71] as well as Pradas et al. [78], the method of stochastic homogenisation was used to explore the effects of additive noise on PDEs via amplitude equations. A key ingredient to this method was that the solutions could be expanded such that $u = \sum_{n=0} a_n e_n$ where a_n and e_n are amplitude-eigenvector pairs. As the RnsaGL gives rise to a quasi-basis, we have tried to apply the same method of deriving amplitude equations in the case of additive noise. The noisy SPDE that we consider is given by

$$\frac{\partial u}{\partial t} = \mathcal{L}^{RGL} u - u^3 + \epsilon \tilde{\delta} u + \epsilon^{\frac{3}{4}} \sum_{n=1}^{N} \alpha_n \beta_n(t) \hat{e}_n \tag{7.1}$$

where β_n is a standard Brownian motion and $\hat{e}_n$ are the eigenvectors for the non-self-adjoint operators. The α_n are constants that determine the strength of the noise that we put along each mode; the sum starts at 1 as we want no noise on the unstable mode. ϵ is the distance from criticality and W is a Q-Wiener process on $\mathcal{H}(G) \cap \mathcal{H}(G)$. We choose a noise strength of $\epsilon^{\frac{3}{4}}$, because in the paper by by Mohammed et al. (2014) [71], it was shown that additive noise of the order $\epsilon^{\frac{3}{4}}$ along the stable eigenvectors results in a deterministic amplitude equation, namely the same first order amplitude equation derived via WNLE. What is interesting is that this approach is fundamentally different from our approach as no modes were discounted as a first step.

Before, we apply the averaging method, we begin by providing the key concepts from stochastic mathematics (Section 6.1). For example, what it means for equation (7.1) to have a solution and the definition of the Backward-Kolmogorov equation. We particularly look at a sequence of proofs from Da Prato and Zabczyk (1992) [32] that establish the existence of a mild solution for (7.1). We also prove that a Wiener process W in $\mathcal{H}(G) \cap \mathcal{H}(G^{-1})$ can be expanded using the quasi-basis of the RnsaGL. In Section 6.2 we derive the first order amplitude equation and in Section 6.3, we perform numerical experiments.

7.1 Definitions and Concepts

In this section, we briefly go over some of the concepts necessary to define (7.1) and ensure that it has a solution. This section is very much analogous to the theorems that we generated in Section 3, but, as well as having conditions such as $\mathcal{L}^{RGL}$'s being the generator of strongly continuous semigroup and a relatively well behaved non-linearity, we also need conditions on the noise. This section is largely her for pedagogical reasons for the reader who may not be au fait with stochastic mathematics, but furthermore the expansion of a Wiener process is a nice result that promises to have applications elsewhere, for instance in the field of Non-Hermitian Quantum Mechanics.

We firstly define what we mean by "noise". For this we need the following definitions; random variable, probability space, stochastic process, and Q-Wiener process, all of which we take from Da Prato and Zabczyk (1992) [32]. These definitions and subsequent theorems form part of the apparatus for showing that (7.1) has a solution, but moreover allow us to define the "Backward-Kolmogorov operator", which we use to perform the stochastic homogenisation.

- Definition (Random Variable). A measurable space is a pair $(\Omega, \mathcal{F})$ where Ω is a non-empty set and $\mathcal{F}$ is also called a σ-algebra of subsets of Ω. This means that the family $\mathcal{F}$ contains the set Ω and is closed under the operator of taking complements and countable unions of its elements. If $(\Omega, \mathcal{F})$ and $(\mathcal{E}, \mathcal{G})$ are two measurable spaces, then a mapping $\mathcal{X}$ form Ω into $\mathcal{E}$ such that the set $\{\omega \in \Omega : X(\omega) \in \mathcal{A}\} = \{X \in \mathcal{A}\}$ belongs to $\mathcal{F}$ for arbitrary $\mathcal{A} \in G$ is called a measurable mapping or a random-variable from $(\Omega, \mathcal{F})$ to $(\mathcal{E}, \mathcal{G})$.

- Definition (Probability Space). A probability measure on a measurable space $(\Omega, \mathcal{F})$ is a σ-additive function $\mathbb{P}$ from $\mathcal{F}$ into $[0, 1]$ such that $\mathbb{P}(\sigma) = 1$. The triple $(\Omega, \mathcal{F}, \mathbb{P})$ is called a probability space.

- Definition (Stochastic Process). Assume that $\mathcal{E}$ is a separable Banach space and let $\mathcal{B}(\mathcal{E})$ be the σ-field of its Borel subsets. Let $(\Omega, \mathcal{F}, \mathbb{P})$ be a probability space on an interval I of $\mathbb{R}^+$. An arbitrary family $X = \{X(t)\}_{t \in I}$ of $\mathcal{E}$-valued random variables $X(t)$, $t \in I$, defined on Ω is called a stochastic process.

- Definition (Q-Wiener Process). Assume $\mathcal{H}$ is a separable Hilbert space and Q is a non-negative trace class operator on $\mathcal{H}$. A $\mathcal{H}$-valued stochastic processes $W(t)$ is called a Q-Wiener process

  1. $W(t = 0) = 0$
  2. W has independent increments: for every $t \geq 0$, the future increments $W(t + u) - W(t)$ are independent of the past values $W(s), s \leq t$.
  3. W has Gaussian Increments, mean that $W(t + u) - W(t)$ is normally distributed with mean 0 and covariance operator Q, i.e. u, $W(t + s) - W(t) \sim \mathcal{N}(0, (t - s)Q)$
  4. W has continuous paths: $W(t)$ is continuous in t, a.s. in Ω.

We recall that as Q is defined as a trace class operator there exists a complete orthonormal system $\{e_k\}$ in $\mathcal{H}$ and a bounded sequence of non-negative real numbers $\{\lambda_k\}$ such that

$$Qe_k = \lambda_k e_k \tag{7.2}$$

We consider now the following important proposition that follows form the definition of a Q-Wiener process.

- Proposition (Properties of Wiener Process in terms of Expansion in the Eigenvectors of Q). Assume $W(t)$ is a Q-Wiener Process. Then the following statements hold.

  1. W is a Gaussian process on $\mathcal{H}$ and

  $$\mathbb{E}(W(t)) = 0, \qquad Cov(W(t)) = tQ, \qquad t \geq 0. \tag{7.3}$$

  2. For arbitrary $t \geq 0$, $\mathcal{W}$ has the expansion

  $$W(t) = \sum_{j=1}^{\infty} \sqrt{\lambda_j}\beta_j(t)e_j \tag{7.4}$$

  where

  $$\beta_j(t) = \frac{1}{\sqrt{\lambda_j}}\langle W(t), e_j\rangle, \tag{7.5}$$

  for all $j \in \mathcal{N}$. Furthermore, $\beta_j(t)$ are all real valued Brownian motions mutually independent on $(\Omega, \mathcal{F}, \mathbb{P})$ and the series in (7.4) is L^2-convergent.

  Proof. See Proposition (4.3) of Da Prato and Zabcyzk [32]. □

We use the same idea to justify the form of the noise in (7.1) into individual Brownian motions. As we want to recreate the stochastic homogenisation method by putting noise down the non-orthogonal eigenvectors, we have to show that we can decompose a general Wiener process W such as

$$W(t) = \sum_{n=0}^{\infty} \langle \hat{e}_n^{\dagger}, W(t)\rangle \hat{e}_n \tag{7.6}$$

We do this through the following theorem;

- Theorem (Expansion of noise in the eigenvectors of $\mathcal{L}^{RGL}$). Let W be a $\mathcal{H}$-valued Wiener process where $\mathcal{H} = \mathcal{H}(G) \cap \mathcal{H}(G^{-1})$. Let $\hat{e}_n^{\perp}$ be the eigenvectors of the RnsaGL when the equation is self-adjoint ($U = 0$). Let these be the eigenvectors of Q such that

$$Q\hat{e}_k^{\perp} = \lambda_k \hat{e}_k^{\perp} \tag{7.7}$$

thus the noise can be expanded as

$$W(t) = \sum_{j=0}^{\infty} \sqrt{\lambda_j} \beta_j(t) \hat{e}_j^{\perp} \tag{7.8}$$

where $\frac{1}{\sqrt{\lambda_j}} \langle \hat{e}_j^{\perp}, W(t) \rangle$. Then the noise can also be expanded as

$$W(t) = \sum_{j=0}^{\infty} \sqrt{\lambda_j} \hat{\beta}_j \hat{e}_j. \tag{7.9}$$

where $\hat{\beta}_j = \frac{1}{\sqrt{\lambda_j}} \langle \hat{e}_j^{\dagger}, W(t) \rangle$.

Proof. The proof follows from the theorem "Expressing elements of $H(G) \cap H(G^{-1})$ in terms of non-orthogonal basis vectors" in Section 4.3.

In Section 3, we showed how the existence of a strongly continuous semigroup allowed us to write our solutions in integral form. A key difference between stochastic equations and deterministic equations is that they must be interpreted in integral form. Often this is the starting point of the definition of a "mild solution". The full definition of a "mild solution" can be given as follows

- Definition (Mild Solution). Let $\mathcal{H}$ be a Hilbert-Space and consider the following stochastic differential equation

$$\frac{du}{dt} = \mathcal{L}u + \mathcal{N}(u) + \frac{dW}{dt} \tag{7.10}$$

with $\mathcal{L}$ is the linear operator, $\mathcal{N}(u)$ is the nonlinear operator and W is a Q-Wiener process. Then (7.10) has a mild solution if it can be written in the following form

$$u(t) = e^{t\mathcal{L}} u_0 + \int_0^t e^{(t-s)\mathcal{L}} \mathcal{N}(u) ds + \int_0^t e^{(t-s)\mathcal{L}} dW(s) \tag{7.11}$$

for arbitrary $t \in [0, T)$ if all terms are "well-defined" in $\mathcal{H}$.

We give the definition of the Stochastic integral in the Itō, as this provides meaning to the last term of (7.11);

- Definition (Itō Integral). Let $\gamma(x, t)$ be a smooth function of (x, t), then we define the Itō integral as

$$\int_0^t \gamma dW = \lim_{n \longrightarrow \infty} \sum_{[t_{i-1}, t_i] \in \pi_n} \gamma(x, t_{i-1})(W(t_i) - W(t_{i-1})) \tag{7.12}$$

where π_n is a sequence of partitions of $[0, t]$.

Given the definition of mild solution, we have the following theorem from Da Prato and Zabcyzk (1992) [32];

- Theorem (Existence and Uniqueness of SPDE with Dissipative Nonlinearity). Let $\mathcal{H}$ be a Hilbert space and let $\mathcal{E}$ be continuously and densely embedded in $\mathcal{H}$. Let us assume the following about the terms in (7.10):

(a) Let $\mathcal{L}$ generates a C_0 semigroup in $\mathcal{H}$.

(b) Let $\mathcal{L}_\mathcal{E}$ be "the part" of $\mathcal{L}$ in $\mathcal{E}$, i.e. $\mathcal{L}_\mathcal{E} : \mathcal{E} \longrightarrow \mathcal{E}$, and let $\mathcal{L}_\mathcal{E}$ also generate a C_0-semigroup on $\mathcal{E}$ such that $||e^{\mathcal{L}_\mathcal{E}}||_\mathcal{H} \leq e^{\omega t}$ where $\omega \in \mathcal{R}$ for all $t \geq 0$.

(c) Let the nonlinearity be uniformly continuous and dissipative on bounded sets of $\mathcal{E}$.

(d) W is a $\mathcal{H}$-valued Q-Wiener process.

(e) $u_0 \in \mathcal{E}$.

then there exists a unique mild solution (7.11) in $C([0,\infty); E)$ to the equation (7.10).

Proof. See Theorem 7.11 Da Prato and Zabcyzk (1992) [32]. □

We can now prove that the (7.1) has a mild solution;

- Corollary (Mild solution to (7.1)). By the above definitions, let $\mathcal{H} = L^2(\mathbb{R})$ and $\mathcal{E} = H^1(\mathbb{R})$. The equation (7.1) has a mild solution.

  Proof. We show that each assumption of the theorem "Existence and Uniqueness of SPDE with Dissipative Nonlinearity" is satisfied. Let $\mathcal{L} = \mathcal{L}^{RGL} + \epsilon\tilde{\delta}$ and let $\mathcal{N}(u) = -u^3$. Furthermore, let us assume that initial condition $u_0 \in \mathcal{E}$ as a starting point, hence (e) is satisfied. By definition, (d) is satisfied as $\mathcal{H}(G) \cap \mathcal{H}(G^{-1}) \subset \mathcal{H}$. Furthermore, W is a Q-Wiener process, as the noise is only placed a long a finite number of global modes. We notice that (a) is also satisfied as we showed previously that $\hat{\mathcal{L}}_n^{RGL}$ is a contraction and thus by adding another bounded operator, we get a C_0-semigroup. We have that (c) is satisfied as we have

$$-\langle u^3 - v^3, u - v\rangle = -\int_{-\infty}^{\infty} (u^2 + v^2)[(u-v)^2 + uv] \leq 0. \tag{7.13}$$

  The uniform continuity follows from

$$||v^3 - u^3||_{H^1} = ||(v-u)(v^2 + u^2 + uv)||_{H^1} \leq C||(v-u)||_{H^1} \tag{7.14}$$

  where C is a constant. Lastly, we have that (b) is satisfied as $||e^{(t-s)(\mathcal{L}^{RGL}+\delta)}|| \leq e^{\omega t}$, as $\mathcal{L}^{RGL}$ is a closed operator that generates a C_0-semigroup. □

Now, we introduce the Backward-Kolmogorov equation, which is the quantity upon which we perform the stochastic homogenisation. It is not necessary to consider the Backward-Kolmogorov equation in order to perform the stochastic homogenisation as the same results can be obtained in a path-wise manner from the governing equations by the application of Itō's lemma. The papers of Blömker and his collaborators (2005, 2007, 2011) [14, 15, 16] used this technique to derive error bounds. In contrast, the procedure we use follows Pradas et al. (2012) [78] by using the Backwards-Kolmogorov equation.

- Definition (Kolmogorov Equation). We define the Backward-Kolmogorov equation as

$$\frac{dv(u,t)}{dt} = \frac{1}{2}Tr[Q\frac{\partial^2}{\partial u^2}v(u,t)] + \langle(\mathcal{L}u + \mathcal{N}(u), \frac{\partial}{\partial u}v(u,t)\rangle \tag{7.15}$$

with $v(u,0)$, for $t \geq 0, u \in D(\mathcal{L})$.

Under certain assumptions, the equation has a solution. The significance of this equation is given in the following theorem

- Theorem (Equivalence of the Solution to the Backward-Kolmogorov Equation and Expectation). Consider the reference equation (7.10). Let $\mathcal{L} : D(\mathcal{L}) \subset \mathcal{H} \longrightarrow \mathcal{H}$ where $\mathcal{L}$ is a symmetric operator that has a set of eigenvectors $\{e_n\}$ that form an orthonormal basis and with corresponding eigenvalues $\{\lambda_n\}$, where $\lambda_n \leq 0$. Furthermore, let W be a Q-Wiener process such that $Q \in (0,1]$ such that $Q = (-\mathcal{L})^{-r}$ for $r \in (0,1]$, and let $\mathcal{N} \in H^1$. Then for any $\phi \in B(\mathcal{H})$, we have

$$v(t,x) = \mathbb{E}[\phi(u,(t,x))], \tag{7.16}$$

$t \in 0$, $x \in \mathcal{H}$ where v is the mild solution of (7.27) and u is the mild solution of (7.10).

Proof. Theorem 9.4.3 of Da Prato and Zabcyzk (1992) [32]

We notice that in the self-adjoint case of the RnsaGL, with $\delta = -0.01$, the assumptions of the theorem "Equivalence of the Solution to the Backward-Kolmogorov Equation and the Expectation" are satisfied with $Q(-(\mathcal{L}^{RGL} + \delta))^{-r}$ with $r \in (0,1]$.

7.2 Derivation of First Order Approximation

soul We note that we derived the first order approximation as it was done in Pradas et al. 2011. [78]. Before, we begin our derivation, we give the theorem that provides similar results in the self-adjoint case. This theorem is from the paper by Mohammed et al. (2014) [71].

- Theorem (Amplitude Equations for a Stochastic Partial Differential Equation (SPDE) with Additive Noise of Order $\epsilon^{\frac{3}{4}}$). Let $\mathcal{H}$ be a Hilbert space with norm $||\cdot||$ and inner product $\langle\cdot,\cdot\rangle$, and consider the following equation

$$\frac{\partial u}{\partial t} = \mathcal{L}u + \epsilon\delta u + \mathcal{F}(u,u,u) + \epsilon^{\frac{3}{4}}\frac{\partial W}{\partial t} \tag{7.17}$$

where

(a) $\mathcal{L}$ is a non-positive self-adjoint operator on $\mathcal{H}$ with real eigenvalues $-\lambda_k$ such that

$$0 = \lambda_0 = \ldots = \lambda_n < \ldots \leq \lambda_k \leq \ldots \qquad \text{and} \qquad \lambda_k \geq C_{km} \tag{7.18}$$

for all sufficiently large k and one $m > 0$ where the corresponding eigenfunctions $\{e_k\}_{k=1}^{\infty}$ form a complete orthonormal system in $\mathcal{H}$ such that $\mathcal{L}e_k = -\lambda_k$

(b) δ is a constant.

(c) $\mathcal{F}$ is a nonlinearity such that $\mathcal{F} : (\mathcal{H}^{\alpha}) \longrightarrow \mathcal{H}$ such that

$$||\mathcal{F}(u, v, w)|| \leq C||u||_{\alpha}||v||_{\alpha}||\omega||_{\alpha} \qquad \forall u, v, w \in \mathcal{H}^{\alpha} \tag{7.19}$$

and furthermore we have that

$$\langle \mathcal{F}(a, a, a), a \rangle \leq -c_0|a|^4 \tag{7.20}$$

(d) W is a finite-dimensional Wiener process of $\mathcal{H}$, such that for $t \geq 0$,

$$W(t) = \sum_k \alpha_k \beta_k(t) e_k \qquad \text{for finitely many} \qquad k \geq n + 1 \tag{7.21}$$

where $(\beta_k))_k$ are independent, standard Brownian motions in $\mathbb{R}$ and $(\alpha_k)_k$ are real numbers.

Then consider the amplitude equation

$$\frac{dA}{dt} = \delta A + P_0(\mathcal{F}(A\hat{e}_0, A\hat{e}_0, A\hat{e}_0)). \tag{7.22}$$

where P_0 is the projection onto the zeroth eigenvector. Provided that (7.17) and (7.22) are initialised such that $u(t = 0) = A(t = 0)e_0$ then for all $p > 1$ and $T_0 > 0$ and all $\kappa \in (0, \frac{1}{18})$, there exists a C such that

$$\mathbb{P}\left(\sup_{t \in [0, \frac{T_0}{\epsilon}]} ||u(x, t) - A\hat{e}_0||_{\alpha} > \epsilon^{(\frac{3}{4} - 10\kappa)} \right) \leq C\epsilon^{\frac{p}{2}}. \tag{7.23}$$

Proof. See the proof of Theorem 16 in Mohammed et al. (2014) [71].

The reader should recognise (7.22) as the Stuart-Landau equation. We see that all the conditions of the above theorem are satisfied for the RnsaGL apart from the self-adjointness; (d) is satisfied owing to the quasi-basis structure. We derive the amplitude equation (7.22) in the following "derivation".

- Derivation (First Order Amplitude Equation in the Stochastic Case).

We put equation (7.1) on a diffusive-timescale by letting $u = \epsilon^{\frac{1}{2}} v(x,\tau)$

$$-\frac{1}{\epsilon}\mathcal{L}v = \Big(-\frac{\partial v}{\partial \tau} + \tilde{\delta} v - v^3 \Big) + \frac{1}{\epsilon^{\frac{1}{4}}} \sum_{n=0}^{N} \alpha_n \beta_n \hat{e}_n. \tag{7.24}$$

where the noise has been such that $\hat{W} = \epsilon W(\tau)$. We expand in terms of the amplitude-eigenvector pairs given by $v = \sum_{n=0}^{\infty} a_n \hat{e}_n$, which is possible owing to the quasi-basis structure and we take the L^2-inner product. We take the L^2 inner product with each $\hat{e}_n^{\dagger}$ in order to isolate the different modes. This gives the following infinite-dimensional system of equations

$$\frac{\partial a_0(\tau)}{\partial \tau} = \tilde{\delta} a_0 - \langle \hat{e}_0^{\dagger}, (\sum_{k=0}^{\infty} a_k \hat{e}_k)(\sum_{l=0}^{\infty} a_l \hat{e}_l)(\sum_{m=0}^{\infty} a_m \hat{e}_m) \rangle \tag{7.25}$$

and for $n \geq 1$

$$\frac{\partial a_n(\tau)}{\partial \tau} = -\frac{1}{\epsilon}\hat{\lambda}_n a_n + \tilde{\delta} a_n - \langle \hat{e}_n^{\dagger}, (\sum_{k=0}^{\infty} a_k \hat{e}_k)(\sum_{l=0}^{\infty} a_l \hat{e}_l)(\sum_{m=0}^{\infty} a_m \hat{e}_m) \rangle + \frac{1}{\epsilon^{\frac{1}{4}}} \alpha_n \beta_n \tag{7.26}$$

where $\hat{\lambda}_n = |\lambda_n|$. The Backward-Kolmogorov equation is for the system of SDEs is

$$\frac{\partial w^{\epsilon}}{\partial \tau} = \mathcal{L}^{bk} w^{\epsilon} \tag{7.27}$$

where we have the "Backward-Kolmogorov operator", $\mathcal{L}^{bk}$, given by

$$\mathcal{L}^{bk} = \frac{1}{\epsilon}\mathcal{L}_0 + \frac{1}{\epsilon^{\frac{1}{2}}}\mathcal{L}_1 + \mathcal{L}_2 \tag{7.28}$$

with

$$\mathcal{L}_0 = \sum_{n=1}^{\infty} -\hat{\lambda} a_n \frac{\partial}{\partial a_n}, \qquad \mathcal{L}_1 = \sum_{n=1}^{\infty} \frac{1}{2} \alpha_n \frac{\partial^2}{\partial a_n^2} \qquad \text{and} \qquad \mathcal{L}_2 = \sum_{n=0}^{\infty} (\tilde{\delta} a_n + \mathcal{N}^n) \frac{\partial}{\partial a_n} \tag{7.29}$$

where we have used the abbreviation

$$\mathcal{N}^n = \langle \hat{e}_n^{\dagger}, (\sum_{k=0}^{\infty} a_k \hat{e}_k, \sum_{l=0}^{\infty} a_l \hat{e}_l, \sum_{m=0}^{\infty} a_m \hat{e}_m) \rangle. \tag{7.30}$$

We let the solution to the Backward-Kolmogorov equation take the following form

$$w^{\epsilon} = w_0 + \epsilon^{\frac{1}{2}} w_1 + \epsilon w_2 + ... \tag{7.31}$$

Putting this into (7.27) the following equations at each order

- $O(\frac{1}{\epsilon^{\frac{1}{2}}})$

$$\mathcal{L}_0 w_0 = 0 \tag{7.32}$$

- $O(\frac{1}{\epsilon})$

$$\mathcal{L}_0 w_1 = -\mathcal{L}_1 w_0 \tag{7.33}$$

- $O(1)$

$$\mathcal{L}_0 w_2 = -\mathcal{L}_1 w_1 + \bigg(- \frac{\partial w_0}{\partial t} + \mathcal{L}_2 w_0 \bigg) \tag{7.34}$$

From the equations (7.32) and (7.33) we ascertain that $w_0(a_0)$ and $w_1(a_0)$ only. From the equation (7.34), we notice that there is no stochastic part as $\mathcal{L}_1 w_1 = 0$. Now, we have to average with respect to the invariant measure given by $\mathcal{L}_0^\dagger \rho = 0$, which is given by $\rho = \delta(a_1)\delta(a_2)...$ for all $n \geq 1$ where δ is the Dirac delta function[1]. This gives the following equation

$$\frac{\partial w_0}{\partial \tau} = \frac{\partial w_0}{\partial a_0} \bigg((\tilde{\delta} a_0 + (a_0)^3 \lambda^1) \bigg) \tag{7.35}$$

Therefore, the resulting amplitude equation is given by

$$\frac{\partial w_0}{\partial a_0} \frac{\partial a_0}{\partial \tau} = \bigg((\tilde{\delta} a_0 + (a_0)^3 \lambda^1) \bigg) \tag{7.36}$$

which corresponds to the following amplitude equation

$$\frac{dA}{d\tau} = \tilde{\delta} A - \lambda^1 A^3. \tag{7.37}$$

We let $B = \epsilon^{\frac{1}{2}} A$ and we put the equation back on the original timescale. This gives

$$\frac{dB}{d\tau} = \tilde{\delta} B - \lambda^1 B^3 \tag{7.38}$$

which is the same result as in the deterministic case. Therefore the first order stochastic approximation u_s^{0th} is given by

$$u_s^{0th} = B \hat{e}_0. \tag{7.39}$$

[1]We notice that the adjoint of the operator $\mathcal{L}_0^\dagger = -\sum_{n=0}^{\infty} \lambda_n (a_n \frac{\partial}{\partial a_n} + 1)$. The kernel of this operator is non-trivial but satisfied by the Dirac Delta function (the reader is invited to consider the paper McKane and Waxman (2007) [65] for a similar example with pure drift). Therefore, we let the invariant measure $\rho = \delta(a_1)\delta(a_2)\delta(a_3)...$, which is such that $\int_{-\infty}^{+\infty} \rho d\mathbf{a} = 1$. Furthermore, every integration of the form $\int_{-\infty}^{\infty} \delta(a_n) a_n da_n$, $\int_{-\infty}^{\infty} \delta(a_n) a_n^2 da_n$ and $\int_{-\infty}^{\infty} \delta(a_n) a_n^3 da_n$ equals zero.

7.2.1 Numerical Experiments

In our numerical experiments, we solve (7.1) with $\alpha_1 = 1$ and for $k \neq 1$, $\alpha_k = 0$. Therefore, there is noise on the eigenvector $\hat{e}_1$ but not along any other eigenvector. In these figures, we have tailored the time-step to the relative size of the noise term. Information on the numerical procedures can be found in the Appendix B.

In Figure 1, we plot side by side the L^2 norm of the solution of (7.1) alongside the stochastic path taken at $x = 0.22$ (the nearest point to the origin on the x-domain) for $U = 0$. We also plot the norm of the approximation given by $A\hat{e}_0$ and the value of $A\hat{e}_0$ at $x = 0.22$. These graphs coincide enough to validate the first order deterministic approximation.

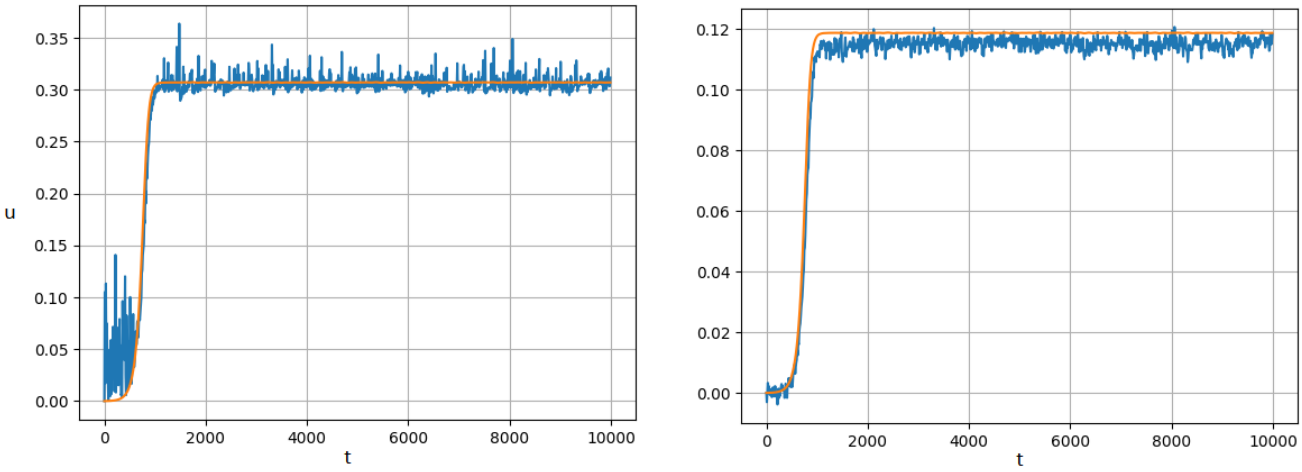

Figure 1. (Left) Figure 1. (Left) The norm of the solution u of (7.1) (blue) and the approximation u_s^{0th} given by (7.39) (orange) for $U = 0$, $\delta = 0.01$. (Right) The solution u (blue) and the approximation u_s^{0th} given by (7.39) for $U = 0$, $\delta = 0.01$ taken at point $x = 0.22$.

For $U = 1$, we compare the same structures namely the difference in norm between the solution of u given by (7.1) and approximation given by the amplitude equation. We see from the picture on the right-hand-side a phenomena of switching, which suggests that the solution is described by the approximation (7.39) is not adequate. We liken this to the deterministic phenomena where the higher order structures, in this case, noisy structures are more significant. In Figure 3, we also plot relative size of the eigenvectors with this normalisation, i.e. $\hat{e}_1$ for $U = 0$ and $\hat{e}_1$ for $U = 1$. We notice that the size of the eigenvector in the case $U = 1$ may have a significant effect on noise strength to have provoked the switching in the numerical experiments.

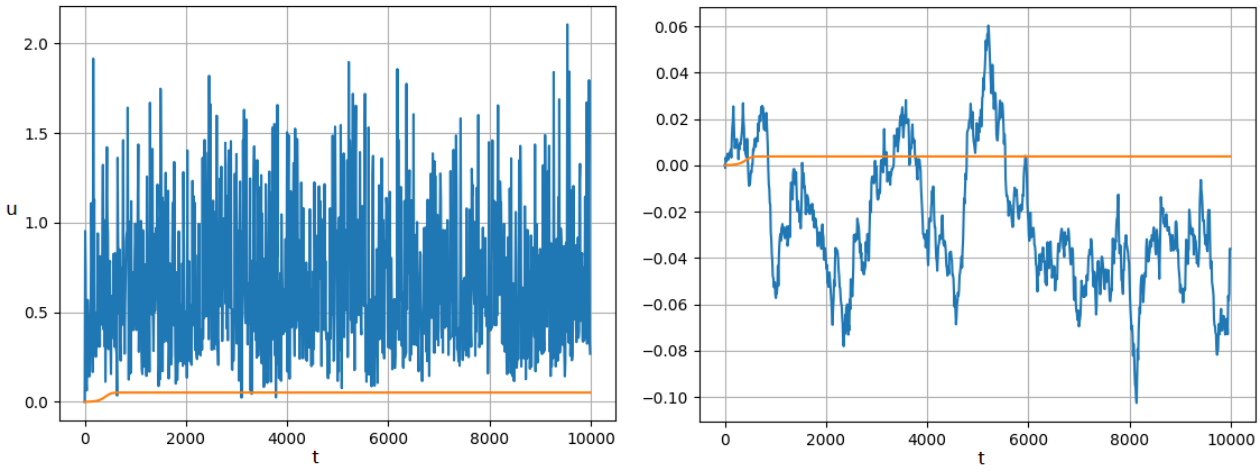

Figure 2. (Left) The norm of the solution u of (7.1) (blue) and the approximation u_s^{0th} given by (7.39) (orange) for $U = 1$, $\delta = 0.01$. (Right) The solution u (blue) and the approximation u_s^{0th} given by (7.39) for $U = 1$, $\delta = 0.01$ taken at point $x = 0.22$.

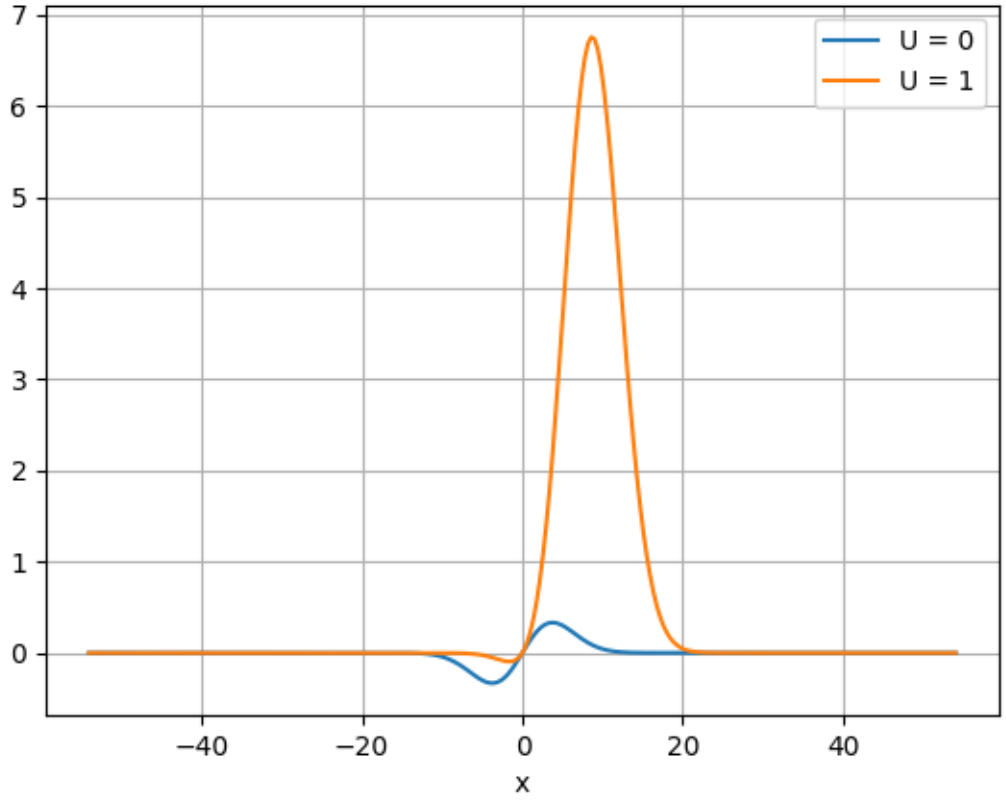

Figure 3. The eigenvectors $\hat{e}_1$ for $U = 0$ (blue) and $U = 1$ (orange).

7.3 Summary of this Chapter

In this chapter, we considered a theorem by Mohammed et al. (2014) [71] which showed for a specific noise strength, the first order approximation to an SPDE was still deterministic. However, one of the assumptions in this theorem was that the operator was self-adjoint thus to allow for a well-defined stochastic convolution. We extended some stochastic concepts for when the linear operator is not self-adjoint, but there exists a quasi-basis structure, and hence showed that in our case the stochastic convolution was well defined. Furthermore, we proved the existence of a mild solution to the noisy RnsaGL and then we then derived a first-order amplitude equation assuming that the solution of the Backward-Kolmogorov equation is equivalent to the expectation even in a situation where the operator is non-self-adjoint but a quasi-basis structure still exists. A theorem equating the solution to the expectation does not exist in the literature to the author's knowledge, but would be a possible direction of future work. We performed numerical experiments that showed the first order deterministic amplitude equation worked well in the self-adjoint case for the value of ϵ considered but poorly in the non-self-adjoint case. Furthermore, in the non-normal case, there was switching between different branches of the pitchfork bifurcation.

Chapter 8

Conclusion

In this thesis, we have used the problem of the failure of first order approximations derived via WNLE to approximate the solutions of non-self-adjoint partial differential equations to explore non-self-adjointness itself. We did this using two test-cases, the RnsaGL and the CnsaGL. These equations exhibited different features; the eigenvectors of the RnsaGL formed a quasi-basis in the space $\mathcal{H}(G) \cap \mathcal{H}(G^{-1})$ and the CnsaGL exhibited the same phenomena seen in numerical experiments as the linearised Navier-Stokes operator where the frequency was well approximated by a first order approximation, but the amplitude was not (Sipp and Lebedev (2007) [92] and Carini et al [21] (2015)). In the following paragraphs, we will go over the main conclusions from each chapter and try to contextualise the significance of the literature in a broader sense as well as talk about avenues of future research. The author believes that this PhD, although not presenting extremely technical results, has strength because the results brought together different fields and in this way created several budding areas for future research.

In the introduction, we surveyed different linear descriptions of Fluid Mechanics and aligned them with different mathematical objects. We also did some rudimentary numerical experiments demonstrating transient growth. Additionally, we split the linear operator $\mathcal{L}^{CGL}$ into two different equations for amplitude and frequency. We showed that, in the case of the CnsaGL, the linear operator for frequency is sub-critical and only demonstrates minimal transient growth. We hypothesize that the frequency operator in the case of the linearised Navier-Stokes equations displays similar phenomena, and hence why the frequency is captured via a first-order approximation. We also connected the different linear approaches via the corresponding mathematical objects. Furthermore, we contextualised the previous work by Hunt and Crighton (1991) [55] by showing that the same result could be derived via an eigenvalue-expansion method despite the eigenvectors only forming a complete set and not satisfying any stronger notion of a basis.

In the second chapter, we provided an argument against higher order amplitude equations by performing numerical experiments that showed non-normality is largely a problem in space - not a problem in time - and that any approximation that disregards the stable modes is not appropriate for modelling a non-normal system. For the

RnsaGL, we showed that a significant part is orthogonal to the leading eigenvector, which will not be captured in an approach that involves building higher order amplitude equations for the zeroth eigenvector. Similar numerical experiments may be elucidating in the case of other non-normal operators where the first order approximation fails to capture the behaviour of the governing equation well, such as the linearised Navier-Stokes equations. This kind of analysis should be performed as a first step.

In the third chapter, we proved that $\mathcal{L}^{RGL}$ and $\mathcal{L}^{CGL}$ generated C_0-semigroups. We also proved local existence and uniqueness of solutions to the RnsaGL and the CnsaGL. For the RnsaGL, we were inspired by the work of Metafune et al. (2005) [67] to define the domains of our operators, but, unlike Metafune et al. (2005), we did not go down the route of proving extra regularity given the regularity of the initial condition. In the fourth chapter, we emphasized that there are different notions of basis and that these are appropriate for different uses. The notion of a Riesz basis allows us to expand functions within that basis such that the corresponding coefficients are finite. When no Riesz basis is present, there is still the possibility of expressing functions in the space $\mathcal{H}(G) \cap \mathcal{H}(G^{-1})$ using a quasi-basis providing the metric operator G is known. A future area of possible research would be to tie the third and fourth chapters together by defining the domain of our operators as the exponentially waited space $\mathcal{H}(G) \cap \mathcal{H}(G^{-1})$ and then to prove that the solution stays in this space.

From a numerical perspective, there is perhaps a possibility for exploring sharper numerical approximations by expressing functions in these quasi-bases. For instance, we used a Hermite-discretisation in order to capture the asymptotic tails of our solution, but this does not capture the asymmetry. The author sees no reason why a quasi-basis structure could not be used in order to provide new discretisation schemes to better express asymmetric functions. A difficulty in the general applications of the quasi-basis structure is to know whether or not the metric operator exists. The pseudospectra gives a good test for the existence of a bounded metric, but as we have seen that in certain scenarios unbounded metrics are very useful, and thus the non-existence of these metric operators is very useful also. In Krejčiřík and Siegl (2019) [60], the non-existence of a metric operator for certain Schrödinger operators was proven on the basis that these had a "significant" complex part. It would be enlightening to reproduce such proofs for the CnsaGL. Furthermore, the splitting of the equation into the frequency operators and the amplitude operator could be a way forward if a complex diffusion term prohibits the existence of a quasi-basis.

In the fifth chapter, we derived higher order approximations using a technique that has not been used previously, namely normalising higher order terms such that they preserved the linear development of the zeroth eigenvector. We used this assumption because it was gifted to us empirically, but we would like to in future work extend this assumption. For example, the assumption can be viewed as ensuring no $O(1)$ terms exist in higher order expansions. However, one could also argue that, in the way $O(1)$ terms do not appear at $O(\epsilon)$, $O(1)$ and $O(\epsilon)$ terms should not appear at $O(\epsilon^2)$ and so on and so forth. For higher values of U and higher values of δ, the approximations did not necessarily improve for higher orders. Therefore, we should consider the radius of convergence of the expansion (5.2), as this could give us possible limitations regarding ϵ. To explore the convergence of the series, it would be use-

ful to implement the numerical procedure using symbolic computing as the higher order terms can get laborious to deal with by hand. On a different note, the derivation of the higher order approximations was inspired predominantly by the work of Vishik and Lyusternik (1960) [100]. We demonstrated how they dealt with the elliptic case, where there is no non-uniqueness at higher terms. In the paper, Vishik and Lyusternik (1960) [100] they consider also the case when there exist "associated eigenvectors"; in today's vocabulary, we would refer to these as associated eigenvectors. This may have applicability to the case of Poiseuille flow where the eigenvectors are nearly parallel (Trefethen et al. (1993) [98]). However, the natural next step is to calculate these higher order approximations for configurations such as cylinder flow at with Reynolds number equal to 47 (the first bifurcation of a cylinder flow) where the non-normality manifests in the same way, with the direct and adjoint eigenvectors becoming further apart.

In the sixth chapter, we derived error bounds for the RnsaGL using a bootstrapping method, but again we purposely did not restrict ϵ or do the bootstrapping with ϵ, as we are interested with how the discrepancy grows for large $\delta = \tilde{\delta}\epsilon$. We found that the coefficient in (6.13) depended on δ as well as the advection velocity U and the time T. The exponential dependence on T in particular made these error bounds large. We re-emphasized that these are theoretical tools only. Furthermore, the error bounds do not reflect the case when the first approximation is better than the second order approximation. The author thinks that, in hindsight, it would have been better to compare the attractors of the solution and the approximation. Arguments regarding the relative size of attractors can be found in Schneider (1994) [84]. An L^P-theory for the Linearised Navier-Stokes equations would allow us to derive use error bounds by writing them in integral form; this is also an extremely difficult problem that has been tackled with the aim of finding solutions to the Navier-Stokes equations. Nevertheless, there is a possibility for similar bounds to be derived between the approximation and the solution in the case of the linearised Navier-Stokes operator via energy methods.

In the seventh chapter, we derived a first-order amplitude equation for the noisy RnsaGL. We derived our amplitude equation by using the Backward-Kolmogorov operator. However, we acknowledged that the appropriate mathematical framework did not exist concerning a quasi-basis. In the numerical experiments, we saw that for $U = 1$ the solution was not approximated well by the first-order amplitude equation at all. The fact that, when $U = 1$, switching occurs suggests is indicative that an order violation has taken place, i.e. the size of the noise term with stable non-self-adjoint eigenvector is greater than the proceeding-in-order spatial structure. The development of the stochastic apparatus in order to deal with the presence of a quasi-basis is another direction for future research, as well as looking at the possible stabilisation effect of additive noise on a non-self-adjoint PDE (a possible stabilisation by additive noise has been explored in self-adjoint cases, the reader is invited to see Blömker et al. (2009) [17]).

To conclude, we hope that the reader can see that the two test cases of the RnsaGL and the CnsaGL provide a wealth of discovery regarding the role of non-normality in Fluid Mechanics, as well as a plethora of new potential research opportunities. The quasi-basis structure really allows the use mathematical techniques from non-Hermitian Quantum Mechanics that have not yet been fully explored in a Fluid Mechanics context. Furthermore, the author

believes that this thesis also has a strong pedagogical aspect. The reasons behind why we do things like resolvent analysis in Fluid Mechanics are given from a mathematical point of view; for example, one is of course interested in the most dangerous frequency response but also when the operator does not generate a strongly-continuous semigroup it is one of the few things that we can do. The author also believes that a key strength of this thesis is its interdisciplinary nature. Often in the study of non-self-adjoint operators, the information is in different places that are sometimes out of the respective purview of the engineer and theoretical physicist; for instance, many of the quasi-basis results were motivated by pseudobosons [6, 9]. This thesis has not only collated research from different fields but provided demonstrative examples that have assisted in elucidating the role of non-normality in Fluid Mechanics.

Appendix A

In this appendix, we prove two versions of the Fredholm Alternative for the RnsaGL and the CnsaGL respectively. We apply these theorems when deriving our amplitude equations throughout the thesis and often just say "by applying the Fredholm Alternative". The sections of this appendix are as follows; in the first section, we give important definitions and theorems, namely the definition of a compact operator and compact embedding, the Kolmogorov-Riesz-Fréchet theorem that criteria for a compact embedding, the Fredholm alternative for compact operators, and the Lax-Milgram theorem in its real and complex forms. We reference these theorems when proving the Fredholm Alternative in the real case and complex case in Sections A.2 and A.3 respectively.

A.1 Useful Theorems and Definitions

In order to prove the Fredholm Alternative, we need a space that is compactly embedded into $L^2(\mathbb{R})$ that represents the boundary conditions in each case, i.e. $u \longrightarrow 0$ as $x \longrightarrow \infty$. We give the definition of a compact embedding and a compact operator before giving the Fredholm Alternative for Compact Operators.

- Definition (Compact Embedding). Let X and Y be Banach spaces, $X \subset Y$. We say that X is compactly embedded in Y, written $X \subset\subset Y$, provided

  (a) $||x||_Y \leq C||x||_X$ ($x \in X$) for some constant C

  (b) each bounded sequence in X is pre-compact in Y (has a convergent subsequence in Y)

- Definition (Compact Operator). Let X, Y be normed spaces and $T : X \longrightarrow Y$ a linear operator. T is a compact operator if for any bounded sequence $x_{nn\in\mathbb{N}}$ in X, the sequence $\{Tx_n\}_{n\in\mathbb{N}}$ contains a converging subsequence.

Often we prove that an embedding is compact by proving the following two criteria of the Kolmogorov-Riesz-Fréchet Theorem;

- Theorem (Kolmogorov-Riesz-Fréchet). Let $\mathcal{F}$ be a bounded set in $L^p(\mathbb{R}^N)$ with $1 \leq p < \infty$. Assume that

(a) $\lim_{|h|\longrightarrow 0} ||f(x+h)-f(x)||_{L^p} = 0$ uniformly in $f(x) \in \mathcal{F}$, ($x \in \mathbb{R}^n$), i.e. for all $\epsilon > 0$, there exists a δ such that $||f(x+h)-f(x)||_{L^p} < \epsilon$ for all $f \in \mathcal{F}$, for all $h \in \mathbb{R}^N$ with $h < \delta$

(b) For all $\epsilon > 0$, there exists $\Omega \subset \mathbb{R}^N$, bounded and measurable such that $||f||_{L^p(\mathbb{R}^n \setminus \Omega)} < \epsilon$ for all $f \in \mathcal{F}$.

Then $\mathcal{F}$ is pre-compact in $L^p(\mathbb{R})$.

Proof. See Brezis (2011) [19], Chapter 4, Theorem 4.26 and Corollary 4.27. on page 111-113.

In our proofs of the respective Fredholm Alternatives, we use the Fredholm Alternative for compact operators. This is given by the following theorem; in this theorem, the nullspace and range of an operator T this is denoted by $N(T)$ and $R(T)$ respectively.

- Theorem (Fredholm Alternative for Compact Operators). Let $K : \mathcal{H} \longrightarrow \mathcal{H}$ be a compact linear operator on a Hilbert space $\mathcal{H}$. Then

  i $N(I-K)$ is finite dimensional,

  ii $R(I-K)$ is closed,

  iii $R(I-K) = N(I-K^*)^{\perp}$

  iv $N(I-K) = \{0\}$ is and only if $R(I-K) = H$,

  v dim$N(I-K) =$ dim$N(I-K^*)$

  Proof. See Appendix D, Theorem 5 of Evans (2010) [44].

A key component to any Fredholm Alternative proof is the underlying Lax Milgram Theorem. The real and complex variations are given as follows;

- Theorem (Lax-Milgram). Let H be a real Hilbert space. Assume that $B : H \times H \longrightarrow \mathbb{R}$ is a bilinear mapping, for which there exist constants α, $\beta > 0$ such that

  (a)
  $$|B[u,v]| \leq \alpha ||u|| ||v|| \qquad (u, v \in H), \tag{A.1}$$

  and

  (b)
  $$\beta ||u||^2 \leq B[u,u] \qquad (u \in H). \tag{A.2}$$

  Finally, let $f : H \longrightarrow \mathbb{R}$ be a bounded linear functional on H. Then there exists a unique element $u \in H$ such that
  $$B[u,v] = \langle f, v \rangle \tag{A.3}$$

for all $v \in H$.

Proof. See Evans (2010) [44], Section 6.2.1.

- Theorem (Complex Lax-Milgram). Let H be a complex Hilbert space. Assume that $B : H \times H \longrightarrow \mathbb{R}$ is a bilinear mapping, for which there exist constants α, $\beta > 0$ such that

  (a)

  $$|B[u,v]| \leq \alpha ||u|| ||v|| \qquad (u, v \in H), \tag{A.4}$$

  and

  (b)

  $$\beta ||u||^2 \leq \Re\{B[u,u]\} \qquad (u \in H). \tag{A.5}$$

  Finally, let $f : H \longrightarrow \mathbb{R}$ be a bounded linear functional on H. Then there exists a unique element $u \in H$ such that

  $$B[u,v] = \langle f, v \rangle \tag{A.6}$$

  for all $v \in H$.

  Proof. This result follows from the generalisation of the Lax-Milgram Theorem by Lions, See Theorem 2.1 in Showalter (2013) [86].

A.2 Fredholm Alternative for RnsaGL

As mentioned previously, we need to create a space that is compactly embedded into $L^2(\mathbb{R})$ that contains the boundary conditions. In order to create this space, we consider the following unbounded operator

$$\mathcal{L}^1 = \frac{\partial}{\partial x} - x. \tag{A.7}$$

Let us consider the norm $|| \cdot ||_{\mathcal{L}^1}$ defined as the norm induced by the inner product $\langle \mathcal{L}^1 \cdot, \mathcal{L}^1 \cdot \rangle$;

$$||u||^2_{\mathcal{L}^1} = \langle \mathcal{L}^1 u, \mathcal{L}^1 u \rangle = ||\frac{\partial u}{\partial x}||^2_{L^2} + ||ux||^2_{L^2} - 2\langle u, x\frac{\partial u}{\partial x} \rangle. \tag{A.8}$$

Via integration by parts, we have

$$2\langle u, x\frac{du}{dx} \rangle = [u^2 x]^{\infty}_{-\infty} - ||u||^2_{L^2} dx \tag{A.9}$$

where the first term on the right-hand-side goes to zero. Therefore, we have that

$$||u||^2_{\mathcal{L}^1} = \langle \mathcal{L}^1 u, \mathcal{L}^1 u \rangle = ||\frac{\partial u}{\partial x}||^2_{L^2} + ||ux||^2_{L^2} + ||u||^2_{L^2}. \tag{A.10}$$

We define the following Hilbert[1] space $\mathcal{H}^{\mathcal{L}^1}$ as i.e.

$$\mathcal{H}^{\mathcal{L}^1} := \{u \in L^2(\mathbb{R}) : ||u||_{\mathcal{L}^1} < \infty\}. \tag{A.11}$$

We want to show that the space $\mathcal{H}^{\mathcal{L}^1}$ is compactly embedded into $L^2(\mathbb{R})$, where the definition of a compact embedding was given in the last section. We do this in the following theorem;

- Theorem (Compact Embedding of $\mathcal{H}^{\mathcal{L}^1}$ into $L^2(\mathbb{R})$). $\mathcal{H}^{\mathcal{L}^1}$ is compactly embedded in $L^2(\mathbb{R})$.

  Proof. The criterion (a) in the definition of a compact embedding follows from the definitions of the norms.

  To prove criterion (b) in the definition of compact operator, we fix a bounded sequence u_n, $n \in \mathbb{N}$ in $\mathcal{H}^{\mathcal{L}^1}$ and set $\mathcal{F} = \{u_n\}_{n=0}^{\infty}$ and show that the terms satisfy the conditions of the Kolmogorov-Riesz-Fréchet theorem. We have that condition (a) of the Kolmogorov-Riesz-Fréchet theorem because the functions u_n are in $H^1(\mathbb{R})$. Therefore, by Morrey's inequality (Theorem 4, Section 5.6.2 in Evans (2010) [44]), the functions u_n are Holder continuous with exponent $\alpha = \frac{1}{2}$ and thereby uniformly continuous. To prove part (b) of Kolmogorov-Riesz-Fréchet theorem, we use the fact that the norm $||u_n||_{\mathcal{L}^1}$ controls of $||xu_n||_{L^2}$. Therefore, we have that for $u_n \in \mathcal{H}^{\mathcal{L}^1}$ and an interval D of radius R

  $$M > ||xu_n||_{L^2(\mathbb{R})} \geq ||xu_n||_{L^2(\mathbb{R}\setminus D)} \geq \sqrt{\int_{|x|>R} x^2 u_n^2 dx} \geq \sqrt{R^2 \int_{|x|>R} u_n^2 dx} = R||u_n||_{L^2(\mathbb{R}\setminus D)}, \tag{A.12}$$

  which gives

  $$||u_n||_{L^2(\mathbb{R}\setminus D)} < \frac{M}{R}. \tag{A.13}$$

  We can always tune R such that $\frac{M}{R} = \epsilon$ for all ϵ, thus part (b) of the Kolmogorov-Riesz-Fréchet theorem is satisfied. Thus, u_n has a convergent subsequence in $L^2(\mathbb{R})$ and thus the embedding is compact. □

We can now prove the following theorem;

- Theorem (Tailored Fredholm Alternative for $\mathcal{L}^{RGL}$). Given $\mathcal{L}^{RGL}$ as in the (RnsaGL). Then

  i Precisely one of the following statements holds:

  either

  (α) For each $f \in L^2(\mathbb{R})$, there exists a unique weak solution u of the equation

  $$-\mathcal{L}^{RGL}u = f \qquad \text{in } L^2(\mathbb{R}) \tag{A.14}$$

[1] We can show that $\mathcal{H}^{\mathcal{L}^1}$ is a Hilbert space by considering a Cauchy sequence $f_n \longrightarrow f$ in $\mathcal{H}^{\mathcal{L}^1}$. We want to show that the limit of this sequence f is in $\mathcal{H}^{\mathcal{L}^1}$. We have owing to the definition of the norms that the space $\mathcal{H}^{\mathcal{L}^1}$ is continuously embedded in $L^2(\mathbb{R})$ so any Cauchy sequence in $\mathcal{H}^{\mathcal{L}^1}$ is also Cauchy in $L^2(\mathbb{R})$. Moreover, as $L^2(\mathbb{R})$ is a complete space, we have that the limit f is also in $L^2(\mathbb{R})$. Furthermore, as we have that $\mathcal{H}^{\mathcal{L}^1}$ is continuously embedded in $L^2(\mathbb{R})$ we have in L^2 that $xf_n \longrightarrow f_1$, $\frac{df_n}{dx} \longrightarrow f_2$ in $L^2(\mathbb{R})$, with $f_1, f_2 \in L^2(\mathbb{R})$. Owing to the uniqueness of limits, we have $xf = f_1$ and $\frac{\partial f}{\partial x} = f_2$, and thus $f \in \mathcal{H}^{\mathcal{L}^1}$.

or else

(β) There exists a weak solution, $u \neq 0$ of the homogeneous problem

$$-\mathcal{L}^{RGL}u = 0 \qquad \text{in } L^2(\mathbb{R}) \tag{A.15}$$

ii Furthermore, should assertion (β) hold, the dimension of the subspace $N \subset \mathcal{H}^{\mathcal{L}^1}$ of weak solutions of (A.15) is finite and equals the dimension of the subspace $N^\dagger \subset \mathcal{H}^{\mathcal{L}^1}$ of weak solutions of

$$-(\mathcal{L}^{RGL})^\dagger v = 0 \qquad \text{in } L^2(\mathbb{R}) \tag{A.16}$$

where $(\mathcal{L}^{RGL})^\dagger$ is the L^2-adjoint operator of $(\mathcal{L}^{RGL})$, i.e. $\langle (\mathcal{L}^{RGL})^\dagger u, v\rangle = \langle u, (\mathcal{L}^{RGL})v\rangle$ where $\langle \cdot, \cdot \rangle$ is the L^2-inner product.

iii Finally, the boundary-value problem (A.14) has a weak solution if and only if

$$\langle v, f\rangle = 0 \qquad \text{for all } v \in N^\dagger. \tag{A.17}$$

Proof. Like in Evans (2010) [44], we split this proof up into steps

1. Let us choose γ such that the the bilinear from $B_\gamma[u, v] := B[u, v] + \gamma\langle u, v\rangle$ where $B[u, v] = \langle u, -\mathcal{L}^{RGL}u\rangle$ that corresponds to the linear operator $\mathcal{L}_\gamma u := -\mathcal{L}^{RGL} + \gamma$ where γ is a constant that facilitates the fulfilment of the coercivity condition (A.5). Then for each $g \in L^2(\mathbb{R})$, there exists a unique function $u \in \mathcal{H}^{\mathcal{L}^1}$ solving

$$B_\gamma[u, v] = \langle g, v\rangle \qquad \text{for all } v \in \mathcal{H}^{\mathcal{L}^1} \tag{A.18}$$

by the Lax-Milgram Theorem. Let us write

$$u = \mathcal{L}_\gamma^{-1} g \tag{A.19}$$

whenever (A.18) holds.

2. We have that $u \in \mathcal{H}^{\mathcal{L}^1}$ is a weak solution of (A.14) if and only if

$$B_\gamma[u, v] = \langle \gamma u + f, v\rangle \qquad \text{for all } v \in \mathcal{H}^{\mathcal{L}^1}. \tag{A.20}$$

Ergo, if and only if

$$u = \mathcal{L}_\gamma^{-1}(\gamma u + f). \tag{A.21}$$

Rewriting this equation as is done in Evans (2010) [44] we have the following

$$u - Ku = h \tag{A.22}$$

where $Ku := \gamma \mathcal{L}_\gamma^{-1} u$ and $h := \mathcal{L}_\gamma^{-1} f$.

3. Now, we claim that $K : L^2(\mathbb{R}) \longrightarrow L^2(\mathbb{R})$ is a bounded, linear, compact operator. This is where we fundamentally differ from Evans (2010) [44] and where the usefulness of space $\mathcal{H}^{\mathcal{L}^1}$ comes in. We have the following inequality

$$C||u||_{\mathcal{L}^1}^2 \leq B_\gamma[u,v] = \langle u, -\mathcal{L}^{RGL} u \rangle + \gamma \langle u, u \rangle = \langle u, g \rangle \leq ||g||_{L^2} ||u||_{\mathcal{L}^1} \tag{A.23}$$

where C is a constant. The first inequality follows from

$$\langle u, -\mathcal{L}u \rangle = -\int_\infty^\infty u \left[\frac{\partial^2 u}{\partial x^2} + U \frac{\partial u}{\partial u} - c_1 u + c_2 x^2 u \right] dx = ||\frac{du}{dx}||^2 - c_1 ||u||^2 + c_2 ||ux||^2 dx. \tag{A.24}$$

Using the definition of $K := \gamma \mathcal{L}_\gamma^{-1}$ and the inequality (A.23), we obtain

$$||Kg||_{\mathcal{L}^1} = ||\gamma u||_{\mathcal{L}^1} \leq C ||g||_{\mathcal{L}^1} \tag{A.25}$$

where C' is a constant.

4. We may now apply the "Fredholm Alternative for Compact Operators" that we gave in the last section; this asserts that either:

   (a) For each h in $L^2(\mathbb{R})$, the equation $u - Ku = h$ has a unique solution $u \in L^2(\mathbb{R})$.

   (b) The equation $u - Ku = 0$ has nonzero solutions in $L^2(\mathbb{R})$.

   Should assertion (a) hold then owing to step 2, there exists a unique solution to (A.14). On the other hand, should (b) be valid, then necessarily $\gamma \neq 0$, and the dimension of the space of solutions, N, to $u - Ku = 0$ is finite and equals the dimension of the space, $N^\dagger$, of solutions to $v - K^\dagger v = 0$ where $K^\dagger$ is the adjoint operator of K in the space $L^2(\mathbb{R})$. Furthermore, by the same construction done in Step 2, we have that $Ku - u = 0$ holds if and only if u is a weak solution of (A.15), and, also, $K^\dagger v - v = 0$ holds if and only if v is a weak solution of (A.16). Thus, points (i) and (ii) of theorem "Tailored Fredholm Alternative for $\mathcal{L}^{RGL}$" are proven.

5. Lastly we prove the third point of the theorem. We notice by the "Fredholm Alternative for Compact Operators" that (A.22) has a solution if and only if

$$\langle v, h \rangle = 0. \tag{A.26}$$

We have that, using the definition of $h = \mathcal{L}_\gamma^{-1} f$ and the definition of $K := \gamma \mathcal{L}_\gamma^{-1}$, we have that

$$\langle h, v \rangle = \frac{1}{\gamma} \langle Kf, v \rangle = \frac{1}{\gamma} \langle f, K^\dagger, v \rangle = \frac{1}{\gamma} \langle f, v \rangle. \tag{A.27}$$

Consequently, we have that (A.14) if and only if $\langle f, v \rangle = 0$ for all weak solutions v of (A.15). □

A.3 Fredholm Alternative for CnsaGL

As in the last case, we need a space that is compactly-embedded in the $L^2(\mathbb{R})$ space. The only difference here is the conjugation that we take on the argument as well as using the complex version of the Lax-Milgram theorem. Otherwise, the proof remains the same. We still give it in full as the use of the Complex Lax Milgram lemma provides an insight as to how more general notions of ellipticity are useful with Fluid Mechanics applications.

As in the last proof, we have

$$\mathcal{L}_c^1 = \frac{\partial}{\partial x} - x. \tag{A.28}$$

where the c just distinguishes the complex case. We define the norm $||\cdot||_{\mathcal{L}_c^1}$, we have

$$||u||_{L_c^1}^2 = \langle \mathcal{L}_c^1 u, \mathcal{L}_c^1 u \rangle = ||\frac{\partial u}{\partial x}||_{L^2}^2 + ||ux||_{L^2}^2 - \langle u, x\frac{\partial u}{\partial x} \rangle - \langle x\frac{\partial u}{\partial x}, u \rangle. \tag{A.29}$$

Therefore, via integration by parts,

$$\langle u, x\frac{du}{dx} \rangle + \langle x\frac{du}{dx}, u \rangle = [|u|^2 x]_{-\infty}^{\infty} - ||u||_{L^2}^2 dx. \tag{A.30}$$

The first term on the right-hand-side goes to zero (the reader is invited to see the discussion in the section on the definition of the operators about the boundary conditions). Therefore, we have that

$$||u||_{L_c^1}^2 = \langle \mathcal{L}_c^1 u, \mathcal{L}_c^1 u \rangle = ||\frac{\partial u}{\partial x}||_{L^2}^2 + ||ux||_{L^2}^2 + ||u||_{L^2}^2. \tag{A.31}$$

We define the following Hilbert[2] space

$$\mathcal{H}^{\mathcal{L}_c^1} := \{u \in L^2(\mathbb{R}) : ||u||_{\mathcal{L}_c^1} < \infty\}. \tag{A.32}$$

We want to show that the space $\mathcal{H}^{\mathcal{L}_c^1}$ is compactly embedded into $L^2(\mathbb{R})$, where the definition of a compact embed-

[2]We can show that $\mathcal{H}^{\mathcal{L}_c^1}$ is a Hilbert space by considering a Cauchy sequence $f_n \longrightarrow f$ in $\mathcal{H}^{\mathcal{L}_c^1}$. We want to show that the limit of this sequence f is in $\mathcal{H}^{\mathcal{L}_c^1}$. We have owing to the definition of the norms that the space $\mathcal{H}^{\mathcal{L}_c^1}$ is continuously embedded in $L^2(\mathbb{R})$ so any Cauchy sequence in $\mathcal{H}^{\mathcal{L}_c^1}$ is also Cauchy in $L^2(\mathbb{R})$. Moreover, as $L^2(\mathbb{R})$ is a complete space, we have that the limit f is also in $L^2(\mathbb{R})$. Furthermore, as we have that $\mathcal{H}^{\mathcal{L}_c^1}$ is continuously embedded in $L^2(\mathbb{R})$ we have in L^2 that $xf_n \longrightarrow f_1$, $\frac{df_n}{dx} \longrightarrow f_2$ in $L^2(\mathbb{R})$, with $f_1, f_2 \in L^2(\mathbb{R})$. Owing to the uniqueness of limits, we have $xf = f_1$ and $\frac{\partial f}{\partial x} = f_2$, and thus $f \in \mathcal{H}^{\mathcal{L}_c^1}$.

ding was given in A.1. We do this in the same way as we did in the real case.

- Theorem (Compact Embedding of $\mathcal{H}^{\mathcal{L}_c^1}$ into $L^2(\mathbb{R})$). $\mathcal{H}^{\mathcal{L}_c^1}$ is compactly-embedded into $L^2(\mathbb{R})$.

  Proof. The first criteria for a compact embedding follows from the definitions of the norms. To prove the second part of the definition, we fix a bounded sequence u_n, $n \in \mathbb{N}$ in $\mathcal{H}^{\mathcal{L}_c^1}$ and set $\mathcal{F} = \{u_n\}_{n=0}^{\infty}$ and show that the terms satisfy the conditions of the Kolmogorov-Riesz-Fréchet theorem. Condition (a) of the Kolmogorov-Riesz-Fréchet theorem is satisfied as the functions u_n are in $H^1(\mathbb{R})$ are Holder continuous with exponent $\alpha = \frac{1}{2}$ and thereby uniformly continuous. To prove part (b) of Kolmogorov-Riesz-Fréchet theorem, we use the fact that the norm $||u_n||_{\mathcal{L}^1}$ controls of $||xu_n||_{L^2}$. Therefore, we have that for $u_n \in \mathcal{H}^{\mathcal{L}^1}$ and an interval D of radius R

$$M > ||xu_n||_{L^2} \geq ||xu_n||_{L^2(\mathbb{R}\setminus D)} \geq \sqrt{\int_{|x|>R} x^2|u_n|^2 dx} \geq \sqrt{R^2 \int_{|x|>R} u_n^2 dx} = R||u_n||_{L^2(\mathbb{R}\setminus D)}, \tag{A.33}$$

  which gives

$$||u_n||_{L^2(\mathbb{R}\setminus D)} < \frac{M}{R} \tag{A.34}$$

  We can always tune R such that $\frac{M}{R} = \epsilon$ for all ϵ, thus part (b) of the Kolmogorov-Riesz-Fréchet theorem is satisfied. Thus, u_n has a convergent subsequence in $L^2(\mathbb{R})$ and thus the embedding is compact. □

We can now prove the following theorem;

- Theorem (Tailored Fredholm Alternative for $\mathcal{L}^{CGL}$). Given $\mathcal{L}^{CGL}$ as in the (CnsaGL) defined as above

  i Precisely one of the following statements holds:

  either

  (α) For each $f \in L^2(\mathbb{R})$, there exists a unique weak solution u of the equation

$$-\mathcal{L}^{CGL}u = f \qquad \text{in } L^2(\mathbb{R}) \tag{A.35}$$

  or else

  (β) There exists a weak solution, $u \neq 0$ of the homogeneous problem

$$-\mathcal{L}^{CGL}u = 0 \qquad \text{in } L^2(\mathbb{R}) \tag{A.36}$$

  ii Furthermore, should assertion (β) hold, the dimension of the subspace $N \subset \mathcal{H}^{\mathcal{L}^1}$ of weak solutions of (A.36) is finite and equals the dimension of the subspace $N^\dagger \subset \mathcal{H}^{\mathcal{L}^1}$ of weak solutions of

$$-(\mathcal{L}^{CGL})^\dagger v = 0 \qquad \text{in } L^2(\mathbb{R}) \tag{A.37}$$

where $(\mathcal{L}^{CGL})^\dagger$ is the L^2-adjoint operator of $\mathcal{L}^{CGL}$, i.e. $\langle(\mathcal{L}^{CGL})^\dagger u, v\rangle = \langle u, (\mathcal{L}^{CGL})v\rangle$ where $\langle\cdot,\cdot\rangle$ is the L^2-inner product.

iii Finally, the boundary-value problem (A.35) has a weak solution if and only if

$$\langle v, f\rangle = 0 \qquad \text{for all } v \in N^\dagger. \tag{A.38}$$

Proof. Like in Evans (2010) [44], we split this up into steps

1. Let us choose γ such that the the bilinear from $B_\gamma[u,v] := B[u,v] + \gamma\langle u, v\rangle$ where $B[u,v] = \langle u, -\mathcal{L}^{CGL}u\rangle$ that corresponds to the linear operator $\mathcal{L}_\gamma u := -\mathcal{L}^{CGL} + \gamma$ where γ is a constant that facilitates the fulfilment of the complex coercivity condition (A.5) in the complex Lax-Milgram lemma. Then for each $g \in L^2(\mathbb{R})$, there exists a unique function $u \in \mathcal{H}^{\mathcal{L}_c^1}$ solving

$$B_\gamma[u,v] = \langle g, v\rangle \qquad \text{for all } v \in \mathcal{H}^{\mathcal{L}^1} \tag{A.39}$$

by the Complex Lax-Milgram Theorem. Let us write

$$u = \mathcal{L}_\gamma^{-1} g \tag{A.40}$$

whenever (A.39) holds.

2. We have that $u \in \mathcal{H}^{\mathcal{L}^1}$ is a weak solution of (A.14) if and only if

$$B_\gamma[u,v] = \langle \gamma u + f, v\rangle \qquad \text{for all } v \in \mathcal{H}^{\mathcal{L}^1}. \tag{A.41}$$

Ergo, if and only if

$$u = \mathcal{L}_\gamma^{-1}(\gamma u + f). \tag{A.42}$$

Rewriting this equation as is done in Evans (2010) [44] we have the following

$$u - Ku = h \tag{A.43}$$

where $Ku := \gamma\mathcal{L}_\gamma^{-1}u$ and $h := \mathcal{L}_\gamma^{-1}f$.

3. Now, we claim that $K : L^2(\mathbb{R}) \longrightarrow L^2(\mathbb{R})$ is a bounded, linear, compact operator. This is where we fundamentally differ from Evans (2010) [44] and where the usefulness of space $\mathcal{H}^{\mathcal{L}_c^1}$ comes in as well as

the Complex Lax-Milgram Lemma. We have the following inequality

$$C||u||^2_{\mathcal{L}^1} \leq \Re\{B_\gamma[u,v]\} \leq |B_\gamma[u,v]| \leq |\langle u, -\mathcal{L}^{CGL}u\rangle + \gamma\langle u,u\rangle| = |\langle u,g\rangle| \leq ||g||_{L^2}||u||_{\mathcal{L}^1} \tag{A.44}$$

where C is a constant. We use the definition of $K := \gamma\mathcal{L}_\gamma^{-1}$ and the inequality (A.44) in order to obtain

$$||Kg||_{\mathcal{L}^1} = ||\gamma u||_{\mathcal{L}^1} \leq C||g||_{\mathcal{L}^1} \tag{A.45}$$

where C is again a constant (note, this is a different C, i.e. not necessarily the same as derived via different means) from C in (A.44). As we proved in the theorem $\mathcal{H}^{\mathcal{L}^1_c} \hookrightarrow L^2(\mathbb{R},\mathbb{C})$ is a compact operator on $\mathcal{H}^{\mathcal{L}^1_c}$.

4. We may now apply the "Fredholm Alternative for Compact Operators" that we gave in the last section; this asserts that either:

   (a) For each h in $L^2(\mathbb{R})$ the equation $u - Ku = h$ has a unique solution $u \in L^2(\mathbb{R})$.

   (b) The equation $u - Ku = 0$ has nonzero solutions in $L^2(\mathbb{R})$

   Should assertion (a) hold then owing to the series of equations in Step 2, there exists a unique solution to (A.35). On the other hand, should (b) be valid, then necessarily $\gamma \neq 0$, and the dimension of the space of solutions, N, to $u - Ku = 0$ is finite and equals the dimension of the space, $N^\dagger$, of solutions to $v - K^\dagger v = 0$ where $K^\dagger$ is the adjoint operator of K in the space $L^2(\mathbb{R})$. Furthermore, by the same construction done in Step 2, we have that $Ku - u = 0$ holds if and only if u is a weak solution of (A.36), and, also, $K^\dagger v - v = 0$ holds if and only if v is a weak solution of (A.37). Thus, points (i) and (ii) of theorem "Tailored Fredholm Alternative for $\mathcal{L}^{RGL}$") are proven.

5. Lastly we prove the third assertion. We notice by the "Fredholm Alternative for Compact Operators" that (A.43) has a solution if and only if

$$\langle v, h\rangle = 0. \tag{A.46}$$

   We have that, using the definition of $h = \mathcal{L}_\gamma^{-1}f$ and the definition of $K := \gamma\mathcal{L}_\gamma^{-1}$, we have that

$$\langle h, v\rangle = \frac{1}{\gamma}\langle Kf, v\rangle = \frac{1}{\gamma}\langle f, K^\dagger, v\rangle = \frac{1}{\gamma}\langle f, v\rangle. \tag{A.47}$$

   Consequently, we have that (A.35) if and only if $\langle f, v\rangle = 0$ for all weak solutions v of (A.36).

□

Appendix B

In this appendix, we go over some numerical methods used. Throughout the thesis, we relied heavily on the SciPy package linear algebra package to compute various norms, inverting various matrices and compute matrix exponentials. Furthermore, all odes were solved via the "solve_ivp" package from NumPy. We do not give details regarding the inbuilt functions in NumPy ans SciPy but we do however give the methods of spatial and temporal discretisation and how we computed the pseudospectra.

B.1 Hermite Discretisation

The numerical experiments are done by discretising the RnsaGL and the CnsaGL operator using Hermite functions, as done in [11]. The differentiation matrices were provided by Weideman and Reddy [103] with corresponding matlab codes and kindly converted into python (https://github.com/ronojoy/pyddx/blob/master/sc/dmsuite.py). To approximate the derivatives in the RnsaGL and the CnsaGL, the solution u is expanded into Physicist's Hermite functions

$$q(x,t) = \sum_{j=1}^{n} c_j(t) \exp(-\frac{1}{2}\alpha_1^2 x^2) H_{j-1}(\alpha_1 x) \tag{B.1}$$

where $H_j(\alpha_1 x)$ refers to the $j-th$ Hermite polynomial. The differentiation process is exact for solutions of the form $f(x) = \exp(-\frac{1}{2}\alpha_1^2 x^2)p(\alpha_1 x)$ where $p(\alpha_1 x)$ is any polynomial of degree $n-1$ or less. The scaling parameter α_1 is used to optimise the accuracy of the discretisation [94], by matching as closely as possible to decay of the (real-part) of the non-self-adjoint eigenvectors (**??**) as $x \longrightarrow \infty$. This particular choice of discretisation means that our boundary conditions are enforced implicitly.

We use 220 points, and our collocation points are given as the roots of $H_n(\alpha_1 x)$. There is a slight discrepancy between our using Probabilist's Hermite polynomials for our eigenvectors and using Physicist's Hermite polynomials for our discretisation, but we still have a highly accurate approximation of $\mathcal{L}$. This discretisation transforms our solution into a flow variable $u(x,t)$ into a flow variable $\hat{u}(t)$ of dimension n. We therefore define our L^2 inner product as

$$\langle f, g \rangle = \int_{\infty}^{\infty} f(x)g(x)dx \approx \hat{f}^T M \hat{g} \tag{B.2}$$

where the T denotes the transpose and M is the positive define matrix that contains the integration weights of the chosen quadrature rule. We use a trapezoidal rule where the integration points are selected as the midpoints of the quadrature points.

B.2 Time-Stepping

We use different time-stepping methods according to whether we are dealing with a SPDE or a PDE. We describe them below before giving the following functions over the page. In the following we denote $\hat{u}$ as the solution to the RnsaGL, CnsaGL, or noisy RnsaGL, given by (7.1) in its discretised form, having been discretised in space using the Hermite Differentiation matrices described in Section 1 of the Appendix.

- PDEs We use the following second order technique. Let us consider the following discretised forms of the PDE

$$\frac{\hat{u}_n - \hat{u}_{n-1}}{dt} = \hat{\mathcal{L}} u_n - u_n^3 \tag{B.3}$$

and

$$\frac{\hat{u}_n - \hat{u}_{n-1}}{dt} = \hat{\mathcal{L}} u_{n+1} - u_n^3. \tag{B.4}$$

Adding these two equations and rearranging gives the following second order scheme

$$\hat{u}_n = (1 - 0.5dt\hat{\mathcal{L}})^{-1}[(1 + 0.5dt\hat{\mathcal{L}})u_{n-1} - dt(\hat{u}_{n-1})^3]. \tag{B.5}$$

In our computations, we use $dt = 0.1$.

- SPDEs We use the Euler-Maruyama technique. Consider the noisy RnsaGL given by u. We denote the discretisation of $\hat{e}_n$ with the extra hat, and $\mathcal{L}^{\hat{RGL}}$ We perform a first order discretisation in time where the subscripts n correspond to the evenly spaced time points $\{t_n\}$ between $t = 0$ and $t = 10000$

$$\frac{\hat{u}_{n+1} - \hat{u}_n}{dt} = \hat{\mathcal{L}}^{RGL}\hat{u}_{n+1} - \hat{u}_n^3 - \epsilon^{\frac{3}{4}}\hat{\hat{e}}_n[\beta_1(t_{n+1}) - \beta_1(t_n)]. \tag{B.6}$$

Furthermore, we have performed a Picard iteration in order to make $\hat{\mathcal{L}}^{RGL}\hat{u}_{n+1}$ a future term. As β_1 is just a standard Brownian motion, we have that $\beta_1(t_{n+1}) - \beta_1(t_n) = z\sqrt{t_2 - t_1}$ where z is an independent normally-distributed variable. For the specifics, the reader is invited to consult [64].

We rearrange this equation in order to obtain

$$\hat{u}_{n+1} = (1 + \hat{\mathcal{L}}^{RGL}dt)^{-1}[-\hat{u}_n^3 dt - \epsilon^{\frac{3}{4}}\hat{\hat{e}}_n z\sqrt{dt}] \tag{B.7}$$

where dt is the time-step. We generate z using the randn function in NumPy. In our calculations $dt = 10^{-5}$.

B.3 Computing Pseudospectra

For computing the pseudospectra, we create a grid of x-points $\{x_m\}$ and y-points $\{y_m\}$ (we used 200 by 200 points) and then find the norm of the inverted matrix $(\mathcal{L} - (x_m + y_m i))^{-1}$ in each instance by using the norm function in the NumPy linear algebra module. This returns the largest singular value of the matrix. We note that faster techniques are possible and described in the following article by Trefethen (1999) [97]. However, as we only considered a one-dimensional example, all of our pseudospectra calculations were finished in minutes as opposed to hours.

In both cases, we divided the domain, shown in figure, into a grid of 200 by 200 evenly spaced points, which we used as our z when calculating the resolvent $(\mathcal{L}^{RGL} - z)^{-1}$ or $(\mathcal{L}^{CGL} - z)^{-1}$. The norm of these operators was calculated via the norm function in the NumPy Linear Algebra package after the operators were discretised via our Hermite discretisation method. The reader is directed to the appendix for further details.

Appendix C

In the first section, we prove that $\mathcal{L}^{CGL}$ generates a C_0-semigroup. In the second section, we prove that $\hat{\mathcal{L}}_n^{CGL}$ is a sectorial operator.

C.1 $\mathcal{L}^{CGL}$ generates a C_0-semigroup

We show that the operator $\mathcal{L}^{CGL}$ generates a C_0-semigroup by firstly proving the conditions of Lumer-Phillips theorem for $\hat{\mathcal{L}}_n^{CGL}$ and then using the theorem "Perturbations by Bounded Operators". The latter theorem was given in the thesis, but we give both theorems here for ease of use of the appendix. We also have the theorem "Conditions on the Domains of Symmetric Operators", which we use to prove one component of the Lumer-Phillips theorem as well as a theorem about the density of $D(\mathcal{L}^{CGL})$ in $L^2(\mathbb{R})$. This density condition needs to be satisfied in order to use the Lumer-Phillips theorem.

- Theorem (Lumer-Phillips). Let $\mathcal{L}$ be a linear operator defined on a dense linear subspace $D(\mathcal{L})$ of the reflexive Banach space X. Then $\mathcal{L}$ generates a contraction semigroup if and only if $\mathcal{L}$ is closed and both $\mathcal{L}$ and its adjoint operator $\mathcal{L}^*$ are dissipative.
  Proof. See Engel and Nagel (2001) Chapter 2, Corollary 3.17 [41]. □

- Theorem (Perturbations by Bounded Linear Operators). Let X be a Banach space and let A be the infinitesimal generator of a C_0-semigroup $T(t)$ on X satisfying $||T(t)|| \leq Me^{\omega t}$. If B is a bounded linear operator on X, then $A + B$ is the infinitesimal generator of C_0-semigroup $S(t)$ on X, satisfying $||S(t)|| \leq Me^{(\omega + M||B||)t}$
  Proof. See Chapter 3, Section 3.1, Theorem 1.1 of Pazy (2012) [75]. □

- Theorem (Conditions on the Domains of Symmetric Operators). A densely-defined operator T is symmetric if and only if $T \subset T^*$ (i.e. if $D(T) \subseteq D(T^*)$, $\forall u \in D(T)$, $Tu = T^*u$).
  Proof. See Proposition 2.57 in Cheverry and Raymond (2019) [23]. □

- Theorem (Density of $D(\mathcal{L}^{CGL})$). The space $C_0^\infty(\mathbb{R})$ is dense in $D(\mathcal{L}^{CGL})$.
  Proof. See Lemma 2.5, Metafune et al. (2005) [67]. □

Firstly, we show that the operator is closed. We do this by using integration by parts. Secondly, we show that the domain of the adjoint $(\hat{\mathcal{L}}_n^{CGL})^\dagger$ operator is smaller than the domain of the direct operator. This allows us to test the dissipativity of the adjoint operator on functions that are in the domain of the direct operator.

- Theorem (Lumer-Phillips Closedness Condition). The operator $(D(\mathcal{L}^{CGL}), \hat{\mathcal{L}}_n^{CGL})$ is closed.
  Proof. Firstly we prove that the operator $(D(\mathcal{L}^{CGL}), \hat{\mathcal{L}}_n^{CGL})$ is closed; i.e. let $\{u_n\}_{n=0}^{\infty} \in D(\mathcal{L}^{CGL})$ be a sequence of functions such that both $u_n \longrightarrow u$ and $\hat{\mathcal{L}}^{CGL} u_n \longrightarrow g$ as $n \longrightarrow \infty$ in $L^2(\mathbb{R})$. We seek to prove that $\hat{\mathcal{L}}^{CGL} u = g$ and $u \in D(\mathcal{L}^{CGL})$.

  We begin by taking the L^2 inner product of $\mathcal{L}u$ with a smooth, compactly supported test function $\phi \in C_0^\infty$; we denote the L^2 inner product using $\langle \cdot, \cdot \rangle$. We perform integration by parts to obtain,

$$\begin{aligned}
\langle \phi, \hat{\mathcal{L}}_n^{CGL} u \rangle &= \langle (\hat{\mathcal{L}}_n^{CGL})^\dagger \phi, u \rangle \\
&= \langle (\hat{\mathcal{L}}_n^{CGL})^\dagger \phi, \lim_{n \longrightarrow \infty} u_n \rangle \\
&= \lim_{n \longrightarrow \infty} \langle (\hat{\mathcal{L}}_n^{CGL})^\dagger \phi, u_n \rangle \qquad \text{(using the continuity of the inner product } L^2\text{)} \\
&= \lim_{n \longrightarrow \infty} \langle \phi, \hat{\mathcal{L}}_n^{CGL} u_n \rangle \\
&= \langle \phi, \lim_{n \longrightarrow \infty} \hat{\mathcal{L}}_n^{CGL} u_n \rangle \qquad \text{(using the continuity of the inner product } L^2\text{)} \\
&= \langle \phi, g \rangle.
\end{aligned}$$

  Furthermore, it follows from the integration by parts that $\mathcal{L}u = g$. It can be seen that $u \in D(\mathcal{L})$. □

- Theorem (Lumer-Phillips Dissipativity Condition A). $D((\hat{\mathcal{L}}_n^{CGL})^\dagger) \subset D(\hat{\mathcal{L}}_n^{CGL}) = D(\hat{\mathcal{L}}^{CGL})$.
  Proof. We have that for $u \in D(\hat{\mathcal{L}}^{CGL})$, $\langle u, \hat{\mathcal{L}}^{CGL} u \rangle$ is not real, and therefore the operator is not symmetric. Therefore, we can use the reverse implication from the theorem "Conditions on the Domains of Symmetric Operators", i.e. $D((\hat{\mathcal{L}}_n^{CGL})^*) \subset D(\hat{\mathcal{L}}_n^{CGL})$. □.

- Theorem (Lumer-Phillips Dissipativity Condition B). $\hat{\mathcal{L}}_n^{CGL}$ and $(\hat{\mathcal{L}}_n^{CGL})^*$ are dissipative.
  Proof. We need to show that $\Re\{\langle u, \hat{\mathcal{L}}_n^{CGL} u \rangle\} \leq 0$ and $\Re\{\langle u, (\hat{\mathcal{L}}_n^{CGL})^\dagger u \rangle\} \leq 0$ are dissipative for all $u \in D(\hat{\mathcal{L}}_n^{CGL})$ and $u \in D((\hat{\mathcal{L}}_n^{CGL})^\dagger)$ respectively. By the last theorem "Lumer-Phillips Dissipativity Condition A", it suffices to just test $u \in D(\hat{\mathcal{L}}_n^{CGL})$. We remark that we have the following quantities

$$\langle u, \frac{\partial^2 u}{\partial x^2} \rangle = -\langle \frac{\partial u}{\partial x}, \frac{\partial u}{\partial x} \rangle = -\left(||\frac{du}{dx}||_{L^2} \right)^2, \qquad \langle u, \frac{\partial u}{\partial x} \rangle = \frac{1}{2}[u^2]_{-\infty}^{+\infty} = 0$$

$$-\langle u, (1 + c_2 x^2) u \rangle = -||u||_{L^2}^2 - \left(||ux||_{L^2} \right)^2$$

  for all $u \in D(\hat{\mathcal{L}}_n^{CGL})$. From these quantities, we can see that $\Re\{\langle u, \hat{\mathcal{L}}_n^{CGL} u \rangle \leq 0$ and $\Re\{\langle u, \hat{\mathcal{L}}_n^{CGL} u \} \leq 0$.

Now, we put the components together;

- Theorem ($(D(\mathcal{L}^{CGL}), \mathcal{L}^{CGL})$ generates a C_0-semigroup). $(D(\mathcal{L}^{CGL}), \mathcal{L}^{CGL})$ generates a C_0-semigroup.

  Proof. By the above theorems "Lumer-Phillips Closedness Condition A", "Lumer-Phillips Dissipativity Condition A", "Lumer-Phillips Dissipativity Condition B" and "Density of $H_V(\mathbb{R})$". We have that $\hat{\mathcal{L}}_n^{CGL}$ generates a contraction semigroup. Therefore, by the theorem "Perturbations by Bounded Operators", we have that $(D(\mathcal{L}^{CGL}), \mathcal{L}^{CGL})$ generates a C_0-semigroup. □

C.2 $\hat{\mathcal{L}}_n^{CGL}$ is a sectorial operator

We proved in the last section that $\hat{\mathcal{L}}_n^{CGL}$ generates a contraction semigroup. We recall the definition of a sectorial operator that we gave in Section 3.2.

- Definition (Sectorial Operator as given in Henry (2006) [51], (Definition 1.3.1)). We call a linear operator $-\mathcal{L}$ a sectorial operator if it is closed, densely-defined operator such that, for some ϕ in $(0, \frac{\pi}{2})$ and some $M \geq 1$ and real a,

  (a) the sector

  $$S_{a,\phi} = \{\phi \leq |arg(\lambda - a)| \leq \pi, \ \ \lambda \neq a\} \tag{C.1}$$

  is contained in the resolvent set $\rho(-\mathcal{L})$, and

  (b)

  $$||(\lambda - \mathcal{L})^{-1}|| \leq \frac{M}{|\lambda - a|} \qquad \text{for all} \qquad \lambda \in S_{a,\phi}. \tag{C.2}$$

We show that $\hat{\mathcal{L}}_n^{CGL}$ coincides with the above definition of the sectorial operator. In the previous section of this appendix, we showed that the operator is closed and densely defined. Therefore, we need to show (a) and (b) of the above definition. In order to show (a), we firstly recognise that often is rephrase (C.1) in terms of the numerical range. We define the numerical range;

- Definition (Numerical Range). Let $\mathcal{L}$ be a linear operator. The numerical range of $\mathcal{L}$ is defined by

  $$\mathcal{F}(\mathcal{L}) = \{z : z = \langle u, \mathcal{L}u \rangle, \text{ where } u \in D(\mathcal{L}), \ \ ||u|| = 1\} \tag{C.3}$$

Let us consider the following quantity $\Sigma(-\mathcal{L}) = \mathbb{C} \backslash cl(\mathcal{F}(-\mathcal{L}))$. Then $\Sigma(-\mathcal{L}) \in \rho(-\mathcal{L})$. Therefore, we can show that $\mathcal{F}(-\mathcal{L})$ lies in a sector $S_{c,\theta} = \{\theta \in \mathbb{C} : |arg(\lambda - c)|\} \leq \theta$ then we have (C.1). We show that $\hat{\mathcal{L}}_n^{CGL}$ satisfies (a) of the definition of a sectorial operator in the following theorem;

- Theorem (Numerical Range Condition of the Definition of a Sectorial Operator). There exists a c and θ such that $\mathcal{F}(-\hat{\mathcal{L}}_n^{CGL})$ lies in the sector

$$S_{c,\theta} = \{\lambda \in \mathbb{C} : |arg(\lambda - c)| \leq \theta\}. \tag{C.4}$$

Proof. We consider the following quadratic form

$$Q(-\hat{\mathcal{L}}_n^{CGL} - c) = -\langle u, (\hat{\mathcal{L}}_n^{CGL} + c)u\rangle. \tag{C.5}$$

Now, as we have

$$\Re\{Q(-\hat{\mathcal{L}}_n^{CGL} - c)\} = ||\frac{\partial u}{\partial x}||_{L^2}^2 + c_2||ux||_{L^2}^2 - c||u||_{L^2}^2 \qquad \text{and} \qquad \Im\{Q(-\hat{\mathcal{L}}_n^{CGL} - c)\} = -||\frac{\partial u}{\partial x}||_{L^2}^2, \tag{C.6}$$

we want to find a c such that $\Re\{Q(-\hat{\mathcal{L}}_n^{CGL} - c)\} \geq \Im\{Q(-\hat{\mathcal{L}}_n^{CGL} - c)\}$

$$2||\frac{\partial u}{\partial x}||_{L^2}^2 + c_2||ux||_{L^2}^2 \geq -c||u||_{L^2}^2. \tag{C.7}$$

We can again take $c = 0$. Regarding θ, it follows that $|\frac{\Im\{Q(-\hat{\mathcal{L}}^{CGL})\}}{\Re\{Q(-\mathcal{L}^{\hat{C}GL})\}}| < 1$. Thus, we can take $\theta = \arctan(1)$. □

For part (b) of the definition of a sectorial operator we can use the Hille-Yosida theorem as we proved in the last section that $\hat{\mathcal{L}}_n^{CGL}$ generates a contraction semigroup

- Theorem (Hille-Yosida, as given in Pazy (2012) [75]). A linear (unbounded) operator $(D(\mathcal{L}), \mathcal{L})$ is the infinitesimal generator of C_0-semigroup of contractions $e^{t\mathcal{L}}$, $t \geq 0$ if and only if

  (a) $\mathcal{L}$ is closed and $Cl(\mathcal{L}) = X$.

  (b) The resolvent set $\rho(\mathcal{L})$ of $\mathcal{L}$ contains $\mathbb{R}^+$ and for every $\lambda > 0$

$$||(\lambda - \mathcal{L})^{-1}|| \leq \frac{1}{\lambda} \tag{C.8}$$

Proof. See Theorem 3.1 of Section 1.3 of Pazy (2012) [75]. □

Now, we can prove the title of this section;

- Theorem ($-\hat{\mathcal{L}}_n^{CGL}$ is a sectorial operator), $-\hat{\mathcal{L}}_n^{CGL}$ is a sectorial operator.

  Proof. As seen in the last section, $\mathcal{L}_n^{CGL}$ is closed and densely-defined. From the theorem, "Numerical Range Condition of the Definition of a Sectorial Operator", (C.1) is satisfied (aspect (a) of the definition of a sectorial operator). We have that As $\hat{\mathcal{L}}^{CGL}$ is contractions, it follows from (C.8) of the Hille-Yosida Theorem that (C.2) is satisfied with $M = 1$ and $a = 0$. Therefore, $\hat{\mathcal{L}}_n^{CGL}$ is a sectorial operator. □

Appendix D

D.1 Compact Resolvents of $\mathcal{L}^{RGL}$ and $\mathcal{L}^{CGL}$

In this appendix, we prove that both $\mathcal{L}^{RGL}$ and $\mathcal{L}^{CGL}$ have compact resolvents. This allows us to satisfy the assumptions of "Condition on the Uniform Boundedness of Projections". We actually go one step further in order to show that both the operators $\mathcal{L}^{RGL}$ and $\mathcal{L}^{CGL}$ have discrete spectrums. This is useful as there is a problem with spectral pollutions when numerically determining the spectra of non-self-adjoint linear operators, but even in self-adjoint cases as well; the reader is invited to see the review article Boulton (2016) [18] about the failure of Galerkin-methods for determining pseudospectra.

We give the following theorems that allow us to ascertain the compact resolvent. What is instrumental in this case is the Kolmogorov-Riesz-Fréchet theorem that was used in Appendix A with the proofs of the Fredholm Alternative, but this time we are using it to show that the domain of the operator is compactly-embedded in the $L^2(\mathbb{R})$ whereas previously we showed that the interim space $H^{\mathcal{L}^1}(\mathbb{R})$ was compactly embedded in $L^2(\mathbb{R})$.

- Theorem (Compact Resolvent Condition). Let H be a Hilbert Space. A closed operator $(D(\mathcal{L}), \mathcal{L})$ has a compact resolvent if and only if the injection $i : (D(\mathcal{L}), ||\cdot||_T) \hookrightarrow (X, ||\cdot||_X)$ is compact.
  Proof. See Proposition 4.24 in Cheverry and Raymond (2019) [23]. □

- Theorem (Discrete Spectrum Condition). Let H be a Hilbert Space. Let $(D(\mathcal{L}), \mathcal{L})$ be a closed operator. Assume that the resolvent set is non-empty and the resolvent set is compact. Then the spectrum of $\mathcal{L}$ is discrete.
  Proof. See Corollary 5.12 in Cheverry and Raymond (2019) [23]. □

- Theorem (Kolmogorov-Riesz-Fréchet). Let $\mathcal{F}$ be a bounded set in $L^p(\mathbb{R}^N)$ with $1 \leq p < \infty$. Assume that

  (a) $\lim_{|h| \longrightarrow 0} ||f(x+h) - f(x)||_{L^p} = 0$ uniformly in $f(x) \in \mathcal{F}$, ($x \in \mathbb{R}^n$), i.e. for all $\epsilon > 0$, there exists a δ such that $||f(x+h) - f(x)||_{L^p} < \epsilon$ for all $f \in \mathcal{F}$, for all $h \in \mathbb{R}^N$ with $h < \delta$

  (b) For all $\epsilon > 0$, there exists $\Omega \subset \mathbb{R}^N$, bounded and measurable such that $||f||_{L^p(\mathbb{R}^n \setminus \Omega)} < \epsilon$ for all $f \in \mathcal{F}$.

  Then $\mathcal{F}$ is pre-compact in $L^p(\mathbb{R})$.
  Proof. See Brezis (2011) [19], Chapter 4, Theorem 4.26 and Corollary 4.27. on page 111-113.

We now have the following two theorems, where we prove that $\hat{\mathcal{L}}_n^{RGL}$ and $\hat{\mathcal{L}}_n^{CGL}$ have a discrete spectrum. Within these proofs, we prove that each operator has a compact resolvent. Again, these proofs are very similar, but as they rely on different proofs regarding the generation of an analytic semigroups, we have kept them separate.

- Theorem (Discrete Spectrum of $(D(\mathcal{L}^{RGL}), \mathcal{L}^{RGL})$). $(D(\mathcal{L}^{RGL}), \mathcal{L}^{RGL})$ has a discrete spectrum.

  Proof. Firstly, we use the theorem "Compact Resolvent Condition", we need to show that the injection

$$(D(\mathcal{L}^{RGL}), ||\cdot||_{H_V}) \hookrightarrow (L^2(\mathbb{R}), ||\cdot||_{L^2(\mathbb{R})}) \tag{D.1}$$

  is compact. The first criteria for a compact embedding follows from the definitions of the norms. To prove the second part, we fix a bounded sequence u_n, $n \in \mathbb{N}$ in $D(\mathcal{L}^{RGL})$ and set $\mathcal{F} = \{u_n\}_{n=0}^{\infty}$ and show that the terms satisfy the conditions of the Kolmogorov-Riesz-Fréchet theorem. We have the first condition of the Kolmogorov-Riesz-Fréchet theorem as the functions u_n are in $H^2(\mathbb{R})$, and therefore by Morrey's inequality (Theorem 4, Section 5.6.2 in Evans (2010) [44]) are Holder continuous with exponent $\alpha = \frac{1}{2}$ and thereby uniformly continuous. To prove part (b) of Kolmogorov-Riesz-Fréchet theorem, we use the fact that the norm $||u_n||_{H_V}$ controls of $||(1+c_2x^2)u_n||_{L^2}$. Therefore, we have that for $u_n \in (D(\mathcal{L}^{RGL}), ||\cdot||_{H_V})$ and an interval D of radius R,

$$\begin{aligned} M > ||(1+c_2x^2)u_n||_{L^2(\mathbb{R})} \geq ||(1+c_2x^2)u_n||_{L^2(\mathbb{R}\setminus D)} &\geq \sqrt{\int_{|x|>R} (1+c_2x^2)^2 u_n^2 dx} \\ &\geq \sqrt{(1+c_2R^2)^2 \int_{|x|>R} u_n^2 dx} = (1+c_2R^2)||u_n||_{L^2(\mathbb{R}\setminus D)}, \end{aligned} \tag{D.2}$$

  which gives

$$||u_n||_{L^2(\mathbb{R}\setminus D)} < \frac{M}{(1+c_2R^2)}. \tag{D.3}$$

  We can always tune R such that $\frac{M}{(1+c_2R^2)} = \epsilon$ for all ϵ, thus part (b) of the Kolmogorov-Riesz-Fréchet theorem is satisfied. Thus, u_n has a convergent subsequence in $L^2(\mathbb{R})$ and thus the embedding is compact.

  Therefore, the operator satisfies the conditions of the theorem "Discrete Spectrum Condition"; the closedness and that $\hat{\mathcal{L}}_n^{RGL}$ generates an analytic semigroup can be obtained from the theorems in Appendix C. Furthermore, there exists a positive constant α follows $\hat{\mathcal{L}}_n^{RGL} + \alpha$ where α such $\hat{\mathcal{L}}_n^{RGL} + \alpha$ is invertible hence the resolvent set is non-empty. □

- Theorem (Discrete Spectrum of $(D(\mathcal{L}^{CGL}), \mathcal{L}^{CGL})$). $(D(\mathcal{L}^{CGL}), \mathcal{L}^{CGL})$ has a discrete spectrum.

  Proof. Firstly, we use the theorem "Compact Resolvent Condition", we need to show that the injection

$$(D(\mathcal{L}^{CGL}), ||\cdot||_{H_V}) \hookrightarrow (L^2(\mathbb{R}), ||\cdot||_{L^2(\mathbb{R})}) \tag{D.4}$$

is compact. The first criteria for a compact embedding follows from the definitions of the norms. To prove the second part, we fix a bounded sequence u_n, $n \in \mathbb{N}$ in $D(\mathcal{L}_{RGL})$ and set $\mathcal{F} = \{u_n\}_{n=0}^{\infty}$ and show that the terms satisfy the conditions of the Kolmogorov-Riesz-Fréchet theorem. We have the first condition of the Kolmogorov-Riesz-Fréchet theorem as the functions u_n are in $H^2(\mathbb{R})$, and therefore by Morrey's inequality (Theorem 4, Section 5.6.2 in Evans (2010) [44]) are Holder continuous with exponent $\alpha = \frac{1}{2}$ and thereby uniformly continuous. To prove part (b) of Kolmogorov-Riesz-Fréchet theorem, we use the fact that the norm $||u_n||_{H_V}$ controls of $||(1 + c_2x^2)u_n||_{L^2}$. Therefore, we have that for $u_n \in (D(\mathcal{L}^{CGL}), ||\cdot||_{H_V})$ and an interval D of radius R,

$$M > ||(1 + c_2x^2)u_n||_{L^2(\mathbb{R})} \geq |||1 + c_2x^2|u_n||_{L^2(\mathbb{R}\setminus D)} \geq \sqrt{\int_{|x|>R} |1 + c_2x^2|^2 u_n^2 dx}$$
$$\geq \sqrt{|1 + c_2x^2|^2 \int_{|x|>R} u_n^2 dx} = \sqrt{|1 + c_2x^2|^2}||u_n||_{L^2(\mathbb{R}\setminus D)}, \quad \text{(D.5)}$$

which gives

$$||u_n||_{L^2(\mathbb{R}\setminus D)} < \frac{M}{|1 + c_2R^2|}. \quad \text{(D.6)}$$

We can always tune R such that $\frac{M}{|1+c_2R^2|} = \epsilon$ for all ϵ, thus part (b) of the Kolmogorov-Riesz-Fréchet theorem is satisfied. Thus, u_n has a convergent subsequence in $L^2(\mathbb{R})$ and thus the embedding is compact.

Therefore, the operator satisfies the conditions of the theorem "Discrete Spectrum Condition"; the closedness and that $\hat{\mathcal{L}}_n^{CGL}$ generates an analytic semigroup can be obtained from the theorems in Appendix C. Furthermore, there exists a positive constant α follows $\hat{\mathcal{L}}_n^{CGL} + \alpha$ where α such $\hat{\mathcal{L}}_n^{CGL} + \alpha$ is invertible hence the resolvent set is non-empty. □

Bibliography

[1] F. Aboud, F. Jauberteau, G. Moebs, and D. Robert. Numerical approaches to compute spectra of non-self adjoint operators and quadratic pencils. *J. Math. Study*, 53(1):12–44, 2020.

[2] G. Adomian. Solving frontier problems of physics: the decomposition method. *Fundamental Theories of Physics, Kluwer Academic Publishers Group, Dordrecht*, 1, 1994.

[3] G. Allaire. Homogenization and two-scale convergence. *SIAM Journal on Mathematical Analysis*, 23(6): 1482–1518, 1992.

[4] G. Allaire and R. Orive. Homogenization of periodic non self-adjoint problems with large drift and potential. *ESAIM: Control, Optimisation and Calculus of Variations*, 13(4):735–749, 2007.

[5] J.-P. Antoine and C. Trapani. Partial inner product spaces, metric operators and generalized hermiticity. *Journal of Physics A: Mathematical and Theoretical*, 46(2):025204, 2012.

[6] J.-P. Antoine and C. Trapani. Some remarks on quasi-hermitian operators. *Journal of Mathematical Physics*, 55(1):025204, 2014.

[7] J.-P. Antoine and C. Trapani. Metric operators, generalized hermiticity and lattices of hilbert spaces. *Non-selfadjoint operators in quantum physics*, pages 345–402, 2015.

[8] F. Bagarello. Examples of pseudo-bosons in quantum mechanics. *Physics Letters A*, 374(37):3823–3827, 2010.

[9] F. Bagarello. Pseudobosons, riesz bases, and coherent states. *Journal of mathematical physics*, 51(2): 023531, 2010.

[10] F. Bagarello. More mathematics for pseudo-bosons. *Journal of Mathematical Physics*, 54(6):063512, 2013.

[11] S. Bagheri, D. Henningson, J. Hoepffner, and P. Schmid. Input-output analysis and control design applied to a linear model of spatially developing flows. *Applied Mechanics Reviews*, 62(2), 2009.

[12] K. Balasubramanian and R. Sujith. Non-normality and nonlinearity in combustion–acoustic interaction in diffusion flames. *Journal of Fluid Mechanics*, 594:29–57, 2008.

[13] C. M. Bender and S. A. Orszag. *Advanced mathematical methods for scientists and engineers I: Asymptotic methods and perturbation theory*. Springer Science & Business Media, 2013.

[14] D. Blomker. Approximation of the stochastic rayleigh–benard problem near the onset of convection and related problems. *Stochastics and Dynamics*, 5(03):441–474, 2005.

[15] D. Blomker. *Amplitude equations for stochastic partial differential equations*, volume 3. World Scientific, 2007.

[16] D. Blömker and W. Mohammed. Amplitude equations for spdes with cubic nonlinearities. *Stochastics An International Journal of Probability and Stochastic Processes*, 01 2011. doi: $10.1080/17442508.2011.624628$.

[17] D. Blömker, M. Hairer, and G. Pavliotis. Some remarks on stabilization by additive noise. 01 2009.

[18] L. Boulton. Spectral pollution and eigenvalue bounds. *Applied Numerical Mathematics*, 99:1–23, 2016.

[19] H. Brézis. *Functional analysis, Sobolev spaces and partial differential equations*, volume 2. Springer, 2011.

[20] R. J. Briggs. *Electron-Stream Interaction with Plasmas*. The MIT Press, 12 1964. ISBN 9780262310741. doi: $10.7551/\mathrm{mitpress}/2675.001.0001$. URL `https://doi.org/10.7551/mitpress/2675.001.0001`.

[21] M. Carini, F. Auteri, and F. Giannetti. Centre-manifold reduction of bifurcating flows. *J. Fluid Mech*, 767: 109–145, 2015.

[22] Y. Cherruault. Convergence of adomian's method. *Kybernetes*, 1989.

[23] C. Cheverry and N. Raymond. Handbook of spectral theory. *Lecture, September*, 2019.

[24] J. Chomaz. Absolute and convective instabilities in nonlinear systems. *Physical review letters*, 69(13):1931, 1992.

[25] J.-M. Chomaz. Global instabilities in spatially developing flows: non-normality and nonlinearity. *Annu. Rev. Fluid Mech.*, 37:357–392, 2005.

[26] J.-M. Chomaz, P. Huerre, and L. G. Redekopp. A frequency selection criterion in spatially developing flows. *Studies in applied mathematics*, 84(2):119–144, 1991.

[27] P. Collet and J.-P. Eckmann. The time dependent amplitude equation for the swift-hohenberg problem. *Communications in mathematical physics*, 132(1):139–153, 1990.

[28] C. Cossu and J. Chomaz. Global measures of local convective instabilities. *Physical review letters*, 78(23): 4387, 1997.

[29] A. Couairon and J.-M. Chomaz. Fully nonlinear global modes in slowly varying flows. *Physics of Fluids*, 11 (12):3688–3703, 1999.

[30] P. Coullet and E. A. Spiegel. Amplitude equations for systems with competing instabilities. *SIAM Journal on Applied Mathematics*, 43(4):776–821, 1983.

[31] J. Crouch and T. Herbert. A note on the calculation of landau constants. *Physics of Fluids A: Fluid Dynamics*, 5(1):283–285, 1993.

[32] G. Da Prato and J. Zabczyk. *Stochastic Equations in Infinite Dimensions*. Encyclopedia of Mathematics and its Applications. Cambridge University Press, 1992. doi: $10.1017/\mathrm{CBO}9780511666223$.

[33] E. Davies. Semigroup growth bounds. *Journal of Operator Theory*, pages 225–249, 2005.

[34] E. B. Davies. *Linear operators and their spectra*, volume 106. Cambridge University Press, 2007.

[35] E. B. Davies and A. B. Kuijlaars. Spectral asymptotics of the non-self-adjoint harmonic oscillator. *Journal of the London Mathematical Society*, 70(2):420–426, 2004.

[36] G. Dee and J. Langer. Propagating pattern selection. *Physical Review Letters*, 50(6):383, 1983.

[37] N. Dencker, J. Sjöstrand, and M. Zworski. Pseudospectra of semi-classical (pseudo) differential operators. *arXiv preprint math/0301242*, 2003.

[38] J. Dieudonné. Quasi-hermitian operators. *Proceedings of the International Symposium on Linear Spaces*, pages 115–120, 1960.

[39] C. Dolph. Recent developments in some non-self-adjoint problems of mathematical physics. *Bulletin of the American Mathematical Society*, 67(1):1–69, 1961.

[40] P. Drazin. On a model of instability of a slowly-varying flow. *The Quarterly Journal of Mechanics and Applied Mathematics*, 27(1):69–86, 1974.

[41] K.-J. Engel and R. Nagel. *One-parameter semigroups for linear evolution equations*, volume 63. 2001.

[42] E. Ergun. Finding of the metric operator for a quasi-hermitian model. *Journal of Function Spaces and Applications*, 2013:1–8, 2013.

[43] L. C. Evans. *Weak convergence methods for nonlinear partial differential equations*. Number 74. American Mathematical Soc., 1990.

[44] L. C. Evans. *Partial differential equations*. American Mathematical Society, Providence, R.I., 2010. ISBN 9780821849743 0821849743.

[45] A. Friedman. *Partial differential equations / Avner Friedman.* Holt, Rinehart and Winston, New York, 1969. ISBN 0030774551.

[46] B. Friedman and L. I. Mishoe. Eigenfunction expansions associated with a non-self-adjoint differential equation. *Pacific Journal of Mathematics*, 6(2):249–270, 1956.

[47] K. Fujimura. The equivalence between two perturbation methods in weakly nonlinear stability theory for parallel shear flows. *Proceedings of the Royal Society of London. A. Mathematical and Physical Sciences*, 424(1867):373–392, 1989.

[48] K. Fujimura. Methods of centre manifold and multiple scales in the theory of weakly nonlinear stability for fluid motions. *Proceedings of the Royal Society of London. Series A: Mathematical and Physical Sciences*, 434 (1892):719–733, 1991.

[49] F. Giannetti and P. Luchini. Structural sensitivity of the first instability of the cylinder wake. *Journal of Fluid Mechanics*, 581:167, 2007.

[50] W. Greenlee. Singular perturbation of non-self-adjoint elliptic eigenvalue problems. In *Theory and Applications of Singular Perturbations*, pages 43–53. Springer, 1982.

[51] D. Henry. *Geometric theory of semilinear parabolic equations*, volume 840. Springer, 2006.

[52] T. Herbert. On perturbation methods in nonlinear stability theory. *Journal of Fluid Mechanics*, 126:167–186, 1983.

[53] F. Hoppensteadt. Asymptotic series solutions for nonlinear ordinary differential equations with a small parameter. *Journal of Mathematical Analysis and Applications*, 25(3):521–536, 1969.

[54] P. Huerre and P. A. Monkewitz. Local and global instabilities in spatially developing flows. *Annual review of fluid mechanics*, 22(1):473–537, 1990.

[55] R. Hunt and D. G. Crighton. Instability of flows in spatially developing media. *Proceedings of the Royal Society of London. Series A: Mathematical and Physical Sciences*, 435(1893):109–128, 1991.

[56] T. Kato. *Perturbation theory for linear operators*, volume 132. Springer Science & Business Media, 2013.

[57] R. Kerswell. Nonlinear nonmodal stability theory. *Annual Review of Fluid Mechanics*, 50:319–345, 2018.

[58] P. Kirrmann, G. Schneider, and A. Mielke. The validity of modulation equations for extended systems with cubic nonlinearities. 1992.

[59] A. I. Koshelev. A priori estimates in l_p and generalized solutions of elliptic equations and systems. *Uspekhi Mat. Nauk*, 13(4):29–88, 1958.

[60] D. Krejčiřík and P. Siegl. Pseudomodes for schrödinger operators with complex potentials. *Journal of Functional Analysis*, 276(9):2856–2900, 2019.

[61] D. Krejčiřík, P. Siegl, M. Tater, and J. Viola. Pseudospectra in non-hermitian quantum mechanics. *Journal of mathematical physics*, 56(10):103513, 2015.

[62] L. Landau and E. M. Lifshits. Mechanics of continuous media. *Gostekhizdat, Moscow*, 81, 1954.

[63] L. LANDAU and E. LIFSHITZ. Chapter iii - turbulence. In L. LANDAU and E. LIFSHITZ, editors, *Fluid Mechanics (Second Edition)*, pages 95 – 156. Pergamon, second edition edition, 1987. ISBN 978-0-08-033933-7. doi: https://doi.org/10.1016/B978-0-08-033933-7.50011-8. URL http://www.sciencedirect.com/science/article/pii/B9780080339337500118.

[64] G. J. Lord, C. E. Powell, and T. Shardlow. *An introduction to computational stochastic PDEs*, volume 50. Cambridge University Press, 2014.

[65] A. McKane and D. Waxman. Singular solutions of the diffusion equation of population genetics. *Journal of theoretical biology*, 247(4):849–858, 2007.

[66] F. G. Mehler. Ueber die entwicklung einer function von beliebig vielen variablen nach laplaceschen functionen höherer ordnung. 1866.

[67] G. Metafune, J. Pruss, A. Rhandi, and R. Schnaubelt. Lp-regularity for elliptic operators with unbounded coefficients. *Advances in Differential Equations*, 10(10):1131–1164, 2005.

[68] A. Mielke and G. Schneider. Attractors for modulation equations on unbounded domains-existence and comparison. *Nonlinearity*, 8(5):743, 1995.

[69] M. Miklavčič. *Applied functional analysis and partial differential equations*. Allied Publishers, 1998.

[70] B. Mityagin, P. Siegl, and J. Viola. Differential operators admitting various rates of spectral projection growth. *Journal of Functional Analysis*, 272, 09 2013. doi: 10.1016/j.jfa.2016.12.007.

[71] W. Mohammed, D. Blömker, and K. Klepel. Multi-scale analysis of spdes with degenerate additive noise. *Journal of Evolution Equations*, 14, 06 2014. doi: 10.1007/s00028-013-0213-3.

[72] A. Mostafazadeh. Pseudo-hermitian representation of quantum mechanics. *International Journal of Geometric Methods in Modern Physics*, 7(07):1191–1306, 2010.

[73] A. Mostafazadeh. Pseudo-hermitian quantum mechanics with unbounded metric operators. *Philosophical Transactions of the Royal Society A: Mathematical, Physical and Engineering Sciences*, 371(1989):20120050, 2013.

[74] R. Novák. On the pseudospectrum of the harmonic oscillator with imaginary cubic potential, August 2015.

[75] A. Pazy. *Semigroups of linear operators and applications to partial differential equations*, volume 44. Springer Science & Business Media, 2012.

[76] C. L. Pekeris and B. Shkoller. Stability of plane poiseuille flow to periodic disturbances of finite amplitude in the vicinity of the neutral curve. *Journal of Fluid Mechanics*, 29(1):31–38, 1967. doi: $10.1017/S0022112067000618$.

[77] H. Poincaré. Mémoire sur les courbes définies par une équation différentielle. *Éditions Jacques Gabay, Sceaux*, 1993.

[78] M. PRADAS, G. PAVLIOTIS, S. KALLIADASIS, D. PAPAGEORGIOU, and D. TSELUIKO. Additive noise effects in active nonlinear spatially extended systems. *European Journal of Applied Mathematics*, 23(5):563–591, 2012. doi: $10.1017/S0956792512000125$.

[79] S. C. Reddy, P. J. Schmid, and D. S. Henningson. Pseudospectra of the orr–sommerfeld operator. *SIAM Journal on Applied Mathematics*, 53(1):15–47, 1993.

[80] W. C. Reynolds and M. C. Potter. Finite-amplitude instability of parallel shear flows. *Journal of Fluid Mechanics*, 27(3):465–492, 1967. doi: $10.1017/S0022112067000485$.

[81] K. Roussopoulos and P. A. Monkewitz. Nonlinear modelling of vortex shedding control in cylinder wakes. *Physica D: Nonlinear Phenomena*, 97(1-3):264–273, 1996.

[82] P. J. Schmid. Nonmodal stability theory. *Annu. Rev. Fluid Mech.*, 39:129–162, 2007.

[83] P. J. Schmid, D. S. Henningson, and D. Jankowski. Stability and transition in shear flows. applied mathematical sciences, vol. 142. *Appl. Mech. Rev.*, 55(3):B57–B59, 2002.

[84] G. Schneider. Global existence via ginzburg-landau formalism and pseudo-orbits of ginzburg-landau approximations. *Communications in mathematical physics*, 164(1):157–179, 1994.

[85] G. Schneider. A new estimate for the ginzburg-landau approximation on the real axis. *Journal of Nonlinear Science*, 4(1):23–34, 1994.

[86] R. E. Showalter. *Monotone operators in Banach space and nonlinear partial differential equations*, volume 49. American Mathematical Soc., 2013.

[87] M. A. Shubov. Basis property of eigenfunctions of nonselfadjoint operator pencils generated by the equation of nonhomogeneous damped string. *Integral Equations and Operator Theory*, 25(3):289–328, 1996.

[88] M. A. Shubov. Asymptotic representation for the eigenvalues of a non-selfadjoint operator governing the dynamics of an energy harvesting model. *Applied Mathematics & Optimization*, 73(3):545–569, 2016.

[89] M. A. Shubov. Spectral analysis of a non-selfadjoint operator generated by an energy harvesting model and application to an exact controllability problem. *Asymptotic Analysis*, 102(3-4):119–156, 2017.

[90] M. A. Shubov. Control problems for energy harvester model and interpolation in hardy space. *Mathematische Nachrichten*, 293(3):585–610, 2020.

[91] P. Siegl and D. Krejčiřík. On the metric operator for the imaginary cubic oscillator. *Physical Review D*, 86 (12), Dec 2012. ISSN 1550-2368. doi: $10.1103/\mathrm{physrevd.86.121702}$. URL `http://dx.doi.org/10.1103/PhysRevD.86.121702`.

[92] D. Sipp and A. Lebedev. Global stability of base and mean flows: a general approach and its applications to cylinder and open cavity flows. *Journal of Fluid Mechanics*, 593:333–358, 2007.

[93] J. Stuart. On the non-linear mechanics of wave disturbances in stable and unstable parallel flows part 1. the basic behaviour in plane poiseuille flow. *Journal of Fluid Mechanics*, 9(3):353–370, 1960.

[94] T. Tang. The hermite spectral method for gaussian-type functions. *SIAM Journal on Scientific Computing*, 14 (3):594–606, 1993.

[95] L. Tartar. *The general theory of homogenization: a personalized introduction*, volume 7. Springer Science & Business Media, 2009.

[96] V. Theofilis. Global linear instability. *Annual Review of Fluid Mechanics*, 43:319–352, 2011.

[97] L. N. Trefethen. Computation of pseudospectra. *Acta numerica*, 8:247–295, 1999.

[98] L. N. Trefethen, A. E. Trefethen, S. C. Reddy, and T. A. Driscoll. Hydrodynamic stability without eigenvalues. *Science*, 261(5121):578–584, 1993.

[99] W. van Saarloos and P. Hohenberg. Fronts, pulses, sources and sinks in generalized complex ginzburg-landau equations. *Physica D: Nonlinear Phenomena*, 56(4):303–367, 1992.

[100] M. I. Vishik and L. A. Lyusternik. The solution of some perturbation problems for matrices and selfadjoint or non-selfadjoint differential equations i. *RuMaS*, 15(3):1–73, 1960.

[101] F. Waleffe. Transition in shear flows. nonlinear normality versus non-normal linearity. *Physics of Fluids*, 7(12): 3060–3066, 1995.

[102] J. Watson. On the nonlinear mechanics of wave disturbances in stable and unstable parallel flows. *J. Fluid Mech*, 9(371-389):219, 1960.

[103] J. A. Weideman and S. C. Reddy. A matlab differentiation matrix suite. *ACM Transactions on Mathematical Software (TOMS)*, 26(4):465–519, 2000.

[104] A. Yagi. *Abstract parabolic evolution equations and their applications*. Springer Science & Business Media, 2009.

[105] L. Zhang, Y. B. Gao, and C. Wang. Green function and perturbation method for dissipative systems based on biorthogonal basis. *Communications in Theoretical Physics*, 51:1017–1022, 2009.

Titre: Une étude des complexités liées à la dérivation d'équations d'amplitude via des développements faiblement non linéaires d'équations aux dérivées partielles non auto-adjointes

Mots clés: les équations d'amplitude, les expansions faiblement non linéaires, l'équation de Ginzburg-Landau, l'équation de Ginzburg-Landau, les équations aux dérivées partielles

Résumé: L'interaction entre la non-normalité et la non-linéarité a fait l'objet de nombreux travaux mais aussi de controverses en mécanique des fluides. Dans cette thèse, nous explorons la relation entre la non-normalité et la non-linéarité en analysant les limitations des approximations au premier ordre des développements faiblement non linéaires (WNLE) pour prédire l'amplitude des branches bifurquées de systèmes non auto-adjoints.

L'approximation du premier ordre correspond à un vecteur propre marginal multiplié par une amplitude régie par une équation, dite équation d'amplitude . Dans la littérature, les auteurs ont utilisé diverses approches pour améliorer cette approximation, comme aller plus haut dans l'ordre dans l'approximation, ce qui nécessite des hypothèses supplémentaires en raison de la non-unicité des termes d'ordre supérieur, ainsi que la construction d'équations d'amplitude d'ordre supérieur pour décrire le développement temporel du vecteur propre considéré. Cette dernière approche peut être considérée comme un moyen pour gérer la non-unicité. Cependant, en ne considérant dans l'approximation que le vecteur propre dominant, même si son développement temporel est régi par une équation d'amplitude d'ordre supérieur, on néglige les structures spatiales différentes de ce vecteur propre.

Dans cette thèse, nous choisissons deux cas tests pour explorer les phénomènes décrits ci-dessus, à savoir l'équation de Ginzburg-Landau non-auto-adjointe réelle (RnsaGL) et l'équation complexe de Ginzburg-Landau non-auto-adjointe (CnsaGL). Nous choisissons ces cas tests car les opérateurs linéaires génèrent dans chaque cas des semi-groupes fortement continus. Également dans le cas réel, il existe une structure de quasi-base. Cela nous permet de rechercher la solution de RnsaGL sous la forme de couples valeur propre-vecteur propre.

Dans un premier temps, nous consolidons les recherches effectuées par d'autres auteurs dans la littérature en dérivant des équations d'amplitude d'ordre supérieur pour le cas RnsaGL. Il est démontré que les équations d'amplitude d'ordre supérieur ont un rayon de convergence plus petit. Nous argumentons également contre les équations d'amplitude d'ordre supérieur en projetant la solution obtenue numériquement sur le vecteur propre dominant : nous constatons que, pour une non-normalité croissante, la solution est de moins en moins alignée avec le vecteur propre dominant. Ainsi, quelle que soit la complexité de l'équation d'amplitude, elle ne peut pas représenter la solution.

Nous dérivons ensuite des approximations d'ordre supérieur en utilisant une hypothèse différente des travaux des auteurs précédents ; à savoir qu'il ne peut y avoir de contributions linéaires dans l'approximation des termes d'ordre supérieur. On voit que dans le cas RnsaGL, cette hypothèse peut être prescrite en imposant que les termes d'ordre supérieur sont orthogonaux au vecteur propre direct ou au vecteur propre adjoint (dans le cas CnsaGL, on ne peut choisir que le vecteur propre direct). Après cela, nous dérivons des bornes d'erreur afin de quantifier la différence entre les solutions numériques et leurs approximations correspondantes. La dérivation de ces bornes d'erreur est facilitée par le fait que les opérateurs linéaires dans les cas considérés génèrent des semi-groupes fortement continus. Ces bornes d'erreur sont des outils théoriques pour montrer l'existence d'un possible rayon de convergence (ils ne nous permettent pas de déterminer le rayon de convergence exact). Nous discutons comment ces bornes d'erreur théoriques peuvent être utilisées concrètement. Enfin, nous profitons de l'existence de la quasi-base en présentant une technique de moyennage stochastique où les modes stables sont soumis à du bruit. Cette technique de moyennage stochastique est différente de la technique WNLE car aucun mode propre n'est négligé dans l'approche, mais les caractéristiques de saturation sont encore sous-estimées dans le cas non auto-adjoint.

Title: A study of the complications regarding the derivation of amplitude equations via weakly nonlinear analysis for non-self-adjoint partial differential equations

Keywords: Amplitude Equations, weakly nonlinear expansions, Ginzburg-Landau Equation, non-self-adjoint, partial differential equations

Abstract: The interplay between non-normality and nonlinearity has been the focus of numerous works but also contention in Fluid Mechanics. In this thesis, we explore the relationship between non-normality and nonlinearity by considering the failure of first-order approximations derived via weakly nonlinear expansions (WNLE) to capture saturation characteristics of non-self-adjoint systems.

The first-order approximation achieved via WNLE is of the form of the leading eigenvector multiplied by an amplitude, which is governed by an amplitude equation. Authors have used various approaches to improve upon this approximation, such as going higher in order in the approximation, which requires additional assumptions owing to the non-uniqueness of higher order terms, as well as also building higher order amplitude equations to describe the temporal development of the leading eigenvector. The latter approach can be seen as a way to circumvent the non-uniqueness. However, by still only approximating with the leading eigenvector, even though its temporal development is elaborated by a higher order amplitude equation, spatial structures different from the leading eigenvector are neglected.

In this thesis, we choose two test-cases to explore the phenomena described above, namely the real non-self-adjoint Ginzburg-Landau equation (RnsaGL) and the Complex non-self-adjoint Ginzburg-Landau (CnsaGL) equation. We choose these test cases because the linear operators in each case generate strongly continuous semigroups, but, also in the real case, there exists a quasi-basis structure. This allows us to expand the solution of the RnsaGL into eigenvalue-eigenvector pairs, which is not always possible for non-self-adjoint linear operators as the eigenvectors' forming an orthonormal basis is not guaranteed as it is in the self-adjoint case.

We begin the thesis by consolidating the research done by other authors in the literature review and in one of the core chapters where we derive higher order amplitude equations for the RnsaGL. It is demonstrated for the RnsaGL that higher order amplitude equations have a smaller radius of convergence, which essentially limits the usefulness of the approximation. We also argue against higher order amplitude equations by projecting the solution of our test cases onto the zeroth eigenvector, where we find that, for increasing non-normality, less of the overall solution is projected onto the zeroth eigenvector. In this way, no matter how elaborate the amplitude equation, it is incapable of representing the entire system.

Following the consolidation of previous research, we derive higher order approximations using an assumption that is different to the work of previous authors; namely that there can be no linear contributions to the approximation at higher order terms. We see that in the case of the RnsaGL, this assumption can manifest by ensuring that the higher order terms are orthogonal to the direct eigenvector or the adjoint eigenvector (in the case of the CnsaGL, we can only choose the direct eigenvector). After this, we derive error bounds in order to quantify the difference between the solutions of the test cases and their corresponding approximations. The derivation of these error bounds is facilitated by the fact that the linear operators in our test cases generate strongly continuous semigroups. These error bounds are theoretical tools to show the existence of a possible radius of convergence rather than telling us what the radius of convergence is. We therefore discuss how to turn these error bounds from theoretical tools to something that can be used for application. Lastly, we profit from the existence of the quasi-basis by using a stochastic averaging technique where noise is put on the stable modes. This stochastic averaging technique is different from WNLE as no eigenmodes are neglected as a first step, but the saturation characteristics are still underestimated in the non-self-adjoint case.

A Study of the Complications regarding the Derivation of Amplitude Equations via Weakly Nonlinear Expansions for Non-self-adjoint Partial Differential Equations

The interplay between non-normality and nonlinearity has been the focus of numerous works but also contention in Fluid Mechanics. In this thesis, we explore the relationship between non-normality and nonlinearity by considering the failure of firstorder approximations derived via weakly nonlinear expansions (WNLE) to capture saturation characteristics of non-self-adjoint systems.
The first-order approximation achieved via WNLE is of the form of the leading eigenvector multiplied by an amplitude, which is governed by an amplitude equation.
Authors have used various approaches to improve upon this approximation, such as going higher in order in the approximation, which requires additional assumptions owing to the non-uniqueness of higher order terms, as well as also building higher order amplitude equations to describe the temporal development of the leading eigenvector. The latter approach can be seen as a way to circumvent the nonuniqueness.
However, by still only approximating with the leading eigenvector, even though its temporal development is elaborated by a higher order amplitude equation, spatial structures different from the leading eigenvector are neglected.
In this thesis, we choose two test-cases to explore the phenomena described above, namely the real nonselfadjoint Ginzburg-Landau equation (RnsaGL) and the Complex non-self-adjoint Ginzburg-Landau (CnsaGL) equation. We choose these test cases because the linear operators in each case generate strongly continuous semigroups, but, also in the real case, there exists a quasi-basis structure. This allows us to expand the solution of the RnsaGL into eigenvalue-eigenvector pairs, which is not always possible for nonself-adjoint linear operators as the eigenvectors' forming an orthonormal basis is not guaranteed as it is in the self-adjoint case.
We begin the thesis by consolidating the research done by other authors in the literature review and in one of the core chapters where we derive higher order amplitude equations for the RnsaGL. It is demonstrated for the RnsaGL that higher order amplitude equations have a smaller radius of convergence, which essentially limits the usefulness of the approximation.
We also argue against higher order amplitude equations by projecting the solution of our test cases onto the zeroth eigenvector, where we find that, for increasing non-normality, less of the overall solution is projected onto the zeroth eigenvector. In this way, no matter how elaborate the amplitude equation, it is incapable of representing the entire system.
Following the consolidation of previous research, we derive higher order approximations using an assumption that is different to the work of previous authors; namely that there can be no linear contributions to the approximation at higher order terms. We see that in the case of the RnsaGL, this assumption can manifest by ensuring that the higher order terms are orthogonal to the direct eigenvector or the adjoint eigenvector (in the case of the CnsaGL, we can only choose the direct eigenvector).
After this, we derive error bounds in order to quantify the difference between the solutions of the test cases and their corresponding approximations.
The derivation of these error bounds is facilitated by the fact that the linear operators in our test cases generate strongly continuous semigroups. These error bounds are theoretical tools to show the existence of a possible radius of convergence rather than telling us what the radius of convergence is. We therefore discuss how to turn these error bounds from theoretical tools to something that can be used for application.
Lastly, we profit from the existence of the quasi-basis by using a stochastic averaging technique where noise is put on the stable modes. This stochastic averaging technique is different from WNLE as no eigenmodes are neglected as a first step, but the saturation characteristics are still underestimated in the non-self-adjoint case.

Keywords :

AMPLITUDE EQUATIONS ; WEAKLY NONLINEAR EXPANSIONS ; GINZBURG-LANDAU EQUATION ; NON-SELF-ADJOINT ; PARTIAL DIFFERENTIAL EQUATIONS

Une étude des complexités liées à la dérivation d'équations d'amplitude via des développements faiblement non linéaires d'équations aux dérivées partielles non auto-adjointes

L'interaction entre la non-normalité et la non-linéarité a fait l'objet de nombreux travaux mais aussi de controverses en mécanique des fluides. Dans cette thèse, nous explorons la relation entre la non-normalité et la non-linéarité en analysant les limitations des approximations au premier ordre des développements faiblement non linéaires (WNLE) pour prédire l'amplitude des branches bifurquées de systèmes non autoadjoints.
L'approximation du premier ordre correspond à un vecteur propre marginal multiplié par une amplitude régie par une équation, dite équation d'amplitude.
Dans la littérature, les auteurs ont utilisé diverses approches pour améliorer cette approximation, comme aller plus haut dans l'ordre dans l'approximation, ce qui nécessite des hypothèses supplémentaires en raison de la non-unicité des termes d'ordre supérieur, ainsi que la construction d'équations d'amplitude d'ordre supérieur pour décrire le développement temporel du vecteur propre considéré. Cette dernière approche peut être considérée comme un moyen pour gérer la non-unicité. Cependant, en ne considérant dans l'approximation que le vecteur propre dominant, même si son développement temporel est régi par une équation d'amplitude d'ordre supérieur, on néglige les structures spatiales différentes de ce vecteur propre.
Dans cette thèse, nous choisissons deux cas tests pour explorer les phénomènes décrits ci-dessus, à savoir l'équation de Ginzburg-Landau non-auto-adjointe réelle (RnsaGL) et l'équation complexe de Ginzburg-Landau non-auto-adjointe (CnsaGL). Nous choisissons ces cas tests car les opérateurs linéaires génèrent dans chaque cas des semi-groupes fortement continus. Également dans le cas réel, il existe une structure de quasi-base. Cela nous permet de rechercher la solution de RnsaGL sous la forme de couples valeur proprevecteur propre.

Dans un premier temps, nous consolidons les recherches effectuées par d'autres auteurs dans la littérature en dérivant des équations d'amplitude d'ordre supérieur pour le cas RnsaGL. Il est démontré que les équations d'amplitude d'ordre supérieur ont un rayon de convergence plus petit. Nous argumentons également contre les équations d'amplitude d'ordre supérieur en projetant la solution obtenue numériquement sur le vecteur propre dominant : nous constatons que, pour une non-normalité croissante, la solution est de moins en moins alignée avec le vecteur propre dominant. Ainsi, quelle que soit la complexité de l'équation d'amplitude, elle ne peut pas représenter la solution.
Nous dérivons ensuite des approximations d'ordre supérieur en utilisant une hypothèse différente des travaux des auteurs précédents ; à savoir qu'il ne peut y avoir de contributions linéaires dans l'approximation des termes d'ordre supérieur. On voit que dans le cas RnsaGL, cette hypothèse peut être prescrite en imposant que les termes d'ordre supérieur sont orthogonaux au vecteur propre direct ou au vecteur propre adjoint (dans le cas CnsaGL, on ne peut choisir que le vecteur propre direct).
Après cela, nous dérivons des bornes d'erreur afin de quantifier la différence entre les solutions numériques et leurs approximations correspondantes. La dérivation de ces bornes d'erreur est facilitée par le fait que les opérateurs linéaires dans les cas considérés génèrent des semi-groupes fortement continus. Ces bornes d'erreur sont des outils théoriques pour montrer l'existence d'un possible rayon de convergence (ils ne nous permettent pas de déterminer le rayon de convergence exact). Nous discutons comment ces bornes d'erreur théoriques peuvent être utilisées concrètement. Enfin, nous profitons de l'existence de la quasi-base en présentant une technique de moyennage stochastique où les modes stables sont soumis à du bruit. Cette technique de moyennage stochastique est différente de la technique WNLE car aucun mode propre n'est négligé dans l'approche, mais les caractéristiques de saturation sont encore sous-estimées dans le cas non autoadjoint.

Mots-clés :

EQUATION AMPLITUDE ; EXPANSION FAIBLEMENT NON-LINEAIRE ; EQUATION GINZBURG-LANDAU ; DERIVEE PARTIELLE

ONERA
THE FRENCH AEROSPACE LAB

BP 80100 - Chemin de la Hunière FR-91123 PALAISEAU CEDEX - Tél. : +33 1 80 38 60 60 - Fax : +33 1 80 38 65 10

www.onera.fr